UNIVERSITÀ DEGLI STUDI DI MILANO

Scuola di Dottorato in Scienze e Tecnologie Chimiche

Dipartimento di Chimica

PhD Course in Industrial Chemistry - XXX Cycle

"Sustainable preparation of Active Pharmaceutical Ingredients (API) in batch & flow mode, and Iron catalyzed transformations"

Tutor: Prof. Maurizio Benaglia

Davide Brenna

R10837

2014 - 2017

Dedico questa tesi al Prof. Franco Cozzi, esempio per tutti noi.

Summary

Abstract

During my PhD, we focused our attention on the application of the green chemistry principles[1] for the preparation of active pharmaceutical ingredients (API) and, more in general, of highly functionalized chiral molecules, as fine chemicals or building blocks of high value for further synthetic manipulations. The work is presented and discussed in three main chapters:

1- The use of a cheap and green reducing agent, $HSiCl_3$, for imines reduction, either in batch and flow mode, to afford chiral amines, including biologically active compounds.

2- The use of 3D-printed reactors for the preparation of APIs, engineering new reactors in order to perform continuous multi-step synthesis.

3- a) The use of Knolker type iron complexes in the catalytic hydrogenations of chiral imines.

b) The use of cheap and readily available Iron complex, $Fe(hmds)_2$, for the trimerization of acetylenes, using for the first time a reducing agent-free protocol.

Chapter 1

The use of $HSiCl_3$ as reducing agent[2] for C=N double bonds, in combination with a Lewis Base (LB) (Scheme a) is well known, since its discovery by Matsumura, in 2001[3].

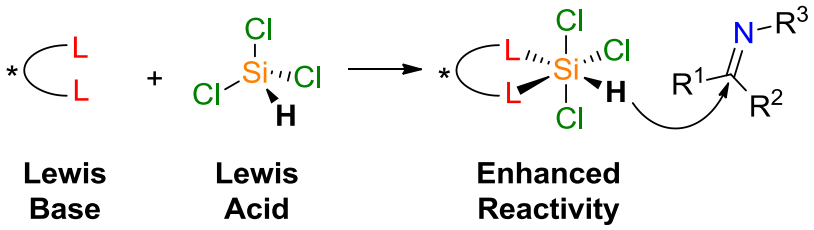

Scheme a

Different catalysts are active in this type of reduction, in particular formyl and picolinic derivatives. In the first case, two carboxyamide groups are able to activate the $HSiCl_3$ trough coordination, while in the second class the amide residue, typically in combination with a pyridine unit, is responsible for the chemical activation of the reducing agent (Figure a).

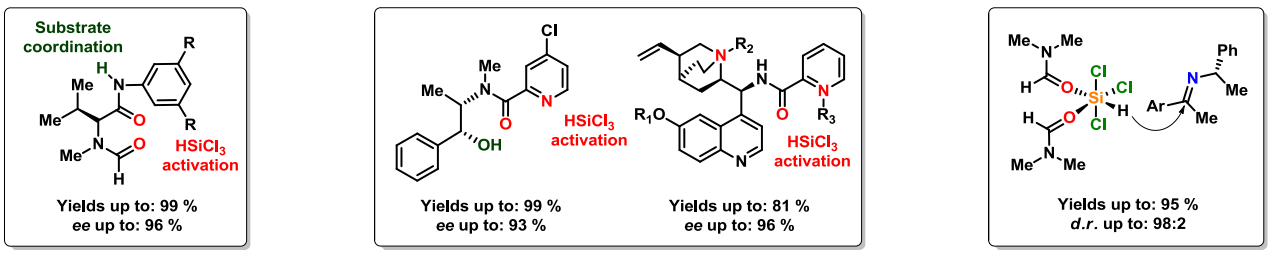

Figure a

Our group is from a long time interested in the development of new and effective catalysts for imines reductions[4]. However, one of the main limitation for organocatalysis is the high catalyst loading often required to guarantee high chemical efficiency. We successfully developed a very active catalyst, based on MacMillan imidazolidinone scaffold, able to work at 0.1% loading, and to promote the reaction in high yield and enantioselectivity (Figure b). This catalyst was also active in the reduction of imines bearing different substituent on the aromatic ring (yields up to 99%, *ee*s up to 98%) and of α and β imino esters.

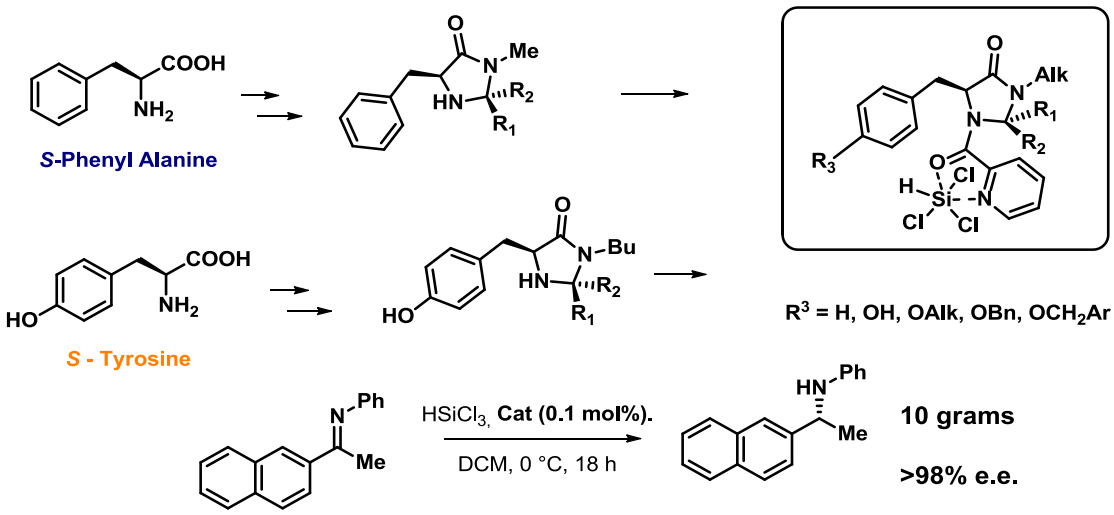

Figure b

A different approach to C=N reduction is represented by the use of a stoichiometric amount of a cheap and achiral LB, such as DMF. The use of these bases in combination with a readily available chiral auxiliary (CA), such as phenylethylamine, was already reported by our group5; in this case, high diastereomeric ratios were observed in the chiral imines reduction. We decided to use this methodology for the reduction of chiral imines which are direct precursors of APIs; moreover, we also explored for the first time the possibility of using $HSiCl_3$ under continuous flow conditions. As target compounds, different amines were selected, in particular 1-(m-hydroxyphenyl)-ethylamine, a key intermediate6 for the synthesis of different API (Figure c).

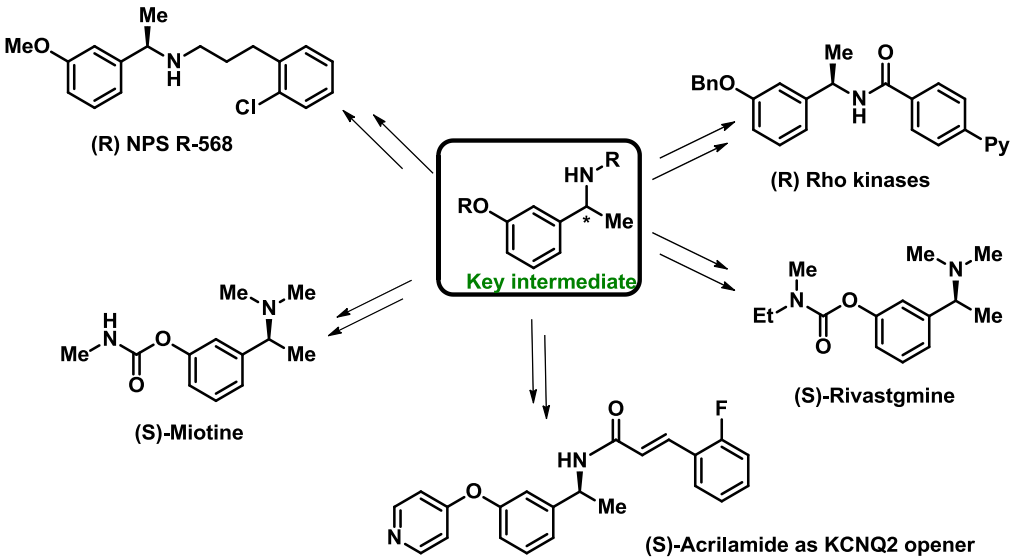

Figure c

The target compound was obtained after reduction of the chiral imine followed by removal of the CA, under continuous flow conditions, using a Pd/C catalyzed hydrogenation performed in H-Cube mini apparatus. High yields and selectivity were observed in the imine reduction, and the removal of the CA proceeded with no epimerization at the benzylic stereocenter (Scheme b).

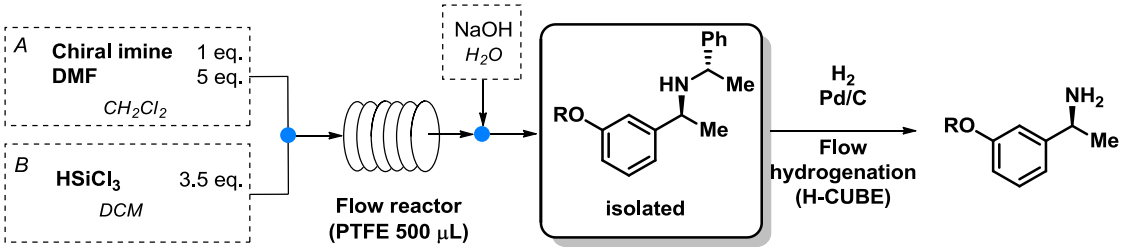

Scheme b

The main limitation of this methodology is the use of Pd/C for the removal of the CA. Looking for a chiral auxiliary that could be removed without the use of a noble metal, we explored the preparation of **Rasagiline** and **Tamsulosin**[7], also in this case using $HSiCl_3$ under continuous flow conditions as reducing agent, in combination both with DMF and a catalytic amount of chiral LB (Figure d).

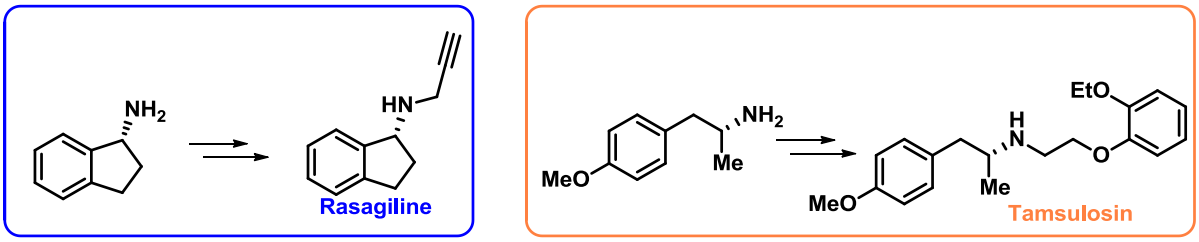

Figure d

Different CAs were tested, but the most effective ones were (*R*)-4-Methoxy-α-methylbenzylamine and (*R*)-2-Methyl-2-propanesulfinamide, both of them removable without the presence of metal catalysts[8]. The first one was very effective for the preparation of **Rasagiline**, while the second one was employed for the preparation of the chiral amine precursor of **Tamsulosin** (Scheme c).

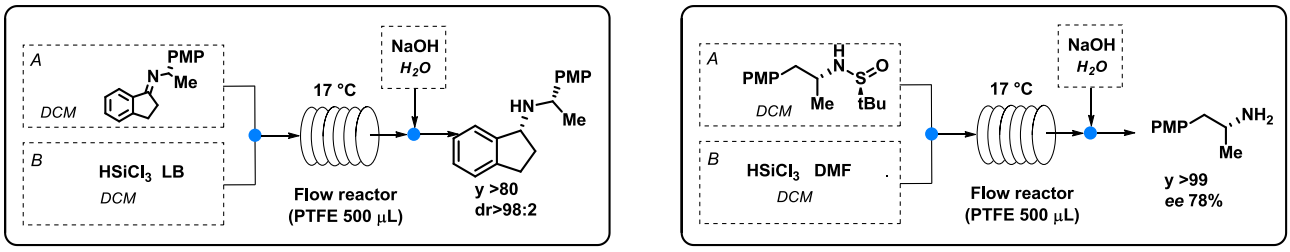

Scheme c

Chapter 2

In the development of the synthesis of APIs in 3D-printed reactors[9], we focused our attention on the preparation of chiral amino alcohols, key building blocks in organic synthesis and important biologically active compounds (Figure e).

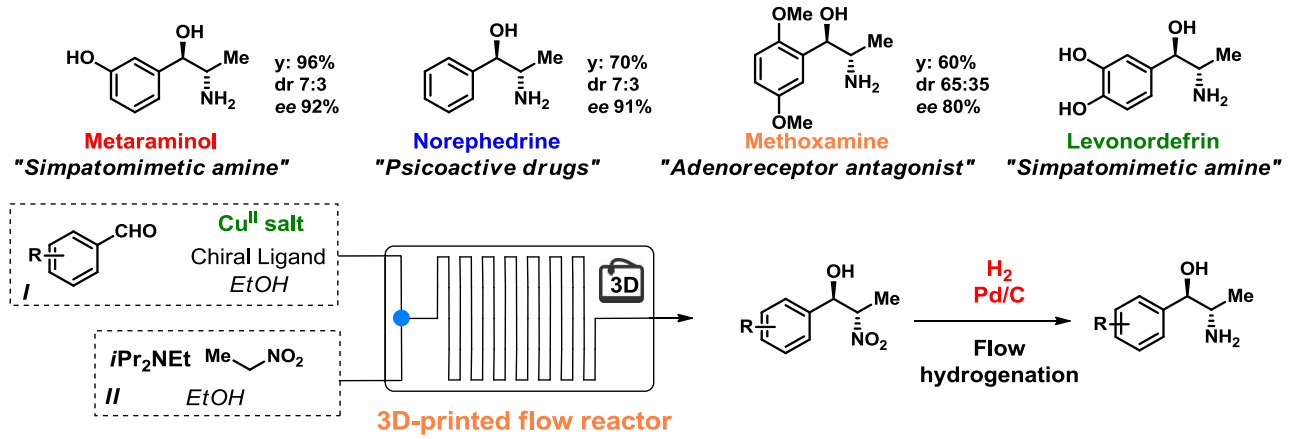

Figure e

The synthesis of these compounds is straightforward, and it can be accomplished through a copper catalyzed stereoselective nitro-aldol reaction performed in a 3D-printed reactor, followed by

a Pd catalyzed hydrogenation of the nitro group. Mesoreactors of different materials, channel size and dimension were printed and successfully used in the stereoselective catalytic Henry reaction. High yields, diasteroselectivities and enantioselectivities were observed in the preparation of the target compounds. In addition, an all-in-flow methodology was developed in order to further optimize the preparation of these amino alcohols (Scheme d).

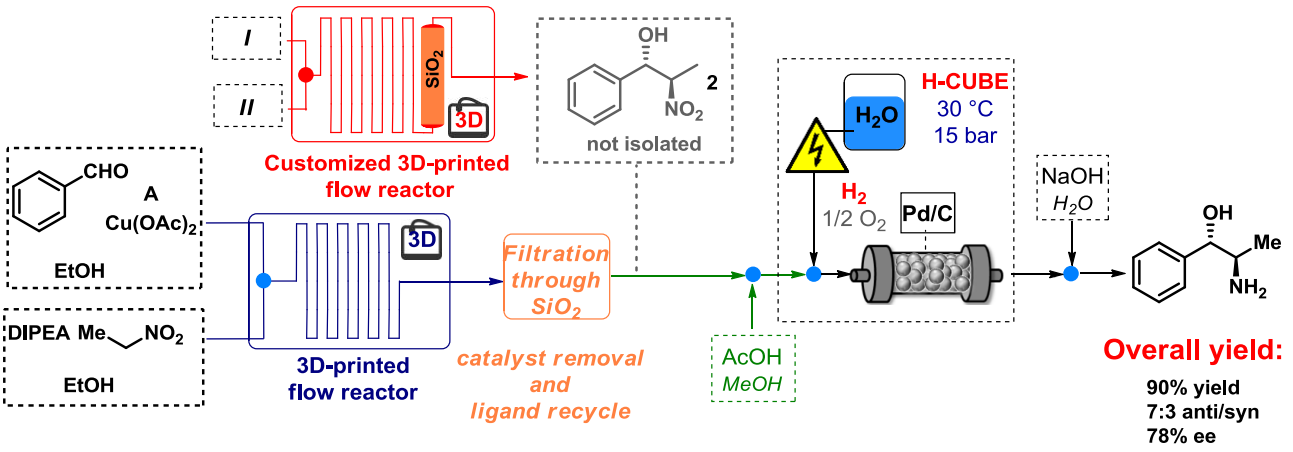

Scheme d

Chapter 3

Regarding the use of iron based catalysts, two different solutions were explored: the use of a Knolker-type Fe^0 complex for chiral imines reduction[10], and the use of $Fe(hmds)_2$ for alkyne trimerization. Due to space limitation, only the use of $Fe(hmds)_2$ will be discussed. The replacement of noble metal catalysts[11] with an earth abundant one, is one of the most challenging goal of the researchers. During my PhD, I spent six months in the laboratories of professor Axel Jacobi in Regensburg's university, where we explored metal catalyzed [2+2+2] cycloadditions[12] of alkynes, a useful synthetic tool for the preparation of substituted aromatic rings[13]. Different transition metals could be used to catalyze alkynes trimerization (e.g. Ru[14], Rh[15], Co[16], Ir[17], Ni[18], Pd[19], Ti[20], Mn[21] and Fe). The development of such synthetic methodology using earth abundant and non-toxic transition metals (Fe[22] and Mn) is a crucial goal in the academic field. Different examples of iron catalyzed trimerization of alkynes have already been reported, however these systems are usually characterized by the presence of a stoichiometric reducing agent for the initial reduction of Fe(II) to Fe(0) or/and harsh reaction conditions (high temperature, long reaction time, high catalyst loading). The first iron (carbonyl) catalyst active in alkynes trimerization was reported by Hübel in 1960[23]. Okamoto and co-workers[24] developed a system, for the intramolecular [2+2+2] cyclization of alkynes using a catalytic amount of Fe(II) and Fe(III) chloride, NHC as ligand, in the presence of zinc powder as reducing agent. Fürstner and co-workers[25] used a well defined Fe(I) ferrate complex for the alkyne trimerization, using high temperature. Iron bis(imino) pyridine complex were successfully applied in combination with zinc dust and ZnI_2 for terminal alkynes

trimerization by Liu[26]. Also, indole containing molecules could be prepared using this methodology as reported by Goswami[27]. Recently, a well defined heteroleptic two-coordinate iron(I) complex was reported by Tilley and co-workers;[28] moreover, heterocyclic rings could be successfully created using iron catalysts[29]. Recently the group of professor Jacobi demonstrated the possibility of using iron(II) bis(1,1,1,3,3,3-hexamethyl-disilazan-2-ide), $Fe(hmds)_2$,[30] activated by various reductants, as very active catalyst for alkenes hydrogenations[31]. There are several reports on the coordination chemistry of $Fe(hmds)_2$ in the presence of various ligands, but only very few catalytic applications have been demonstrated[32].[20] The reactivity of this complex was further explored, in particular its use in alkynes trimerization reactions. For the first time we were able to use $Fe(hmds)_2$ in absence of any reducing agent for the trimerization of alkynes. Different aromatic substituents were successfully tested, and high yields (up to 99%) and complete selectivity towards the 1,2,4 isomer were always observed (Scheme e).

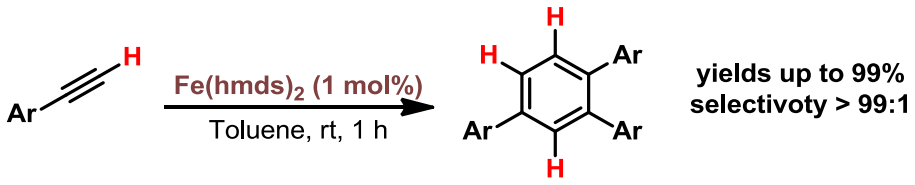

Scheme e

Also, alkyl substituted alkynes were reactive in the 2+2+2 cyclotrimerizations (Scheme f).

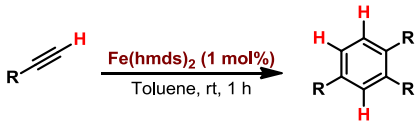

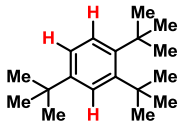
Yield: 80 %
95:5

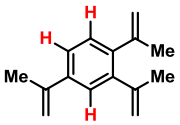
Yield: 73 %
99:1

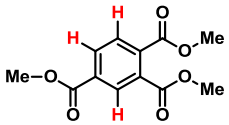
Yield: 69 %
99:1

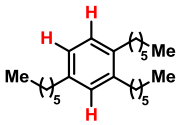
Yield: 92 %
98:2

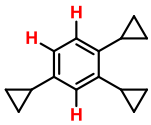
Yield: 60 %
60:40

Scheme f

General Introduction

Brief introduction to pharmaceutical industry

The major aim of chemistry should be the increasing of life expectation and its quality. Since the development of the modern medicine the duration of human life is dramatically increased, different factors played a crucial role (alimentation, migration and plagues), certainly the contribution of the pharmaceutical industry is remarkable, since its birth and the development through the XX century. (Figure 0-1)

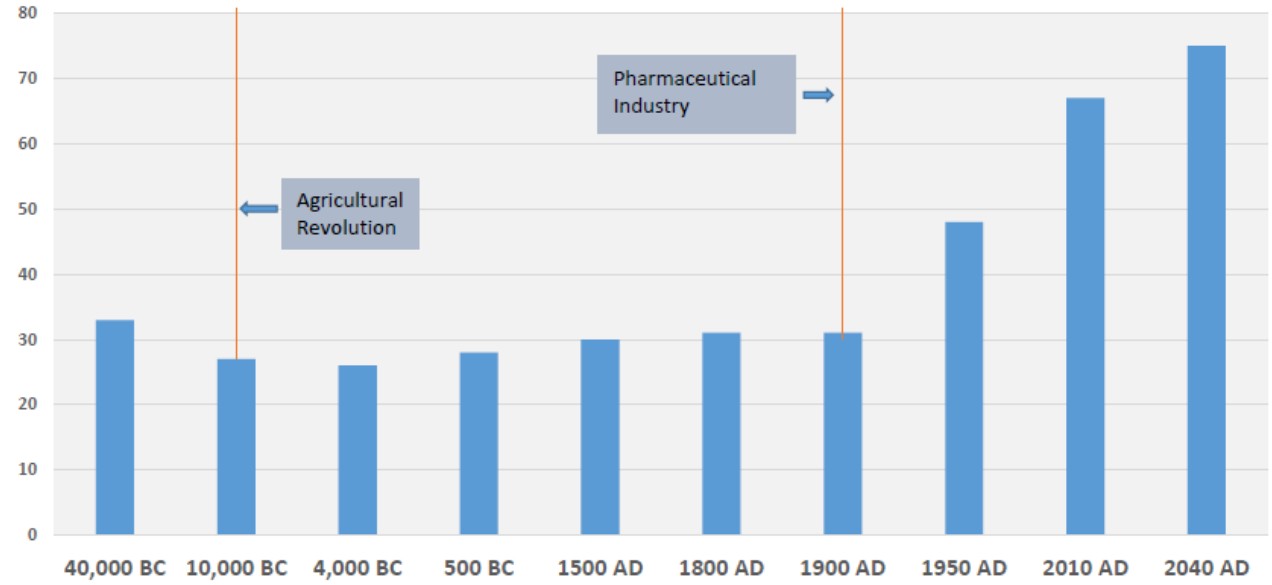

Figure 0-1[33]

The born of modern pharmaceutical industry coincides within the first commercialization of natural products, as drugs, in the first half of the 19th century; Morphine was sold as a pain killer (Merck in 1827) and Quinine (produced in Paris from the Cinchona bark in1820) was used for the treatment of Malaria during the colonization of Africa. It is remarkable to note that some of them are still on the market nowadays. Another milestone for pharmaceutical industry coincides with the first synthetic analgesics, commercialized from Hoechst Pharma in 1880 (Antipyrine and Amidopyrine), followed by Bayer with phenacetin[34]. (Figure 0-2)

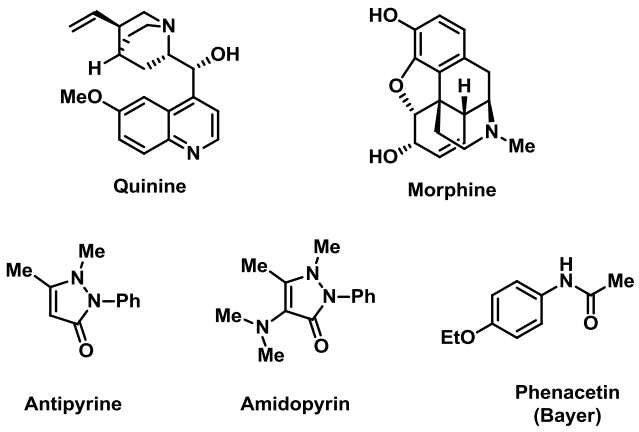

Figure 0-2

In 1898 Bayer lunched the first blockbuster drug; during the summer, an 18 years old student, prepared synthetic Aspirine for the first time; this breakthrough was followed by the discovery and commercialization of different drugs in a short period of time: The slipping pills Veronal, (1902, Emily Fisher), the first synthetic local anesthetic Procaine (Alfred Einhorn, 1905). (Figure 0-3)

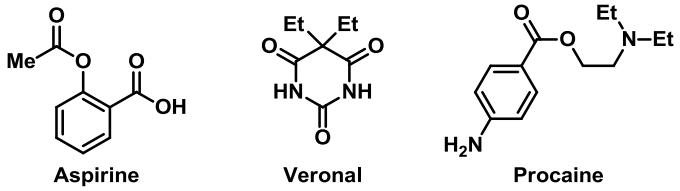

Figure 0-3

In the first years of the 20th century there is also the creation of the first multinational company indeed, Bayer bought "*Hudson river aniline and color co."* and the new world of multinational pharmaceutical companies has started. Traveling through the history and the development of the pharmaceutical industry is compulsory to cite the role of the antibacterial substances. In 1935 the first antibiotic, Prontosil, was prepared and sold by Bayer; this compound plays a crucial role in modern history, saving the life of common and powerful people, such as Franklin D. Roosevelt's son (1936) and Winston Churchill (1937). However, the first blockbuster antibiotic drugs, Penicillin, was produced on large scale, after two years of development in 1942, helping in saving the life of wounded soldiers during the second world war. The low price of this compound (15 $/Kg in the developed world) lead to the abuse of this antibiotic and to the resulting resistance. Different type families of antibiotic were developed, however probably the most powerful and promising family is the cefalosporine one. (Figure 0-4)

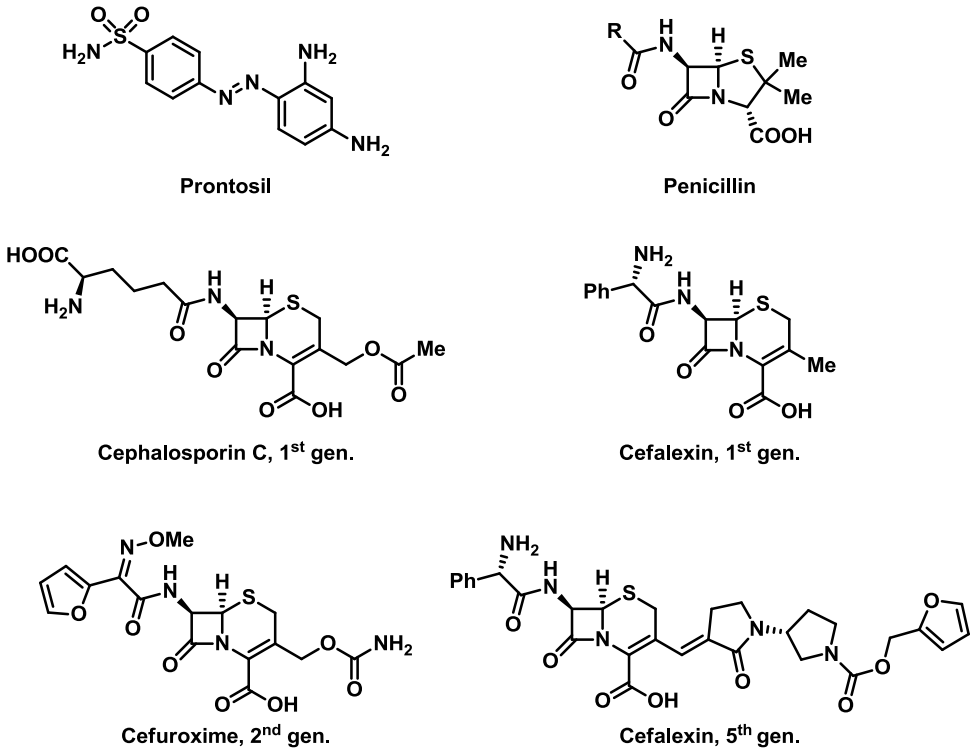

Figure 0-4

The years between 1950 and 1965 are called the Golden era of the pharmaceutical industry, an enormous amount of new drugs were discovered and commercialized in few years; not only antibiotics but also Cortison (1949, anti-rheumatoid and other inflammatory disease), Chloropyrazine (1952, tranquilizer), Mercaptopurine (1953, used against leukemia), Diazepam (1962, anxiolytic), Ibuprofen (1964,first non steroids anti-inflammatory drug), Propranolol (1965, anti-arrhythmic) and the life style changer drug Norethisterone, the pill, prepared for the first time in Palo alto California in 1951 and marked 6 years later under the name of Nortulin. (Figure 0-5).

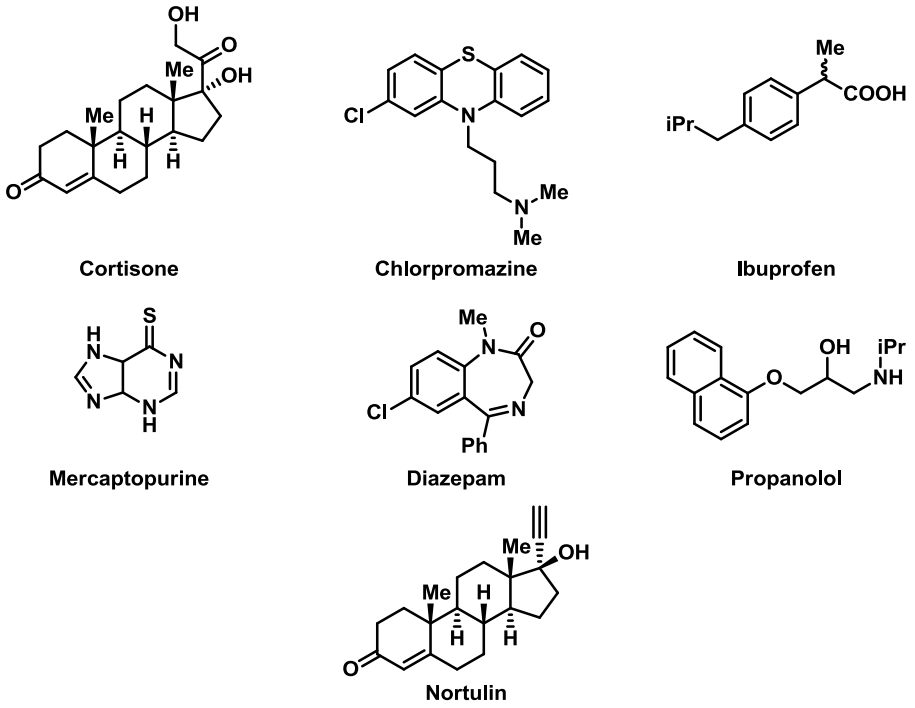

Figure 0-5

The golden age dramatically ended with the Thalidomide disaster. In 1958 the drug was marketed by Grünenthal Chemie, as a sleeping pill for pregnant women in Europe (Figure 0-6); the FDA, however in 1960 refused the approval for the U.S. market due to “insufficiency of safety”. In 1961, 10000 children born with deformations, and it was lately discovered that one of the two enantiomer was Teratogenic; in 1962 the drug was finally retired from the market. This tragedy is often reported as example in favor of the development and commercialization of enantiopure drugs. Without doubt an enantiopure drug is better compared to the racemate (see following paragraph for more details). However, as demonstrated by Testa and co-workers[35], both by in vivo and in vitro studies, the acid proton on the stereogenic center of Thalidomide is unstable and lead to the racemization of the compound; hence, selling the thalidomide as an enantiopure compound would not have avoided the disaster.

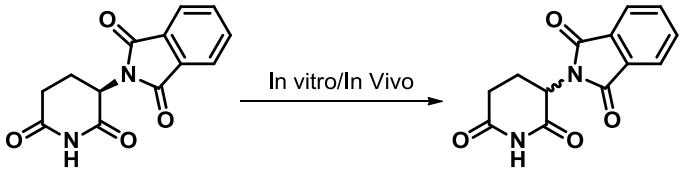

Figure 0-6

After this tragedy, the rate of the approval for the new drugs decreased by 50 % (between the 1965-1969); in the same years the FDA published the first guideline for good manufacturing practice (GMP) (1963) and a complete description of the trials necessary in order to get the drug approved for the US market. The time necessary for the commercialization of the drug rose rapidly from 2 years in 1940-1950 to 10 years in 1970, the longer period required for the approval was during 80's, up to 13 years for a new drug. During these 15-20 years the number of new approved dropped down. The regulatory body recognized that a longer period of time was a damage also for the patients. Some modifications on the guidelines were introduced such as: Faster approval for drugs against life threatened disease and elongation of patent protection up to 20 years. These changes lead to a 10 year of waiting period between the drug discovery and the drug commercialization.

Chiral drugs, regulation, and strategies

"And I should not I spare Nineveh, that great city, wherein and more than sixscore thousand person that cannot discern between their right hand and their left hand; and also, much cattle"[36]

Since the rationalization of the molecular recognition in key events for the drugs action[37], a new focus on the development and the commercialization of enantiopure drug has become interest for the pharmaceutical industry. In the second part of 1980 the so called "rediscovery of stereochemistry" started, influenced by the discovery of the different bioavailability, pharmacokinetics, and adsorption properties of two enantiomer of the same drug. This is due chiral and extremely selective enzymes present in the human body, that are influencing all the major aspects of the drug response and adsorption. Between 1987 and 1992 the guideline of FDA and the other regulatory agencies clarified that the commercialization of a defined stereoisomer of a drug was better than the commercialization of the mixture of stereoisomers[38].

Different advantages are endemic in the commercialization of a single enantiomer of an active pharmaceutical ingredient API; considering a racemic mixture, 3 different scenarios could be possible[39]:

1- Only one enantiomer is active, and the other is completely inactive.

2- One enantiomer is active towards the selected target, and the other one is toxic.

3- One enantiomer is active towards the selected target, and the other one cause interaction in drugs behavior.

Hence the commercialization of a pure enantiomer of the drug lead to a lower toxicity, reducing the total dose of the compound, and gave simpler dose-response relationship. The production of single

enantiomer drugs has been increasing enormously in the last 30 years, and at the present new drugs are directly developed as a single enantiomer. (Figure 0-7[40])

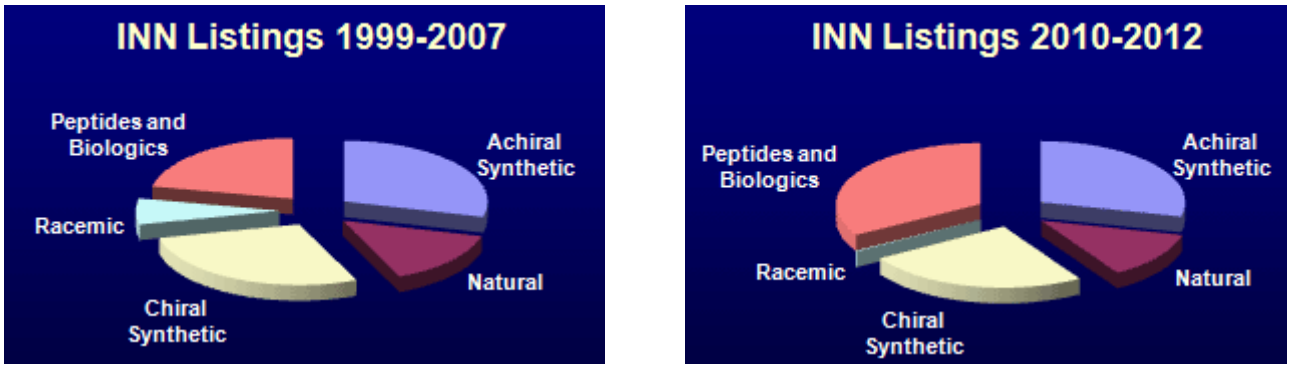

Figure 0-7

A phenomenon that is quite relevant in industry is the rediscovery of one enantiomer of a previously commercialize racemic mixture[41], this is called “chiral switches”. Some compounds showed different activities if taken as single-enantiomer drugs respect to the racemic mixture; this strategy was used by the originator of the drug in order to extended the patent‘s life.

During the commercialization of a new drug, a complete structure elucidation, absolute stereochemistry, and methods for the detection of the undesired stereoisomer are required for the drug approval

Different strategies could be applied to the preparation of the selected chiral API, depending on the technology mastered by the company:

1- Resolution of racemic mixtures

2- The use of chiral auxiliaries

3- The use of chiral catalysts

4- Separation of the two enantiomers

5- The use of enzymes and biocatalysts.

All these techniques could be used in principle but there are some drawbacks: a method that is for example, the resolution of racemic mixture (still largely applied in industry) lead at least to the loss of 50% of the reaction outcome, with a huge impact on the environment. One of the aim of the academic research is the development of sustainable and efficient technique to synthesize enantiopure/enantioenriched API; different options are possible such as the use of more efficient and greener catalysts(organocatalysis, iron, manganese) and flow chemistry combined with enabling technologies.

The regulatory aspect

By taking a closer look to the companies that are producing the API for the market, we can identify mainly three different categories:

The innovative pharmaceutical companies: they are the first to develop a new drug, to afford the huge cost linked to trials and approval process, to face the high rate of failures (less than 10% of the drugs reach the market). In this companies, the IP department has a great importance, they could build or use specific facilities/technologies for a targeted product. These companies have the resources and the time to perform complete toxicologic screen on the impurity profile of the final product.

The generics APIs producers: these companies start to commercialize the drug when the patent has expired, hence their main target is to produce a competitive product in terms of price. The target quality of the compound is referenced to the drug already on the marker, however since usually these companies have no time and resources for the complete toxicologic screen of the impurity profile on the final drug, they aim to produce a purer product compare to the generator. Typically, they have highly versatile factories since the market for the generic API is really dynamic.

The customer synthesis provider: these companies are devoted to custom synthesis and to the preparation of key intermediate. The production of intermediates require complete flexibility on the production in terms of machinery and multi-purpose equipment, speed is the key for these companies.

All these companies have different goals and objective. However, each one must follow the rules and the guidelines of the regulatory agencies in order to obtain the approval for their API (or advanced intermediates) into the market.

The definition of an API according to the World Health Organization is: "active pharmaceutical ingredient (API) Any substance or combination of substances used in a finished pharmaceutical product (FPP), intended to furnish pharmacological activity or to otherwise have direct effect in the diagnosis, cure, mitigation, treatment or prevention of disease, or to have direct effect in restoring, correcting, or modifying physiological functions in human beings."

In order to be commercialized the API must be **effective** against the targeted disease, and have to be clearly **safe** for the patient. Two actors play a crucial role in the APIs commercialization and registration: the *pharma companies*, and the *regulatory agencies*. There are different regulatory agencies (FDA, AIFA, EMEA, FMDA, swiss medic); in particular the agencies responsible for the registration of an API are two, the one from the country of production and the one for the country of destination.

In sight of a global compatibility, a harmonized guideline was developed; in order to obtain the registration of pharmaceutical compounds for human use (ICH guidelines[42]) in the mayor world market (USA, Europe and Japan).

Four main areas are covered by the ICH Guidelines:

Quality: *stability studies*, defining relevant thresholds for *impurities testing* and a more flexible approach to pharmaceutical quality based on *Good Manufacturing Practice (GMP)*.

Efficacy: heading is concerned with the *design, conduct, safety and reporting of clinical trials.*

Safety: comprehensive set of *safety Guidelines* to uncover potential risks like *carcinogenicity, genotoxicity and reprotoxicity.*

Multidisciplinary: cross-cutting topics which do not fit uniquely into one of the Quality, Safety, and Efficacy categories.

The attention will be now focused on the quality, evaluating the different aspects that must be taken into account for the production of a high-quality API.

According to the ICH guidelines, the quality of the API is not only related to the analysis on the final product, but all the *productive process steps* are crucial for the API's final quality definition. In order to meet the specifics requested for the registration and the following commercialization of the API, it is crucial to decide when the GMP should be applied during the productive process. (Table 0-1)

Type of Manufacturing	Application of the GMP (yellow) in the manufacturing of an API				
Chemical	Production of API stating material	Introduction of the API starting material into the process	Production of intermediates	Isolation and purification	Physical processing and packaging

Table 0-1

The GMP manipulation starts when a clearly identifiable API starting material is insert into the productive process.

The guideline definition of API starting material: "Is a raw material, intermediate, or an API that is used in the production of an API and that is incorporated as a significant structural fragment into the structure of the API. An API Starting Material can be an article of commerce, a material purchased from one or more suppliers under contract or commercial agreement, or produced in-house. API Starting Materials normally have defined chemical properties and structure.". From the introduction of the API starting material into the process, all the operation and all the intermediates must be run under GMP.

GMP required a dedicated complete track of all the analysis related to the product and to the intermediates, and the identification of the process key parameters to assure constant product quality. Moreover, the guidance also describes all the aspect that is necessary to control such as:

Quality management: the responsibility for production activities, internal audit and quality control.

Personal: the qualification required by the personnel, the grade of training and education.

Building characteristics: design, utilities, water, containment, lighting, sewage and sanitation and maintenance.
Process equipment: the design, construction, maintenance and cleaning of the process machinery, the calibration and the data storage.
Material Management: Quarantine, storage, sampling and testing procedures are required.
Documentation and Records: all the documentation should be prepared, validated and store.
Production and in process control: production operations, time limits, in process sampling and control, contamination control.
Packaging and identification labelling of APIs and intermediates: packaging material, label control, packing and labeling operation are needed.
Storage and distribution
Laboratory controls: General control, testing intermediates and APIs, validation of analytical procedures, analysis certificates, stability over time and temperature of the API.
Validation: validation policy, validation documentation, qualification, process validation, reviews of the validated systems, validation of analytical methods.
Rejection and reuse of the material: reprocessing, reworking, recovery of material and solvents, returns.
Complains and recall
APIs for clinical trials: quality, facilities, control of raw materials, production, validation, changes, laboratory control, documentation.

In this complex scenario, one of the main actor (FDA) is strongly pushing towards the implementation of new technologies for the API production. In particular the regulatory body focused its attention on flow chemistry. According to the FDA different problems, present in the batch based manufacturing could be tacked such as: the lack of flexibility in the volumes of production in case of pandemic events, and the gap between the customers and the producer.

In both cases a flow manufacturing could help, in case of a continuous flow process is easier to rapidly increase the quantity of the product (in case of pandemic events), in addition to that a flow plant is usually small compared to a vessel based one and could be place closer to the final users of the API. To better understand the power of this technology a short introduction is reported in the following paragraphs

Introduction to flow chemistry

As organic chemists, we are usually prone to set up a reaction using batch technique and performing step by step a series of different operations such as: Adding solvent, reagents and eventually the catalyst, in the same reaction vessel stirring the reaction mixture for the desired time at the selected temperature; and subsequently proceeding with the quench, purification, and

analysis of the product. The main advantages of this technology are its extremely versatility and the multi-purpose ability of the single machinery used for those operation. (Figure 0-8[43]) These advantages and a know-how for the scale up of the process led to a great predominance of the batch process for the production of APIs.

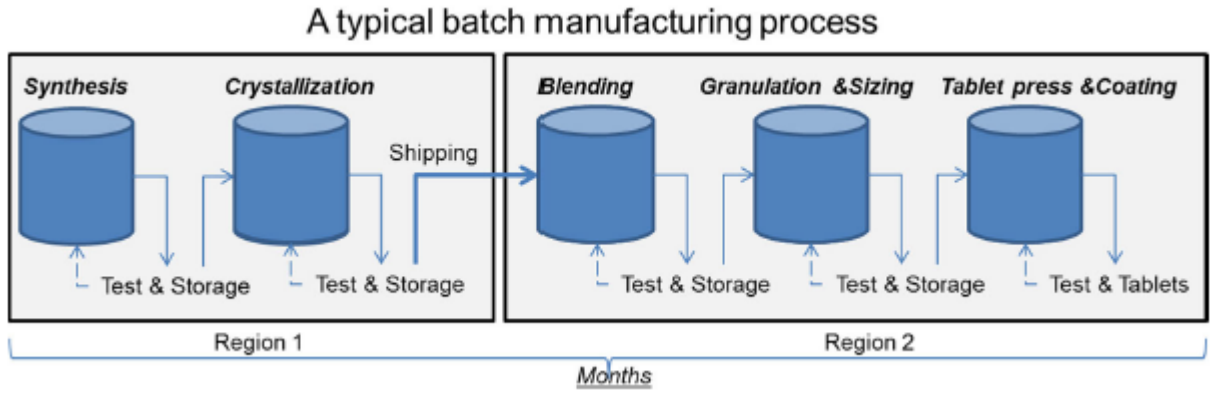

Figure 0-8

The traditional batch chemistry presents some disadvantages, such as: slow temperature control, not always efficient heat and mass transfer. In particular, some transformations could be very dangerous or "forbidden" for a plant scale using standard batch procedures. (Azide, Oxygen, aliphatic nitro compounds). An alternative to batch process is a flow process, where the reagents are continuously pumped through a series of tubes (reactors) in order to perform in a series of different continuous operations. (Figure 0-9[43])

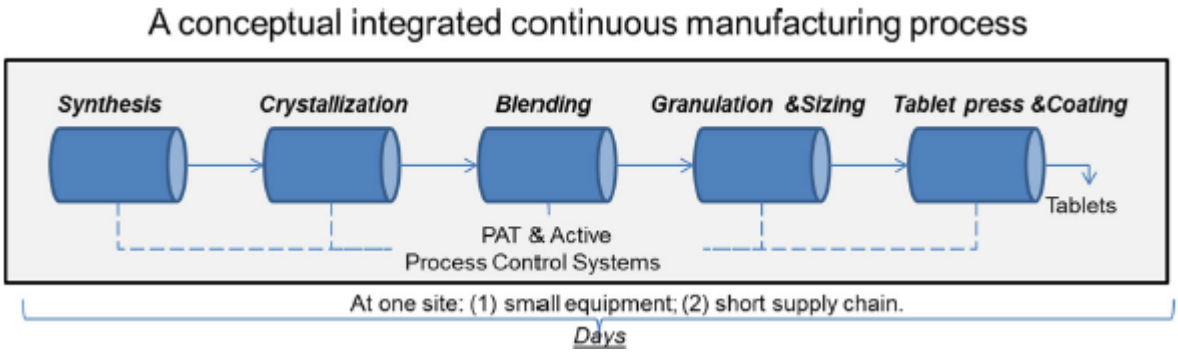

Figure 0-9

Flow devices are usually coiled tubing or chip-based components, that lead to a higher surface/volume ratio compared to a standard batch reactor. The direct result is a better heat and mass transfer compared to the batch process, almost absolute temperature control that reduces the formation of byproducts due to possible hot-spots present in the standard reaction vessel. Not only temperature, but also the reaction time could be strictly controlled, by modulating the flow rate, in function of the volume of the reactor. The smaller volume of a standard flow reactor and the close environment lead to benefits regarding safety issues; toxic, hazardous or explosives reagents could be produced in situ and directly used, thus reducing the risks for the operator, as

brilliantly showed by Kappe et al: they generated dry diazomethane in situ,[44] using a tube in tube solution[45] and directly used it for esterification and alkylation reactions (Figure 0-10).

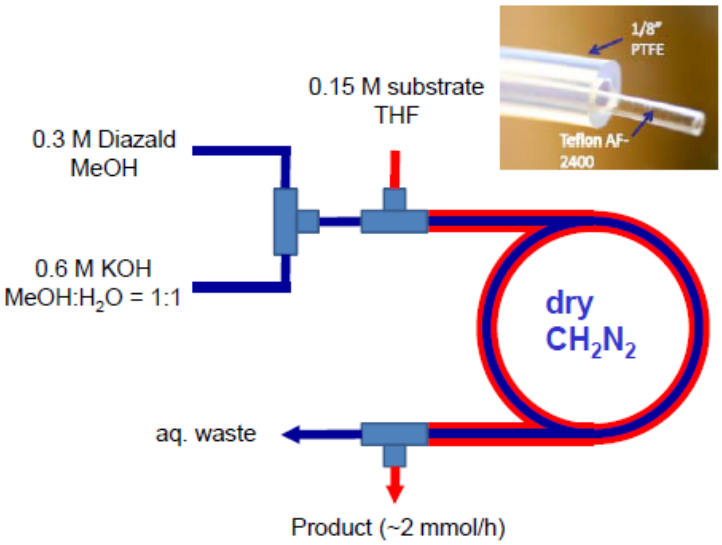

Figure 0-10

An additional advantage is the possible automatization that could be achieved by the process, with direct on-line analysis. That leads to faster screening of reaction conditions and, enhanced control on the parameters of the reaction/process leading to a maximum productivity, minimization of the waste and constant quality of the product. [46]

The main drawbacks of the flow reactors are due to their very specific set up compared with a standard batch vessel and are linked to the solubility (in case of solids precipitations blockages and leakages are possible) and the physical state of the reagents (solid, liquid, gases). In every reaction it is of course necessary to carefully evaluate the thermodynamic, the kinetic, the mixing, the mass and heat transfer. On the market, different systems are present in order to meet the requirements of the users: the reactors could be made of stainless steel hastelloy, copper, PEEK, PTFE; also, the volume of the reactor is flexible, from 1 µl to several liters.

One of the main advantage of a flow system is the easier possibility of scaling up, compared with standard batch chemistry. In the case of a flow process the scaling up usually requires a minimal re-optimization and in principle two different strategies could be used: The standard scaling up with a bigger reactor size, or the use of different parallel flow reactors (numbering-up).

Notably the use of a heterogeneous catalyst in flow is possible, however, generally the TON of those catalytic systems are low, that led to deactivation and subsequently a quite frequent replacement of the catalyst, however different systems are available and could be successfully applied for general transformations (H-Cube Thales Nano).

In the academia, a huge interest has recently emerged towards the preparation of APIs using continuous flow techniques[47]; despite this boost, in the fine chemical industry and in particular in the pharmaceutical one the switch towards the flow chemistry is very slow and in some cases completely absence.

The reason why continuous flow technologies are rarely used in industry are copious and very complex. One possible explanation can be found in the peculiarity of the molecules that are produced by these companies.

Usually a standard synthesis is composed by 10 or more steps (sequential or convergent); moreover the commercial life of the compound is shorter compared to the standard bulk chemistry products, and in addition the production volume of the compounds is smaller compared to petrochemical and bulk chemicals all these reasons lead to the preferential selection of a small number of multi-purpose reactors that can operate in pressure and temperature control and can be used for all the reactions and steps and purification needed for the preparation of APIs.

The rapid development and lunch on the market of new modular and commercially available systems that could be used for continuous flow transformation led to the growing interest of the scientific community toward flow chemistry. The continuous manufacturing of pharmaceutical is rapidly expanding, thus becoming an alternative option for the medicinal chemists and the researcher in general.

Two leading examples to produce final drugs under continuous flow conditions were recently reported. The first one is the Aliskiren hemifumarate[48] continuous production, carried out by MIT and Novartis group (Figure 0-11). Here, the flow technology is not only related to the synthetic aspect, but all the operations (quench, phase separation, crystallizations, drying, and formulation) involved in the production of the final drug were carried out under continuous flow mode in a complete automated process. The productivity of the apparatus is impressive: with a reactor volume of 0.7 Liter, 100 g/hour API could be prepared, that means 0.8 tons/year on two different synthetic steps.

Figure 0-11.

The second example was reported by Adamo et al[49] in 2016, in MIT laboratories a platform able to prepare thousands of different liquids formulation in one day was developed (Figure 0-12). With this work the challenge of a multipurpose machinery for the synthesis of different APIs was tackled; using a complete integrated system, able not only to perform the synthesis but also all the purification steps required (crystallization) and the liquid formulate preparation. The machine has

little dimensions, comparable to a commonly used refrigerator, and it is composed by single and independent module, synthesis, in line analysis, work up, phase separations, crystallizations, in line purification and formulation of drugs in accord with FDAs standards. Four different APIs were prepared in accord with GMP practice (fluoxetine, lidocaine hydrochloride, diazepam and diphenhydramine hydrochloride). The instrument controlled by a single operator, is divided into two main sections, the upper part is dedicated to the synthesis, while the lower one is used for the purification and formulation processes.

Figure 0-12. Reconfigurable flow platform for the synthesis of drugs.

This reconfigurable apparatus, after the FDA approval, could be used for the “on demand” and “on situ” production of different APIs (humanitarian missions, military outposts, ships, and submarines). This multipurpose machinery would be more flexible and easy to use compare to a standard pilot plant; moreover, the use of liquid formulation directly after the API preparation has a reduced complexity compared with the standard tablets one.

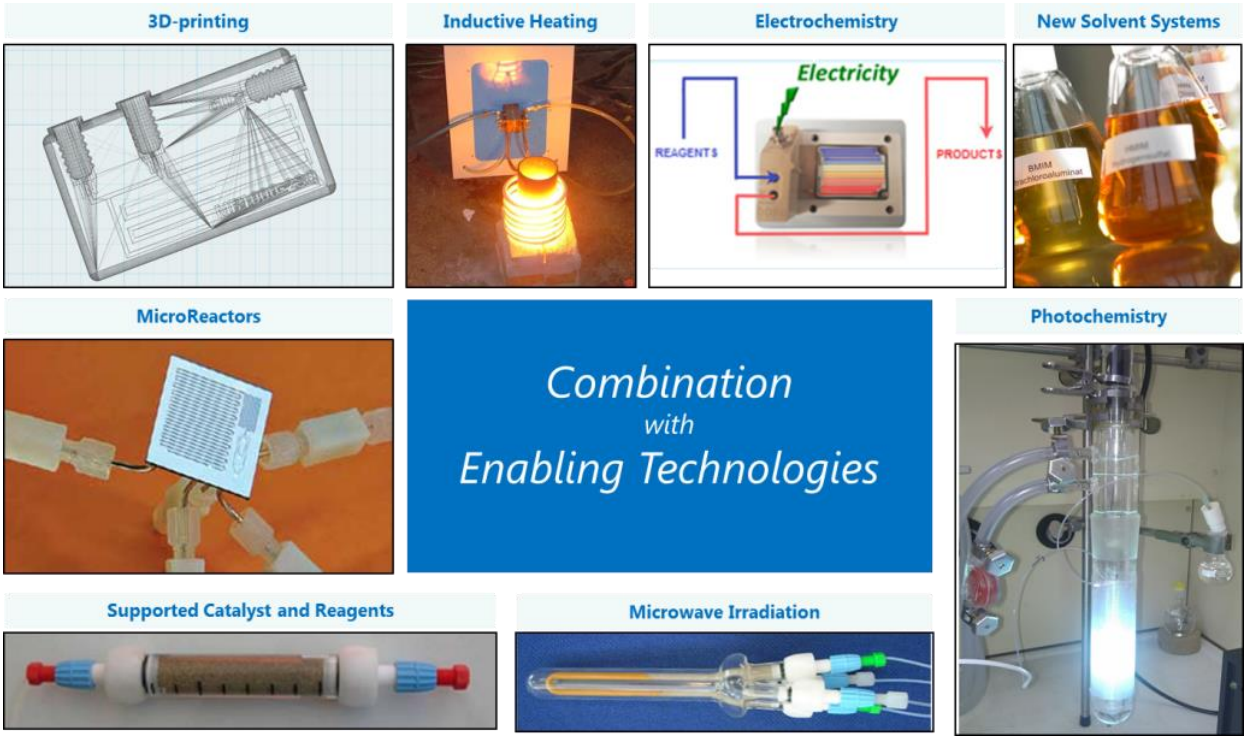

Figure 0-13. Enabling technologies generally combined to flow processes.

Flow methodologies can be used in combination with enabling technologies to boost the efficiency of the process.[50] Enabling technologies combined to continuous processes could be 3D printing, microreactor technology, microwave irradiation, supported reagents or catalysts, photochemistry, inductive heating, or new solvent systems (Figure 0-13).

Chapter 1:

Stereoselective reduction of C=N double bonds using $HSiCl_3$

The pharmaceutical industry is gradually shifting towards the production of enantiopure API, as shown in the introduction. The number of chiral amines present in the active pharmaceutical ingredient is incredibly large, moreover this class of compounds is also present in other derivates, such as agrochemicals, fragrance, and cosmetic products[51]. (Figure 1-1)

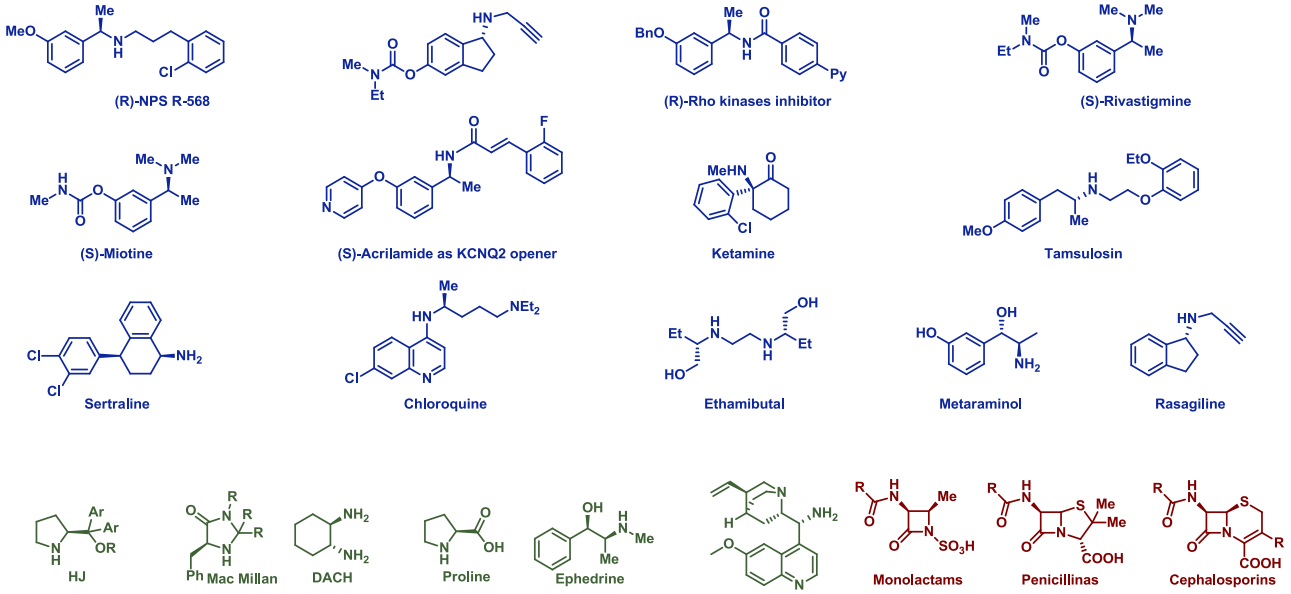

Figure 1-1

The resolution of racemic chiral amines is still one of the most applied technique in the industrial preparation of nitrogen-based chiral compounds, via the formation of diasteroisomeric salt, using chiral acids readily available from the chiral pool. However, the maximum yield in this preparation technique is, in the best case, 50%. The stereoselective reduction of C=N double bond using metal catalysts is challenging because the product itself, generated after the reduction, is a possible ligand for the metal that can interfere with the catalytic cycle. However, in the last decade, either metal base[52] or organocatalyzed[53] methodologies were successfully developed for the stereoselective reduction of imines, testimony an increased interest in this particular field of research.

In this first part of the thesis the attention will be focused on the use of a $HSiCl_3$ in combination with a chiral or achiral Lewis Base, as a reducing agent for C=N double bonds, in order to obtain APIs adopting a robust and metal free strategy solution.

$HSiCl_3$ is a cheap reducing agent, is a by-product of Silicon industry[54], and it is used to wash the pipeline to remove moisture before flowing SiH_4 for the preparation of layers of ultrapure silicon compounds. Its synthesis is quite simple and starts from very cheap starting materials such as silicon and HCl. (Figure 1-2)

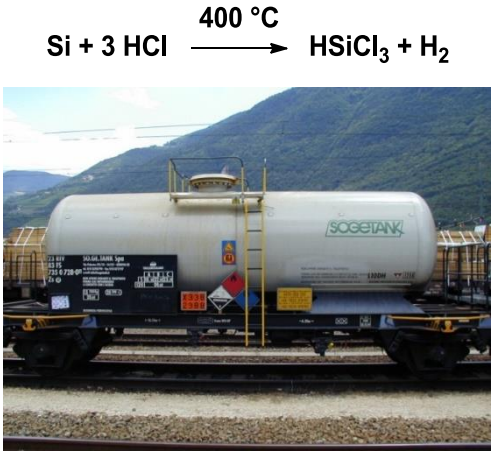

Figure 1-2

$HSiCl_3$ is sensitive to moisture, but it could be easily handled adopting standard techniques for moisture sensitive compounds. The standard work-up procedures, an aqueous basic solution ($NaHCO_3$ or NaOH) produces non-toxic inorganic salts. The hydride character of $HSiCl_3$ could be rationalized using the "*hypervalent bonding analysis*". Trichlorosilane is a weak Lewis Acid (LA) able to form a new and more reactive adduct in the presence of a Lewis Base (LB). The electron density of the LB is distributed on the ligand of the $HSiCl_3$ and, at the same time the positive charge on the silicon atom is increased, enhancing its LA character. (Figure 1-3)

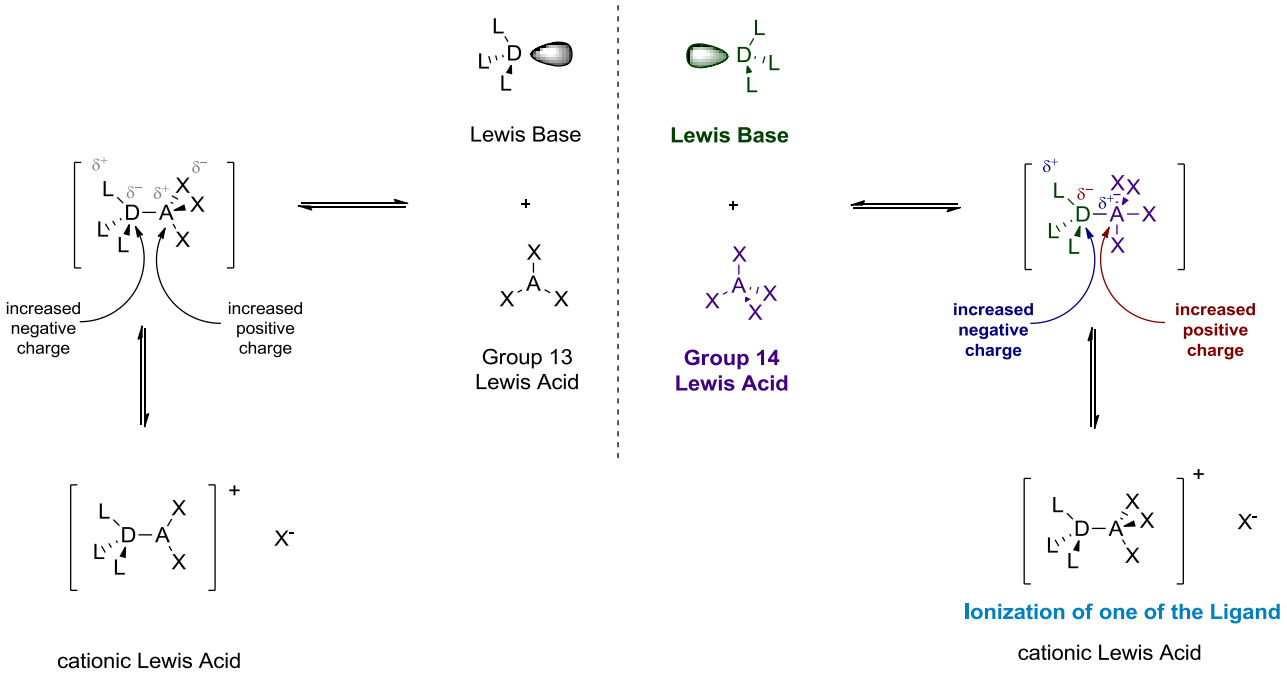

Figure 1-3

According to the hypervalent bonding analysis[2], the coordination of two LBs leads the silicon atom to the formation of hypervalent bonds (3-centers 4- electrons). The hybridization of the silicon atom changes from sp3 to sp; notably the new molecular orbitals show a reduced electron density on the silicon and the increased presence of the electrons on the ligands. The stronger is the Lewis Base

the stronger is the negative charge on the ligands, the more the hydrogen atom can act as a hydride and could be used for the reduction of C=N and C=O[55]. Figure 1-4

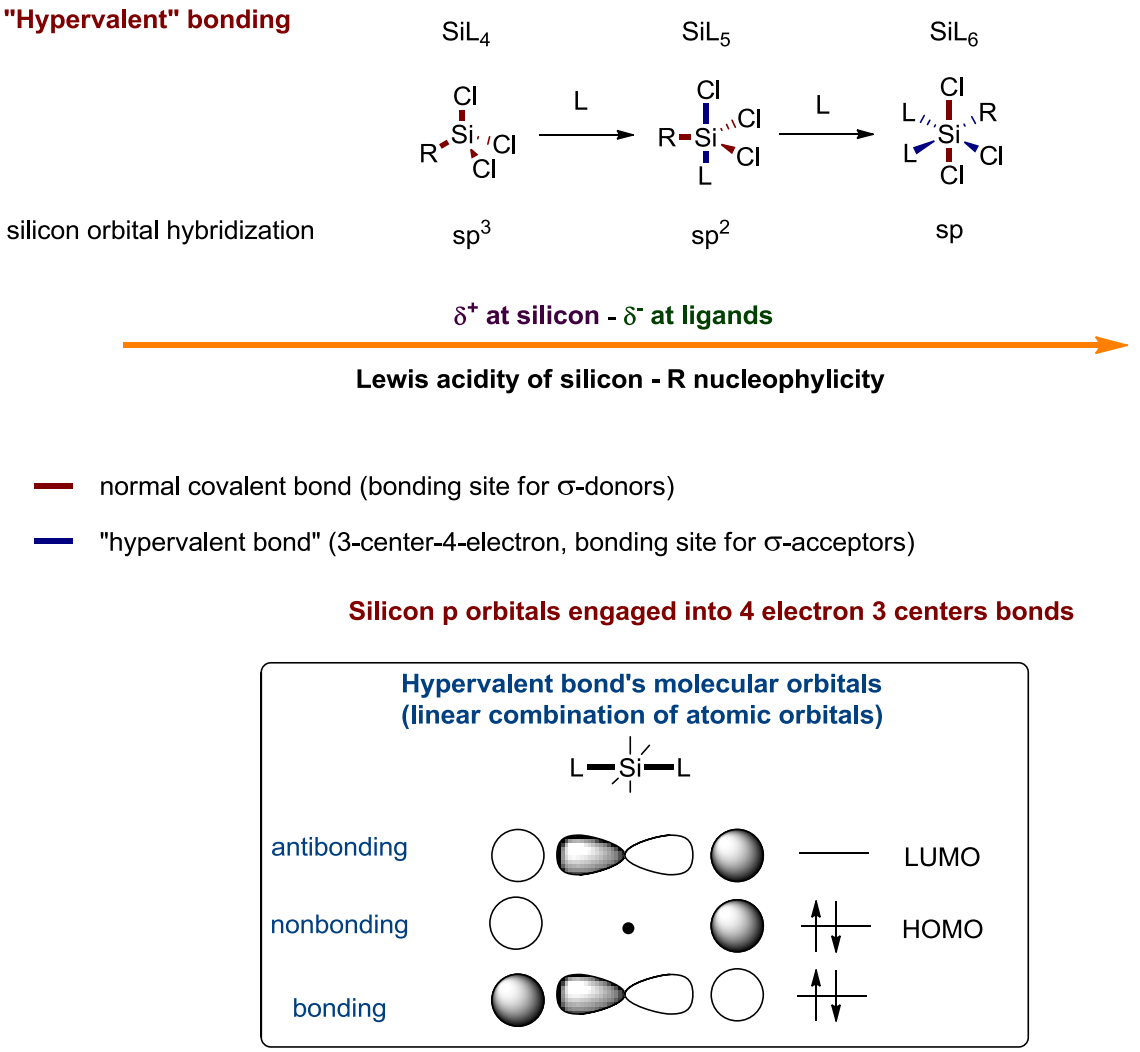

Figure 1-4: Hypervalent bonding theory, and molecular orbitals

The nucleophilicity of silicon substituents allows the delivery of the hydride into an electrophilic substrate (C=O, C=N or Michael acceptors), that could be also coordinated by the silicon atom, due to its increased Lewis Acidity. Hence, using an enantiomerically pure LB for the activation of $HSiCl_3$, it could be possible to perform stereoselective reduction of C=N double bonds. (Scheme 1-1)

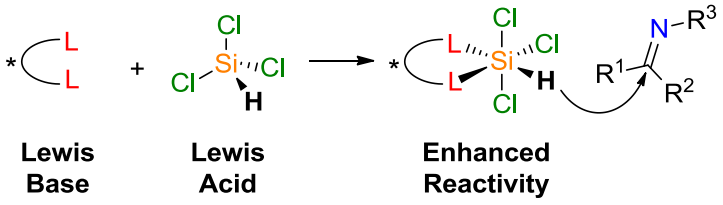

Scheme 1-1: Activation of $HSiCl_3$

Strategies for stereoselective reductions of carbonyl compounds:

In order to control the stereochemical outcome of a $HSiCl_3$-mediated reduction of carbonyl compounds two different solutions are possible: (Scheme 1-2):

1- The use of an imine bearing a chiral auxiliary, using an **achiral LB in a catalytic or stoichiometric amount.**

2- The use of a chiral Lewis base in a **catalytic** amount. Obviously, to improve the stereoselectivity of the reaction, it is also possible to employ a match couple between the chiral auxiliary and a chiral catalyst.[56].

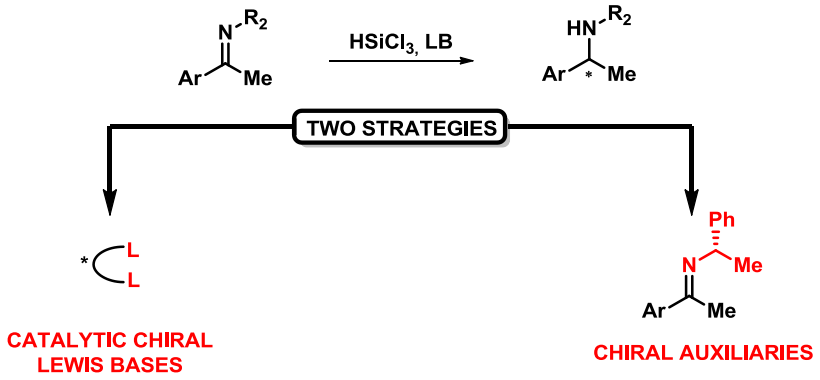

Scheme 1-2. Strategies for stereoselection control

In 1993, for the first time, the group of Kobayashi[57] reported the use of $HSiCl_3$ as a reducing agent for aldehydes, ketones and aldimines. The best Lewis Base for the transformation was DMF.

In 2010 our group[558] demonstrated that it was possible to achieve high stereocontrol in the diasteroselective reduction of ketoimines bearing simple chiral residue, commercially available in both the enantiomers, such as phenylethylamine, using $HSiCl_3$ activated by DMF (yields up to 99%, *d.r.* up to 98:2).

Chiral Lewis Bases

Different chiral ligands were developed for the stereoselective reduction of C=N double bonds using $HSiCl_3$ as a reducing agent. Usually, different LBs can be used, but it was proved that the most effective catalysts are bidentate, such as N- formyl, picolinamide and sulfoxide derivatives. Several examples of these classes are extensively reported in two reviews. [5960] In this chapter, the development of these chiral LBs will be analysed, focusing the attention on the milestone events and the catalysts developed in our laboratories.

The first organocatalyzed and stereoselective reduction with $HSiCl_3$ was reported by Matsumura in 2001[61]; using a *N*- formylprolinamide derivative, the authors demonstrated the possibility of performing a stereoselective reduction using $HSiCl_3$ even if the enantiomeric excess of the final amine was only up to 66%(Scheme 1-3). After this pioneering work, new and more efficient catalysts were developed.

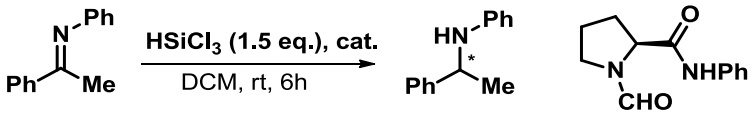

Scheme1-3. *N*-formylprolinamide as chiral Lewis base in $HSiCl_3$ reductions

After three years, the group of professor Kočovský[62] reported the use of a valine based catalyst for the reduction of ketoimines, obtaining the desired amines with *ee* up to 95% employing 10% of catalyst loading

(Scheme 1-4)

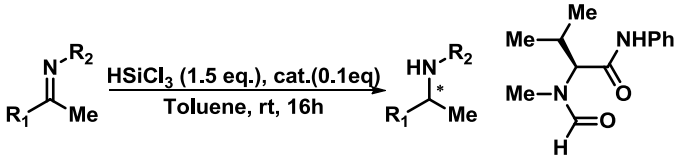

Scheme 1-4: Valine based catalyst, for efficient imines reductions

A library of different catalysts was subsequently developed, however the most performing catalyst remained the Valine based one. Two structural requirements for the catalyst were identified, a formyl moiety needed for the coordination with the silicon, the second amide coordinating the imine trough H- bonding. In addition, also π interaction with the aryl residue was proposed (Figure 1-5).

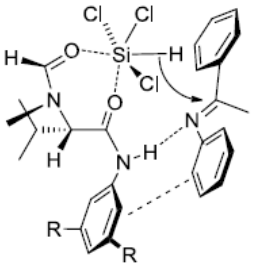

Figure1-5 Model of stereoselection for (*S*)-valine-derived organocatalysts

Meanwhile new classes of catalysts featuring a picolinamide residue, for the activation of $HSiCl_3$ have been developed.[4]

[63]

The first example was reported by Matsumura and co-workers, in 2006[64] in which pyrrolidine derivative was used for the enantioselective reduction of ketoimines, obtaining *ee* up to 80%, the authors proposed that both the hydrogen of the tertiary alcohol and the oxygen of the amide were coordinated to the silicon. (Figure 1-6)

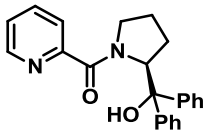

Figure 1-6. *N*-picolinic derivative, based on prolinol scaffold

The use of a picolinamide condensed with (1*R*, 2*S*)-ephedrine skeleton (Figure 1-7) was investigated by our[65] group and Zhang[66] one. The best yields and selectivity were achieved

working at -20°C, using 1 mole % of catalyst only, in two hours of reaction time, *ee* up to 95% and yield up to 90% were obtained. (Figure 1-7)

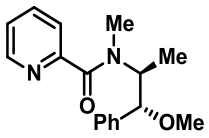

Figure 1-7. Picolinic ephedrine derivative

Because of the straightforward synthesis of these catalysts a small library was prepared and tested in catalysis[63c], the best derivatives of this class were the one bearing the 4-chloro picolinic residue. This class of catalysts was also tested in the diasteroselective reduction of chiral imines, evaluating the match and miss match couple. Diasteroselectivity up to 99:1 were obtained using the match couple and the phenyl ethyl amine as chiral auxiliary. (Scheme 1-5)

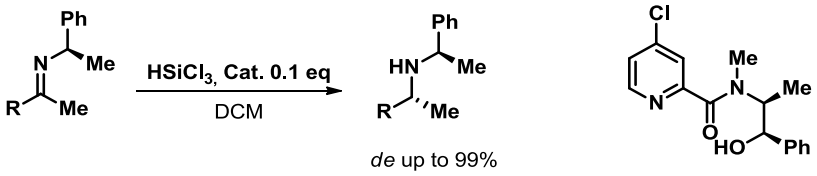

Scheme 1-5: match couple in high stereoselective chiral imines reductions

The best catalyst was also used the for reduction of β-enaminoesters[67] and α-trifluoromethyl imines[68] obtaining the desired amines in good yields and with high enantioselectivity. In addition to that, different catalysts based on the picolinamide moiety were developed in our group during the last 10 years using different chiral scaffolds. In particular 1,2 diamines[69] were used as starting material for the preparation of picolinamides, however lower level of enantioselectivity (only up to 63%) were achieved. (Figure 1-8)

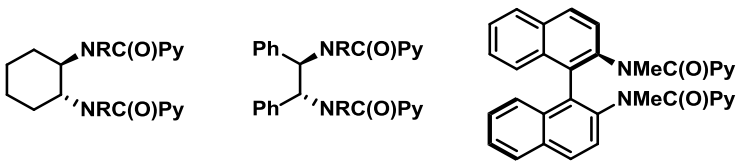

Figure 1-8: chiral picolinamides developed in our laboratories

In 2013 picolinamides and picolinesters based on the Cinchona alkaloids scaffold were developed in our laboratories in collaboration with the group of professor Anthony J. Burke of the University of Évora (PT). [70] (Figure 1-9).

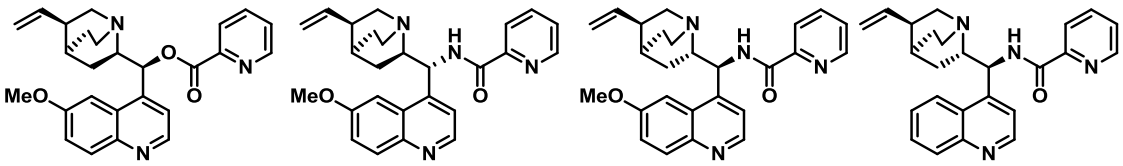

Figure 1-9: cinchona alkaloids derivatives used as chiral catalysts for imines reduction.

The catalyst bearing the ester bond was active in catalysis, however no stereoselection was observed in the imine reduction; on the other hand, using the amide derivatives it was possible to achieve high yields and *ee* up to 88%, working at -40°C with 1 mole % of catalyst loading.
The scope of the reaction included *N*-aryl alkyl- and arylketones, α-imino- and β-enaminoesters, unfortunately the reduction of α-trifluoromethyl imine proceeded with no stereocontrol.
Recently a solid supported version of these catalysts was developed[71] , the supported ones showed a similar reactivity compared to the batch one and also the same stereochemical outcome was observed

In the first part of this chapter the attention will be focused on the use, for the first time, of $HSiCl_3$ under continuous flow conditions, to perform stereoselective reductions of imines that are direct precursors of different APIs; the problem of obtaining free chiral primary amine would be faced and the use of different chiral auxiliaries will be tested. In the second part of this chapter a new class of picolinamides based on imidazolidinone scaffold will be prepared and tested in catalysis.

Stereoselective metal-free reduction of chiral imines in batch and in flow mode. A convenient strategy for the synthesis of chiral APIs.

The experimental work described in this chapter resulted in three different articles. [72]

Catalysis is one of the foundation of a green synthesis; however, when the industrial synthesis of a chiral pharmaceutical product must be planned, issues like chemical efficiency and robustness of the procedure, general applicability and economic considerations become crucially important. For these reasons, the application of many of the known chiral catalytic systems very often is not feasible and the use of inexpensive and readily available chiral auxiliaries becomes an attractive and economically competitive alternative. This holds true also for the synthesis of chiral amines,[73] that heavily relies on the diastereoselective reduction of *N*-functionalized imines with chiral, removable residues.[74]

We thought to take advantage of this approach to realize an efficient synthesis of both enantiomers of 1-(*m*-hydroxyphenyl)-ethylamine, a key intermediate for the preparation of several, valuable pharmaceutically active compounds (Scheme 1-6).

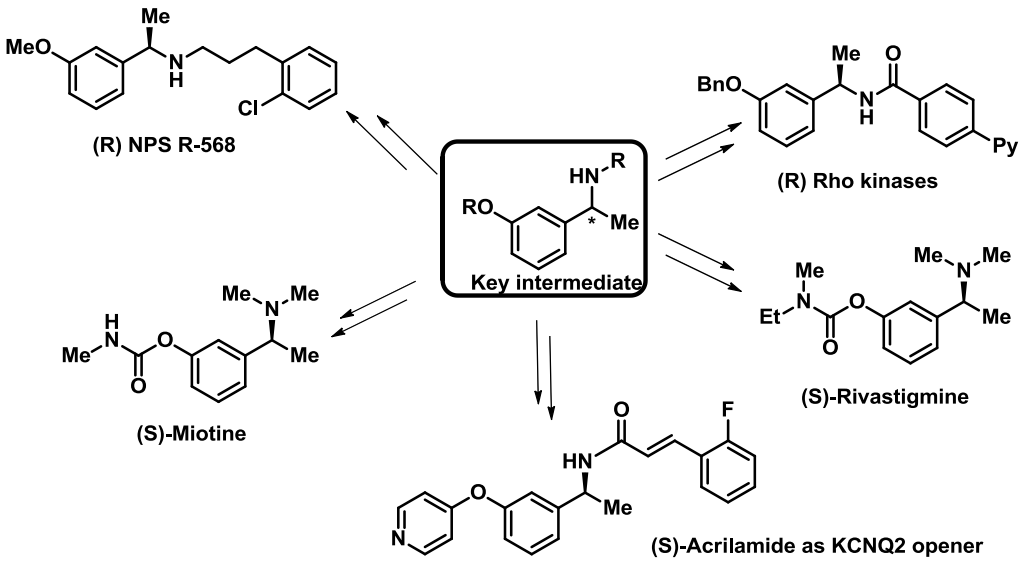

Scheme 1-6: Biologically active amines featuring the 1-(m-alcoxyphenyl)-ethylamine moiety.

Rivastigmine finds application in the treatment of mild to moderate dementia in Alzheimer's type and Parkinson diseases. Miotine, the first synthetic carbamate used clinically, is an anticholinesterase drug. Rho Kinases inhibitors have proved to be efficacious in animal models of stroke, inflammatory diseases, Alzheimer's disease, and neuropathic pain, and therefore have potential for preventing neurodegeneration and stimulating neuroregeneration in various neurological disorders. (*R*)-NPS 568 is a calcimimetic compound used in the treatment of hyperparathyroidism, while Acrylamide (*S*)-A, a potent and efficacious KCNQ2 opener, is currently under study for the treatment of neuropathic pain, including diabetic neuropathy. The importance of *N*-alkyl chiral amines in medicinal chemistry, that encompasses a large variety of compounds with different biological activity, has been recently highlighted.[75]

In this part of the thesis an efficient, metal-free reduction of imines bearing an inexpensive and easily removable chiral residue will be developed and discussed, in addition the transformation under continuous flow conditions will be presented.[76] In order to obtain the selected amino alcohols the chiral auxiliary[77] removal will be performed, in particular using an H-cube mini[78] hydrogenation system equipped with a Pd/C cartridge.

First, we studied the preparation of the direct precursor of the *R*)-NPS 568 (**1-4**) in batch. The first metal free reduction of the imine (**1-2**) proceeded with high yield and complete stereocontrol at -20°C in DCM overnight, amine **1-3** was obtained with 95% yield and 98:2 *d.r.* **.** Subsequently the removal of the chiral auxiliary was performed using Pd/C at rt for 56 hours, without observing racemization of the final chiral primary amine (**1-4**). (Scheme 1-7)

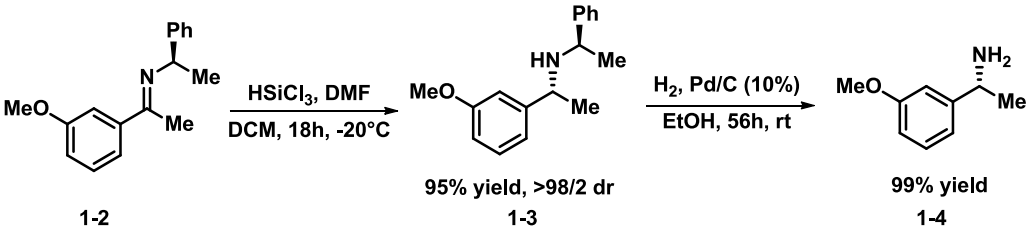

Scheme 1-7. Synthesis of (*R*)-1-(3-methoxyphenyl)-ethylamine 3, direct precursor of (R)-NPS 568.

The preparation of the key intermediate **1-1** was also explored. First the reduction of the 3-benzyloxy protected imine **1-5** was studied. (Scheme 1-8) Running the first reduction in the same condition of the 3-Methoxy derivative led to high yield and complete control of the diasteroselectivity, obtaining compound **1-6** in 91% yield and 98:2 *d.r.*.

In addition, the removal of the phenylethylamine residue and the benzyloxy ether was successfully performed using a catalytic amount of Pd/C in the presence of H_2, obtaining the desired compound in 83 % of yield after chromatographic purification[79].

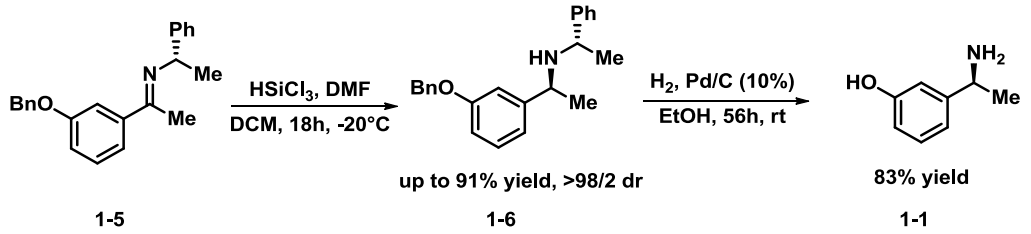

Scheme 1-8. In batch synthesis of (*S*)-1-(3-hydroxyphenyl)-ethylamine **1-2** and of amine **1-1**, immediate precursors of Rivastgmine and analogous derivatives.

The influence of the DMF equivalents on the reduction was studied, (Table 1-1) and it was found out that running the imine reduction using 5 equivalents of DMF instead of 10, do not affect neither the yield or the stereochemical outcome. It was also possible to perform the reduction at 0 °C obtaining 92:8 *d.r.*. The stereoselective reduction could be carried out in 6 hours without any erosion on the chemical yield, (Table 1-1). Moreover, the use of more eco-friendly solvents

(toluene and anisole)[80] was tested and good yields (up to 77) and high diasterocontrol (up to 96:4) were obtained.

Table 1-1. In batch reduction of O-Bn protected chiral imine **1-5.**

Entry	T (°C)	DMF (eq)	Solvent	Yield (%)[a]	*d.r.*[b]
1	0	10	DCM	85	92:8
2	-20	10	DCM	81	>98:2
3	0	5	DCM	91	92:8
4	-20	5	DCM	90	97:3
5[c]	-20	5	DCM	83	97:3
6	-20	5	Toluene	67	92:8
7	-20	5	Anisole	77	96:4

[a] Isolated yield; reaction time: 18h; [b] Determined by ^{1}H-NMR spectroscopy; [c] Reaction time: 6 h.

The trichlorosilane-mediated reduction was effective also on the chiral imine **1-7**, featuring the carbamate group on the aromatic ring, and led to the isolation, after methylation, of *N*-methyl chiral amine **1-8** in 81% yield as a single isomer (>98:2 *d.r.*), immediate precursor to (*S*)-Rivastigmine (Scheme 1-9). To the best of our knowledge this is the first example of the stereoselective reduction of that class of imines, achieved in mild conditions, without observing any degradation of the carbamate moiety.

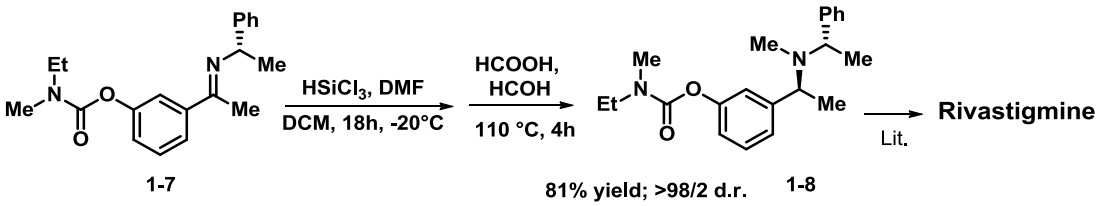

Scheme 1-9.

After the successful development of the batch chemistry, the attention was focused on the set up for the flow[81] reduction of the imine and the following deprotection.

As already reported in the introduction of this thesis the flow and versatile manufacture of chiral intermediates is a hot topic both for academic and industrial researchers. In this case the safety concerns about the use of $HSiCl_3$ could be overcame by taking advantage of the safer reaction condition related to the flow set-up[82]. Therefore, the development of a continuous flow process for the preparation of both enantiomers of 1-(m-alkoxyphenyl)-ethylamine derivatives is an attractive option. At the best of our knowledge this was the first time that $HSiCl_3$ was used under continuous flow conditions, for the in-flow reduction of imines.

As experimental set-up, a coil-reactor made of PTFE tubing (1.58 mm outer diameter, 0.58 mm inner diameter, 1.89 m length, 500 µL effective volume) coiled in a bundle was used. The reactor

was immersed in a cooled bath at the selected temperature. (Scheme 1-10, see the experimental part for pictures).

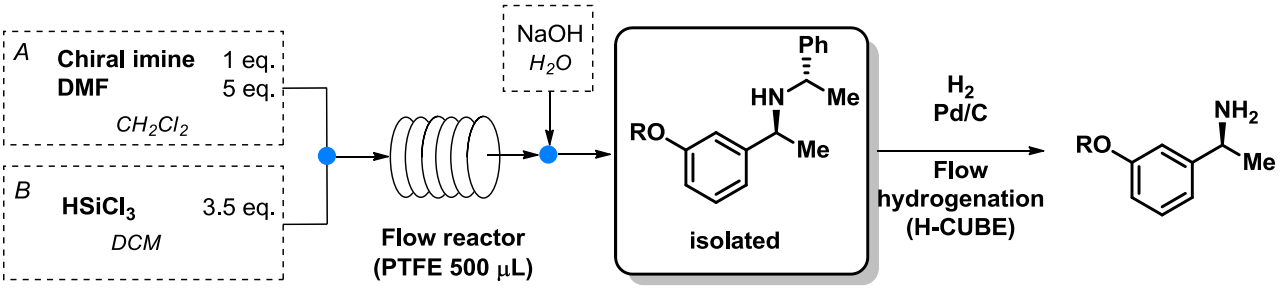

Scheme 1-10. Continuous flow reduction of chiral imines and removal of the chiral auxiliary by continuous flow hydrogenation to afford pure primary amines.

The optimization of the reaction conditions was performed on imine **1-5**, in CH_2Cl_2 by using different temperatures and flow rates (Table 1-2). With 5 minutes of residence time at 15 °C the desired amine was obtained in 70% yield with 90:10 as dr (entry 1). Running the reaction at 0°C with 10 minutes of residence time better stereocontrol (d.r. 93:7) and yield (80%) were achieved (entry 3). Working at -20°C the chiral amine was isolated in 75 % yield and complete stereoselection (entry 4). Notably, it was possible to increase the reaction concentration up to 0.4 M without erosion in chemical yield or in the stereocontrol, demonstrating the possibility of developing more concentrated, efficient, and green process. Once the best conditions were set up, the reduction of the 3-Methoxy functionalized imine 1-**2** and imine **1-5** were successfully performed under continuous flow condition with good yields and excellent diasteroselectivity (Table 1-2, entries 6 and 7).

Table 1-2. Reduction of chiral imines 1-5, 1-2 and 1-7 under continuous flow conditions.

Entry	Imine	T (°C)	Flow rate (μl/min)	Residence Time (min)	Yield (%)[a]	*d.r.*[b]
1	**1-5**	15	50	5	70	90:10
2	**1-5**	0	50	5	57	96:4
3	**1-5**	0	25	10	83	93:7
4	**1-5**	-20	25	10	81	98:2
5[c]	**1-5**	0	25	10	75	96:4
6	**1-2**	-20	25	10	82	95:5
7	**1-7**	-20	25	10	80	98:2

[a] Yields given as average of five different samples collected at different times; reaction concentration: 0.1M; [b] Determined by ^{1}H-NMR spectroscopy; [c] Reaction concentration: 0.5M.

The hydrogenolysis[83] of the obtained amine was performed in a ThalesNano H-Cube Mini™ (Scheme 1-11) equipped with a 10% Pd/C cartridge. Amine **1-3** was used as a model system: at 50°C and with 50 bar of pressure the starting compound was recovered unreacted (entry 1, Table

1-3), while working at 80 °C and 80 bar amine **1-4** was isolated in 70% yield (entry 2). Increasing the pressure and the temperature up to 100 bars did not improve the yield (entries 3 and 4), however with longer reaction time (a recycle loop was installed) the desired compound was obtained in 95% yield working at 70 °C and 70 bar of pressure (entry 6). Notably, no epimerization at the benzylic stereocenter was observed, even using these harsh reaction conditions.

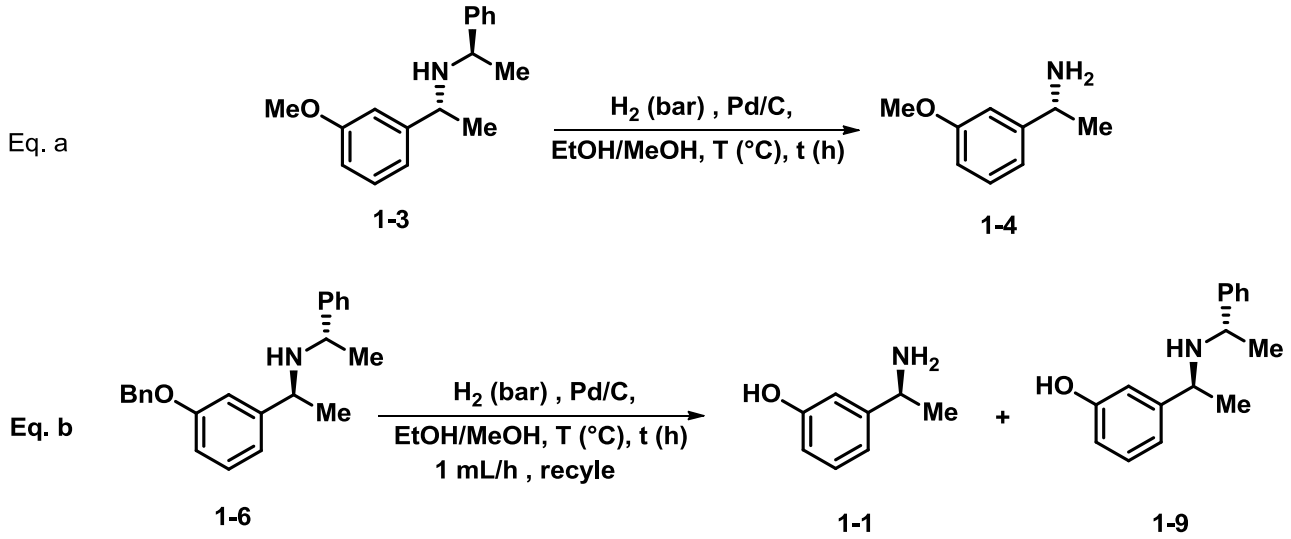

Scheme 1-11. Continuous flow deprotection of amines **2** and **5** to afford chiral primary amines.

Having the best conditions in our hands, obtained using amine **1-3** we tested the double deprotection of amine **1-6**.

In this case the deprotection at 90 °C after 2 hours gave the *O*-debenzylated product **1-9** in 90% yield (entry 7). After 4 hours of reaction at 80 °C, the desired chiral amine **1-1** was isolated in 70% yield, that was further increased up to 85% by running the hydrogenolysis in continuo for 6 hours (entry 9).

Table 1-3. Continuous flow hydrogenolysis of chiral amines.

Entry	Amine	T (°C)	Flow rate (ml/min)	Pressure(bar)	Time (min)	Yield (%)[a]
1	**1-3**	50	1	50	10	n.r.
2	**1-3**	80	1	80	10	70
3	**1-3**	95	0.5	95	20	70
4	**1-3**	95	0.3	95	23	80
5[b]	**1-3**	80	1	80	120	95
6[b]	**1-3**	70	1	70	360	93
7[b]	**1-6**	90	1	80	120	90[c]
8[b]	**1-6**	80	1	80	240	70

9 [b]	**1-6**	80	1	80	360	85

a Isolated yield, reaction concentration: 0.1M; b Reaction run using a closed loop system; c Product 1-9 was obtained as major product in 90% yield.

In conclusion, the first protocol for an efficient, continuous flow, stereoselective reduction of imines was successfully developed. In addition, also the in flow removal of the chiral auxiliary was explored. This flow set up was used for the preparation of key intermediates for the synthesis of different API's.

However, a major drawback of this method is the use of a precious metal catalyst for the chiral auxiliary removal. In order to have a green, robust, and competitive protocol a complete metal free route of synthesis should be developed. Hence, in the following part, studies on protecting groups that could be removed under metal free conditions will be reported.

A stereoselective, catalytic and metal free strategy for the in-flow synthesis of advanced precursors of Rasagiline and Tamsulosin.

In order to apply a complete metal free and in flow protocol for the synthesis of pharmaceutical intermediates, we selected two new target molecules. Rasagiline mesylate (Figure 1-10), also known as *R*-(+)-*N*-propargyl-1-aminoindan mesylate, is a commercially marketed pharmaceutically active substance, under the brand name Azilect®. The racemic form of the drug was invented and patented by Aspro Nicholas in the early 1979, and was later found to be indicated for treatment of Parkinson's disease (PD), being effective both as monotherapy in early PD and as adjunctive in patients with advancing PD and motor fluctuations.[84]This chiral amine is a potent second-generation propargylamine pharmacophore that selectively and irreversibly inhibits the B-form of the monoaminoxidase enzyme (MAO-B) over type A by a factor of fourteen.[85] European drug-regulatory authorities approved this potent MAO-B inhibitor in February 2005 and the US FDA in May 2006.[86] Although the *S*-(−)-enantiomer of *N*-propargyl-1-aminoindane still exerts some neuroprotective properties, the potency of *R*-(+)-enantiomer against the MAO-B enzyme is approximately 1000-fold higher. Different strategies aimed at the preparation of the enantiopure compound have been explored,[87] but, at the best of our knowledge, a stereoselective organocatalytic approach for the preparation of Rasagiline has never been reported so far. The second one is Tamsulosin, sold under the trade name Flomax as single enantiomer. It is used to treat symptomatic benign prostatic hyperplasia and to treat urinary retention. Tamsulosin acts as antagonist for α1a adrenergic receptor. Starting from its common precursor **1-11**, different pharmaceutically active compounds could be prepared, as active compounds on different receptors such as cholinesterase and monoamine oxidase inhibition[88] , σ-Receptors [89] and human Adenosine A2A Receptor.[90]

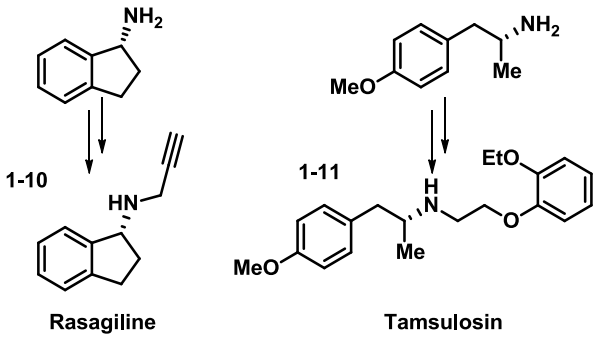

Figure 1-10: Target compounds

For the preparation of chiral amines **1-10** and **1-11**, the use of $HSiCl_3$ as reducing agent in combination with different LB was explored. As already reported in the introduction, in order to control the stereochemical outcome of the reaction different strategies could be used. (Scheme 1-12)

The use an achiral imine, in the presence of a catalytic amount of a chiral LB (LB*), for the activation of the $HSiCl_3$ (Eq. A); it is also possible to use a chiral auxiliary (CA) (Eq. B), as already explored for the preparation of the advanced precursor of Rivastigmine (**1-1**); for achieving a complete stereocontrol the use of a CA in combination with a LB* was also studied (Eq. C).

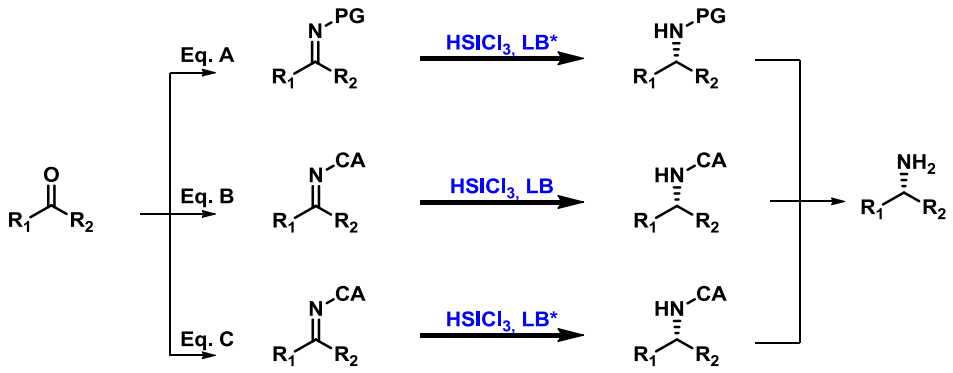

Scheme 1-12: Strategies for stereoselection

For the first strategy (Eq. A) we started to develop the batch chemistry, in order to prepare the target molecule **1-10**. Two achiral protecting group on the nitrogen were selected (Benzyl residue and a PMP one). The selected catalysts were two picolinamides derivatives, one based on ephedrine (A) and the second one based on cinchona (B). (Scheme 1-13)

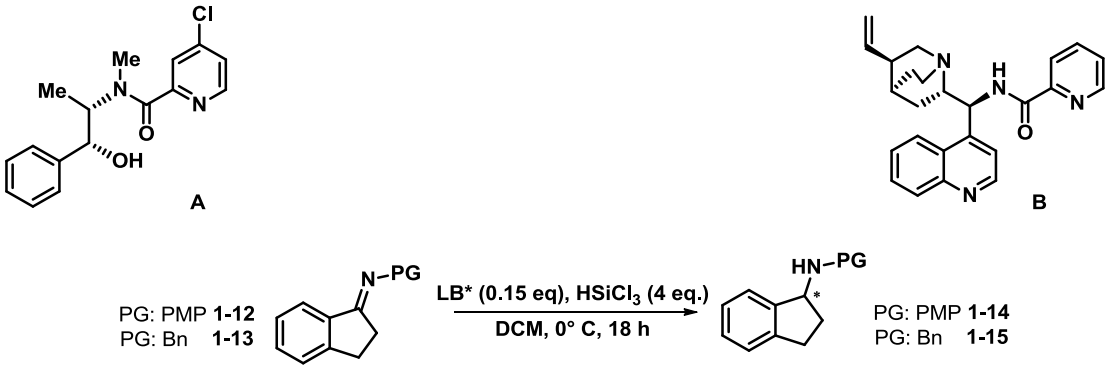

Scheme 1-13: Enantioselective reductions of imines

Using catalyst A, high yields were obtained with PMP and Benzyl protected imines (Table 1-5), however low enantioselection was achieved: using the Bn protected imine **1-13** only 60% *ee* was observed (entry 3).

Table 1-4: chiral LB catalyzed reductions

Entry	PG	Cat.	Yield (%)[a]	*ee* (%)[b]
1	PMP	A	0	--
2[c]	PMP	A	92	35
3[d]	Bn	A	85	60

4	Bn	B	80	55

[a] yields on isolated products, [b] enantiomeric excess was evaluated by chiral HPLC, [c] catalyst loading 0.3 eq., [d] reaction performed at -20 °C

In order to enhance the stereocontrol of the reduction the use of a chiral auxiliary was investigated (Scheme 1-12 Eq. B). For the initial screening phenyl ethyl amine was used. The chiral imine (**1-15**) was obtained with a 9:1 E/Z ratio and subsequently reduced using $HSiCl_3$ in combination with DMF as achiral and cheap LB. Different reaction conditions were screened (Table 1-5). It was found that in order to achieve a high diasteroselection the optimal temperature was -20°C (Table 1-5, entry 5), but with these reaction conditions only 49% of isolated yield was obtained. For achieving 88% of conversion was necessary to work at higher temperature, (entry 6) and in this case the stereoselectivity dropped to 90:10. The use of a match and mismatch couple, using the CA and the chiral catalysts A and B was investigated (Scheme 1-12, Eq. C). In the reduction, using catalyst A, (Table 1-5, entry 7) complete conversion was achieved, but only 90:10 of *d.r.* was obtained. In the case of catalyst B (Table 1-6, entry 8), a mismatched couple was observed, low yield and low *d.r.* were achieved, however running the reaction using the pseudo enantiomer of the catalyst, conversion up to 80% and *d.r.* of 98:2 were observed (Table 1-5, entry 9).

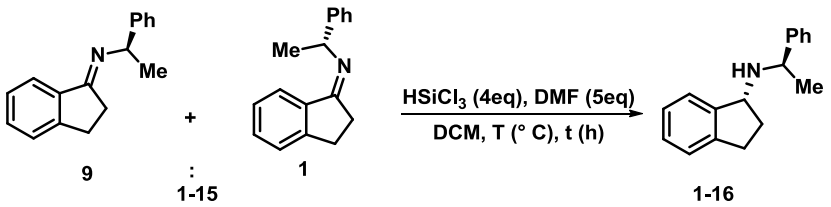

Table 1-5

Entry	LB	T (° C)	t(h)	Conv. (%)[a]	*d.r.*[b]
1	DMF	0	18	67	90:10
2	DMF	-10	18	44	90:10
3	DMF	-10	36	42	90:10
4[c]	DMF	0	36	77	90:10
5[c]	DMF	-20	36	49	98:2
6	DMF	0 to rt	18	88	90:10
7[d]	A	-20	36	90	90:10
8[d]	B	-20	36	20	76:24
9[d,f]	B	-20	36	80	98:2

[a] conversions were evaluated on ^{1}H-NMR, [b] *d.r.* were evaluated on crude mixtures using ^{1}H-NMR, [c] $HSiCl_3$ was further added every 12 hours, [d] reaction was performed using 0.15 eq. of chiral LB, [f] performed with the enantiomer of catalyst B.

As already observed, for the removal of the chiral auxiliary the use of a precious metal catalyst (Pd) is needed.[91] To tackle this problem, different chiral auxiliaries were selected such as: (*R*)-4-

Methoxy-α-methylbenzylamine and (*R*)-2-Methyl-2-propanesulfinamide, both removable without the presence of metal catalysts[9293] (Scheme 1-14). Imines **1-17** and **1-18**, were prepared and tested in the reaction with $HSiCl_3$.

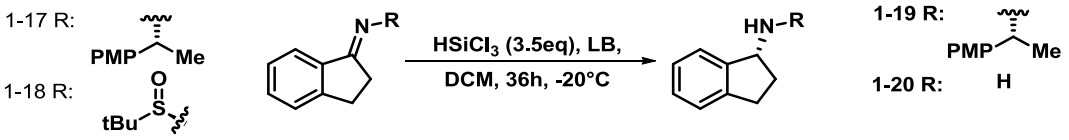

Scheme 1-14: Stereoselective reductions of chiral imines.

Imine **1-17** was completely reduced with 5 equivalents of DMF as achiral LB (Table 1-6, entry 1) high conversion (80 %) and complete diasteroselection (98:2) was observed. By using chiral catalyst A, complete conversion and high stereocontrol (98:2) were achieved (Table 1-6, entry 2), this confirming that catalyst A and the substrate were match couple. Notably, after reduction and basic aqueous quench, imine **1-18** afforded pure unprotected amine **1-20** in a very convenient process (entry 4). The long reaction time (36 hours), the same described in literature [91], prompted us to explore the possibility of developing a continuous flow methodology for the preparation of Rasagiline, in accordance with the raising interesting for the flow preparation of API's [94].

Table 1-6: Reductions of chiral imines

Entry	Imine	LB	Eq.	Conv. (%)	*d.r.*
1[a]	**1-17**	DMF	5	80	98:2
2[b]	**1-17**	A	0.15	98	98:2
3	**1-18**	DMF	5	<5	ND
4[c]	**1-18**	A	0.15	99	60[d]

[a]5 eq. of DMF were used, [b]0.15 eq of catalyst were used [c] the product was obtained as primary amine directly after the work up, [d]*ee* %..

As reported in the previous paragraph the possibility of running the reduction using $HSiCl_3$ under flow conditions present some advantages, such as better temperature control and better yield in shorter reaction time. Hence, we decided to use this set up to obtain a direct precursor of Rasagiline. (Scheme 1-15) The same reaction set up already used for the preparation on the key precursor **1-1** was used. (for pictures, see the experimental section).

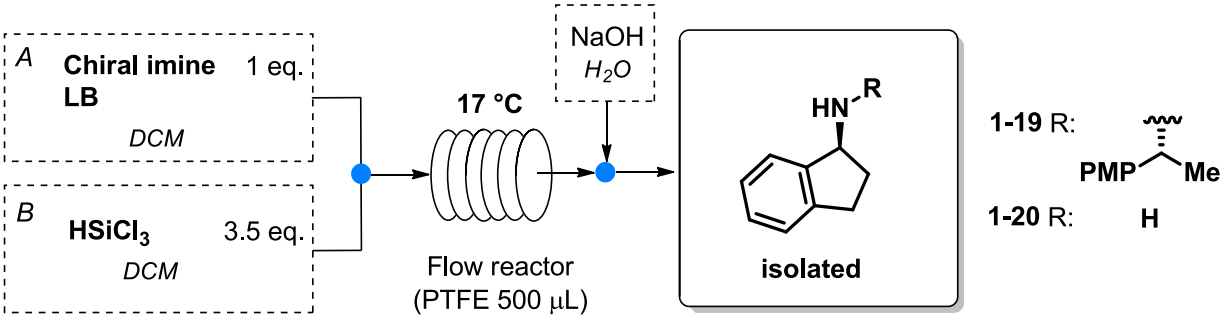

Scheme 1-15: continuous flow preparation of an advanced precursor of Rasagiline.

First, the use of five equivalents of DMF as achiral LB was tested, (Table 1-8, entries 1-4). Working at 30°C in only 20 minutes we reached 83% conversion and 92:8 *dr* (entry 4). pleasantly in only 20 minutes of residence time, the conversion was up to 80%, working at 30°C and the stereoselection was complete. Notably in only 20 minutes of reaction time, using continuous flow conditions, we reached the same results of 36 hours of reaction time in batch. Also, the match couple with catalyst A was used (Table 1-7, entry 5); however, working in the same condition of DMF, the conversion was lower (70%). The chiral imine **1-18**, bearing an easier to remove group was reduced under continuous flow conditions (Table 1-7, entries 6-7). The primary amine was directly recovered, however low conversion and low enantiomeric excess were observed in the final product.

Table 1-7: flow reductions of chiral imines

Entry	LB	Imine	T (° C)	Residence time (min.)	Eq.	Conv. (%)	*d.r.*
1	DMF	**1-17**	17	10	5	20	98:2
2	DMF	**1-17**	17	20	5	34	98:2
3	DMF	**1-17**	17	30	5	35	98:2
4	DMF	**1-17**	30	20	5	83	92:8
5	A	**1-17**	30	20	0.2	70	98:2
6	A	**1-18**	-20	20	0.2	22	55[a]
7	A	**1-18**	0	20	0.2	22	56[a]

[a]*ee*%

The in-flow reduction of imine **1-21**, and **1-22** were also studied. In this case, the use of 4-methoxy phenyl ethyl amine derivative was not feasible, since the oxidative removal was not compatible with the electron rich aromatic group present on this Tamsulosin precursor, and the use of a Pd/C based deprotection was the first choice (Scheme 1-16).

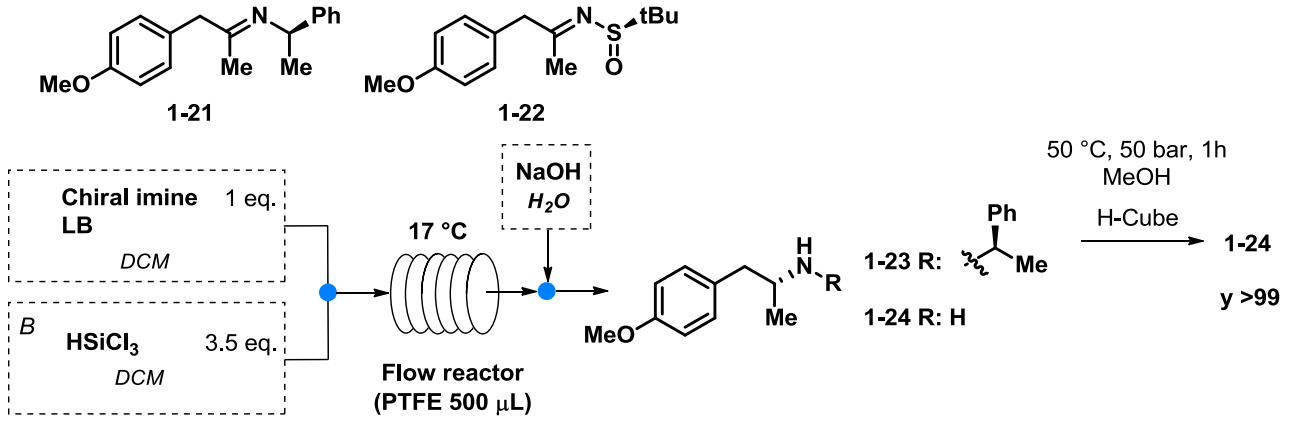

Scheme 1-16

In order to achieve a better stereocontrol in the reduction of imine **1-21**, the match couple with catalyst B was employed (Table 1-8, entries 1-2), in 30 minutes was possible to achieve good conversion up to 75% and fairly good diasteroselection up to 92:8. In addition the following

deprotection using H-Cube mini apparatus proceeded with excellent yield, obtaining the final amine as enantioenriched product. Also, the flow reduction of imine **1-22** was performed (Table 1-8, entries 3-4); in this case using DMF as achiral LB was possible to achieve, after the work up the primary amine with enantiomeric excess up to 88% and with good yields up to 70%.

Table 1-8

Entry	LB	Imine	Residence time (min.)	Eq.	Conv. (%)	*d.r.*
1	B	1-21	20	0.2	60	92:8
2	B	1-21	30	0.2	75	92:8
3[a]	DMF	1-22	20	5	60	88[c]
4[b]	DMF	1-22	30	5	70	88[c]

[a] reaction performed from 0°C to room temperature, [b] reaction performed at 0°C, [c]*ee*%

In conclusion, a complete metal free preparation of two advanced precursors of APIs Rasagiline and Tamsulosin was performed, the flow preparation of these compounds was studied and showed improved productivity and shorter reaction time. The use of a catalytic amount of LB* in the presence of a chiral auxiliary in order to control the selectivity of the reaction was successfully explored.

In the next paragraph, the attention will be focused on the development of a new class of chiral LB for the imines reduction using $HSiCl_3$.

A new class of low-loading catalysts for a highly enantioselective, metal-free imine reduction of general applicability

The major drawback of the chiral Lewis Bases developed until now is the high catalyst loading necessary for the effective and stereoselective reduction of C=N double bonds.

Despite all the recent achievements in the field, the combination of inexpensive, non-toxic, easily disposable reagents with very low catalyst loadings, comparable to those of the metal-based chiral catalysts, is an unmet challenge in organocatalysis today.[95] Trichlorosilane-based reduction methodology may offer this opportunity.

In this paragraph the design, the synthesis, the optimization, and the application of a new class of easy accessible chiral Lewis bases is reported. These compounds could be prepared in few steps starting from cheap and commercially available aminoacids. (Figure 1-11)

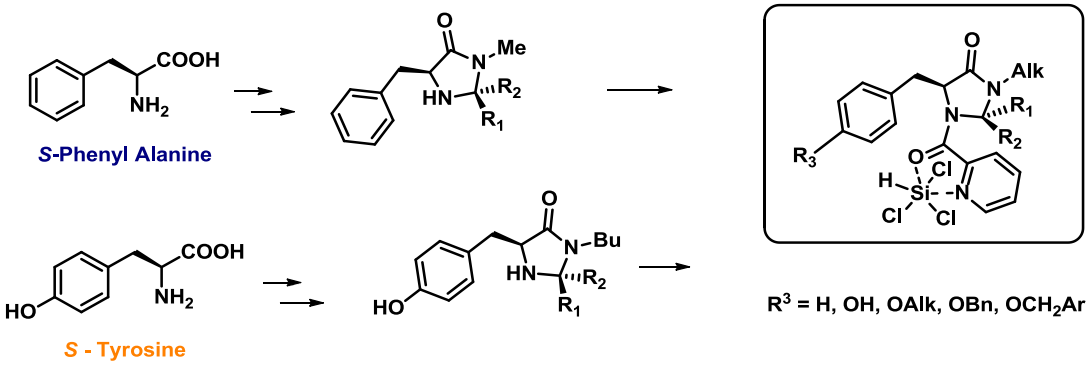

Figure 1-11. A new class of chiral Lewis bases for enantioselective catalytic hydrosilylation of imines.

Picolinamides could be easily obtained by condensation between picolinic acid/chloride/anhydride with different chiral scaffolds, and have been extensively studied as activators of trichlorosilane[63].

The inspiration for the design of this new class of LB* was taken by the well-established and efficient scaffold of imidazolidinones developed by Professor MacMillan, successfully used for the activation of carbonyl compounds in organocatalysis[96]. (Figure 1-12)

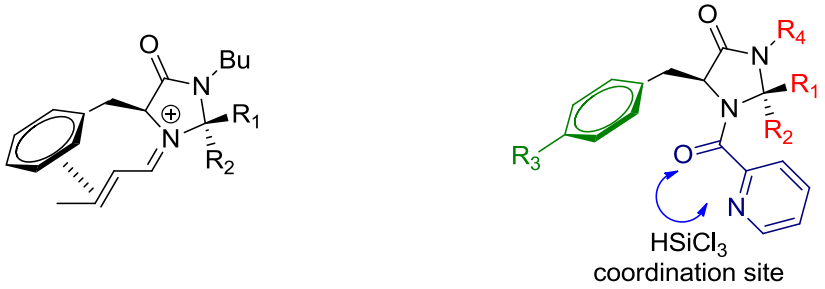

Figure 1-12

The picolinamide residue is responsible of $HSiCl_3$ coordination and chemical activation, while the imidazolidinone scaffold offers many opportunities to tune and modify the steric hindrance and the stereoelectronic properties of the catalytic system (Figure 1-13). Therefore, a series of new

chemical entities, featuring different substituents on the imidazolidinone ring and on the aromatic ring of the amino acid moiety, were synthesized.

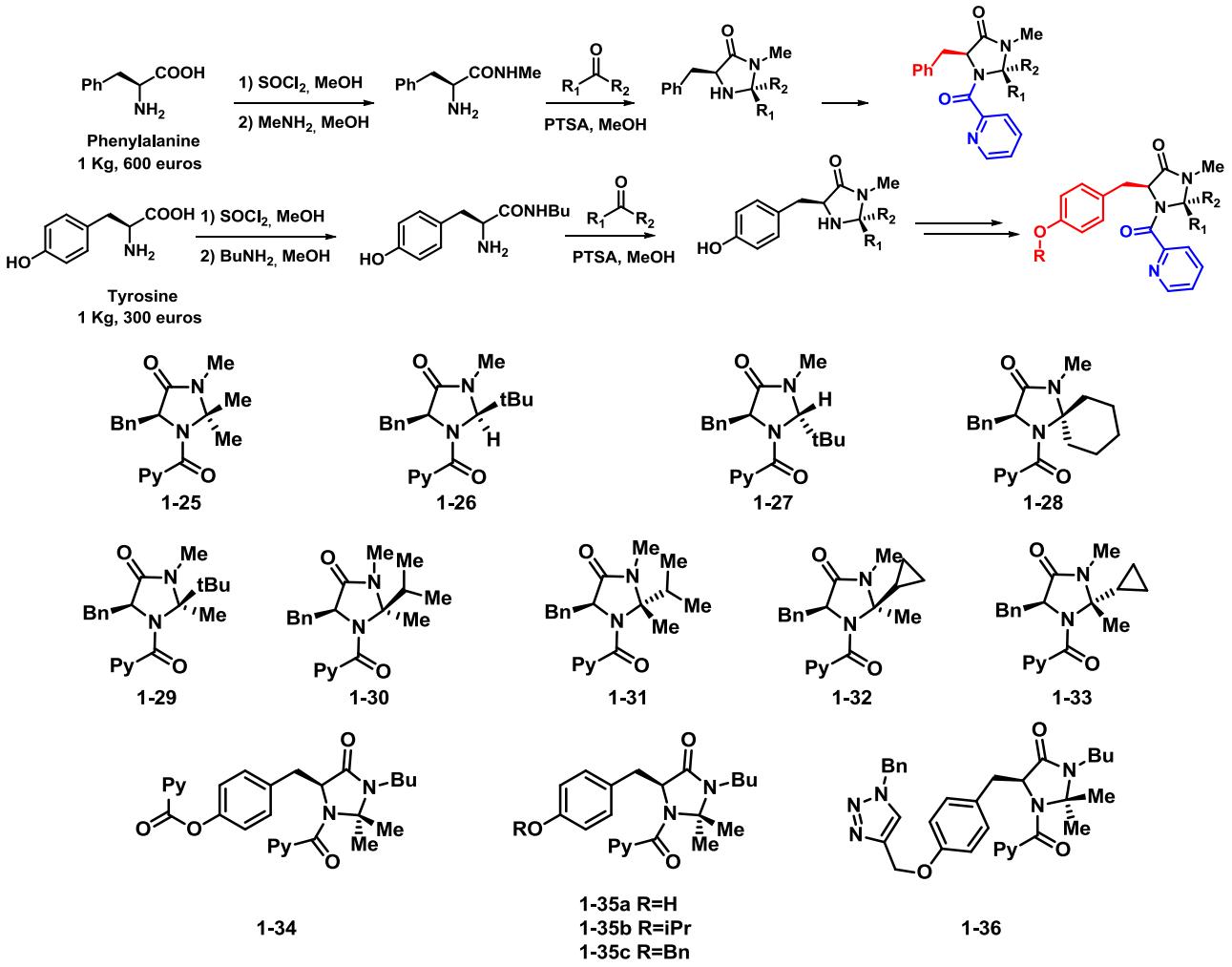

Figure 1-13

Starting from (*S*)-phenyl alanine, enantiopure Lewis bases **1-25** to **1-33** were prepared; the imidazolidinone ring was assembled via reaction of the *N*-methyl (*S*)-phenyl alanine carboxyamide with different carbonyl derivatives, and then conjugated to picolinic acid. Analogously, (*S*)-tyrosine was used to prepare catalysts **1-34** to**1-35,** featuring a 4-substituted phenyl ring (Figure 1-13). (For detailed description of the synthesis see the experimental section).

In order to identify the most promising and efficient catalyst, an initial screening on the model imine derived from the condensation of acetophenone and aniline was performed at 0°C. (Table 1-9)

Table 1-9. Catalyst screening.

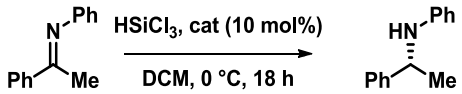

1-37 1-38

Entry [a]	Catalyst	Yield (%) [b]	*e.e.* (%) [c]
1	1-25	76	85
2[d]	1-25	73	92
3	1-26	57	10
4	1-27	13	<5
5	1-28	73	64
6	1-29	90	<5
7	1-30	80	72
8	1-31	75	<5
9	1-32	76	89
10	1-33	60	48
11	1-34	78	23
12	1-35a	98	94
13	1-35b	81	97
14	1-35c	98	98
15	1-36	99	92

[a] Reaction conditions: **5a** (0.1 mmol, 20 mg), **cat**. 0.01 mmol, $HSiCl_3$ (0.35 mmol, 35 μL) in CH_2Cl_2 (1 mL) at 0°C; [b] isolated yield; [c] determined by HPLC on chiral stationary phase; [d] reaction performed at -10 °C.

Catalyst **1-25,** showed interesting performance in terms of yield and enantioselection, (Table 1-10, entries 1,2). Different group in R1 R2 position should force the phenyl ring of the benzyl residue for a better shielding of the imines[96], however the variation on the structure did not improve the catalysts activity, lower yields and lower enantioselection were observed (Table 1-9, entries 3-11). Surprisingly the introduction of a para substituent on the aromatic ring lead to the identification of very efficient catalysts. LB* **1-35** (a,b,and c, table 1-9 entries 12-14) showed very high activity and incredible stereocontrol, *ee* up to 98%. Catalyst **1-36**, was developed for the study on possible compatibility of the triazole ring in the reaction conditions, in prevision of the development of a supported version of the catalyst[97] and showed good activity (entry 15).

For studying the performance of catalysts, **1-25**, **1-35a**,**1-35b**, **1-35c**, **1-36** less reactive imines were used (Table 1-10). In particular the aim was the observe the chemical activity of those catalyst when the electron density on the carbonyl of the imine was increased. (Table 1-10)

The reduction of imine **1-39** bearing a simple phenyl ring residue was accomplished with all the catalysts, (Table 1-10, entries 1-5), obtaining good yields and high enantiomeric excess. Using a para methyl substituted imine (**1-40**), the reactivity of catalysts **1-25** and **1-35b**, dropped dramatically and in these two cases low yield and low *ee* were observed, (Table 1-10, entries 6 and 8), however using the other catalysts amine (**1-43**) was obtained with high yield and enantioselectivity. The most electron rich imine employed, bearing a 4-OMe substituent on the aromatic ring, was successfully reduced only by catalysts **1-35a**, **1-35c**, and **1-36**, in the first two cases the desired amine (**1-44**) was recovered in 99% yield and *ee* up to 93%.

Table 1-10

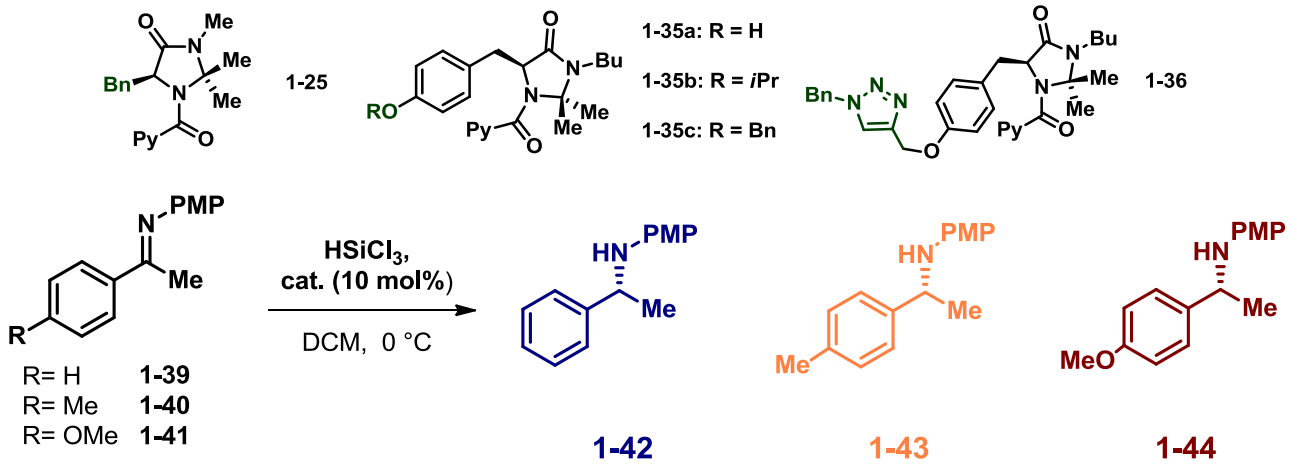

Entry [a]	R:	Catalyst	Yield (%) [b]	*e.e.* (%) [c]
1	**H**	1-25	77	89
2	**H**	1-35a	93	96
3	**H**	1-35b	81	95
4	**H**	1-35c	99	97
5	**H**	1-36	99	93
6	**Me**	1-25	<10	Nd
7	**Me**	1-35a	95	93
8	**Me**	1-35b	55	60
9	**Me**	1-35c	99	93
10	**Me**	1-36	99	91
11	**OMe**	1-25	--	-
12	**OMe**	1-35a	99	85
13	**OMe**	1-35b	--	-
14	**OMe**	1-35c	99	91

15	**OMe**	1-36	89	90

[a] Reaction conditions: **5** (0.1 mmol), **cat**. 0.01 mmol, $HSiCl_3$ (0.35 mmol, 35 μL) in CH_2Cl_2 (1 mL) at 0°C; [b] isolated yield; [c] determined by HPLC on chiral stationary phase; [d] reaction performed at -10 °C.

Catalysts 1-**35c** and **1-36** were selected for further studies in particular with the aim of lowering down the catalyst loading[98]. In the attempt to lower the catalyst loading, the reduction of imine **1-39** was performed with reduced amounts of chiral Lewis base (Table 1-11). Using catalyst **1-36** it was possible to perform the reduction with only 1 mol%, obtaining the product in 93% yield and 92% *ee* (Table 1-11, entries 1-4). Catalyst **1-35c** showed an even better reactivity, and the amine **1-42**, was obtained in 80% yield and 97 % *ee*, using only 0.1% mol of catalyst (Table 1-11 entry 7).

Working with 0.1% of catalyst the ACE (Asymmetric Catalyst Efficiency)[99], evaluated on entries 6-7 of table 1-12, is 375-400, a comparable value with organometallic systems and better than the most organocatalysts. [100[

Table 1-11.

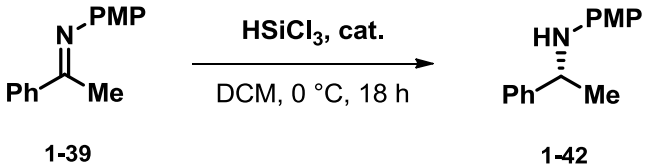

1-39 **1-42**

Entry [a]	Catalyst	Cat. loading	Yield (%) [b]	*e.e.* (%)[c]
1	1-36	5 mol%	95	92
2[a]	1-36	5 mol%	95	81
3[b]	1-36	5 mol%	87	92
4	1-36	1 mol%	92	92
5	1-35c	1 mol%	99	97
6	1-35c	0,1 mol%	93	90
7[c]	1-35c	0,1 mol%	80	97

[a] Reaction conditions: **5** (0.1 mmol), **cat**. 0.01 mmol, $HSiCl_3$ (0.35 mmol, 35 μL) in CH_2Cl_2 (1 mL) at 0°C; [b] isolated yield; [c] determined by HPLC on chiral stationary phase.

To demonstrate the applicability of the methodology on multi gram scale, the preparation of 10 grams of amine **1-46** was accomplished using only 10 mg of catalyst, obtaining the desired compound in 86% yield and 98% ee. (Scheme 1-17)

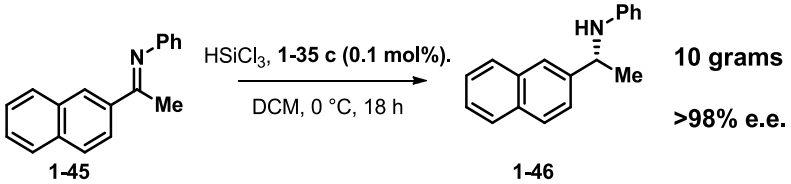

1-45 **1-46**

Scheme 1-17

To test the general applicability of catalysts 1-**35c** and **1-36** the reduction of a wide variety of imines was investigated (Table 1-12).

Both catalysts **1-35c** and **1-36** were active and very efficient in the synthesis of different chiral amines. Notably LB* **1**-**35c** was able to promote the reduction of *N*-aryl and *N*- alkyl substituted imines in >90% yield and enantioselectivities constantly ranging from 90% to 98%. The synthesis of α– and β-amino esters (Table 1-12, entriesm16-19) was also accomplished, in up to 96% *ee*. The reduction of 3-alkoxy-substituted acetophenone imines (**1-51, 1-52**), either *N*-benzyl protected (as precursor of primary amine derivatives), or *N*-(3-phenylpropyl) substituted (imine **1-53**), represents a practical and efficient entry to the synthesis of enantiomerically pure valuable pharmaceutical compounds, as previously reported (scheme 1-6, page 27), used in the treatment of Alzheimer and Parkinson disease, hyperparathyroidism, neuropathic pains and neurological disorders (Figure 1-14).

Table 1-12

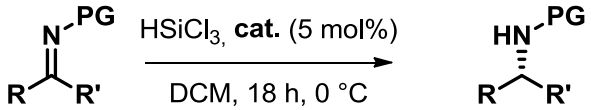

Entry	Imine	Cat.	R	R’	PG	Yield (%)	e.e. (%)
1	1-45	1-35c	α-napht	CH_3	Ph	99	98
2[a]	1-45	1-36	α-napht	CH_3	Ph	99	90
3	1-47	1-36	4-F-C_6H_4	CH_3	PMP	93	95
4	1-48	1-36	4-CF_3-C_6H_4	CH_3	PMP	92	96
5	1-49	1-35c	4-NO_2-C_6H_4	CH_3	PMP	99	97
6	1-49	1-36	4-NO_2-C_6H_4	CH_3	PMP	94	93
7	1-50	1-35c	4-Cl-C_6H_4	CH_3	PMP	98	96
8	1-50	1-36	4-Cl-C_6H_4	CH_3	PMP	95	94
9[a]	1-51	1-35c	3-OMe-C_6H_4	CH_3	PMP	98	90
10	1-51	1-36	3-OMe-C_6H_4	CH_3	PMP	97	90
11[a]	1-52	1-36	3-OBn-C_6H_4	CH_3	PMP	80	96
12	1-53	1-36	3-OBn-C_6H_4	CH_3	Bn	80	93
13[a]	1-54	1-35c	Ph	CH_3	$(CH_2)_3$Ph	99	98
14[a]	1-54	1-36	Ph	CH_3	$(CH_2)_3$Ph	99	90
15[a]	1-55	1-35c	Ph	CH_3	*n*-Bu	80	96
16[a]	1-56	1-35c	Ph	COO_2CH_3	PMP	99	90
17[a]	1-56	1-36	Ph	COO_2CH_3	PMP	95	90
18[a]	1-57	1-35c	Ph	$CH_2COO_2CH_3$	PMP	85	96
19	1-57	1-36	Ph	$CH_2COO_2CH_3$	PMP	65	95
20[a]	1-58	1-35c	Ph	CH_2NO_2	PMP	99	93

[a] reaction performed at -20 °C.

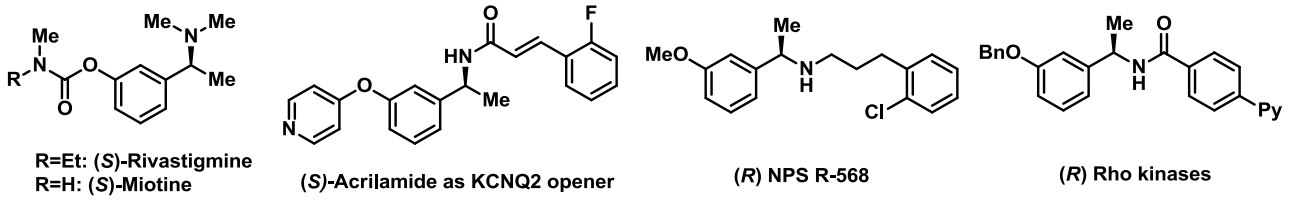

Figure 1-14. Chiral amines as valuable pharmaceutically active compounds.

In conclusion, a new class of chiral Lewis bases for imines hydrosilylation was developed; the most active catalyst promoted the reduction of a wide variety of functionalized substrates, very often in quantitative yields and enantioselectivities typically higher than 90%, up to 98%. Remarkably, the chiral Lewis base of choice efficiently catalyzed the reaction with only 0.1% mol loading, without losing stereoselectivity. The synthesis of enantiopure chiral amines on gram scale was also accomplished with only milligrams of catalyst. The simple experimental procedure, the low cost of the reagents, the mild reaction conditions and straightforward isolation of the product after an aqueous work up, the extremely low catalyst loading and the possibility to realize *in continuo* processes, make the methodology attractive also for industrial applications.

Experimental section chapter 1

NMR spectra: ^{1}H-NMR and ^{13}C-NMR spectra were recorded with instruments at 300 MHz (Bruker AMX 300 and Brucker F300). The chemical shifts are reported in ppm (δ), with the solvent reference relative to tetramethylsilane (TMS).

Mass spectra: Mass spectra were registered on an APEX II & Xmass software (Bruker Daltonics) instrument or on a thermo Finnigan LCQ Advantage instrument, equipped with an ESI ion source.

$[\alpha]^{T}_{D:\ Optical}$ rotations were obtained on a Perkin-Elmer 241 polarimeter at 589 nm using a 5 mL cell, with a length of 1 dm.

HPLC: For HPLC analyses on chiral stationary phase, to determine enantiomeric excesses, it was used an Agilent Instrument Series 1100. The specific operative conditions for each products are reported from time to time.

GC: Gas chromatography was performed on a GC instrument equipped with a flame ionization detector, using a chiral capillary column Chiral Dex CB column (30m x 0.32 x 0.25μL

TLC: Reactions and chromatographic purifications were monitored by analytical thin-layer chromatography (TLC) using silica gel 60 F254 pre-coated glass plates and visualized using UV light, phosphomolybdic acid or ninhydrin.

Chromatographic purification: Purification of the products was performed by column chromatography with flash technique (according to the Still method) using as stationary phase silica gel 230-400 mesh (SIGMA ALDRICH).

Dry solvents: Dichloromethane (DCM) was dried by distillation under nitrogen atmosphere on CaH_2. The other dry solvents used are commercially available and they are stored under nitrogen over molecular sieves (bottles with crown cap).

Reactions work-up: The organic phases, if necessary, were dried over Na_2SO_4. The solvents were removed under reduced pressure and then at high vacuum pump (0.1-0.005 mmHg).

Trichlorosilane: Commercially available $HSiCl_3$ was used without any further purification

Fluidic device: The device was realized by assembling one coil-reactor according to the scheme reported in figure S-1. Coil-reactors were connected by T-junctions using standard HPLC connectors.

Coil-reactor: This module was realized by using PTFE tubing (1.58 mm outer diameter, 0.58 mm inner diameter, 1.89 m length, 500 µL effective volume) coiled in a bundle and immersed in an MeOH bath cooled to the desired temperature.

Syringe pump: Chemix Fusion 100, equipped with two 2.5 ml Hamilton gastight syringes, fed the solution containing the imine and the DMF dissolved in DCM, and the solution of $HSiCl_3$ in DCM through a T-junction into the coil-reactor.

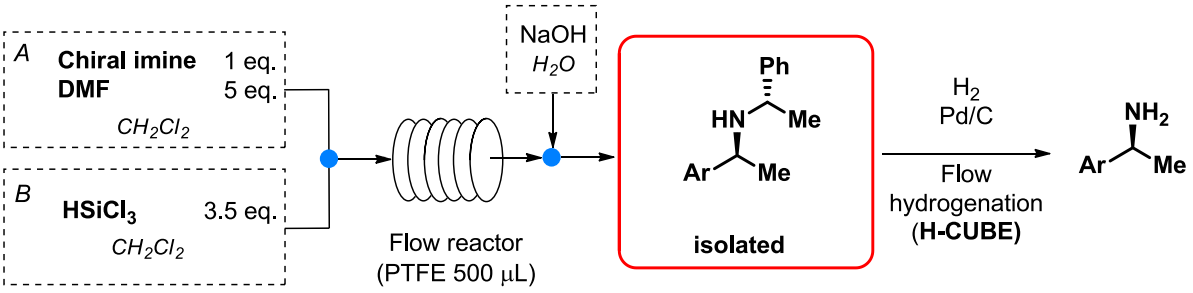

Continuous hydrogenation: The continuous hydrogenations were performed with a Thales Nano H Cube mini, equipped with a cartridge with 10% Pd/C.

Batch hydrogenations*:*The hydrogenations were run in a 450 mL Parr autoclave equipped with a removable aluminium block that can accommodate up to 4 magnetically stirred 20 mL-glass vials, fitted with a Teflon septum.

General procedures for imines synthesis

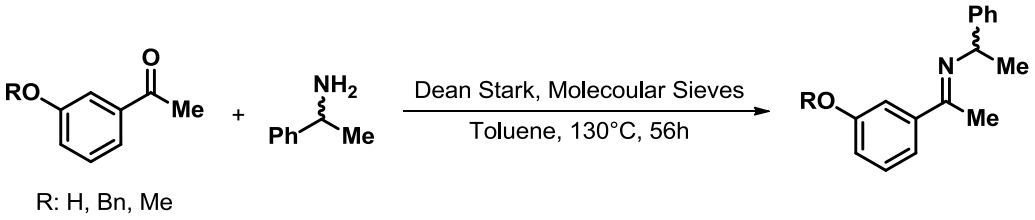

R: H, Bn, Me

General procedure (A): Toluene (8 mL), 4 Å molecular sieves, amine (6.6 mmol, 1.5 eq.) and ketone (4.4 mmol, 1 eq.) were introduced in a one necks 25 mL round-bottomed flask provided with a condenser and a Dean-Stark apparatus. The reaction mixture was heated to 130 °C and stirred at this temperature for 56 h. After cooling to room temperature, molecular sieves were removed filtering over Na_2SO_4 pad and washed with DCM. The solvent was removed under reduced pressure. The residual starting materials were removed by fractional distillation at P = 3 x 10^{-2} mbar at 150 °C with Glass Oven B-585 Kugelrohr (only terminal round flask inserted). in order to remove the excess of amine.

General procedure (B): Toluene (6 mL), molecular sieves (350 mg), amine (1.5 eq, 6.6 mmol) and ketone (1 eq, 4.4 mmol) were introduced in a 25 mL vial without inert atmosphere. The stirred mixture was subjected to 200 W microwave irradiation and heated to 130 °C for 6 h 30 min. Constant microwave irradiation as well as simultaneous air-cooling (2 bar) were used during the entire reaction time. After cooling to room temperature, the reaction mixture was filtered on Na_2SO_4 , and washed with DCM, the solvent was removed under reduced pressure. The residual starting materials were removed by fractional distillation at P = 3 x 10^{-2} mbar at 150 °C with Glass Oven B-585 Kugelrohr (only terminal round flask inserted).

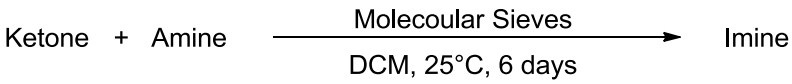

General procedure (C): Dry DCM (0.1M), molecular sieves, amine (1.5 eq.) and ketone (1 eq.) were introduced in a two necks round bottomed flask provided with a nitrogen inlet. The reaction mixture was stirred for 6 days at 25° C, then filtered over a Na_2SO_4 pad, and the solvent was removed under reduced pressure.

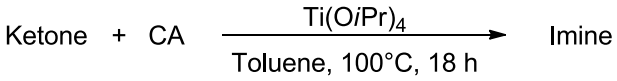

General procedure (D): The selected ketone was charged in a two round bottomed flask, posed under nitrogen and dissolved in dry Toluene (0.1M). At this solution was added Ti(*i*PrOH)$_4$ (2 eq.), after 5 minutes of mixing the (*R*)-(+)-2-Methyl-2-propanesulfinamide was added. The reaction mixture was stirred for 18 hours at 110 ° C, then poured into a same volume solution of brine. The

resulting slurry was filtered over celite and the cake was washed with AcOEt. The two phases were separated, and the organic phase was further washed with brine. The organic layer was dried with Na_2SO_4 pad, and the solvent was removed under reduced pressure. The desired imines were obtained pure after chromatographic purification.

General procedures for imines reductions

General procedures for $NaBH_4$ reductions: A solution of imine in ethanol (0.1 M) is introduced into a round bottomed flask, the temperature was cooled to 0° C and the $NaBH_4$ was added in two portions. After 18 hours, a stoichiometric amount of water was added and after 10 minutes the solvent was removed under reduced pressure. The diasteroisomeric ratio was evaluated on the crude mixture.

General procedures for batch imines reduction with $HSiCl_3$: Dry DMF (5 eq.) and a 0.9 M solution of the imine in dry solvent were introduced in a 10 mL round bottomed flask under N_2 atmosphere and further diluted in 2 mL of dry solvent. The mixture was cooled to the reaction temperature. A 1.6 M solution of $HSiCl_3$ (0.7 mmol, 3.5 eq.) in selected solvent was added to the reaction mixture. After the desired time, the reaction was quenched with a 0.1 M solution of NaOH until the basic pH was reached. The resulting slurry was stirred at room temperature for 10 minutes, then Na_2SO_4 was added as drying agent. The mixture was filtered over a celite pad and washed with CH_2Cl_2 (10 mL) and ethyl acetate (10 mL). The solvent was removed under reduced pressure. The diasteroisomeric ratio was evaluated on the crude mixture. The resulting amines were purified by flash chromatography on silica gel or by crystallization.

General procedures for continuous flow imines reduction with $HSiCl_3$: The 500 µL coil-reactor at the desired temperature was fed with two 2.5 ml Hamilton gastight syringes, at the desired flow rate. Syringe A was filled with a solution of imine (1 mol eq.) and dry DMF (5 mol eq.) in dry DCM. Syringe B: was filled with a solution of $HSiCl_3$ in DCM. The concentration of the reagent in the syringes was fixed according to the desired concentration in the reactor. The reaction mixture was collected into a one round bottomed flask, filled with a 0.1 M solution of NaOH at the same reaction temperature.

After the first volume was discharged, the steady-state conditions were reached; the reported yield values are given as average of five different samples collected at different times.

General procedure for LB catalyzed imines reduction: The imine (1 mmol) and the catalyst were introduced into a vial and dissolved in dry CH_2Cl_2 (1 mL) under inert atmosphere. $HSiCl_3$ (1 M solution in CH_2Cl_2, 3,5 equiv.) was added at 0° C and then the reaction was stirred at the indicated temperature and for the desired reaction time. After reaction time the crude mixture was treated with NaOH 10% aq. until basic pH = 9. The aqueous layer was extracted twice with CH_2Cl_2. The

organic layer was collected, dried with Na_2SO_4 and concentrated under vacuum. The residue was purified by column chromatography on silica gel. The enantiomeric excess was determined by HPLC on chiral stationary phase.

Advanced precursors of Rivastigmine and Miotine: products descriptions

3-Benzyloxyacetophenone

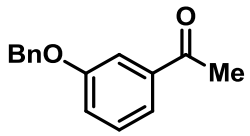

3-hydroxyloxyacetophenone (1 eq.) was charged into a one round bottomed flask, and dissolved in CH_3CN (0.5 M), K_2CO_3 (10 eq.) was added to the reaction mixture. At the heterogeneous suspension was added BnBr (3 eq.). The resulting solution was stirred at 50 °C for 24 hours. After the removal of the solvent and the excess of BnBr the resulting slurry was dissolved in DCM and washed with a 0.5 M solution of NaOH. The collected organic phase was dried with $MgSO_4$ and the solvent was removed under reduced pressure to give a brown oil that was used without further purification.

^{1}H NMR (300 MHz, $CDCl_3$) δ 7.64 – 7.55 (m, 2H), 7.42 (m, 6H), 7.21 (m 1H), 5.14 (s, 2H), 2.62 (s, 3H).

N-ethyl-N-methyl carbamic chloride:

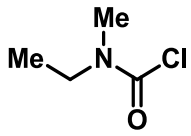

This compound was prepared following literature procedure[101]

N-ethyl-N-methyl carbomyl acetophenone:

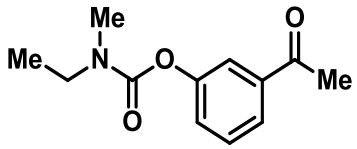

This ketone was prepared following literature procedure.[102]

N-(1-(*S*)-phenylethyl)-ethan-1-(3-(benzyloxy)phenyl)-1-imine **(1-5)**

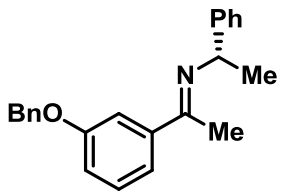

Synthetized according to general procedure A and B starting from the corresponding ketone and (*S*)-phenylethylamine. The pure product was obtained in 45% (Procedure A) and 25% (Procedure B) yield after purification by fractional distillation at P = 3 x 10^{-2} mbar °C with Glass Oven B-585 Kugelrohr set to 95 °C. The imine is a 91:9 mixture of the *E* and the *Z* isomers.

Major isomer:

^{1}H NMR (300 MHz, $CDCl_3$) *E* δ: 7.99-7.94 (m, 1H), 7.58-7.31 (m, 12H), 5.19 (s, 2H), 4.94 (q, 1H, *J* = 9.0 Hz), 2.25 (s, 3H), 1.66 (d, 3H, *J* = 9.0 Hz).

Imines description

N-(1-(*R*)-phenylethyl)-ethan-1-(3-(methoxy)phenyl)-1-imine **(1-2)**

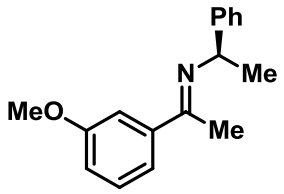

Prepared according to general procedure A and B starting from the corresponding ketone and (*R*)-phenylethylamine. The pure product was obtained in 50% (Procedure A) and 35% (Procedure B) yield after purification by fractional distillation yield after purification by fractional distillation at P = 3 x 10^{-2} mbar °C with Glass Oven B-585 Kugelrohr set to 95 °C. The imine was a 90:10 mixture of the *E* and the *Z* isomers as reported in literature.[103]

Major isomer:

^{1}H NMR (300 MHz, $CDCl_3$) *E* δ 7.55–7.20 (m, 9H), 4.86 (q, *J* = 6.6 Hz, 1H), 3.88 (s, 3H), 2.28 (s, 3H), 1.56 (d, *J* = 6.6 Hz, 3H).

N-(1-(*S*)-phenylethyl)-ethan-1-(3-(*N-ethyl-N-methyl carbamate*)phenyl)-1-imine: **(1-7)**

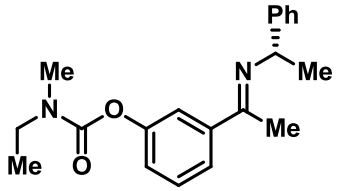

Prepared according to general procedure A starting from the corresponding ketone and (*S*)-phenylethylamine. The pure product was obtained in 89% conversion. The imine was used in the following reduction without further purification.

^{1}H NMR (300 MHz, $CDCl_3$) δ 7.67–7.61 (m, 2H), 7.24-7.45 (m, 7 H), 4.88 (q, *J* = 6.6 Hz, 1H) , 3.45 (m, 2H), 3.04 (br, 3H), 2.25 (s, 3H), 1.53 (d, *J* = 6.6 Hz, 3H), 1.26 (m, 3H).

N-(1-(3-benzyloxyphenyl)ethyl)-(*S*)-α-methylbenzylamine **(1-6)**

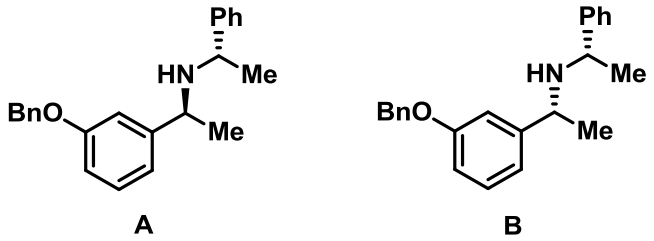

The reaction leaded to a mixture of the two diasteroisomers. Major (A) Minor (B).

^{1}H NMR (300 MHz, $CDCl_3$) δ: Selected signals for the evaluation of the diasteroisomeric ratio: 3.77 (m, 2H, diast. B), 3.49 (m, 2H diast. A).

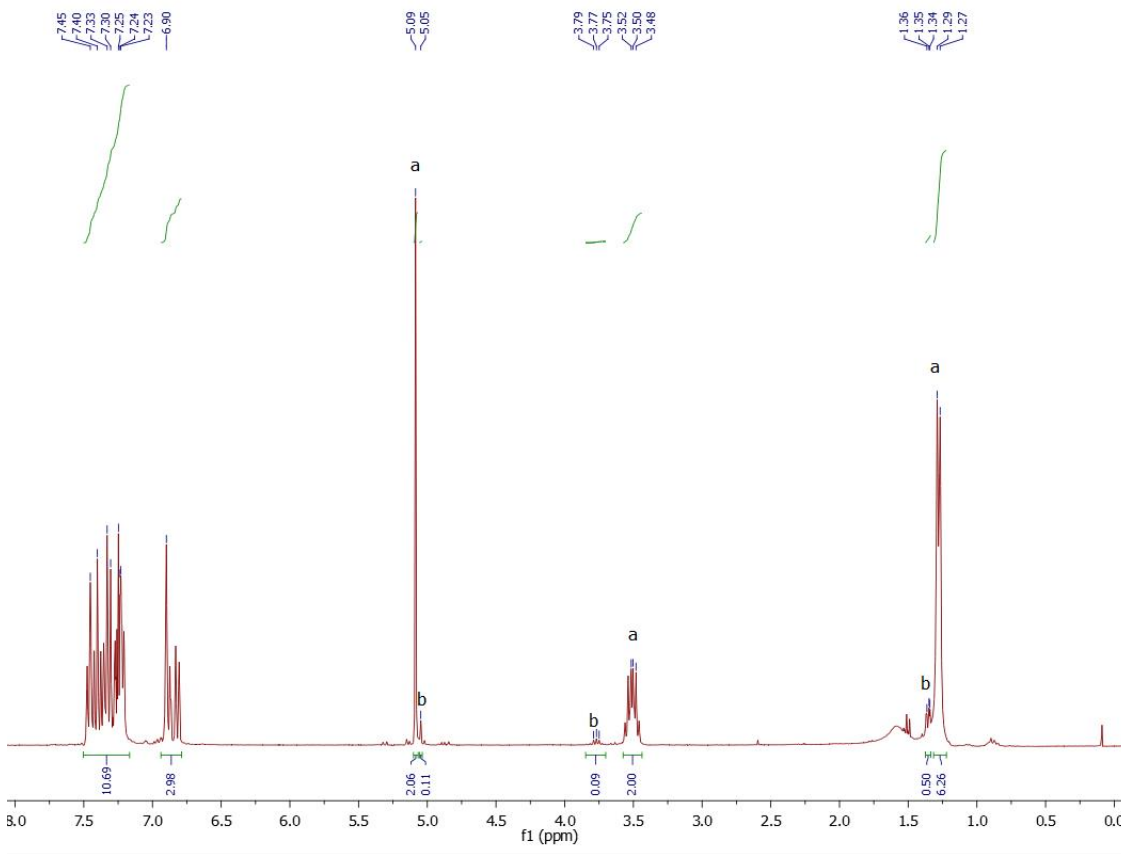

The major diasteroisomer A was obtained pure after flash column chromatography on silica gel with a 90:10 hexane/ethyl acetate mixture as eluent. Rf = 0.18.

(*S*)-*N*-(1-(3-benzyloxyphenyl)ethyl)-(*S*)-α-methylbenzylamine

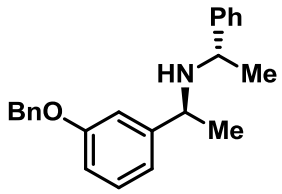

^{1}H NMR (300 MHz, $CDCl_3$) δ: 7.47-7.20 (m, 11H), 6.89-6.87 (m, 2H), 6.81 (d, 1H, *J* = 7.5 Hz), 5.08 (s, 2H), 3.49 (m, 2H), 1.26 (d, 6H, J=6.3 Hz)

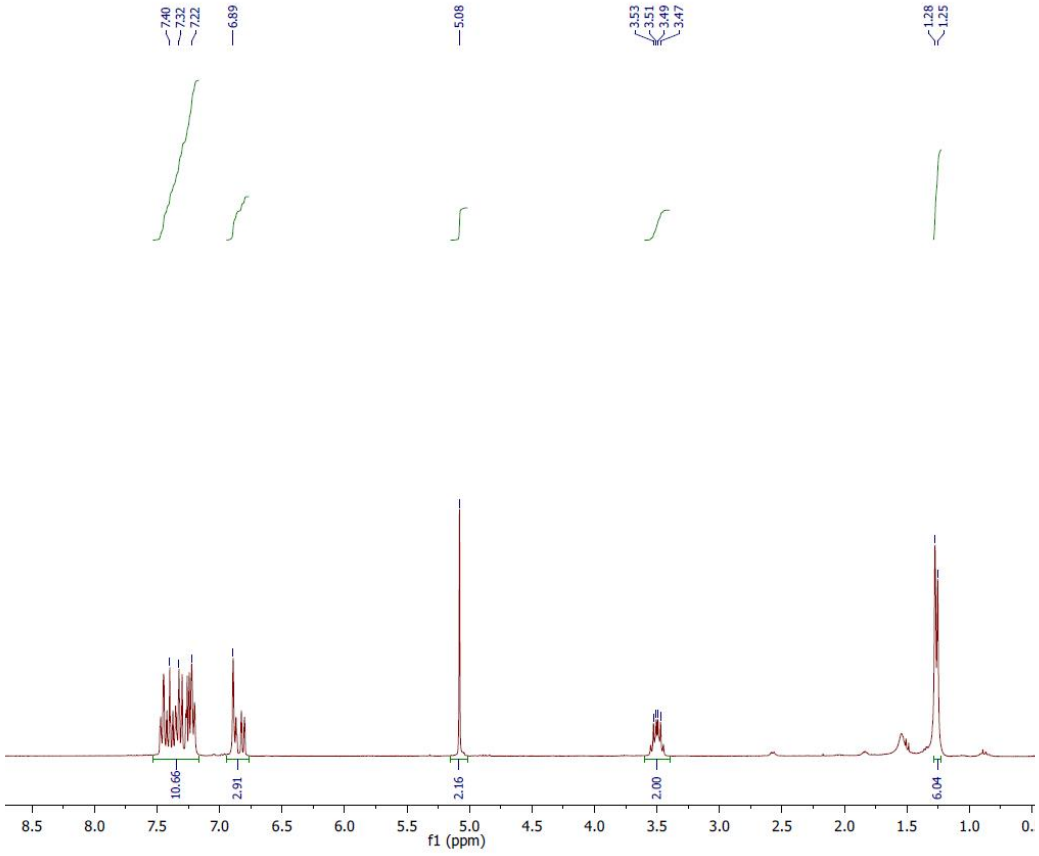

N-(1-(3-methoxyphenyl)ethyl)-(*S*)-α-methylbenzylamine **(1-3)**

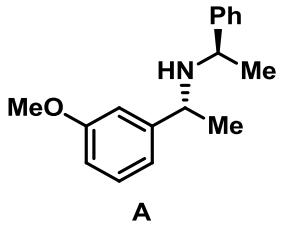

A

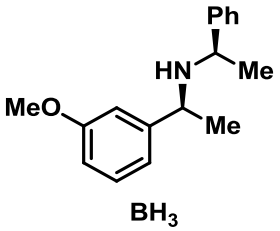

BH_3

The reaction leaded to a mixture of the two diasteroisomers. Major (A) Minor (B).

^{1}H NMR (300 MHz, $CDCl_3$): Selected signals for the evaluation of the diasteroisomeric ratio: 3.79 (m, 2H, diast. B), 3.50 (m, 2H, diast. A).

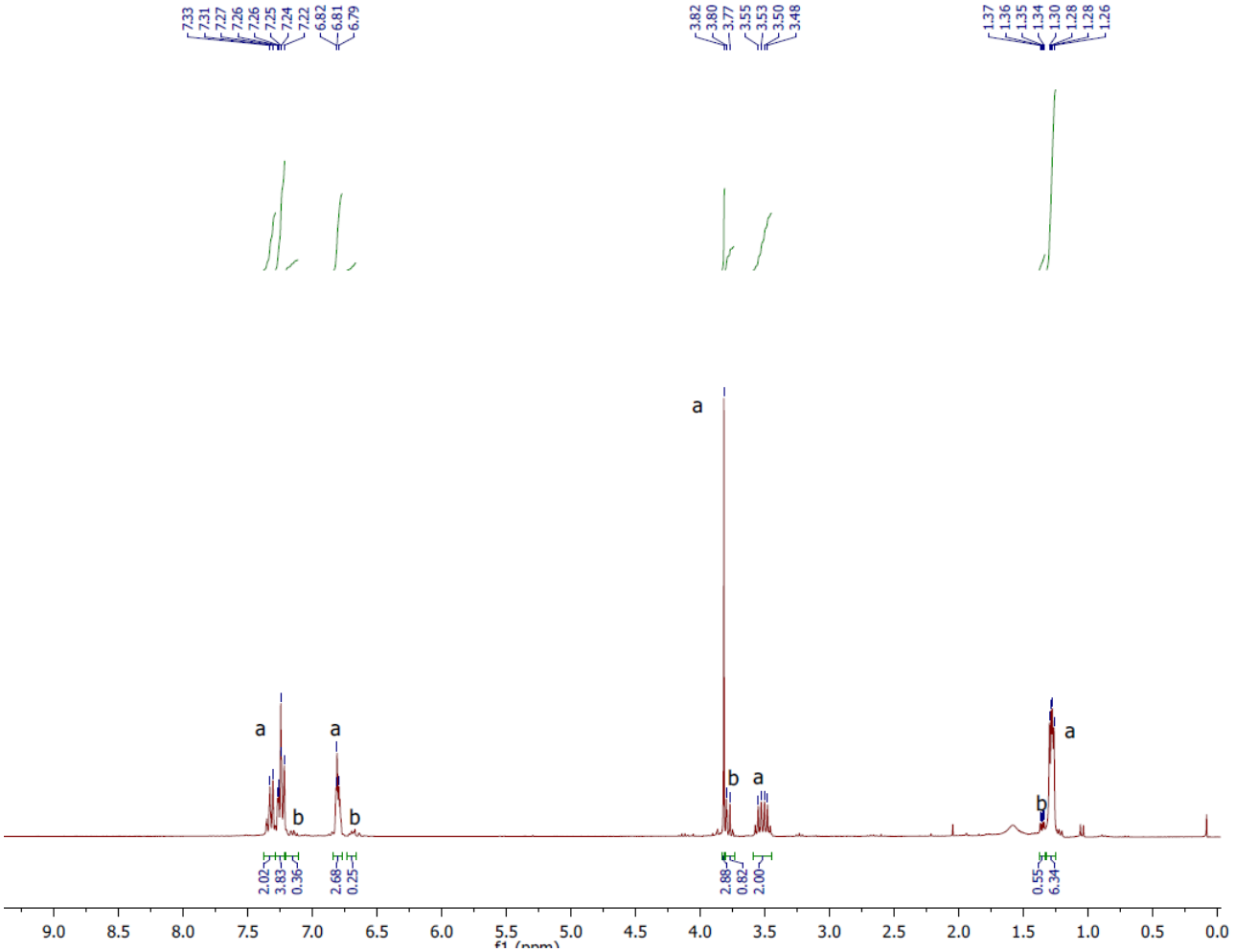

The major diasteroisomer A was obtained pure after flash column chromatography on silica gel with a 90:10 hexane/ethyl acetate mixture as eluent. Rf = 0.20.

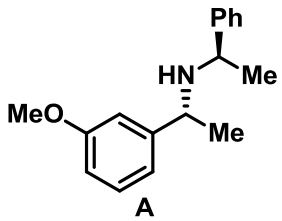

^{1}H NMR (300 MHz, $CDCl_3$) δ 7.39–7.05 (m, 6H), 6.81 (m, 3H), 3.82 (s, 3H), 3.50 (m, 2H), 1.54 (br, 1H), 1.28 (dd, 6H, J=6.5 Hz).

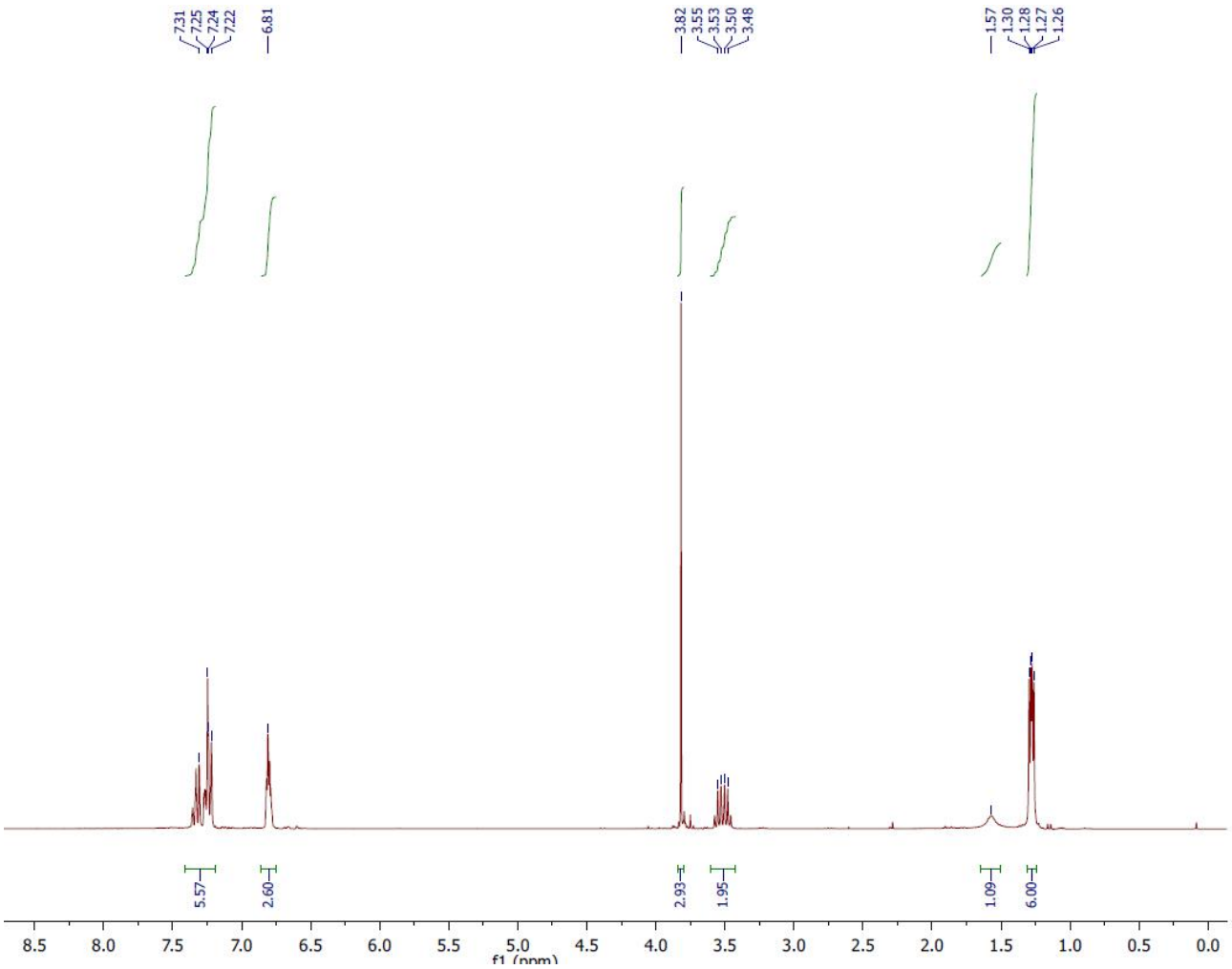

3-(((*S*)-1-phenylethyl)amino)ethyl)phenyl ethyl (methyl) carbamate

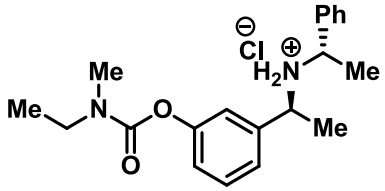

The amine was obtained as HCl salt. In a round bottom flask, the crude mixture was solved into Et_2O. The solution was cooled to 0 °C and one equivalent of a 2M HCl solution in Et_2O was added dropwise, leading to the formation of a precipitate. The salt was collected and washed with cold Et_2O. The product was used without any further purification in the next step.

^{1}H NMR (300 MHz, $CDCl_3$): 7.56 – 7.12 (m, 9H), 3.89 (m, 2H), 3.48 (m, 2H), 3.07 (br, 3H), 1.89 (d, *J* = 6.1 Hz, 6H), 1.23 (m, 3H).

^{13}C NMR (75 MHz, $CDCl_3$) δ 154.27, 151.85, 137.42, 136.05, 134.97, 130.25 (2C), 129.59, 129.20 (3C), 128.43, 60.14, 57.06, 44.20, 34.32, 33.96, 21.28, 13.27, 12.49.

HRMS: m/z calc. for $C_{20}H_{27}N_2O_2$(+1) = 327.20670; found = 327,20664

HRMS: m/z calc. for $C_{20}H_{26}N_2O_2Na_1$(+1) = 349.18865; found = 349,18880

3-((*S*)-1-(methyl((*S*)-1-phenylethyl)amino)ethyl)phenyl ethyl(methyl)carbamate (**1-8**)

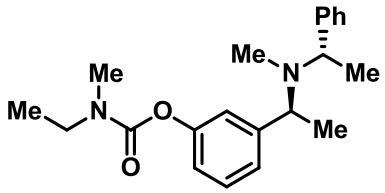

In a vial containing the amine 98% aqueous formic acid solution (2 eq.) followed by 37% aqueous formaldehyde solution (3 eq.) were added. The reaction mixture was heated to reflux for 4 h. After cooling to room temperature, 1 mL water was added. Na_2CO_3 was added until neutral pH was reached. The resulting mixture was extracted with ethyl acetate (5 ml X 3). The combined organic phases were washed with 5 mL water and dried over anhydrous Na_2SO_4. The solvent was removed under reduced pressure and the product purified by distillation.

^{1}H NMR (300 MHz, $CDCl_3$) δ 7.56 – 7.11 (m, 9H), 4.23 (m, 2H), 3.43 (m, 2H), 3.05 (br, 3H), 2.76 (s, 3H), 1.67 (dd, *J* = 6.4, 4.0 Hz, 6H), 1.25 (m, 3H)

Amine deprotection

General procedure for batch amine deprotection: A 0.5 M solution of the amine in ethanol charged into a vial for high pressure hydrogenation (PARR instrument), 10 % of Pd/C was added to the solution and the hydrogenation was carried out at 10 bar for 48 hours.

*Compound **1-1***: The Ethanol suspension was filtered through a celite pad and washed with 50 mL of MeOH, the solution was then treated with 1 equivalent of a 2M solution of HCl in Et_2O. The solvents were removed under pressure. The residue was dissolved in DCM and treated with Amberlyst IRA-400 (OH-) resin in order to get the free amine.

Compound **1-4***:* The Ethanol suspension was filtered through a celite pad and washed with 50 mL of MeOH, the solvents were removed under pressure and the compound was obtained as free amine.

General procedure for H-Cube Mini deprotection:

For the synthesis of **6:** A 0.1M solution of the amine (1.51mmol, 0,5 g) in ethanol (15mL) was charged into a vial connected with the pump of the H CUBE Mini, equipped with a 30 mm cartridge of 10% Pd/C. The instrument was previously stabilized at the desired temperature and pressure and at 1 mL7min as flow rate. The reaction was run in a close loop for the desired time.

*Compound **1-1*** : The Ethanol suspension was filtered through a celite pad and washed with 50 mL of MeOH, the solution was then treated with 1 equivalent of a 2M solution of HCl in Et_2O. The solvents were removed under pressure. The residue was dissolved in DCM and treated with Amberlyst IRA-400 (OH-) resin in order to get the free amine.

*Compound **1-4***: The Ethanol suspension was filtered through a celite pad and washed with 50 mL of MeOH, the solvents were removed under pressure and the compound was obtained as free amine.

1-*S*-(3-hydroxyphenyl)ethylamine (**1-1**)

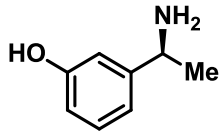

^{1}H NMR (300 MHz, MeOD) δ 7.19 (t, *J* = 8.1 Hz, 1H), 6.91–6.81 (m, 2H), 6.82–6.72 (m, 1H), 4.27–4.13 (m, 1H), 1.51 (d, *J* = 6.8 Hz, 3H).

$[\alpha]^T_{D:}$ 1g/100mL methanol 589 nm = -22.1 deg

The spectroscopic data, $[\alpha]^T$was in accord with the one reported by the literature.[104]

GC method: injector 200 °C; flow 2mL/min; temperature program 100 °C/hold 2 min.; 130 °C/rate 1 °C per min./hold 5 min; 170°C/rate 2 °C per min/hold 5 min.: t_{ret}: 58.219 min[105]

1-*R*-(3-methoxyphenyl)ethylamine (**1-4**)

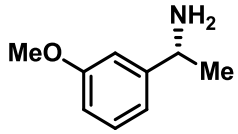

^{1}H NMR (300 MHz, MeOH) δ 7.18 (d, J = 8.3 Hz, 1H), 6.90 (t, J = 4.3 Hz, 1H), 6.82 – 6.69 (m, 2H), 3.97 (q, J = 6.7 Hz, 1H), 3.76 (s, 3H), 1.35 (d, J = 6.7 Hz, 3H).

The spectroscopic data and the $[\alpha]^T_D$[106] were in accord with the one reported in the literature.[107]

$[\alpha]^T_{D:}$ 0.4g/100mL methanol 589 nm = 24.3 deg

.

Advanced precursors of Rasagiline and Tamsulosin: products description

Imines description

N-(4-Methoxyphenyl)-indanimine (**1-12**)

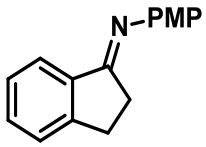

Synthetized according to general procedure A, starting from 1-indanone and *p*-anisidine. The pure product was obtained in 90% yield after purification by precipitation of the excess of starting amine using hexane.

^{1}H NMR (300 MHz, $CDCl_3$) *E:* δ: 7.94 (m, 1 H), 7.48-7.43 (m, 1H), 7.39-7.33 (d, 2H *J* = 9.0 Hz), 6.91 (m, 4H), 3.82 (s, 3H), 3.08-3.04 (m, 2H,), 2.75-2.70 (m, 2H).

Compound **1-12** is known, and all analytical data are in agreement with literature[108]

N-benzyl-1-indanimine (**1-13**)

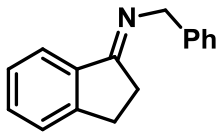

Synthetized according to general procedure C starting from 1-indanone and benzylamine.

The product was obtained in 60% yield after purification by fractional distillation at P = 3 x 10^{-2} mbar with Glass Oven B-585 Kugel Rohr set to 95 °C.

^{1}H NMR (300 MHz, $CDCl_3$)*:* δ: 7.92 (d, 1H J = 7.5 Hz), 7.45-7.24 (m, 8H), 4.74 (s, 2H), 3.16-3.12 (m, 2H), 2.84-2.80 (m, 2H).

Compound **1-13** is known, and all analytical data are in agreement with literature[109]

(*R*)-*N*-(α-methylbenzyl)indanimine (**1-15**)

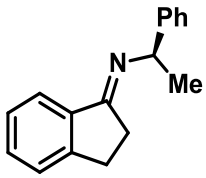

Synthetized according to general procedure B starting from 1-indanone and (*R*)-phenylethylamine. The pure product was obtained in 93% yield after purification by fractional distillation at P = 3 x 10^{-2} mbar with Glass Oven B-585 Kugel Rohr set to 95 °C. The imine was a 9:1 mixture of the *E* and the *Z* isomers.

Major isomer:

^{1}H NMR (300 MHz, $CDCl_3$) *E:* δ: 7.99 (d, 1H), 7.58-7.31 (m, 8H), 4.70 (q, 1H), 3.05 (m, 2H), 2.83 (m, 1H), 2.57 (m, 1H), 1.60 (d, 3H, *J* = 9.0 Hz).

Compound **1-15** is known, and all analytical data are in agreement with literature[110]

(*R*)-*N*-(4-methoxyphenylethyl)indanimine (**1-17**)

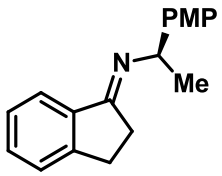

Synthetized according to general procedure A starting from 1-indanone and (*R*)-4-Methoxy-α-methylbenzylamine. The pure product was obtained in 60% yield after purification by crystallization in Et_2O. The imine was a pure *E* isomer.

^{1}H NMR (300 MHz, $CDCl_3$)*:* δ: 7.99 (d, 1H, J = 6.5 Hz), 7.41-7.31 (m, 5H), 6.91 - 6.88 (m, 2H), 4.66 (q, 1H, J = 6.6 Hz), 3.81 (s, 3H), 3.11-3.05 (m, 2H), 2.90-2.83 (m, 1H), 2.72-2.57 (m, 1H), 1.50 (d, 3H, *J* = 6.6 Hz).

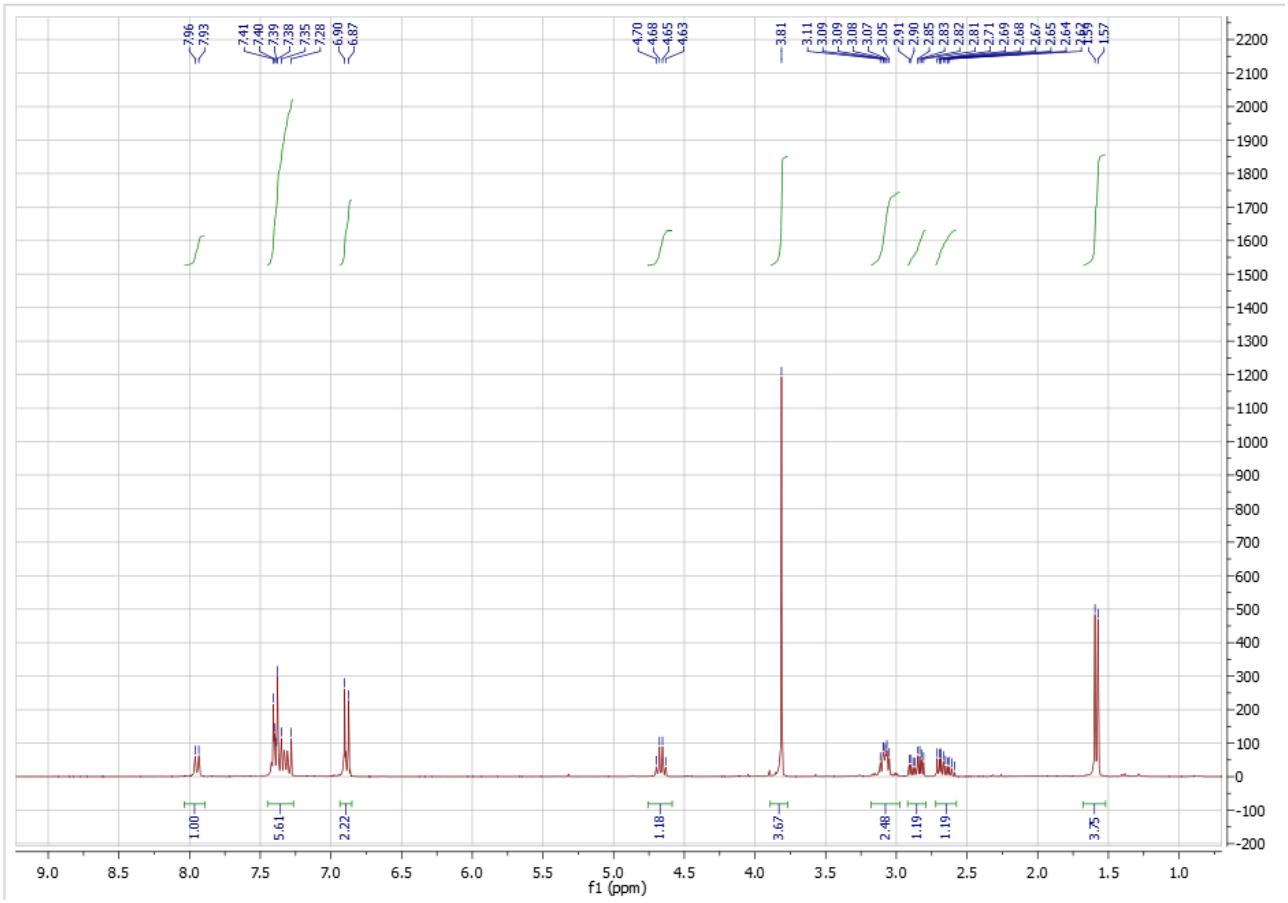

^{13}C NMR (75 MHz, $CDCl_3$) δ 172.35, 158.24, 149.39, 140.17, 138.23, 130.98, 127.65 , 126.83, 125.47, 122.67 (2C), 113.72 (2C), 61.03 , 55.27, 28.09 (2 C), 24.89.

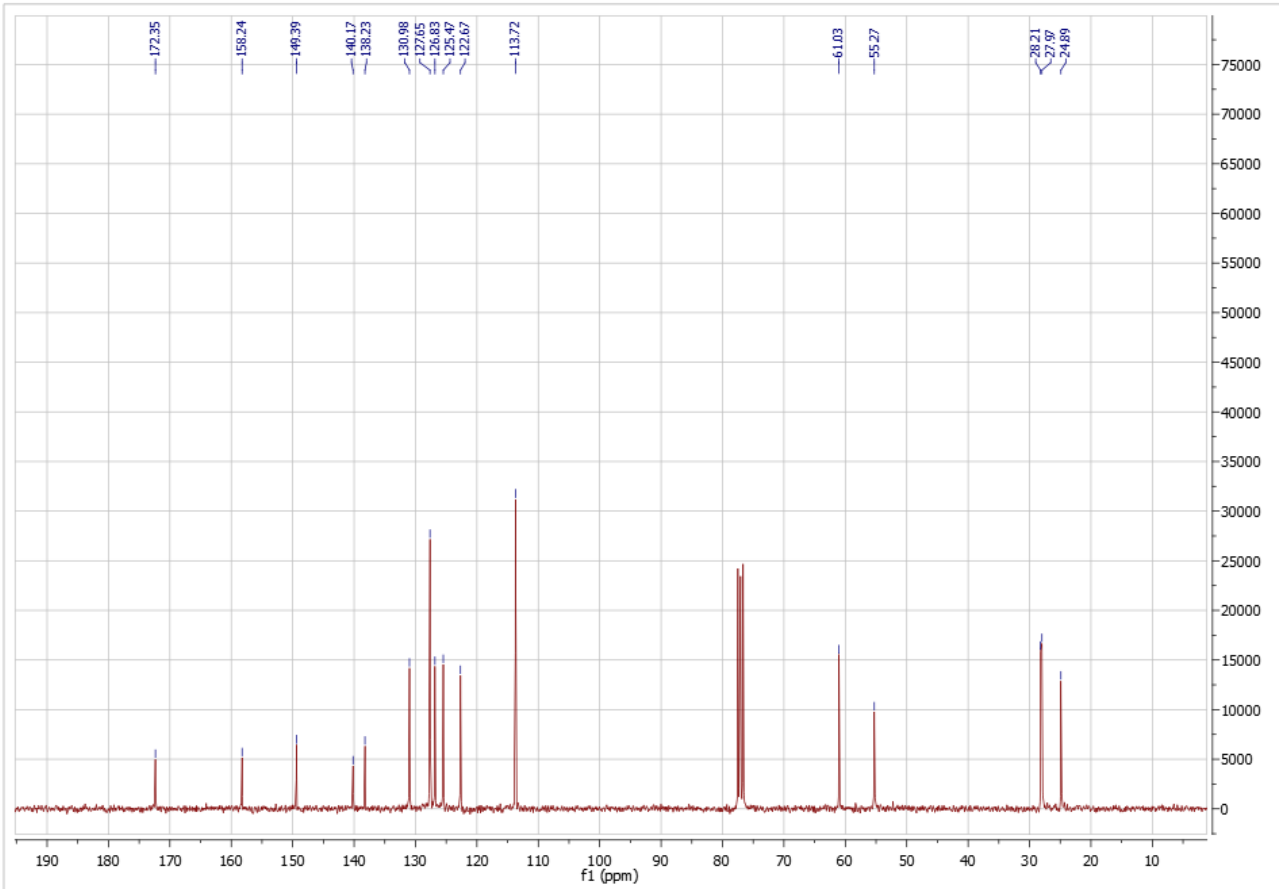

HRMS: m/z calc. for $C_{18}H_{19}NO$ (+1) = 266.15394; found = 266.15439

(*R*)-*N*-(2,3-dihydroinden-1-ylidene)-2-methylpropane-2-sulfinamide (**1-18**)

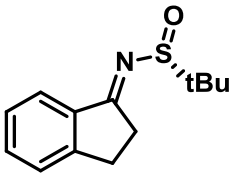

Synthetized according to general procedure D starting from 1-indanone and (*R*)-(+)-2-Methyl-2-propanesulfinamide. The product was obtained in 40% yield after chromatographic purification. (8:2 Hexane:AcOEt).

^{1}H NMR (300 MHz, $CDCl_3$)*:* δ: 7.83 (d, *J* = 7.7 Hz, 1H), 7.50 - 7.32 (m, 3H), 3.56 – 3.41 (m, 1H), 3.17 (m, 3H), 1.34 (s, 9H).

Compound **1-18** is known and all analytical data are in agreement with literature[111]

N-(1-(*R*)-phenylethyl)-propan-1-(4-methoxyphenyl)-1-imine (**1-21**)

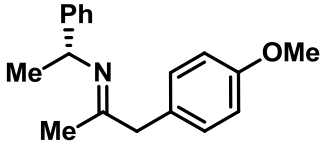

Synthetized according to general procedure B starting from 4-methoxyphenylacetone and (*R*)-phenylethylamine. The pure product was obtained in 85% yield after purification by fractional distillation at P = 3 x 10^{-2} mbar with Glass Oven B-585 Kugel Rohr set to 95 °C. The imine was obtained as yellow oil a 7:3 E/Z mixture.

Major isomer: (*E*)

^{1}H NMR (300 MHz, $CDCl_3$) *E:* δ: 7.45 – 7.11 (m, 7H), 6.86-6.84 (m, 2H), 4.63 (q, 1H, J = 6.6 Hz), 3.90 (s, 3H), 3.56 (s, 2H),1,77 (s, 3H), 1.53 (d, 3H, *J* = 6.6 Hz).

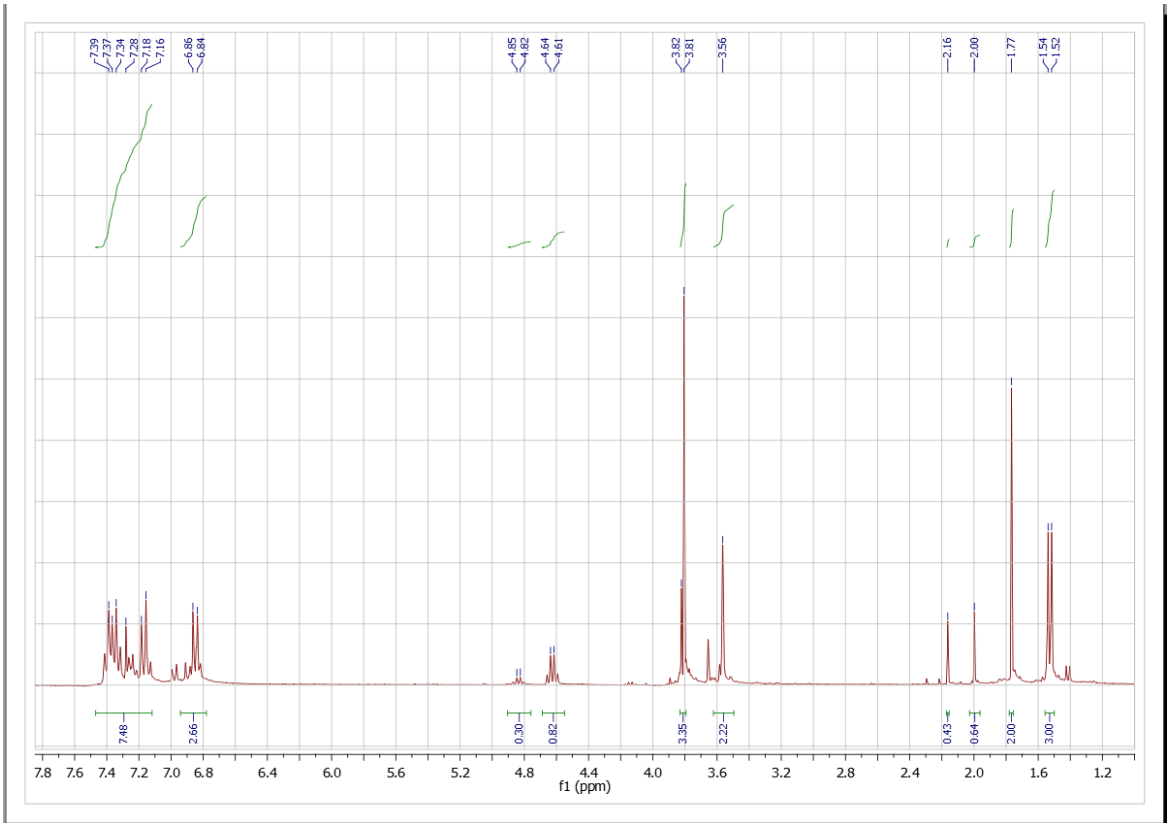

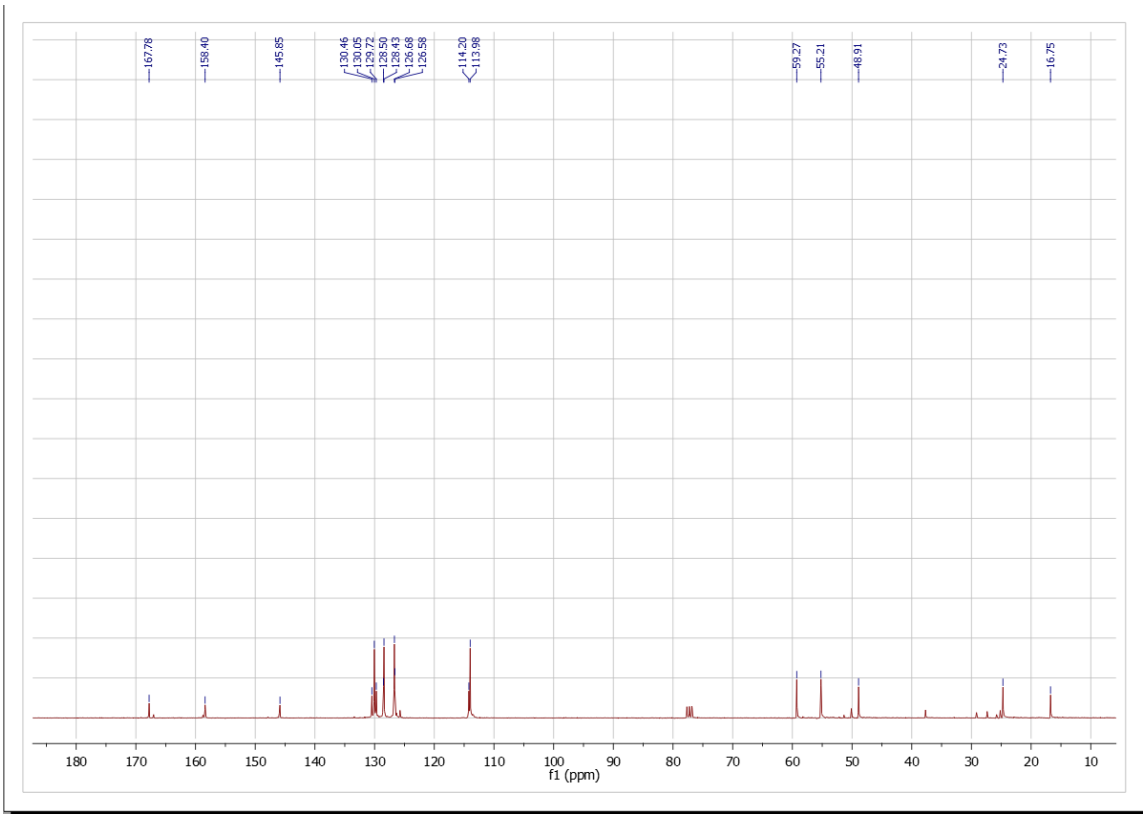

^{13}C NMR (75 MHz, $CDCl_3$) δ 167.78, 158.40, 145.85, 130.46, 130.05, 129.72 (2C), 128.46 (2 C), 126.63 (2C), 114.09 (2C), 59.27, 55.21, 48.91, 24.73, 16.75.

HRMS: m/z calc. for $C_{18}H_{21}NO$ (+1) = 290,11852; found = 290,11938

N-(2-methylpropane-2-sulfinamide)-propan-1-(4-(methoxy)phenyl)-1-imine (**1-22**)

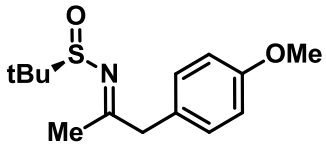

Synthetized according to general procedure D starting from 1-indanone and (*R*)-(+)-2-Methyl-2-propanesulfinamide. The product was obtained in 30% yield as brown oil after chromatographic purification. (9:1 Hexane:AcOEt).

^{1}H NMR (300 MHz, $CDCl_3$) δ 7.14 (d, *J* = 8.6 Hz, 2H), 6.87 (d, *J* = 8.6 Hz, 2H), 3.81 (s, 3H), 3.70–3.55 (AB system, 2H), 2.28 (s, 3H), 1.22 (s, 9H).

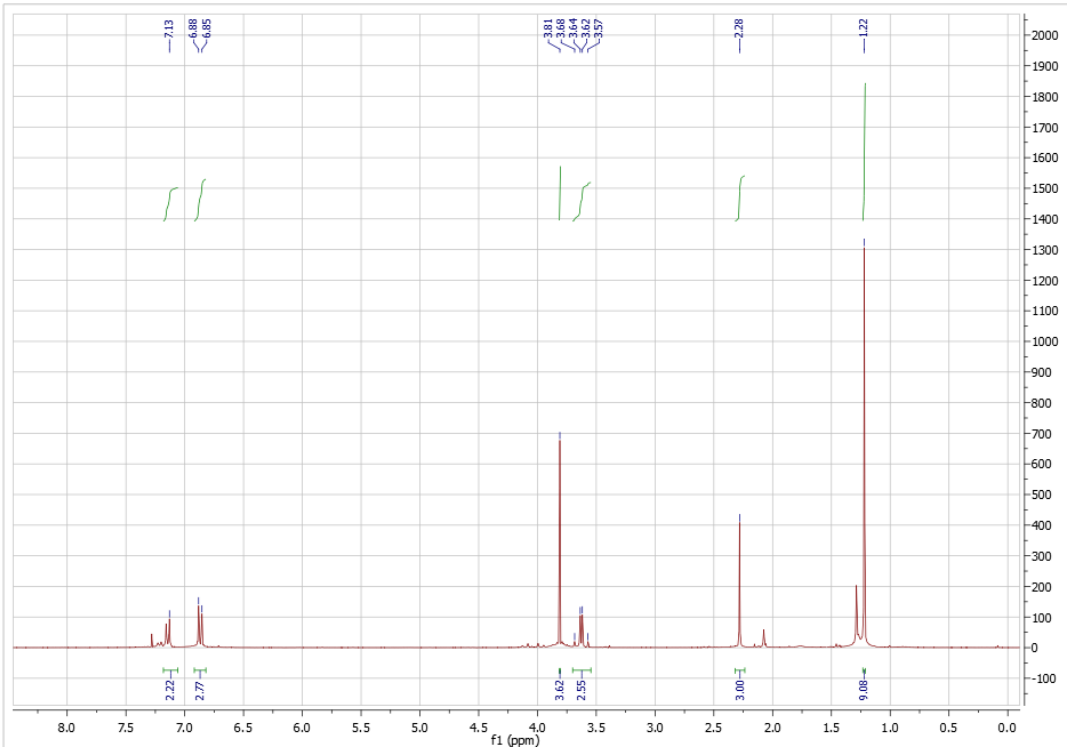

^{13}C NMR (75 MHz, $CDCl_3$) δ 183.73, 158.69, 130.33, 127.70 (2C), 114.14 (2C), 56.58, 55.26, 49.31, 38.05, 22.14 (3C).

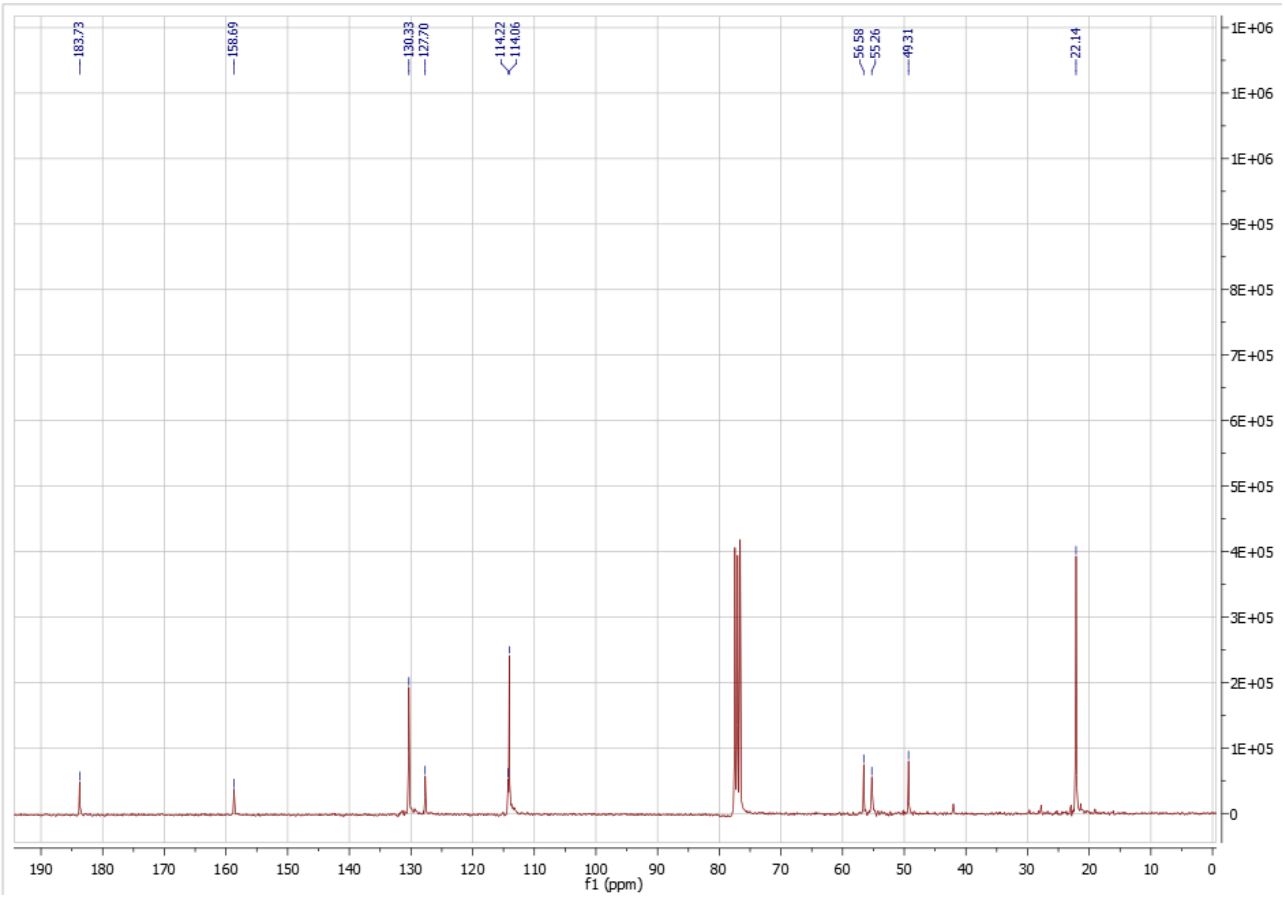

HRMS: m/z calc. for $C_{14}H_{21}NO_2S$ Na (+1) = 290.1554; found = 290.15275

HRMS: m/z calc. for $C_{14}H_{21}NO_2S$ (+1) = 260.16959; found = 260.17060

Amines precursors of Rasagiline and Tamsulosin

(*R*)-*N*-1-indan-(*p*-methoxyphenil)amine (**1-14**)

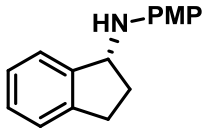

^{1}H NMR (300 MHz, $CDCl_3$) δ: 7.37 (d, 1H J = 7.3 Hz), 7.26-7.7.15 (m, 3H), 6.83 (d, 2H J = 9.0 Hz),6.74 (d, 2H J = 9.0 Hz), 4.98 (t, 1H), 3.79 (s, 3H), 3.09 (m, 1H), 2.85 (m, 1H), 2.57 (m, 1H), 1.95 (m, 1H).

The enantiomeric excess was determined by chiral HPLC with Daicel Chiralcel IB column, eluent: 99:1 Hex/IPA; 0.75 mL/min flow rate, detection: 254 nm, t_R 13.50 min (major), t_R 14.40 min.(min)

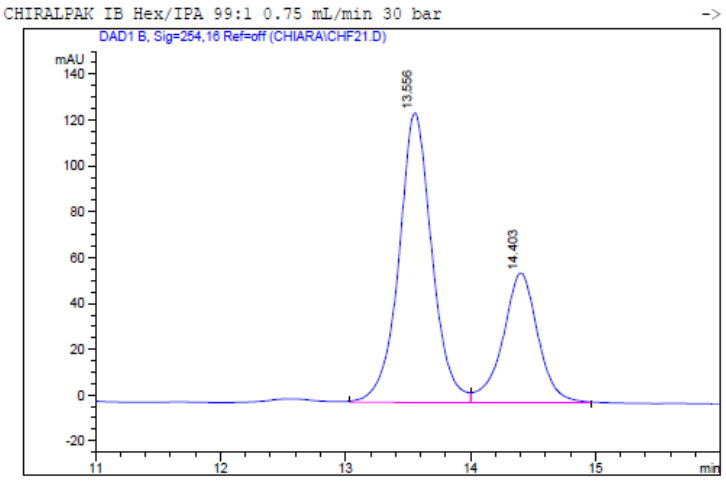

Signal 1: DAD1 B, Sig=254,16 Ref=off

Peak #	RT [min]	Type	Width [min]	Area	Area %	Name
1	13.556	BV	0.274	2323.444	67.771	
2	14.403	VB	0.292	1104.937	32.229	

Compound **1-14** is known and all analytical data are in agreement with literature[112]

(*R*)-*N*-1-benzyl-indanamine **1-15**

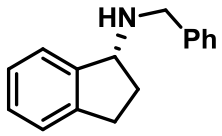

^{1}H NMR (300 MHz, $CDCl_3$) δ: 7.54 (d, 1H), 7.48 (d, 2H), 7.33 (m, 1H), 7.26-7.22 (m, 5H), 4.37 (t, 1H), 3.88 (s, 2H), 3.09 (m, 1H), 2.85 (m, 1H), 2.39 (m, 1H), 2.09 (m, 1H).

Compound **1-15** is known, and all analytical data are in agreement with literature [113]

The enantiomeric excess was determined by chiral HPLC with Phenomenex Amylose 2 column, eluent: 9:1 Hex/IPA; 0.8 mL/min flow rate, detection: 220 nm, t_R 5.50 min, (minor) t_R 5.90 min.(major) Racemic compound was obtained by reduction with $NaBH_4$ of the corresponding amine.

```
Injection Date  : Tue, 6. Sep. 2016            Seq Line   :          0
Sample Name     : oan amy2 10ipa               Location   :      Vial 1
Acq Operator    : 1                            Inj. No.   :          0
                                               Inj. Vol.  :          -
```

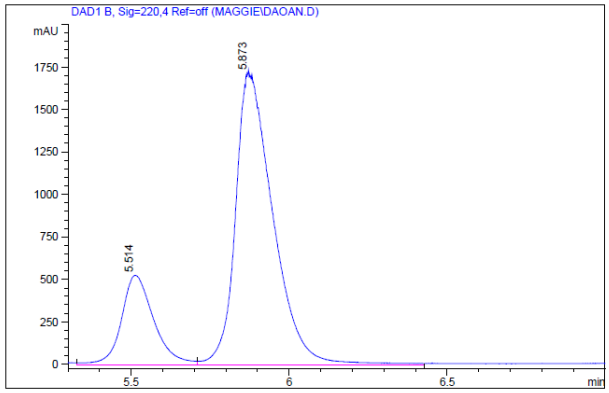


```
Signal  1: DAD1 B, Sig=220,4 Ref=off

|Peak|   RT    | Type  | Width |   Area    | Area % |     Name      |
| #  |  [min]  |       | [min] |           |        |               |
|----|---------|-------|-------|-----------|--------|---------------|
|   1|    5.514|VV     |  0.107|  3739.803|  20.898|               |
|   2|    5.873|VV     |  0.121| 14155.527|  79.102|               |
-------------------------------------------------------------------
```

```
Injection Date  : Tue, 6. Sep. 2016            Seq Line   :          0
Sample Name     : racn amy2 10ipa              Location   :      Vial 1
Acq Operator    : 1                            Inj. No.   :          0
                                               Inj. Vol.  :          -
```

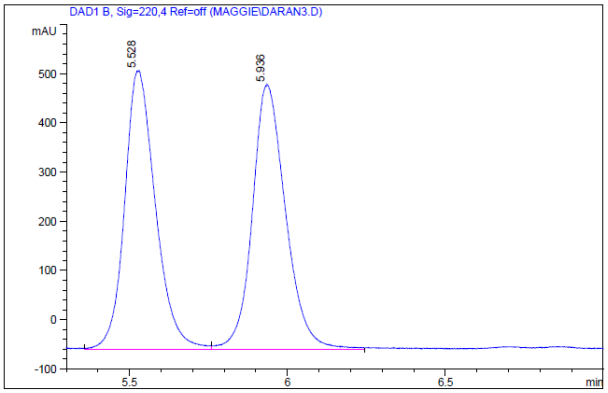


```
Signal  1: DAD1 B, Sig=220,4 Ref=off

|Peak|   RT    | Type  | Width |   Area    | Area % |     Name      |
| #  |  [min]  |       | [min] |           |        |               |
|----|---------|-------|-------|-----------|--------|---------------|
|   1|    5.528|VV     |  0.104|  3852.656|  49.364|               |
|   2|    5.936|VV     |  0.108|  3951.975|  50.636|               |
-------------------------------------------------------------------
```

(*R, R*)-*N*-1-indan-(1-phenylethyl)amine (**1-16**)

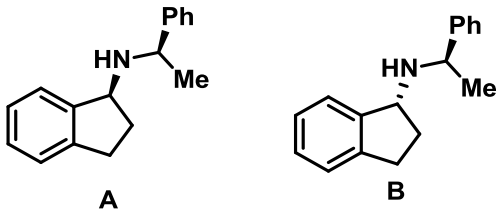

The reaction leaded to a mixture of the two diasteroisomers. Major (B) Minor (A).

^{1}H NMR (300 MHz, $CDCl_3$) δ: Selected signals for the evaluation of the diasteroisomeric ratio: 4.18 (m, 2H, diast. B), 4.09 (m, 2H, diast. A).

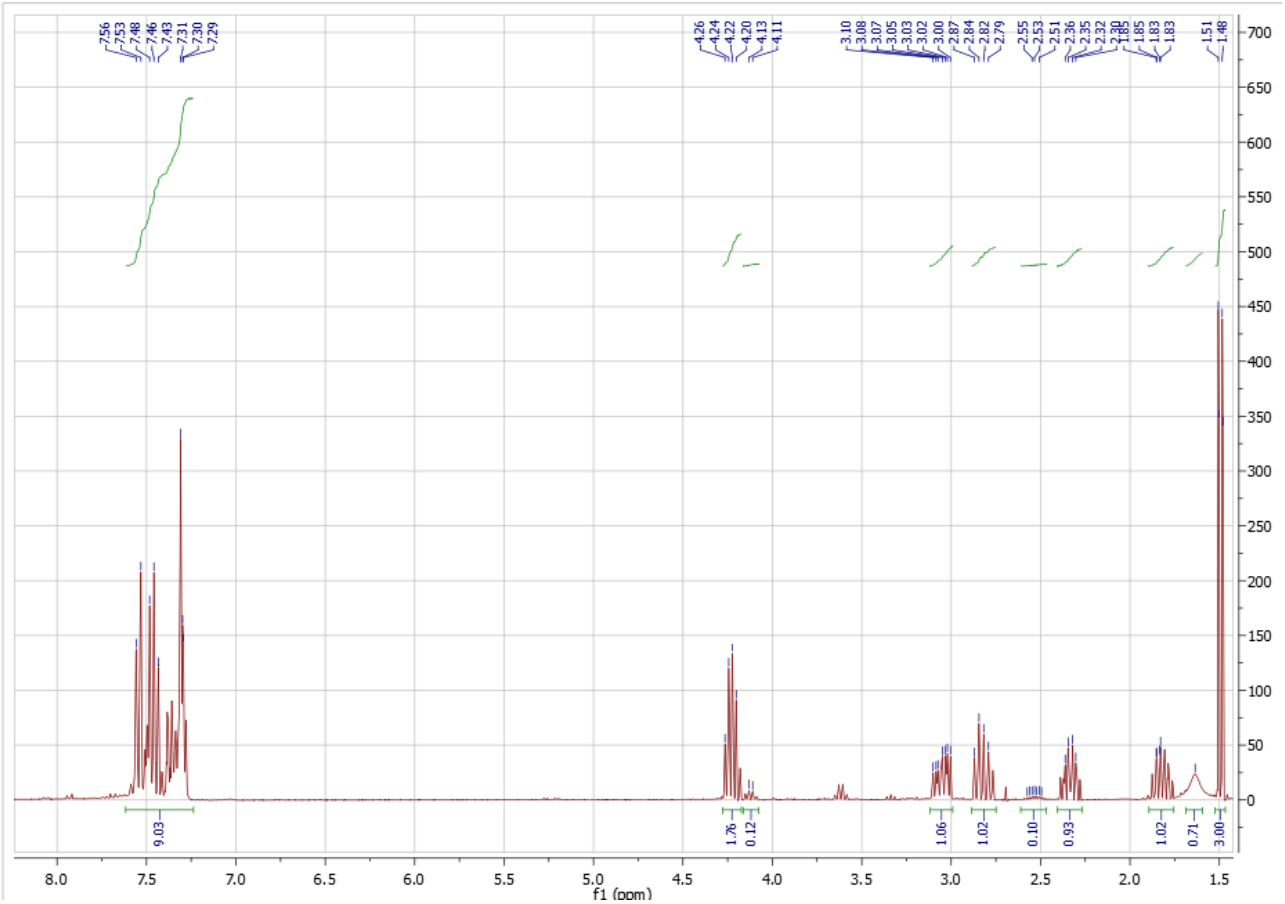

Major isomer:

^{1}H NMR (300 MHz, $CDCl_3$) δ: 7.24-7.52 (m, 9H), 4.15-4.22 (m, 2H), 2.98-3.05 (m, 1H), 2.75-2.82 (m, 1H), 2.26-2.34 (m, 1H), 1.74-1.82 (m, 1H), 1.60 (s, 1H), 1.46 (d, 3H).

Compound **1-16** is known, and all analytical data are in agreement with literature [110]

(*R, R*)-*N*-1-indan-(1-*p*-methoxyphenylethyl)amine (**1-19**)

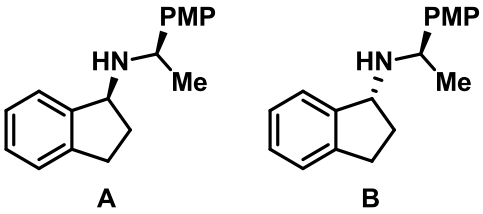

The mixtures of the two diasteroisomers is a transparent oil

The reaction leaded to a mixture of the two diasteroisomers. Major (B) Minor (A).

^{1}H NMR (300 MHz, $CDCl_3$) δ: Selected signals for the evaluation of the diasteroisomeric ratio: 2.45 (m, 1H, diast. A), 2.20 (m, 1H, diast. B).

Major isomer:

^{1}H NMR (300 MHz, $CDCl_3$) δ: 7.38 (d, 2H, J = 8.6 Hz), 7.25-7.19 (m, 4H), 6.92 (d, 2H. J = 8.6 Hz) 4.15-4.22 (m, 2H), 3.84 (s, 3H), 2.98-3.05 (m, 1H), 2.75-2.82 (m, 1H), 2.28-2.22 (m, 1H), 1.74-1.82 (m, 1H), 1.40 (d, 3H, J = 6.5 Hz).

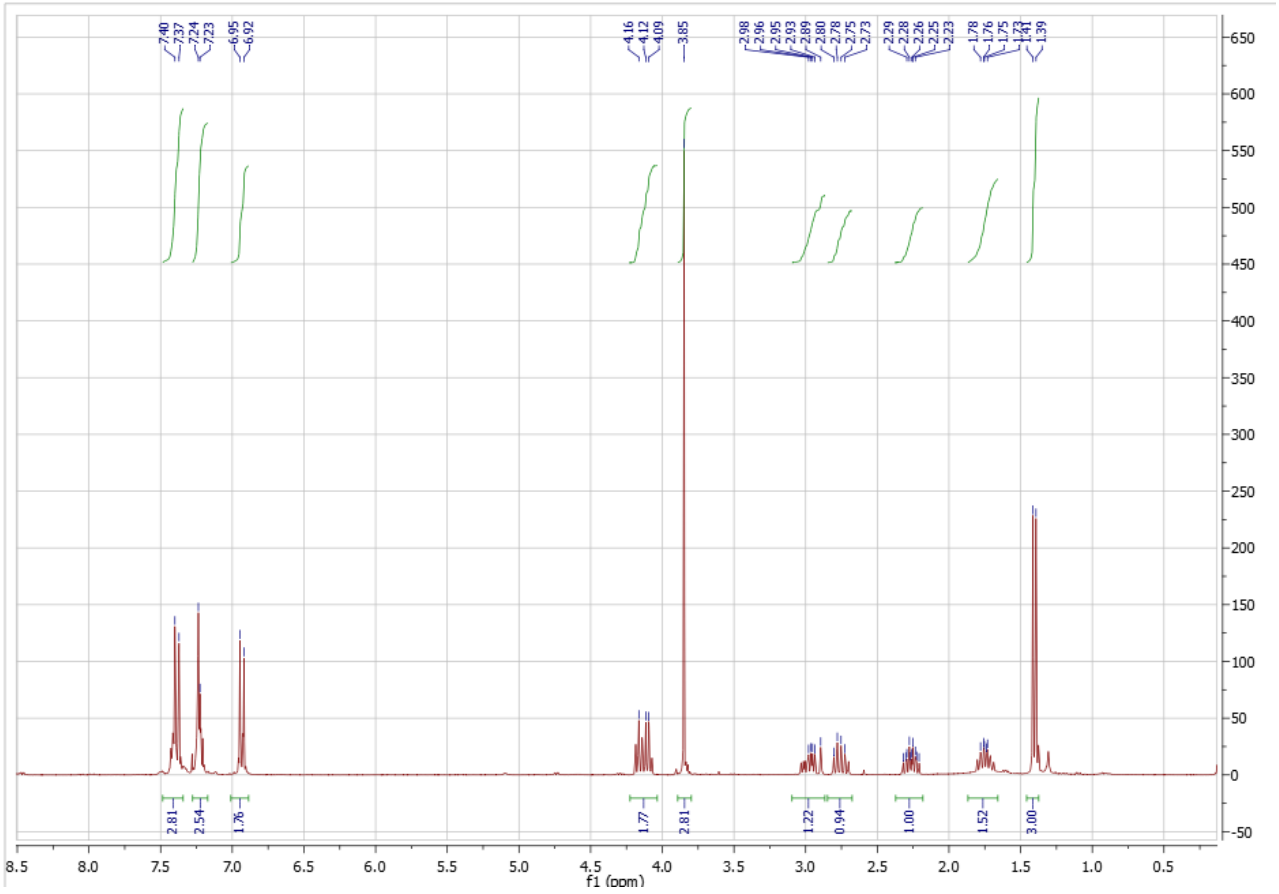

^{13}C NMR (75 MHz, $CDCl_3$) δ 172.36, 158.25, 149.39, 140.18, 138.24, 130.99, 127.65, 126.83, 125.47, 122.67 (2C), 113.72 (2C), 61.02, 55.27, 28.09 (2C), 24.88.

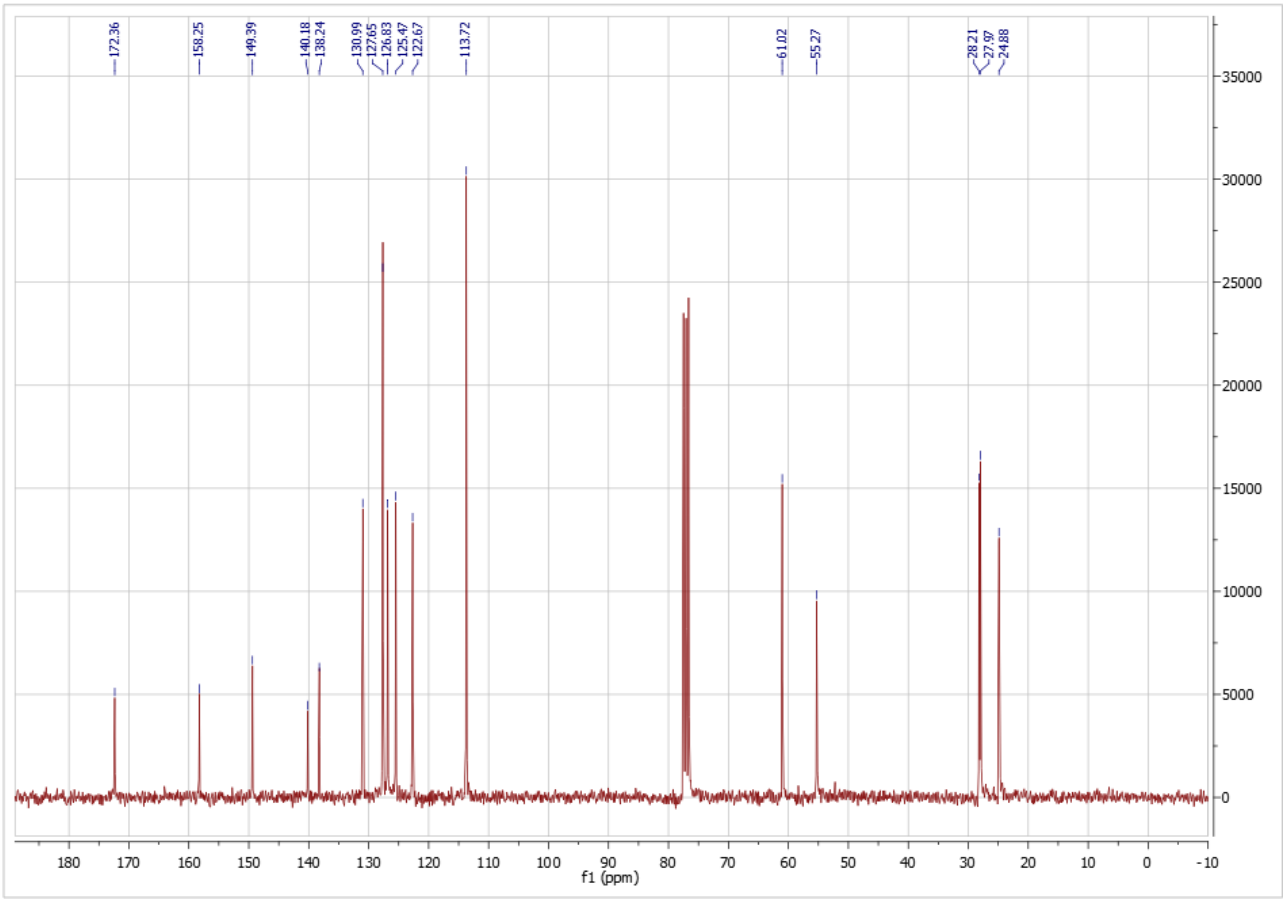

HRMS: m/z calc. for $C_{18}H_{21}NO$ (+1) = 268.16959; found = 268,17018

HRMS: m/z calc. for $C_{18}H_{21}NONa$ (+1) = 290.15154; found = 290,15231

(*R*)-Indanamine (**1-20**)

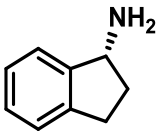

^{1}H NMR (300 MHz, $CDCl_3$) δ 7.53 – 7.12 (m, 4H), 4.39 (t, *J* = 7.4 Hz, 1H), 3.07 – 2.74 (m, 2H), 2.64 – 2.43 (m, 1H), 2.01 (br, 2H), 1.78 -1.65 (m, 1H).

The enantiomeric excess was determined by chiral HPLC on the benzoyl derivatives with Daicel Chiralcel OD-H column, eluent: 9:1 Hex/IPA; 0.5 mL/min flow rate, detection: 254 nm, t_{rue} 27.296 min (major), t_R 39.047 min.(min)

```
================================================================================
Injection Date  : Fri, 16. Dec. 2016            Seq Line   :           0
Sample Name     : DBP289_BENZOIL                Location   :
Acq Operator    : DAVIDE BRENNA                 Inj. No.   :           0
                                                Inj. Vol.  :           -

DBP289_BENZOIL
CHIRALCEL OD-H  Hex/IPA 9:1 1 mL/min 44 Bar 0.5mL/min                   ->
```

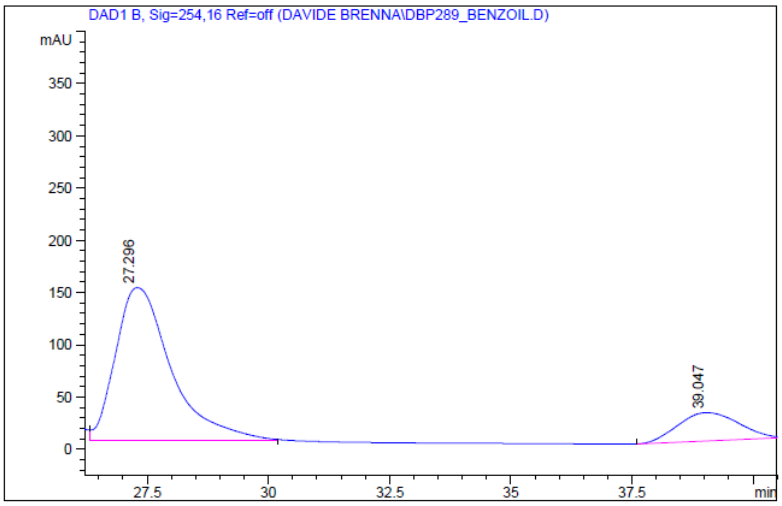


```
Signal  1: DAD1 B, Sig=254,16 Ref=off

|Peak|   RT    | Type  | Width |    Area    | Area % |     Name      |
| #  |  [min]  |       | [min] |            |        |               |
|----|---------|-------|-------|------------|--------|---------------|
|   1|  27.296|VB     |  1.181| 11626.629|  82.968|               |
|   2|  39.047|MM     |  1.466|  2386.685|  17.032|               |
--------------------------------------------------------------------------
```

Compound **1-20** is known and all analytical data are in agreement with literature [114]

(*R*)-1-(4-methoxyphenyl)-*N*-((*R*)-1-phenylethyl)propan-2-amine (**1-23**)

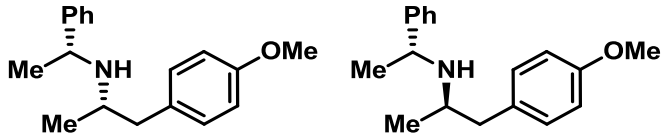

A **B**

The mixtures of the two diasteroisomers is a light-yellow oil

The reaction leaded to a mixture of the two diasteroisomers. Major (B) Minor (A).

^{1}H NMR (300 MHz, CDCl3) δ: Selected signals for the evaluation of the diasteroisomeric ratio: 1.07 (d, 3H, diast. A), 0.95 (d, 3H, diast. B).

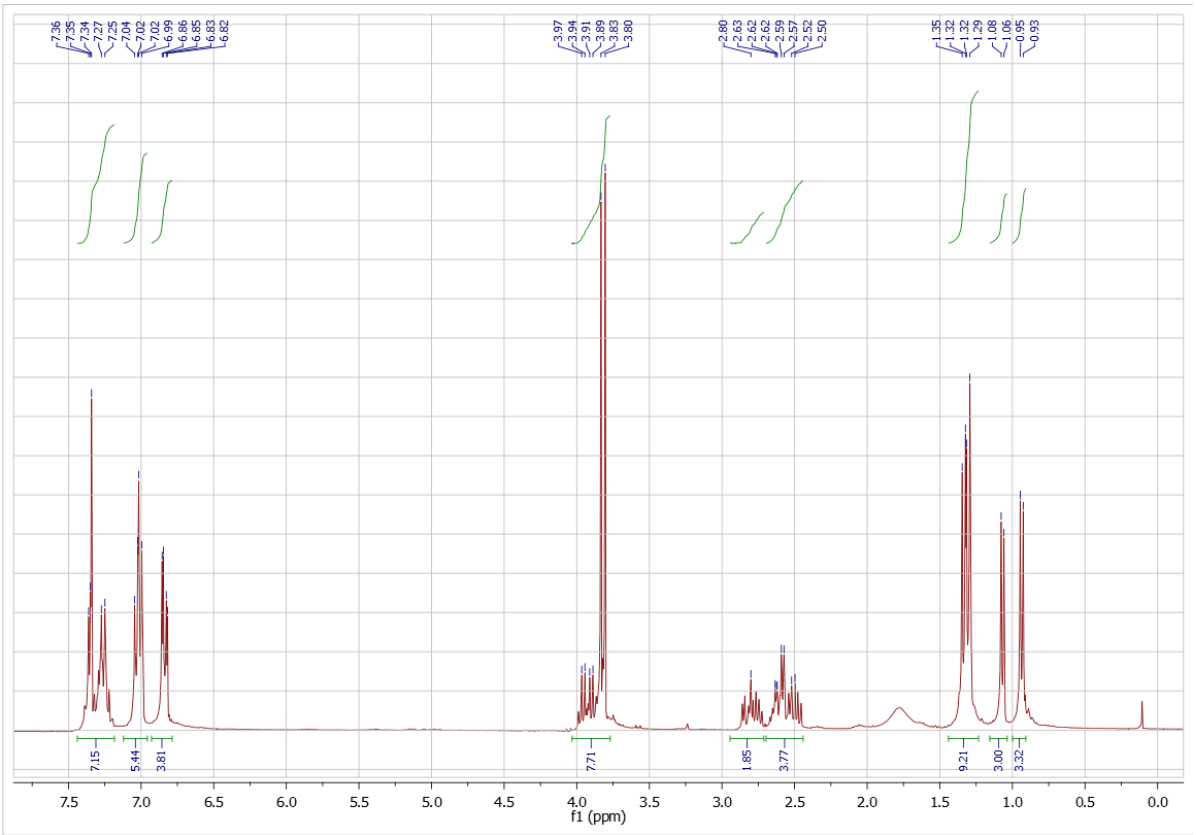

Major isomer:

^{1}H NMR (300 MHz, CDCl3) δ 7.42 – 7.22 (m, 5H), 7.02 (d, J = 8.6 Hz, 2H), 6.82 (d, J = 8.6 Hz, 2H), 3.98 (m, 1H), 3.80 (s, 3H), 2.93 – 2.73 (m, 2H), 2.54-2.47 (m, 1H), 1.37 (d, J = 6.6 Hz, 3H), 0.97 (d, J = 6.2 Hz, 3H).

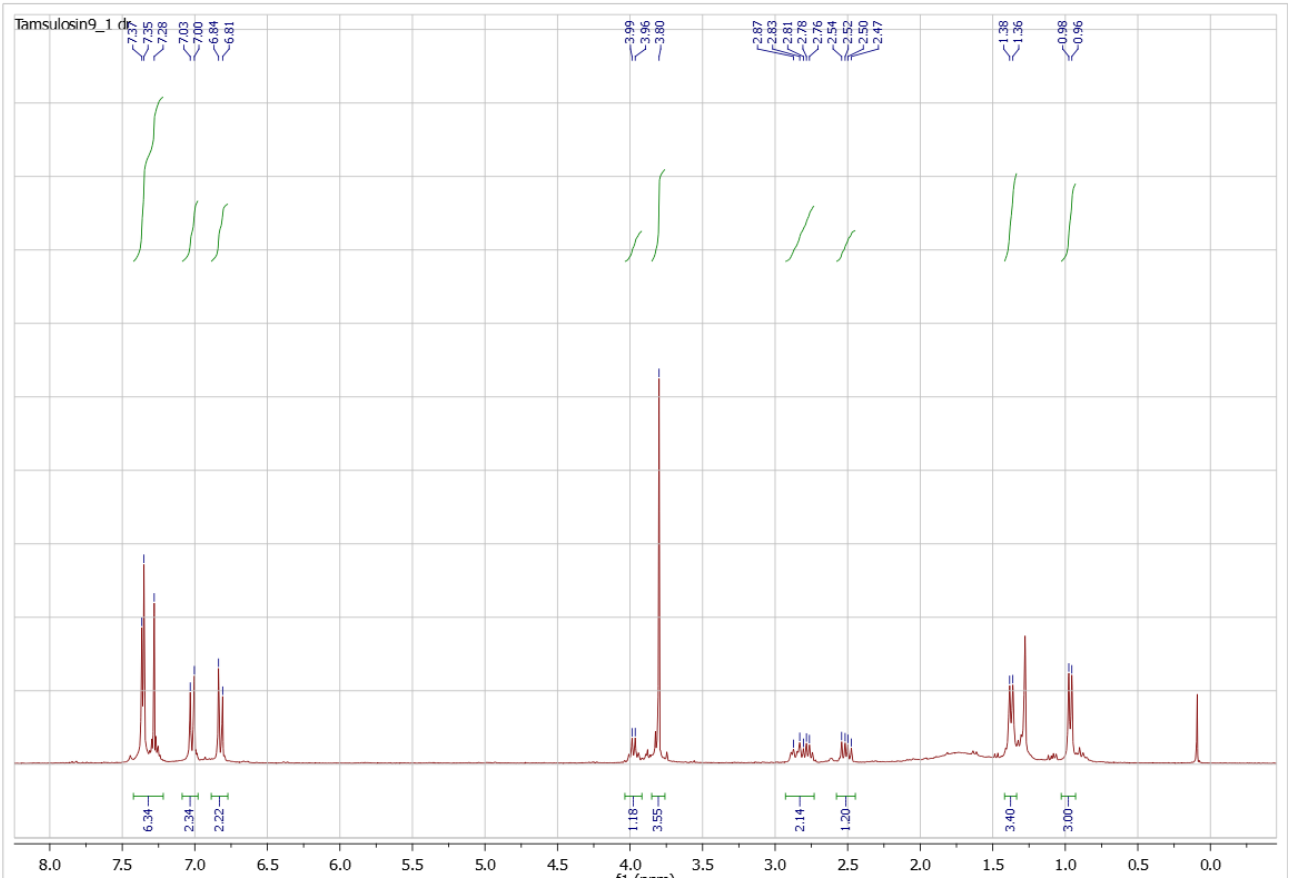

Compound **1-20** is known, and all analytical data are in agreement with literature [115]

(*R*)-4-methoxyamphetamine (**1-24**)

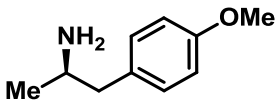

^{1}H NMR (300 MHz, CDCl3) δ 7.11 (d, J = 8.6 Hz, 2H), 6.85 (d, J = 8.6 Hz, 2H), 3.80 (s, 3H), 3.13 – 3.11 (m, 1H), 2.77 – 2.40 (AB, system 2H), 1.11 (d, J = 6.3 Hz, 3H).

The enantiomeric excess was evaluated following literature procedures, using Mosher acid[116]

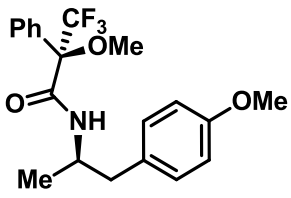

Compound **1-11** is known, and all analytical data are in agreement with literature [117]

Amine deprotection

General procedure for H-Cube Mini deprotection:

For the synthesis of **2:** A 0.1M solution of the amine (1.51mmol, 0,4 g) in ethanol (15mL) was charged into a vial connected with the pump of the H CUBE Mini, equipped with a 30 mm cartridge of 10% Pd/C. The instrument was previously stabilized at the desired temperature and pressure and at 1 mL\min as flow rate. The reaction was run in a close loop for the desired time.

Picture of the flow system

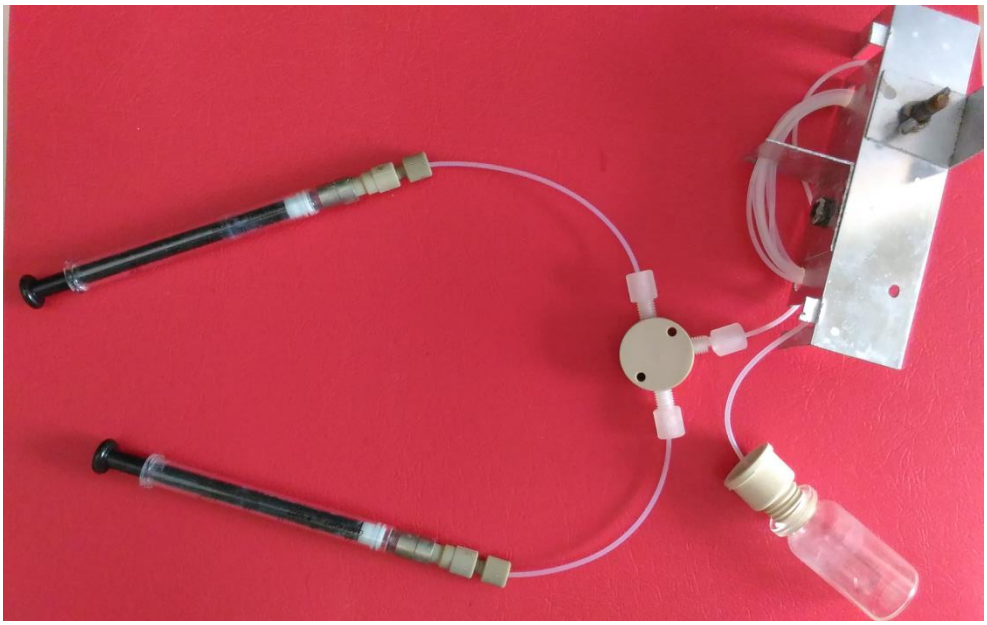

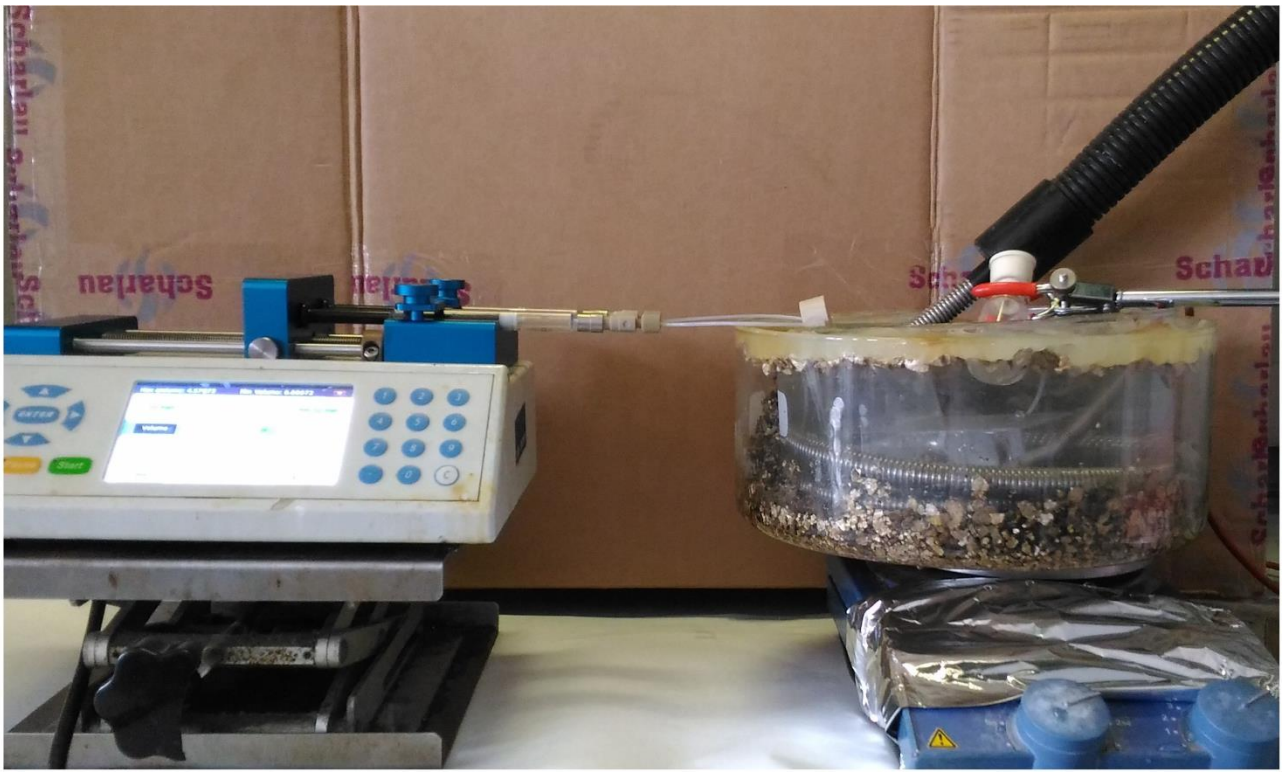
Schanlau
Schanlau
Schanlau
Schanlau
Volume
Start

A new class of low-loading, metal-free catalysts for the enantioselective imine reduction of wide general applicability

Catalysts synthesis

Synthesis amide of alanine

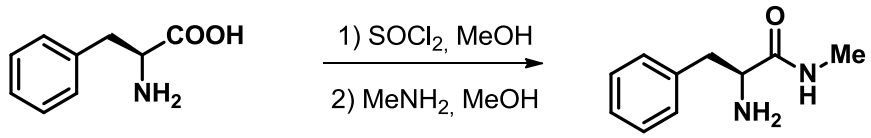

(*L*)- Phenyl Alanine

The amide was prepared starting from (*L*)- Phenyl Alanine according to a published procedure[118]

^{1}H-NMR (300 MHz, $CDCl_3$): δ 7.30-7.19 (m, 5H), 3.62-3.58 (dd, 1H), 3.30-3.27 (dd, 1H), 2.81-2.79 (d, 3H), 2.71-2.68 (m, 1H).

The **amide** is known, and all analytical data are in agreement with literature[118]

Synthesis of imidazolidinones **26**

Compound **IIa**

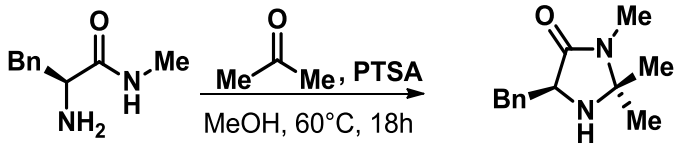

The amide (6 mmol) and PTSA (0.3 mmol) were dissolved in MeOH (15 mL) and acetone (20 mL) and the mixture was heated at 60 °C for 18 hours. After reaction time the crude was concentrated under vacuum. Compound **IIa** was obtained as a yellowish oil (6 mmol, 98% yield) and used in the following step without further purification. All analytical data are in agreement with literature.[1]

^{1}H-NMR (300 MHz, $CDCl_3$): δ 7.28-7.20 (m, 5H), 3.77 (m, 1H), 3.15-3.10 (dd, 1H), 3.09-3.05 (dd, 1H), 2.74 (s, 3H), 1.24 (s, 3H), 1.14 (s, 3H).

Compound **26** is known and all analytical data are in agreement with literature[118]

Compounds **27a** and **27b**

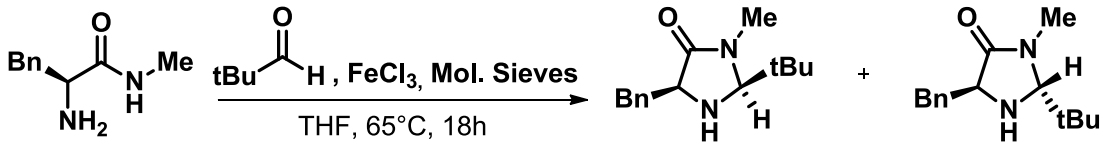

The amide (5 mmol) and $FeCl_3$ (0.5 mmol) were dissolved in THF (25 mL). Pivalic aldehyde (6 mmol) and molecular sieves were added, and the mixture was heated at 65 °C for 18 hours. After reaction time the crude was filtered over celite, concentrated under vacuum and purified by flash column chromatography on silica gel (eluent: Hex/AcOEt=7/3) to afford **27a** (1.1 mmol) and **IIc** (1.9 mmol) as a yellowish oils (60% yield overall yield).

27a

^{1}H-NMR (300 MHz, $CDCl_3$): δ 7.27-7.21 (m, 5H), 4.02 (s, 1H), 3.69-3.66 (m, 1H), 3.16-3.09 (dd, 1H), 2.94-2.88 (dd, 1H), 2.87 (s, 3H), 0.82-0.81 (d, 9H).

^{1}H-NMR (300 MHz, $CDCl_3$): δ 7.27-7.20 (m, 5H), 3.84-3.82 (m, 1H), 3.79 (s, 1H), 3.12-3.06 (dd, 1H), 2.89-2.84 (dd, 1H), 2.87 (s, 3H), 0.89-0.88 (d, 9H).

Compounds **27a and 27b** are known and all analytical data are in agreement with literature [119]

Compound **28**

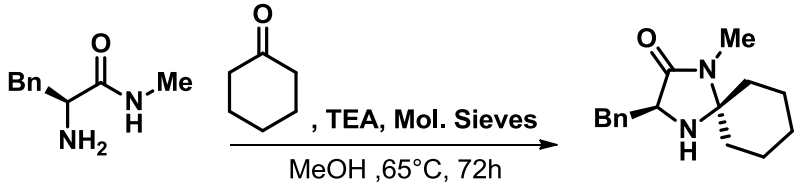

The amide (2.7 mmol) and TEA (2.7 mmol) were dissolved in MeOH (20 mL). Cyclohexanone (5.4 mmol) and molecular sieves were added, and the mixture was heated at 65 °C for 72 hours using a Dean-Stark apparatus. After reaction time the crude was filtered over celite, concentrated under vacuum and purified by flash column chromatography on silica gel (eluent: Hex/AcOEt=6/4) to afford **28** as a yellowish oil (2.3 mmol, 86% yield).

^{1}H-NMR (300 MHz, $CDCl_3$): δ 7.31-7.23 (m, 5H), 3.80-3.76 (m, 1H), 3.16-3.10 (dd, 1H), 3.02-2.96 (dd, 1H), 2.76 (s, 3H), 1.68-1.62 (m, 6H), 1.59-1.52 (m, 2H), 1.50-1.47 (m, 2H).

Compound **28** is known, and all analytical data are in agreement with literature.[120]

Compound **29**

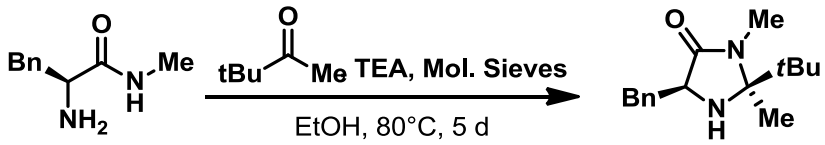

The amide (2.5 mmol) and TEA (2.5 mmol) were dissolved in EtOH (20 mL). *t*-Butyl-methyl ketone (5 mmol) and molecular sieves were added, and the mixture was heated at 80 °C for 5 days using a Dean-Stark apparatus. After reaction time the crude was filtered over celite, concentrated under vacuum and purified by flash column chromatography on silica gel (eluent: Hex/AcOEt=6/4) to afford **IIe** as a brownish oil (0.57 mmol, 23% yield).

Compound **29** is known, and all analytical data are in agreement with literature[121]

^{1}H-NMR (300 MHz, $CDCl_3$): δ 7.30-7.25 (m, 5H), 3.75-3.71 (m, 1H), 3.16-3.11 (dd, 1H), 3.08-3.00 (dd, 1H), 2.85 (s, 3H), 1.24 (s, 3H), 0.81 (s, 9H).

Compounds **30** and **31**

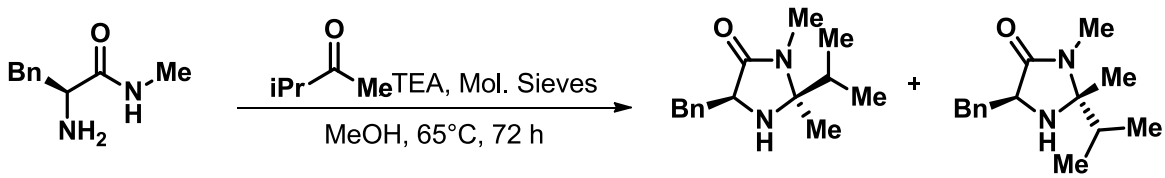

The amide (2.2 mmol) and TEA (2.2 mmol) were dissolved in MeOH (16 mL). *i*-Propyl-methyl ketone (4.4 mmol) and molecular sieves were added, and the mixture was heated at 65 °C for 72 hours using a Dean-Stark apparatus. After reaction time the crude was filtered over celite, concentrated under vacuum and purified by flash column chromatography on silica gel (eluent: Hex/AcOEt=1/1) to afford **IIf** (0.9 mmol) and **IIg** (0.86 mmol) as a brownish oils (80% overall yield).

30

^{1}H-NMR (300 MHz, $CDCl_3$): δ 7.28-7.23 (m, 5H), 3.82-3.78 (m, 1H), 3.14-3.10 (dd, 1H), 3.05-3.01 (dd, 1H), 2.70 (s, 3H), 1.84-1.80 (m, 1H), 1.28 (s, 3H), 0.88-0.85 (d, 3H), 0.43-0.40 (d, 3H);

^{13}C-NMR (75 MHz, $CDCl_3$): δ 173.19, 137.54, 129.72(2C), 128.58(2C), 126.69, 79.79, 58.62, 37.22, 33.53, 25.31, 23.07, 16.37, 15.41.

31

^{1}H-NMR (300 MHz, $CDCl_3$): δ 7.31-7.19 (m, 5H), 3.80-3.78 (m, 1H), 3.12-3.09 (dd, 1H), 3.07-3.04 (dd, 1H), 2.68 (s, 3H), 1.83-1.77 (m, 1H), 0.91 (s, 3H), 0.89-0.87 (d, 3H), 0.75-0.72 (d, 3H);

^{13}C-NMR (75 MHz, $CDCl_3$): δ 173.12, 136.96, 129.70(2C), 128.50(2C), 126.78, 80.27, 60.56, 38.16, 35.05, 25.20, 16.65, 16.28.

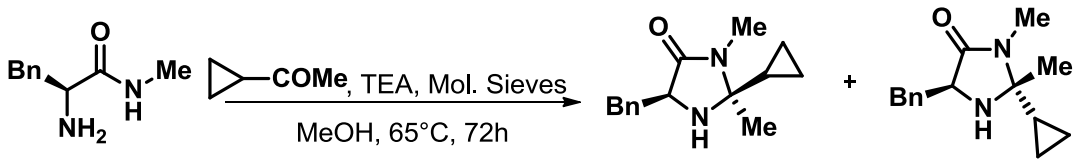

The amide (2.8 mmol) and TEA (2.8 mmol) were dissolved in MeOH (16 mL). Cyclopropyl-methyl ketone (5.6 mmol) and molecular sieves were added, and the mixture was heated at 65 °C for 72 hours using a Dean-Stark apparatus. After reaction time the crude was filtered over celite, concentrated under vacuum and purified by flash column chromatography on silica gel (eluent: Hex/AcOEt=1/1) to afford **32** (1.26 mmol) and **33** (0.95 mmol) as a brownish oils (79% overall yield).

32

^{1}H-NMR (300 MHz, $CDCl_3$): δ 7.28-19 (m, 5H), 3.81-3.77 (m, 1H), 3.17-3.11 (dd, 1H), 2.84-2.77 (dd, 1H), 2.81 (s, 3H), 1.20 (s, 3H), 0.75-0.71 (m, 1H), 0.43-0.38 (m, 2H), 0.28-0.23 (m, 2H);

^{13}C-NMR (75 MHz, $CDCl_3$): δ 172.10, 137.97, 129.51(2C), 128.44(2C), 126.52, 76.76, 58.71, 38.55, 25.06, 23.01, 18.29, 1.50, 0.27.

33

^{1}H-NMR (300 MHz, $CDCl_3$): δ 7.29-7.16 (m, 5H), 3.77-3.74 (m, 1H), 3.03-3.02 (d, 2H), 2.84 (s, 3H), 1.24 (m, 1H), 0.93 (s, 3H), 0.41-0.36 (m, 2H), 0.29-0.25 (m, 2H);

^{13}C-NMR (75 MHz, $CDCl_3$): δ 172.83, 136.88, 129.60(2C), 128.55(2C), 126.81, 77.53, 59.89, 37.87, 25.27, 24.82, 18.27, 1.68, 0.63.

Synthesis of imidazolidinones **34, 35a, 35b, 35b, 36**

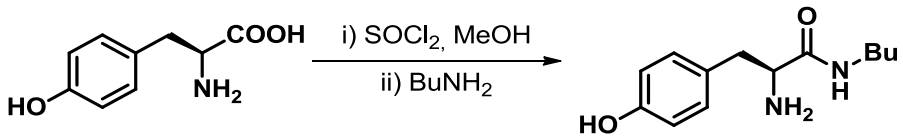

(*L*)- Tyrosine

The Amide was prepared starting from (*L*)- Tyrosine according to a published procedure.[122]

^{1}H-NMR (300 MHz, $CDCl_3$): δ 6.99 (d, 2H); 6.70 (d, 2H); 3.42 (t, 1H); 3.10 (m, 2H); 2.84 (dd, 1H); 2.72 (dd, 1H); 1.35 (m, 2H); 1.19 (m, 2H); 0.87 (t, 3H).

The amide is known, and all analytical data are in agreement with literature**Errore. Il segnalibro non è definito.**

The imidazolidonone of tyrosine:

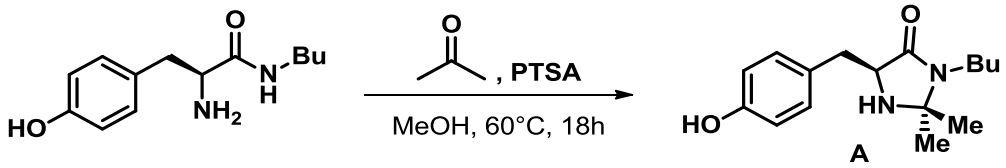

A

The amide of (*S*)-Tyrosine (6 mmol) and PTSA (0.3 mmol) were dissolved in MeOH (15 mL) and acetone (20 mL) and the mixture was heated at 60 °C for 18 hours. After reaction time the crude was concentrated under vacuum. Compound **A** was obtained as a yellowish oil (6 mmol, 98% yield) and used in the following step without further purification

^{1}H-NMR (300 MHz, $CDCl_3$): δ 7.04 (d, 2H); 6.74 (d, 2H); 3.73 (t, 1H, *J* = 5.8 Hz); 3.29 (ddd, 1H, *J* = 12.0 , 6.7, 3.1 Hz); 3.04 (ddd, 2H, *J* = 12.0, 5.8, 5.4 Hz);2.89 (ddd, 1H, *J* = 12.0, 6.2, 3.1 Hz); 1.49-1.43 (m, 2H); 1.31-1.21 (m, 2H); 1.27 (s, 3H); 1.17 (s, 3H); 0.90 (t, 3H, *J* = 7.3 Hz) ppm.
^{13}C-NMR (75 MHz, $CDCl_3$): δ 174.2; 155.8; 130.7 (2C); 127.2; 115.7(2C); 76.4; 58.9; 40.4; 35.5; 31.3; 27.8; 26.3;20.3; 13.7 ppm.

Compound **A** is known, and all analytical data are in agreement with literature

Alkylation of the phenol:

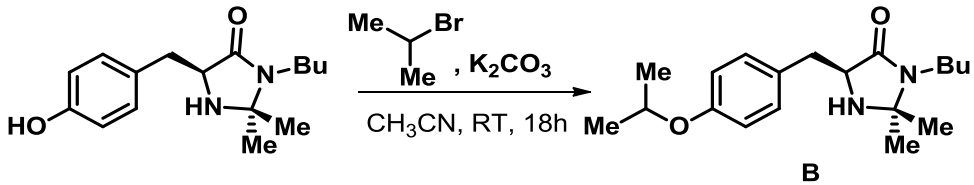

B

Compound **A** (0.5 mmol) was dissolved in dry CH_3CN (5 mL) under nitrogen atmosphere and K_2CO_3 (1.5 mmol) was added. After 10 minutes isopropyl bromide (0.7 mmol) was slowly added and the mixture was stirred 18 h at room temperature. After reaction time the crude was filtered over celite and concentrated under vacuum. The crude was purified by flash column chromatography on silica gel (eluent: Hex/AcOEt=2/8) to afford **B** as a yellowish oil (0.5 mmol, 98% yield).

^{1}H-NMR (300 MHz, $CDCl_3$): δ 7.12-7.11 (d, 2H), 6.82-6.80 (d, 2H), 4.51-4.48 (m, 1H), 3.74-3.71 (m, 1H), 3.31-3.26 (m, 1H), 3.05-2.89 (m, 3H), 1.50-1.46 (m, 2H), 1.32-1.26 (m, 11H), 1.15 (s, 3H), 0.94-0.89 (m, 3H).

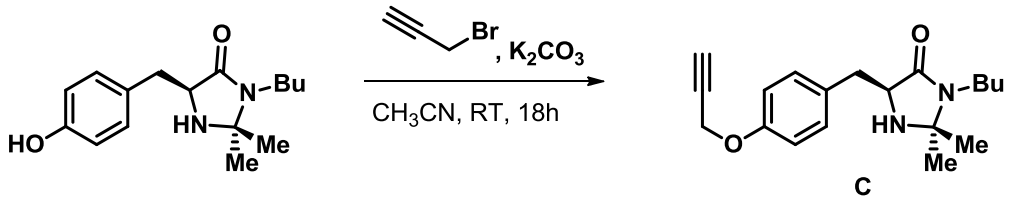

Compound **A** (1.5 mmol) was dissolved in dry CH_3CN (12 mL) under nitrogen atmosphere and K_2CO_3 (3 mmol) was added. After 10 minutes propargyl bromide (2 mmol) was slowly added and the mixture was stirred 18 h at room temperature. After reaction time the crude was filtered over celite and concentrated under vacuum. The crude was purified by flash column chromatography on silica gel (eluent: Hex/AcOEt=2/8) to afford **C** as a yellowish oil (1.2 mmol, 78% yield).
Compound **C** is known, and all analytical data are in agreement with literature.[123]

^{1}H-NMR (300 MHz, $CDCl_3$): δ 7.12 (d, 2H); 6.85 (d, 2H); 4.59 (d, 2H); 3.65 (t, 1H) 3.23-3.20 (m, 1H); 2.97 (dd, 2H); 2.96-2.84 (m, 1H); 2.46 (t, 1H); 1.41 (m, 2H); 1.29-1.24 (m, 2H); 1.20 (s, 3H); 1.09 (s, 3H); 0.86 (t, 3H) ppm.
^{13}C-NMR (75 MHz, $CDCl_3$): δ 174.1, 156.8, 131.0 (2C), 130.1, 115.2 (2C), 78.8, 76.3, 75.7, 59.1, 56.1, 40.5, 36.2, 31.7, 28.3, 26.8, 20.6, 14.0 ppm.

Compound **D**

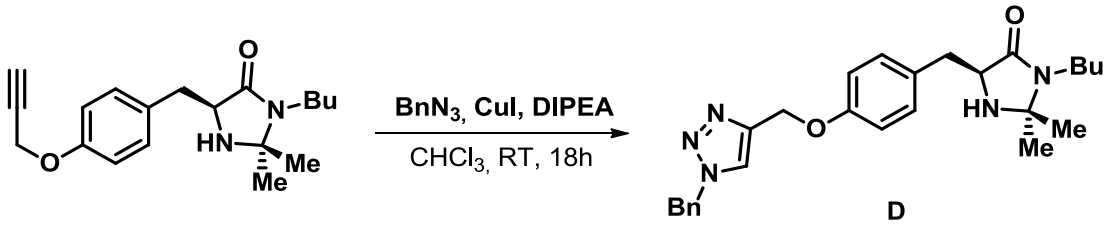

Compound **C** (1.2 mmol) was dissolved in dry chloroform (10 mL) under nitrogen atmosphere then CuI (0.06 mmol) and DIPEA (4 mmol) were added. The mixture was stirred at room temperature for 15 minutes, then a solution of BnN_3 (1.3 mmol) in dry chloroform (3 mL) was slowly added. The mixture was stirred for 24 hours at room temperature then the crude was concentrated *in vacuo*. The residue was purified by column chromatography on silica gel (eluent: AcOEt) to afford **D** as yellowish oil (1.1 mmol, 95% yield).
Compound **D** is known, and all analytical data are in agreement with literature. ref

^{1}H NMR (300 MHz, $CDCl_3$): δ 7.55 (s, 1H), 7.38-7.41 (m, 2H), 7.28-7.31 (m, 2H), 7.16 (d, 2H), 6.91 (d, 2H), 5.55 (s, 2H), 5.16 (s, 2H), 3.75 (bs, 1H), 3.29-332 (m, 1H), 3.06 (t, 2H), 1.86 (bs, 1H), 1.45-1.52 (m, 2H), 1.25-1.30 (m, 2H), 1.29-1.31 (m, 5H), 1.17 (s, 3H), 0.93 (t, 3H) ppm.

^{13}C-NMR (125 MHz, $CDCl_3$): δ 173.7, 157.2, 144.6, 134.5, 130.8, 129.3, 129.1(2C), 128.8(2C), 128.1, 122.9, 114.8, 76.1, 62.0, 58.8, 54.3, 40.3, 35.9, 31.4, 28.1, 26.5, 20.3, 13.8 ppm.

General Procedure for the synthesis of catalysts ***26-27a, 27b, 28, 29, 30, 31, 32, 33***

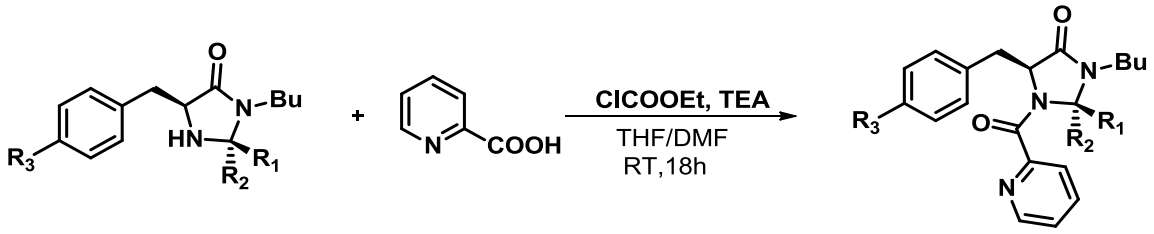

Picolinic acid (1.6 mmol) was dissolved in dry THF (12 mL) under nitrogen atmosphere. N-methyl-morpholine (2.4 mmol) was added and the mixture was cooled at 0 °C. Ethyl chloroformate (1.6 mmol) was added dropwise and the mixture was stirred for 15 minutes at same temperature, then 2 h at room temperature. After reaction time a solution of imidazolidinone **II** (1.6 mmol) in dry DMF (8 mL), was slowly added. The reaction was stirred at room temperature overnight. After reaction time the solvent was evaporated under vacuum and the crude product was dissolved in AcOEt then washed with H_2O. Collected organic layers were dried with Na_2SO_4, concentrated *in vacuo,* and the residue was purified by column chromatography on silica gel.

Catalyst (**1-29**)

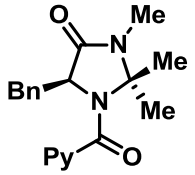

Prepared according to the general procedure starting from the corresponding imidazolidinone. The product was purified by flash column chromatography on silica gel (eluent: Hex/AcOEt=2/8) to afford a brownish oil (70% yield).

^{1}H-NMR (300 MHz, $CDCl_3$): δ 8.60-8.58 (m, 1H), 7.88-7.86 (m, 2H), 7.43-7.39 (m, 1H), 7.18-7.15 (m, 3H), 6.93-6.90 (m, 2H), 5.73-5.70 (m, 1H), 3.10-3.04 (dd, 1H), 2.74 (s, 3H), 2.20-2.14 (dd, 1H), 1.69 (s, 3H), 0.82 (s, 3H).

^{13}C-NMR (75 MHz, $CDCl_3$): δ 167.62, 164.82, 153.83, 147.64, 136.85, 135.28, 129.57(2C), 127.83(2C), 126.53, 124.84, 123.65, 60.52, 36.70, 29.13, 23.04, 21.96.

MS (ESI) m/z (%): calc. for $C_{19}H_{21}N_3O_2Na$ = 346.4; found = 346.2.

$[\alpha]^{25}_D$ = -129.1 (c: 0.42 $CHCl_3$).

Catalyst (**1-27a**)

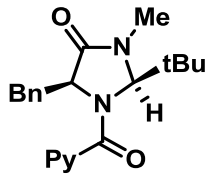

Prepared according to the general procedure starting from the corresponding imidazolidinone. The product was purified by flash column chromatography on silica gel (eluent: CH_2Cl_2/MeOH=95/5) to afford a brownish oil (80% yield).

^{1}H-NMR (300 MHz, $CDCl_3$): δ 8.46-8.44 (m, 1H), 7.73-7.69 (m, 1H), 7.62-7.61 (m, 1H), 7.34-7.30 (m, 1H), 7.20-7.17 (m, 5H), 5.66 (m, 1H), 4.86-4.82 (m, 1H), 3.62-3.58 (dd, 1H), 3.25-3.21 (dd, 1H), 3.08 (s, 3H), 1.18 (s, 9H).

^{13}C-NMR (75 MHz, $CDCl_3$): δ 171.59, 147.84, 138.00, 137.12, 129.28(2C), 128.23(2C), 126.31, 125.17, 124.51, 81,69, 61.53, 40.98, 37.46, 31.36, 27.19.

MS (ESI) m/z (%): calc. for $C_{21}H_{25}N_3O_2Na$ = 374.4; found = 374.4.

$[\alpha]^{26}_D$ = -7.3 (c: 0.40 $CHCl_3$).

Catalyst (**1-27b**)

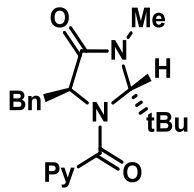

Prepared according to the general procedure starting from the corresponding imidazolidinone. The product was purified by flash column chromatography on silica gel (eluent: CH_2Cl_2/MeOH=95/5) to afford a brownish oil (97% yield).

^{1}H-NMR (300 MHz, $CDCl_3$): δ 8.67-8.57 (m, 1H), 8.00-7.85 (m, 2H), 7.46-7.44 (m, 1H), 7.16-7.14 (m, 3H), 6.84-6.83 (m, 2H), 5.29-5.23 (m, 2H), 3.10-3.06 (dd, 1H), 2.84 (s, 3H), 2.35-2.28 (dd, 1H), 1.00 (s, 9H).

^{13}C-NMR (75 MHz, $CDCl_3$): δ 171.69, 168.48, 153.37, 148.80, 137.22, 134.86, 129.63(2C), 128.06(2C), 126.95, 126.15, 125.60, 80.73, 62.13, 41.60, 37.64, 31.84, 26.53.

MS (ESI) m/z (%): calc. for $C_{21}H_{25}N_3O_2Na$ = 374.4; found = 374.4.

$[\alpha]^{26}_D$ = 122.9 (c: 0.40 $CHCl_3$).

Catalyst (**1-28)**

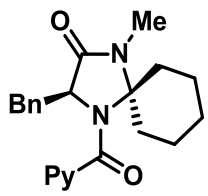

Prepared according to the general procedure starting from the corresponding imidazolidinone. The product was purified by flash column chromatography on silica gel (eluent: CH_2Cl_2/MeOH=97/3) to afford a brownish oil (72% yield).

^{1}H-NMR (300 MHz, $CDCl_3$): δ 8.57-8.55 (d, 1H), 7.85-7.76 (m, 2H), 7.39-7.37 (m, 1H), 7.17-7.15 (m, 3H), 6.92-6.89 (m, 2H), 5.71-5.69 (m,2H), 3.12-3.08 (dd, 1H), 3.04 (s, 3H), 2.97-2.95 (m, 1H), 2.52-2.49 (m, 1H), 2.20-2.14 (dd, 1H), 1.77-1.57 (m, 5H), 1.41-1.37 (m, 2H).

^{13}C-NMR (75 MHz, $CDCl_3$): δ 168.1, 165.0, 154.5, 147.7, 136.9, 135.4, 129.8, 128.0(2C), 126.7(2C), 124.9, 123.7, 60.2, 37.3, 32.4, 31.7, 28.2, 23.9, 23.7, 22.7.

MS (ESI) m/z (%): calc. for $C_{22}H_{25}N_3O_2Na$ = 386.4; found = 386.1.

$[\alpha]^{22}_D$ = 294.6 (c: 0.26 $CHCl_3$).

Catalyst (**1-29)**

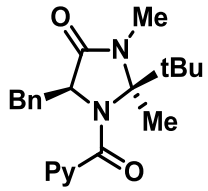

Prepared according to the general procedure starting from the corresponding imidazolidinone. The product was purified by flash column chromatography on silica gel (eluent: CH_2Cl_2/MeOH=97/3) to afford a brownish oil (77% yield).

^{1}H-NMR (300 MHz, $CDCl_3$): δ 8.29-8.27 (m, 1H), 7.61-7.60 (m, 1H), 7.29-7.25 (m, 2H), 7.19-7.17 (m, 1H), 7.05-7.02 (m, 2H), 6.72-6.69 (m, 2H), 5.55-5.53 (m, 1H), 3.03 (s, 3H), 2.98-2.94 (dd, 1H), 2.77-2.21 (dd, 1H), 1.98 (s, 3H), 1.21 (s, 9H).

^{13}C-NMR (75 MHz, $CDCl_3$): δ 170.45, 167.48, 155.20, 147.58, 137.27, 137.15, 129.74, 128.88, 128.64, 128.13, 126.16, 124.07, 123.19, 59.88, 57.99, 42.04, 40.65, 28.98, 28.41, 25.44, 19.49, 18.54.

MS (ESI) m/z (%): calc. for $C_{22}H_{27}N_3O_2Na$ = 388.5; found = 388.4.

$[\alpha]^{22}_D$ = 42.1 (c: 0.20 $CHCl_3$).

Catalyst (**1-30)**

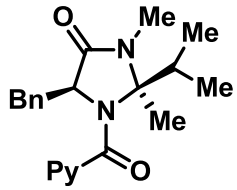

Prepared according to the general procedure starting from the corresponding imidazolidinone. The product was purified by flash column chromatography on silica gel (eluent: CH_2Cl_2/MeOH=97/3) to afford a brownish oil (60% yield).

^{1}H-NMR (300 MHz, $CDCl_3$): δ 8.39-8.38 (d, 1H), 7.74-7.71 (m, 1H), 7.53-7.50 (m, 1H), 7.27-7.25 (m, 1H), 7.08-7.06 (m, 3H), 6.81-6.80 (m, 2H), 5.62-5.60 (m, 1H), 3.03-3.00 (dd, 1H), 2.95 (s, 3H), 2.69-2.65 (dd, 1H), 1.85 (s, 3H), 1.11-1.09 (d, 3H), 1.05-1.04 (m, 1H), 0.94-0.91 (d,3H).

^{13}C-NMR (75 MHz, $CDCl_3$): δ 169.24, 165.82, 154.04, 147.28, 136.70, 128.71(2C), 127.72(2C), 127.61, 125.85, 124.33, 123.31, 58.87, 40.13, 39.94, 33.61, 26.81, 20.27, 18.30, 18.18, 17.19.

MS (ESI) m/z (%): calc. for $C_{21}H_{25}N_3O_2Na$ = 374.4; found = 374.3.

$[\alpha]^{24}_D$ = 111.7 (c: 0.20 $CHCl_3$).

Catalyst (**1-31)**

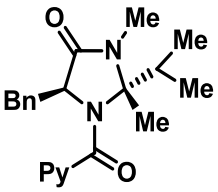

Prepared according to the general procedure starting from the corresponding imidazolidinone. The product was purified by flash column chromatography on silica gel (eluent: CH_2Cl_2/MeOH=97/3) to afford a brownish oil (64% yield).

^{1}H-NMR (300 MHz, $CDCl_3$): δ 8.61-8.59 (d, 1H), 7.90-7.88 (m, 1H), 7.42-7.40 (m, 1H), 7.25-7.18 (m, 4H), 6.94-6.92 (d, 2H), 5.67-5.65 (m, 1H), 3.11-3.05 (dd, 1H), 2.76 (s, 3H), 2.08-2.02 (dd, 1H), 1.01-0-98 (d, 3H), 0.95-0.90 (m, 6H), 0.74-0.72 (d, 1H).

^{13}C-NMR (75 MHz, $CDCl_3$): δ 169.39, 165.65, 154. 76, 148.27, 137.29, 135.76, 130.01, 128.25(2C), 127.02(2C), 125.29, 124.30, 61.66, 37.04, 33.59, 27.13, 25.23, 19.66, 17.93, 16.58, 16.30.

MS (ESI) m/z (%): calc. for $C_{21}H_{25}N_3O_2Na$ = 374.4; found = 374.4.

$[\alpha]^{24}_D$ = 71.8 (0 c: 0.20 $CHCl_3$).

Catalyst (**1-32)**

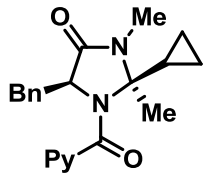

Prepared according to the general procedure starting from the corresponding imidazolidinone. The product was purified by flash column chromatography on silica gel (eluent: CH_2Cl_2/MeOH=97/3) to afford a brownish oil (95% yield).

^{1}H-NMR (300 MHz, $CDCl_3$): δ 8.55-8.54 (d, 1H), 8.00 (s, 1H), 7.81-7.73 (m, 1H), 7.39-7.34 (m, 1H), 7.13-7.08 (m, 3H), 6.97-6.95 (d, 2H), 5.73-5.71 (m, 1H), 3.04-3.00 (dd, 1H), 2.85 (s, 3H), 2.35-2.30 (dd, 1H), 1.44 (s, 3H), 1.30-1.25 (m, 1H), 0.38-0.27 (m, 4H).

^{13}C-NMR (75 MHz, $CDCl_3$): δ 167.69, 164.73, 161.90, 154.07, 147.97, 147.36, 136.71, 135.42, 129.55, 127.68, 126.25, 124.46, 123.37, 60.10, 37.33, 25.10, 16.54, 15.84, 2.70, 2.58.

MS (ESI) m/z (%): calc. for $C_{21}H_{23}N_3O_2Na$ = 372.4; found = 372.3.

$[\alpha]^{24}_D$ = 203.9 (c: 0.21 $CHCl_3$).

Catalyst (**1-32)**

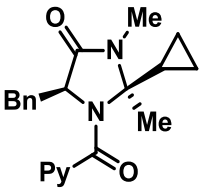

Prepared according to the general procedure starting from imidazolidinone **32**. The product was purified by flash column chromatography on silica gel (eluent: CH_2Cl_2/MeOH=97/3) to afford a brownish oil (49% yield).

^{1}H-NMR (300 MHz, $CDCl_3$): δ 8.64-8.63 (d, 1H), 7.93-7.91 (d, 1H), 7.46-7.43 (q, 1H), 7.22-7.18 (m, 3H), 6.97-6.94 (m, 3H), 5.74-5.72 (m, 1H), 3.13-3.08 (dd, 1H), 2.78 (s, 3H), 2.18-2.14 (dd, 1H), 1.28-1.23 (m, 1H), 0.79 (s, 3H), 0.63-0.57 (m, 4H).

^{13}C-NMR (75 MHz, $CDCl_3$): δ 168.66, 165.64, 159.7, 154.53, 148.22, 137.34, 135.77, 130.10(2C), 128.29(2C), 127.04, 125.36, 124.16, 61.12, 37.21, 25.75, 18.82, 18.44, 4.68, 2.72.

MS (ESI) m/z (%): calc. for $C_{21}H_{23}N_3O_2Na$ = 372.4; found = 372.4.

$[\alpha]^{24}_D$ = 226.0 (c: 0.21 $CHCl_3$).

Catalyst (**1-34**)

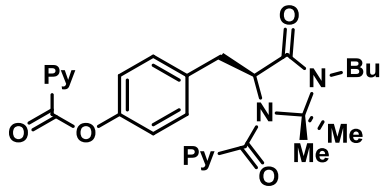

Prepared according to the general procedure starting from the corresponding imidazolidinone. The product was purified by flash column chromatography on silica gel (eluent: Hex/AcOEt=3/7) to afford a brownish oil (18% yield).

^{1}H-NMR (300MHz, $CDCl_3$): δ 8.85-8.83 (m, 2H), 8.67-8.66 (m, 1H), 8.55-8.52 (m, 1H), 8.27-8.21 (m, 2H), 7.94-7.89 (m, 2H), 7.34-7.31 (m, 2H), 7.19-7.14 (m, 2H), 7.03-6.97 (m, 2H), 5.57 (s, 1H), 5.20 (s, 1H), 3.85-3.75 (m, 2H), 3.12-3.00 (m, 2H), 1.60-1.50 (m, 2H), 1.25-1.20 (m, 2H), 1.04 (s, 9H), 0.88 (m, 3H).

Catalyst (**1-31a**)

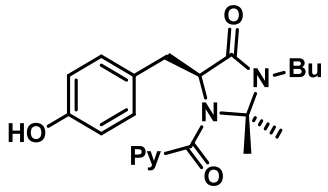

Prepared according to the general procedure starting from the corresponding imidazolidinone. The product was purified by flash column chromatography on silica gel (eluent: Hex/AcOEt=3/7) to afford a brownish oil (76% yield).

^{1}H-NMR (300 MHz, $CDCl_3$): δ 8.61 (d, 1H), 7.92 (m, 3H), 7.03-7.12 (m, 4H), 5.70 (m, 1H), 3.09 (m, 3H), 2.20 (m, 1H), 1.74 (s, 3H), 1.64 (m, 1H), 1.48 (m, 1H), 1.31 (m, 2H), 1.10 (s, 3H), 0.94 (t, 3H).

^{13}C-NMR (75 MHz, $CDCl_3$): δ 168.6, 165.5, 156.1, 154.0, 148.3, 137.5, 131.2 (2C), 126.3, 125.5, 124.0, 115.4 (2C), 81.0, 61.1, 40.0, 36.2, 30.7, 24.6, 24.0, 20.5, 13.7 ppm.

HRMS (ESI+) m/z calculated for $C_{22}H_{27}O_3N_3Na_1$(+1): 404.1945; found 404.1941.

$[\alpha_D]^{23}$ = + 268.2 (c: 0.58 $CHCl_3$).

Catalyst (**1-31b**)

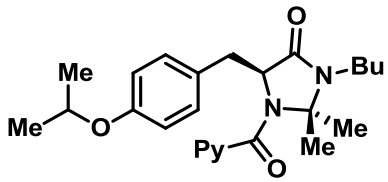

Prepared according to the general procedure starting from the corresponding imidazolidinone. The product was purified by flash column chromatography on silica gel (eluent: CH_2Cl_2/MeOH=98/2) to afford a brownish oil (75% yield).

^{1}H-NMR (300 MHz, $CDCl_3$): δ 8.62-8.61 (d, 1H), 7.91-7.87 (m, 3H), 7.44-7.43 (m, 1H), 6.89-6.86 (d, 2H) 6.75-6.72 (d, 2H), 5.65-5.63 (m, 1H), 4.51-4.45 (m, 1H), 3.23-3.18 (m, 1H), 3.06-3.01 (m, 2H), 2.13-2.06 (dd, 1H), 1.73 (s, 3H), 1.30-1.28 (d, 9H), 0.97-0.95 (d, 6H).

^{13}C-NMR (75 MHz, $CDCl_3$): δ 168.40, 165.35, 156.97, 154.49, 148.18, 137.38, 131.40, 131.27(2C), 127.58, 125.32, 124.03, 116.06(2C), 69.95, 60.82, 39.81, 36.26, 30.83, 24.58, 24.01, 21.87, 20.49, 13.70.

MS (ESI) m/z (%): calc. for $C_{25}H_{33}N_3O_3Na$ = 446.5; found = 446.4.

$[\alpha]^{26}_D$ = 37.3 (c: 0.40 $CHCl_3$).

Catalyst (**1-36**)

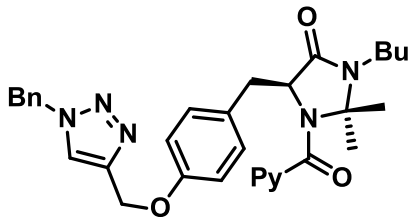

Prepared according to the general procedure starting from the corresponding imidazolidinone. The product was purified by flash column chromatography on silica gel (eluent: Hex/AcOEt=2/8) to afford a brownish oil (78% yield).

^{1}H-NMR (300 MHz, $CDCl_3$): δ 8.60-8.61 (d, 1H), 7.87-7.90 (m, 2H), 7.52 (s, 1H), 7.41-7.37 (m, 3H), 7.30-7.27 (m, 2H), 6.87 (d, 2H), 6.80 (d, 2H), 5.62-5.65 (m, 1H), 5.53 (s, 2H), 5.11 (s, 2H), 4.13 (q, 1H), 3.12-3.18 (m, 1H), 3.00-3.08 (m, 2H), 2.05-2.13 (m, 1H), 1.57-1.63 (m, 2H), 1.39-1.52 (m, 2H), 1.36-1.39 (m, 3H), 0.87-0.97 (m, 3H), 0.95 (s, 3H) ppm.

^{13}C-NMR (300 MHz, $CDCl_3$): δ 168.3, 165.3, 157.4, 154.4, 148.2, 144.4, 138.2, 137.4, 134.5, 131.3, 129.1 (2C), 128.7, 128.3, 128.1 (2C), 125.4, 124.0, 122.7, 114.6 (2C), 80.6, 61.9, 60.7, 54.2, 39.8, 36.3, 30.8, 24.6, 24.1, 20.5, 13.7 ppm.

HRMS (ESI+) m/z calculated for $C_{32}H_{36}O_3N_6Na_1$(+1): 575.2741; found 575.2748.

$[\alpha_D]^{23}$ = + 201.3 (c: 0.65 $CHCl_3$).

Synthesis of catalyst (**1-31c**)

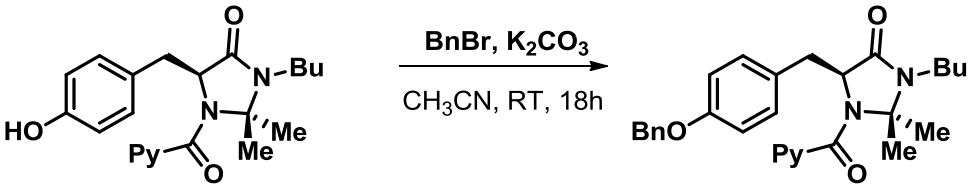

Compound **3a** (1.5 mmol) was dissolved in dry CH_3CN (12 mL) under nitrogen atmosphere and K_2CO_3 (3 mmol) was added. After 10 minutes BnBr (2 mmol) was slowly added and the mixture was stirred 18 h at room temperature. After reaction time the crude was filtered over celite and concentrated under vacuum. The crude was purified by flash column chromatography on silica gel (eluent: Hex/AcOEt=2/8) to afford **3c** as a yellowish oil (1.3 mmol, 85% yield).

^{1}H-NMR (300 MHz, $CDCl_3$): δ 8.60 (d, 1H), 7.87 (m, 3H), 7.39 (m, 5H), 6.80-6.90 (m, 4H), 5.63 (m, 1H), 5.03 (s, 2H), 3.17 (m, 1H), 3.04 (m, 2H), 2.09 (m, 1H), 1.72 (s, 3H), 1.65 (m, 1H), 1.44 (m, 1H), 1.32 (m, 2H), 0.95 (t, 3H), 0.92 (s, 3H) ppm.

^{13}C-NMR (75 MHz, $CDCl_3$): δ 168.3, 165.3, 157.8, 154.4, 148.2 137.3, 136.9, 131.2 (2C), 128.5 (2C), 128.0, 127.9, 127.3 (2C), 125.3, 124.0, 114.9 (2C), 80.6, 69.9, 60.8, 39.8, 36.3, 30.8, 24.6, 24.1, 20.5, 13.7 ppm.

HRMS (ESI+) m/z calculated for $C_{29}H_{33}O_3N_3Na_1$(+1): 494.2414; found 494.2404.

$[\alpha_D]^{23}$ = + 122.3 (c: 0.41 $CHCl_3$).

Imines descriptions

(E)-N-phenyl-ethan-1-phenyl-1-imine (**1-37**)

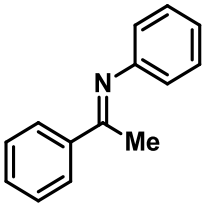

The desired product was prepared according to general procedure A. The imine was purified by crystallization from ethanol.

^{1}H-NMR (300 MHz, $CDCl_3$): δ_H 8.03-7.99 (m, 2H), 7.49-7.45 (m, 3H), 7.39-7.35 (m, 2H), 7.14 -7.09 (m, 1H), 6.85-6.82 (m, 2 H), 2.27 (s, 3H).

(*E*)-4-methoxy-*N*-(1-phenylethyliden)aniline (**1-39**)

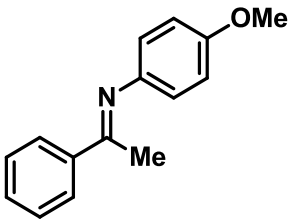

The desired product was prepared according to general procedure A. The imine was purified by crystallization from ethanol

^{1}H-NMR (300 MHz, $CDCl_3$): δ_H 7.97-7.95 (m, 2H), 7.47-7.44 (m, 3H), 6.92-6.89 (m, 2H), 6.77-6.74 (m, 2H), 3.81 (s, 3H), 2.25 (s, 3H).

(E) 4-methoxy-*N*-(1-p-tolylethyliden)aniline (**1-40**)

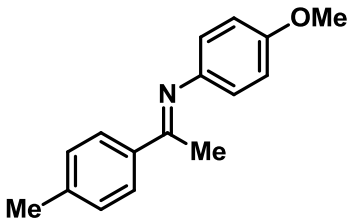

The desired product was prepared according to general procedure B The residual starting materials were removed by fractional distillation at p=3x10-2 mbar at 150 °C with Glass Oven B-585 Kugel Rohr (only terminal round flask inserted).

^{1}H-NMR (300 MHz, $CDCl_3$): δ_H 7.98-7.95 (d, J = 9 Hz, 2H), 6.97-6.92 (m, 4H), 6.79 (d, J = 9 Hz, 2H), 3.89 (s, 3H), 2.33 (s, 3H), 2.25 (s, 3H).

(E) 4-methoxy-*N*-(1-p-methoxyethyliden)aniline (**1-41**)

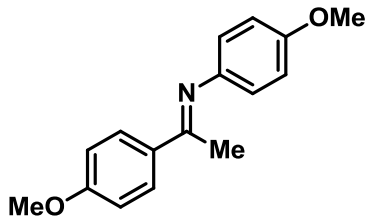

The desired product was prepared according to general procedure A . The residual starting materials were removed by crystallization from ethanol.

^{1}H-NMR (300 MHz, $CDCl_3$): δ_H 7.98-7.95 (d,, 2H), 6.97-6.92 (m, 4H), 6.79 (d, 2H), 3.89 (s, 3H), 3.84 (s, 3H), 2.25 (s, 3H).

(E) N-Phenyl-[1-(2-naphthyl)ethylidene]amine (**1-45**)

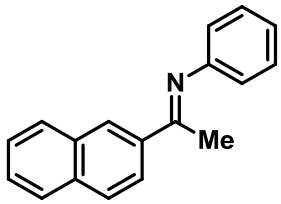

The desired product was prepared according to general procedure A . The residual starting materials were removed by crystallization from ethanol.

^{1}H-NMR (300 MHz, $CDCl_3$): δ_H 8.35 (s, 1H), 8.23 (m, 1H), 7.96 -7.86 (m, 3H), 7.58-7.50 (m, 2H), 7.41-7.35 (m, 2H), 7.11 (m, 1H), 6.85 (m, 2H), 2.36 (s, 3H).

(*E*)-*N*-(1-(4-fluorophenyl)ethylidene)-4-methoxybenzenamine (**1-47**)

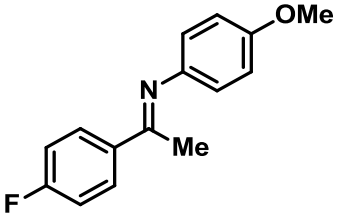

The desired product was prepared according to general procedure **A**. The residual starting materials were then removed by fractional distillation at p=3x10^{-2} mbar at 150 °C with Glass Oven *B-585 Kugelrohr* (only terminal round flask inserted).

^{1}H-NMR (300 MHz, $CDCl_3$): δ_H 8.02-7.98 (d, J = 9 Hz, 2H), 7.50-7.52 (d, J = 9 Hz, 2H), 6.95-6.92 (d, J = 8 Hz, 2H), 6.79-6.76 (d, J = 8 Hz, 2H), 3.84 (s, 3H), 2.25 (s, 3H).

(*E*)-*N*-(1-(4-trifluomethylrophenyl)ethylidene)-4-methoxybenzenamine (**1-48**)

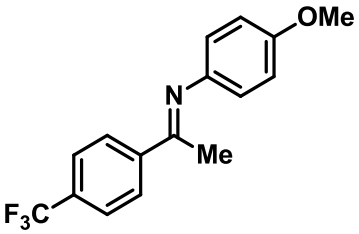

The desired product was prepared according to general procedure **A.** Purification: crystallization from hexane.

^{1}H-NMR (300 MHz, $CDCl_3$): δ_H 8.06 (d, 2H), 7.70 (d, 2H), 6.97-6.92 (d, 2H), 6.79 (d, 2H), 3.89 (s, 3H), 2.26 (s, 3H).

(*E*)-*N*-(1-(4-nitrophenyl)ethylidene)-4-methoxybenzenamine (**1-49**)

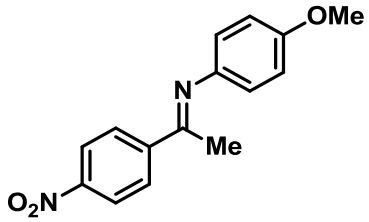

The desired product was prepared according to general procedure A. The desired imine was purified by crystallization from toluene.

^{1}H-NMR (300 MHz, $CDCl_3$): δ_H 8.31 (d, 2H), 8.15 (d, 2H), 6.95 (d, 2H), 6.79 (d, 2H), 3.85 (s, 3H), 2.30 (s, 3H).

(*E*)-*N*-(1-(4-Clorophenyl)ethylidene)-4-methoxybenzenamine (**1-50**)

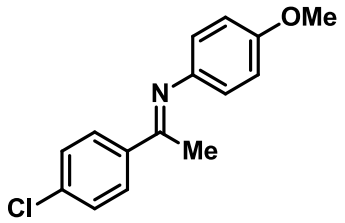

The desired product was prepared according to general procedure **A**. The residual starting materials were then removed by fractional distillation at p=3x10^{-2} mbar at 150 °C with Glass Oven *B-585 Kugel Rohr* (only terminal round flask inserted).

^{1}H-NMR (300 MHz, $CDCl_3$): δ_H 7.95-7.92 (d, J = 9 Hz, 2H), 7.44-7.41 (d, J = 9 Hz, 2H), 6.95-6.92 (d, J = 8 Hz, 2H), 6.79-6.76 (d, J = 8 Hz, 2H), 3.84 (s, 3H), 2.26 (s, 3H).

(*E*)-*N*-(1-(3-methoxyphenyl)ethylidene)-4-methoxybenzenamine (**1-51**)

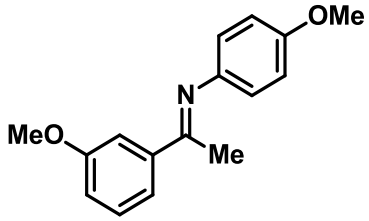

The desired product was prepared according to general procedure B. The crude mixture was used without further purification.

^{1}H-NMR (300 MHz, $CDCl_3$): δ_H 7.60-7.58 (m, 3H), 7.34 (m, 2H), 3.89 (s, 3H), 3.84 (s, 3H), 2.25 (s, 3H).

(*E*)-N-(1-(3-benzyloxyphenyl)ethylidene)-4-methoxybenzenamine (**1-52**)

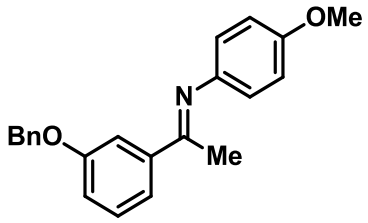

The desired product was prepared according to general procedure B.

^{1}H NMR (300 MHz, $CDCl_3$) δ: 7.71 (s, 1H), 7.57-7.36 (m, 7H), 7.12 (d, 1H), 6.95 (d, 2H, *J* = 3.0 Hz), 6.80 (d, 2H), 5.17 (s, 2H), 3.86 (s, 3H), 2.27 (s, 3H).

(*E*) 1-phenyl-*N*-(1-(3-benzyoxy)ethylidene)methenamine (**1-53**)

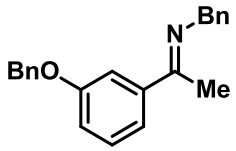

The desired product was prepared according to general procedure B. The residual starting materials were then removed by fractional distillation at p=3x10-2 mbar at 150 °C with Glass Oven B-585 Kugel Rohr (only terminal round flask inserted).

^{1}H NMR (300 MHz, $CDCl_3$) δ: 7.40-7.28 (m, 14H), 5.17 (s, 2H), 4.78 (s, 2H), 2.35 (s, 3H).

N-3-phenylpropyl-(1-phenylethylidene)amine (**1-54**)

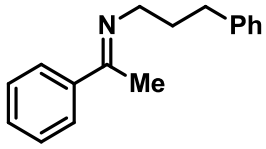

The desired product was prepared according to general procedure B. The residual starting materials were then removed by fractional distillation at p=3x10-2 mbar at 135 °C with Glass Oven B-585 Kugel Rohr (only terminal round flask inserted).

^{1}H NMR (300 MHz, $CDCl_3$) δ: 7.81-7.79 (m, 2H), 7.40-7.20 (m, 7H), 3.51 (t, 2H), 2.65 (t, 2H), 2.22 (s, 3H), 2.12 (m, 2H)

N-butyl-(1-phenylethylidene)amine (**1-55**)

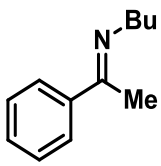

The desired product was prepared according to general procedure B. The residual starting materials were then removed by fractional distillation at p=3x10-2 mbar at 35 °C.

^{1}H NMR (300 MHz, $CDCl_3$) δ_H: 7.79-7.77 (m, 2H), 7.40-7.37 (m, 3H), 3.51 (t, 2H), 2.25 (s, 3H), 1.75 (m, 2H), 1.50 (m, 2H), 1.00 (t, 3H).

(*Z*)-methyl 2-((4-methoxyphenyl)imino)-2-phenylacetate (**1-56**)

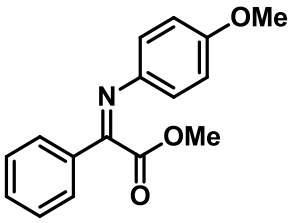

The desired product was prepared according to general procedure C. The product was purified by flash column chromatography on silica gel (eluent 9:1 ETP\AcOEt)

^{1}H NMR (300 MHz, $CDCl_3$) δ_H: 7.84(d, 2H), 7.46 (m, 3H), 6.93(m, 4H), 3.81 (s, 3H) 3.69 (s, 3H).

(*Z*)-methyl 3-((4-methoxyphenyl)amino)-3-phenylacrylate (**1-57**)

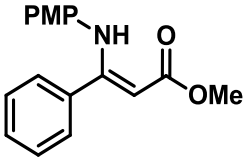

The desired product was prepared according to general procedure C. The product was purified by flash column chromatography on silica gel (eluent 9:1 ETP\AcOEt)

^{1}H NMR (300 MHz, $CDCl_3$) δ_H: 7.29(s, 4H), 6.65 (s, 4H), 4.95 (s, 1H), 3.75 (s, 3H), 3.70 (s, 3H).

(*Z*)-4-methoxy-N-(2-nitro-1-phenylvinyl)aniline (**1-58**)

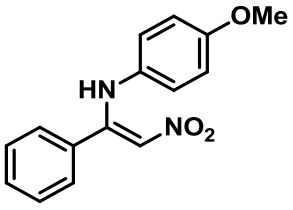

This product was prepared according to literature.[124]

^{1}H NMR (300 MHz, CDCl3): δ (ppm) 11.50 (s,1H), 7.38 (t, 1H), 7.31 (t, 2H), 7.26 (d,2H), 6.75 (d, 2H), 6.72 (s, 1H), 6.67 (d, 2H), 3.70 (s,3H).

General procedure for LB catalyzed imines reduction

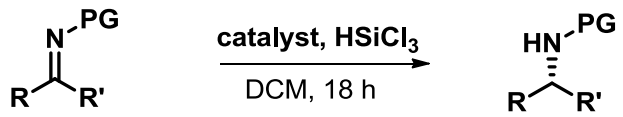

The imine (1 mmol) and the catalyst were introduced into a vial and dissolved in dry CH_2Cl_2 (1 mL) under inert atmosphere. $HSiCl_3$ (1 M solution in CH_2Cl_2, 3,5 equiv.) was added at 0° C and then the reaction was stirred at the indicated temperature and for the desired reaction time. After reaction time the crude mixture was treated with NaOH 10% aq. until basic pH = 9. The aqueous layer was extracted twice with CH_2Cl_2. The organic layer was collected, dried with Na_2SO_4, and concentrated under vacuum. The residue was purified by column chromatography on silica gel. The enantiomeric excess was determined by HPLC on chiral stationary phase.

Amines characterization

(*R*)-*N*-(1-phenylethyl)aniline (**1-38**)

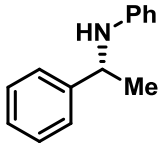

Prepared according to the general procedure. The crude mixture was purified by column chromatography on silica gel eluting with hexane/ethyl acetate 95:5 afford the title product as a yellowish solid. All analytical data are in agreement with literature.[125]

^{1}H-NMR (300 MHz, $CDCl_3$) δ_H 7.23-7.19 (m, 7H), 6.61-6.49 (m, 3H), 4.48 (q, 1H), 1.53 (d, 3H) ppm.

The enantiomeric excess was determined by HPLC on chiral stationary phase with Daicel Chiralcel OD-H column: eluent Hexane/*i*PrOH = 99/1, flow rate 0.8 mL/min, λ=254 nm, τ_{minor} = 13.2 min, τ_{major} = 15.9 min.

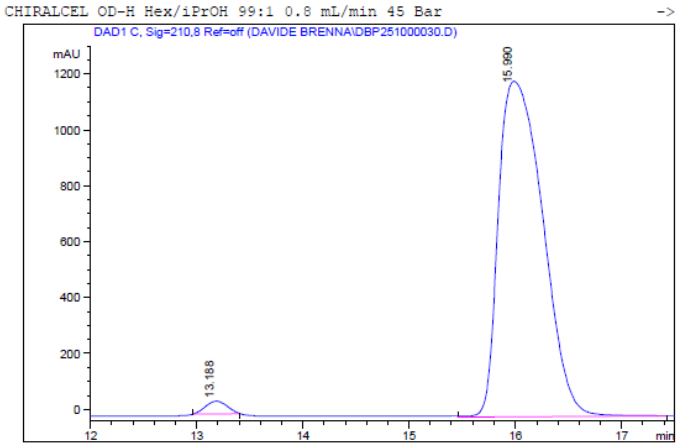

Signal 1: DAD1 C, Sig=210,8 Ref=off

Peak #	RT [min]	Type	Width [min]	Area	Area %	Name
1	13.188	MM	0.236	641.066	1.808	
2	15.990	MM	0.484	34822.816	98.192	

(*R*)-4-methoxy-*N*-(1-phenylethyl)aniline (**1-42**)

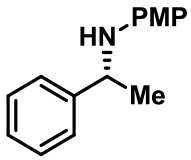

Prepared according to the general procedure. The crude mixture was purified by column chromatography on silica gel eluting with hexane/ethyl acetate 95:5 afford the title product as a yellowish solid. All analytical data are in agreement with literature.[125]

^{1}H-NMR (300 MHz, $CDCl_3$) δ_H 7.43-7.26 (m, 5H), 6.73 (d, 2H), 6.58 (d, 2H), 4.46 (q,1H), 3.74 (s, 3H), 1.58 (d, 3H) ppm.

The enantiomeric excess was determined by HPLC on chiral stationary phase with Daicel Chiralcel OD-H column: eluent Hexane/*i*PrOH = 99/1, flow rate 0.8 mL/min, λ=254 nm, τ_{major}=17.9 min, τ_{minor}=21.0 min.

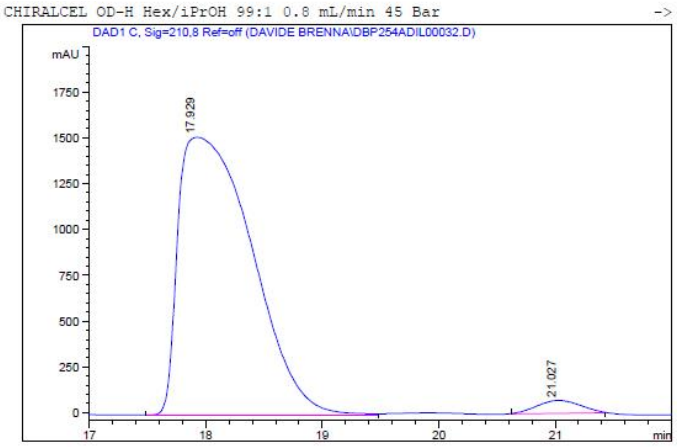

Signal 1: DAD1 C, Sig=210,8 Ref=off

Peak #	RT [min]	Type	Width [min]	Area	Area %	Name
1	17.929	BB	0.527	66942.359	97.342	
2	21.027	MM	0.435	1827.936	2.658	

(*R*)-4-methoxy-*N*-(1-(p-tolyl)ethyl)aniline (**1-43**)

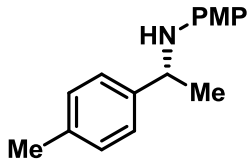

Prepared according to the general procedure. The crude mixture was purified by column chromatography on silica gel eluting with hexane/ethyl acetate 95:5 afford the title product as a yellowish solid. All analytical data are in agreement with literature.[126]

^{1}H-NMR (300 MHz, $CDCl_3$) δ_H 7.29-7.26 (d, 2H), 7.16-7.14 (d, 2H), 6.73-6.70 (d, 2H), 6.54-6.52 (d, 2H), 4.45-4.38 (q, 1H), 3.72 (s, 3H), 2.35 (s, 3H), 1.53(d, 3H) ppm.

The enantiomeric excess was determined by HPLC on chiral stationary phase with Daicel Chiralcel OD-H column: eluent Hexane/*i*PrOH = 98/2, flow rate 0.8 mL/min, λ=254 nm, τ_{major}=12.4 min, τ_{minor}=14.5 min.

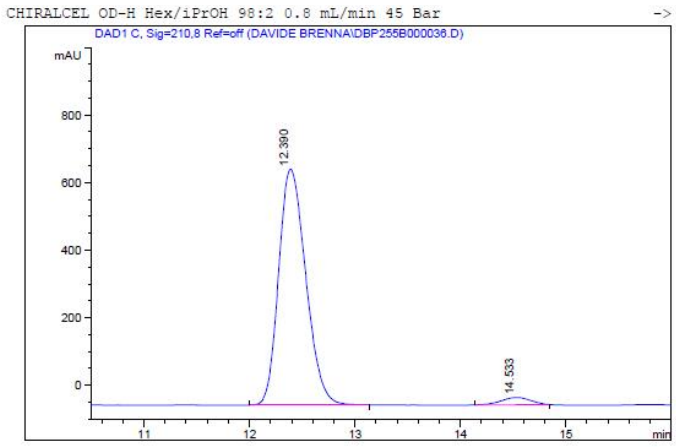

Signal 1: DAD1 C, Sig=210,8 Ref=off

Peak #	RT [min]	Type	Width [min]	Area	Area %	Name
1	12.390	BB	0.281	12496.647	96.751	
2	14.533	MM	0.325	419.646	3.249	

(*R*)-4-methoxy-*N*-(1-(4-methoxyphenyl)ethyl)aniline (**1-44**)

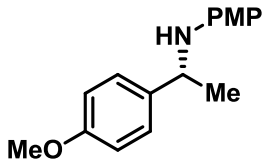

Prepared according to the general procedure. The crude mixture was purified by column chromatography on silica gel eluting with hexane/ethyl acetate 95:5 afford the title product as a yellowish solid. All analytical data are in agreement with literature.[125]

^{1}H-NMR (300 MHz, $CDCl_3$) δ_H 7.30 (d, 2H), 6.87 (d, 2H), 6.71 (d, 2H), 6.49 (d, 2H), 4.40 (q, 1H), 3.80 (s, 3H), 3.72 (s, 3H), 1.49 (d, 3H) ppm.

The enantiomeric excess was determined by HPLC on chiral stationary phase with Daicel Chiralcel OD-H column: eluent Hexane/*i*PrOH = 9/1, flow rate 0.8 mL/min, λ=254 nm, τ_{major}=11.5 min, τ_{minor} = 12.9 min.

CHIRALCEL OD-H Hex/iPrOH 9:1 0.8 mL/min 45 Bar

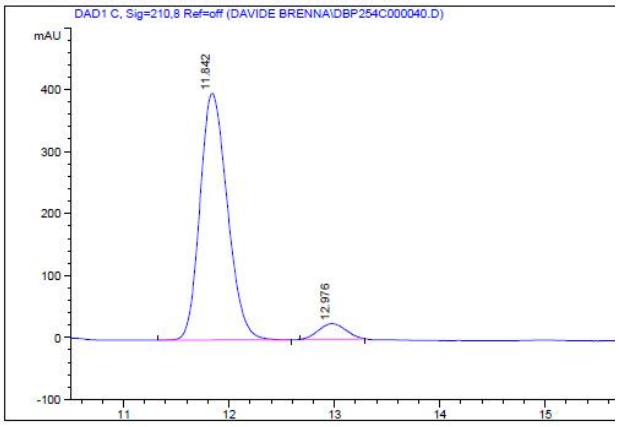

Signal 1: DAD1 C, Sig=210,8 Ref=off

Peak #	RT [min]	Type	Width [min]	Area	Area %	Name
1	11.842	MM	0.301	7188.565	94.144	
2	12.976	MM	0.298	447.114	5.856	

(*R*)-*N*-(1-(naphthalen-2-yl)ethyl)aniline (**1-46**)

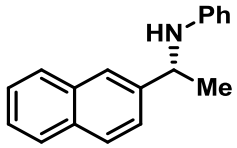

Prepared according to the general procedure. The crude mixture was purified by column chromatography on silica gel eluting with hexane/ethyl acetate 95:5 afford the title product as a yellow solid. All analytical data are in agreement with literature.[125] The product was also cristalized. The free amine was dissolved in Et_2O, than a stoichiometric amount of 1 M HCl in Et_2O was added. Formed precipitated was collected.

^{1}H-NMR (300 MHz, $CDCl_3$) δ_H 7.78-7.82 (m, 5H), 7.41-7.51 (m, 3H), 6.65-6.69 (m, 2H), 6.48-6.52 (m, 2H), 4.55 (q, 1H), 3.88 (br, 1H), 1.56 (d, 3H) ppm.

The enantiomeric excess was determined on the free amine by HPLC on chiral stationary phase with Daicel Chiralcel OD-H column: eluent Hexane/*i*PrOH = 99/1, flow rate 1.0 mL/min, λ=254 nm, τ_{major} = 21.6 min, τ_{minor} = 22.86 min.

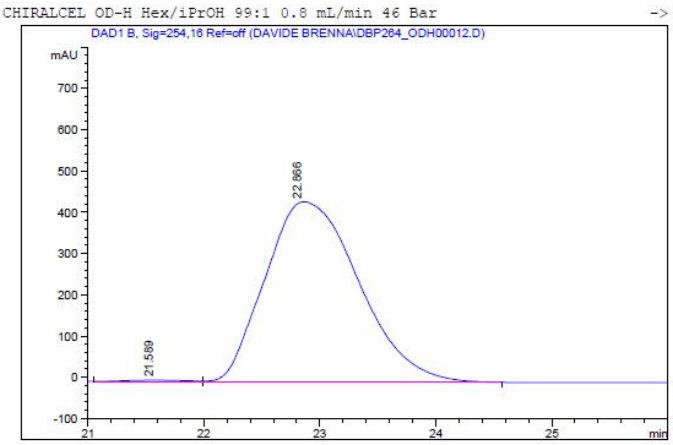

Signal 1: DAD1 B, Sig=254,16 Ref=off

Peak #	RT [min]	Type	Width [min]	Area	Area %	Name
1	21.589	VV	0.527	249.259	1.002	
2	22.866	VB	0.863	24629.781	98.998	

(*R*)-4-methoxy-*N*-(1-(4-fluorophenyl)ethyl)-4-methoxyaniline (**1-59**)

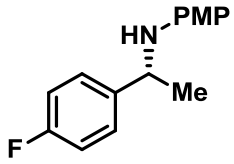

Prepared according to the general procedure. The crude mixture was purified by column chromatography on silica gel eluting with hexane/ethyl acetate 95:5 afford the title product as a yellowish solid. All analytical data are in agreement with literature.[127]

^{1}H-NMR (300 MHz, $CDCl_3$) δ_H 7.28-7.33 (m, 2H), 6.95-7.00 (m, 2H), 6.68 (d, 2H), 6.43 (d, 2H), 4.37 (q, 1H), 3.68 (s, 3H), 1.45 (d, 3H)ppm.

The enantiomeric excess was determined by HPLC on chiral stationary phase with Daicel Chiralcel OD-H column: eluent Hexane/*i*PrOH = 98/2, flow rate 0.8 mL/min, λ=254 nm, τ_{major}=19.6 min, τ_{minor} = 22.9 min.

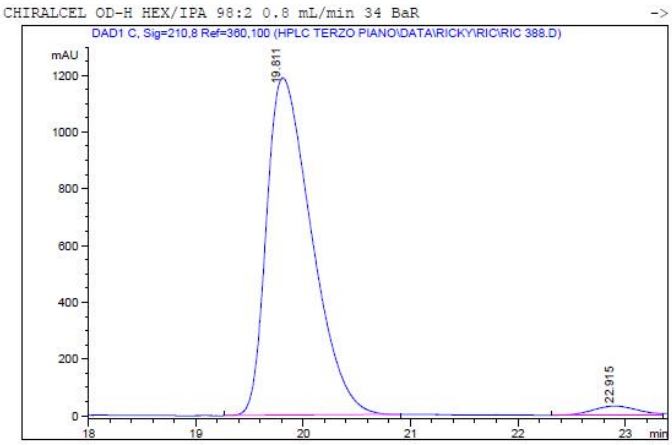

Signal 1: DAD1 C, Sig=210,8 Ref=360,100

Peak #	RT [min]	Type	Width [min]	Area	Area %	Name
1	19.811	BB	0.344	34618.781	97.284	
2	22.915	BV	0.355	966.477	2.716	

(*R*)-4-methoxy-*N*-(1-(4-(trifluoromethyl)phenyl)ethyl)aniline (**1-60**)

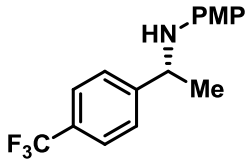

Prepared according to the general procedure. The crude mixture was purified by column chromatography on silica gel eluting with hexane/ethyl acetate 95:5 afford the title product as a yellowish solid. All analytical data are in agreement with literature.[125]

^{1}H-NMR (300 MHz, $CDCl_3$) δ_H 7.56 (d, 2H), 7.47 (d, 2H), 6.69 (d, 2H), 6.42 (d, 2H), 4.44 (q, 1H), 3.81 (bs, 1H), 3.68 (s, 3H), 1.48 (d, 3H) ppm.

The enantiomeric excess was determined by HPLC on chiral stationary phase with Daicel Chiralcel OD column: eluent Hexane/*i*PrOH = 98/2, flow rate 0.8 mL/min, λ=254 nm, τ_{major} = 22.2 min, τ_{minor} = 29.3 min.

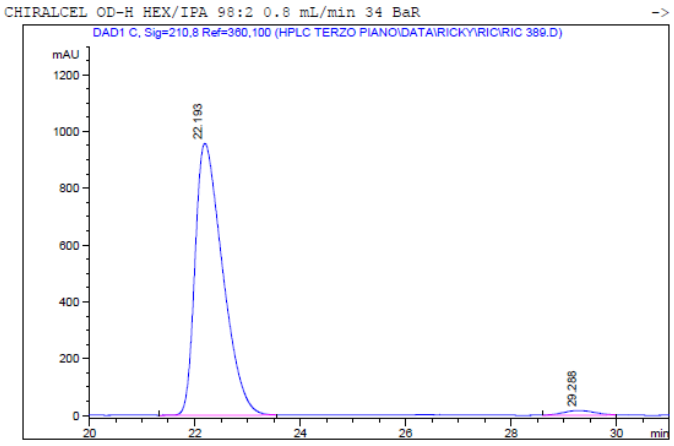

Signal 1: DAD1 C, Sig=210,8 Ref=360,100

Peak #	RT [min]	Type	Width [min]	Area	Area %	Name
1	22.193	VB	0.437	34731.688	98.103	
2	29.288	MM	0.674	671.542	1.897	

(*R*)-4-methoxy-*N*-(1-(4-nitrophenyl)ethyl)aniline (**1-61**)

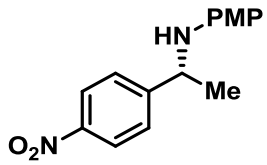

Prepared according to the general procedure. The crude mixture was purified by column chromatography on silica gel eluting with hexane/ethyl acetate 90:10 afford the title product as a orange solid. All analytical data are in agreement with literature.[126]

^{1}H-NMR (300 MHz, $CDCl_3$) δ_H 8.18 (m, 2H), 7.55 (d, 2H), 6.70 (m, 2H), 6.40(m, 2H), 4.50 (q, 1H), 3.86 (bs, 1H), 3.69 (s, 3H), 1.52(d, 3H) ppm.

The enantiomeric excess was determined by HPLC on chiral stationary phase with Daicel Chiralcel OD-H column: eluent Hexane/*i*PrOH = 99:1, flow rate 0.8 mL/min, λ=254 nm, τ_{major} = 37.5 min, τ_{minor} =44.5

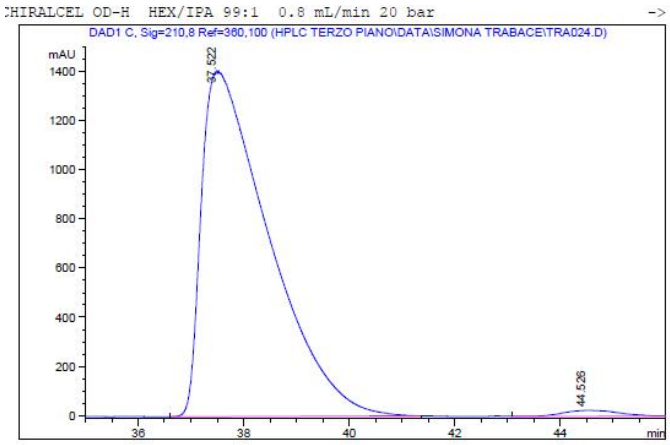

Signal 1: DAD1 C, Sig=210,8 Ref=360,100

Peak #	RT [min]	Type	Width [min]	Area	Area %	Name
1	37.522	BB	1.042	124581.422	98.609	
2	44.526	VV	0.853	1757.109	1.391	

(*R*)-4-methoxy -*N*-(1-(4-chlorophenyl)ethyl)-4-methoxyaniline (**1-62**)

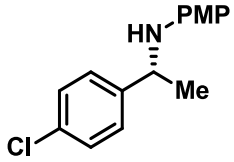

Prepared according to the general procedure. The crude mixture was purified by column chromatography on silica gel eluting with hexane/ethyl acetate 95:5 afford the title product as a yellowish solid. All analytical data are in agreement with literature.[127]

^{1}H-NMR (300 MHz, $CDCl_3$) δ: 7.31-7.25 (m, 4H), 6.70-6.67 (d, 2H), 6.44-6.42 (d, 2H), 4.40 (q, 1H), 3.72 (s, 3H), 1.48 (d, 3H).

The enantiomeric excess was determined by HPLC on chiral stationary phase with Daicel Chiralcel OD-H column: eluent Hexane/*i*PrOH = 98/2, flow rate 0.5 mL/min, λ=254 nm, τ_{major} = 33.4 min, τ_{minor}= 37.7 min.

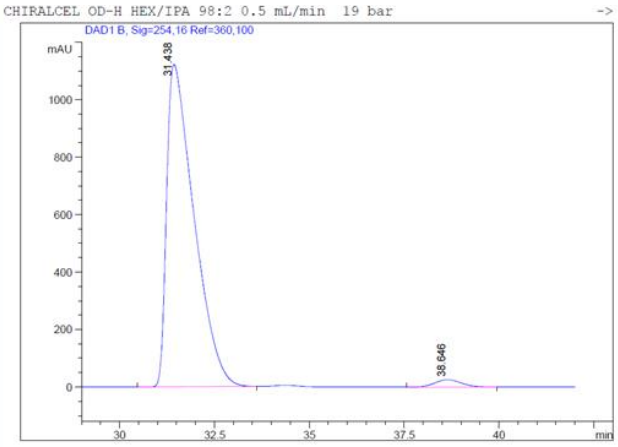

Signal 1: DAD1 B, Sig=254,16 Ref=360,100

Peak #	RT [min]	Type	Width [min]	Area	Area %	Name
1	31.438	MM	0.834	56122.465	97.775	
2	38.646	MM	0.828	1276.857	2.225	

(*R*)-4-methoxy-*N*-(1-(3-methoxyphenyl)ethyl)aniline (**1-63**)

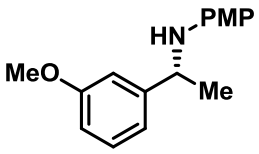

Prepared according to the general procedure. The crude mixture was purified by column chromatography on silica gel eluting with hexane/ethyl acetate 95:5 afford the title product as a yellowish solid. All analytical data are in agreement with literature.[128]

^{1}H-NMR (300 MHz, $CDCl_3$) δ_H 7.5-7.1 (m, 4H), 6.72 (d, 2H), 6.51 (d, 2H), 4.40 (q, 1H), 3.82 (s,3H), 3.73 (s, 3H), 1.52 (d, 3H).

The enantiomeric excess was determined by HPLC on chiral stationary phase with Daicel Chiralcel OD-H column: eluent Hexane/*i*PrOH = 98/2, flow rate 0.5 mL/min, λ=254 nm, τ_{major} = 25.9 min, τ_{minor} = 30.5 min.

CHIRALPAK OD-H Hex/i-PrOH 98:2 0.5 mL/min 19bar ->

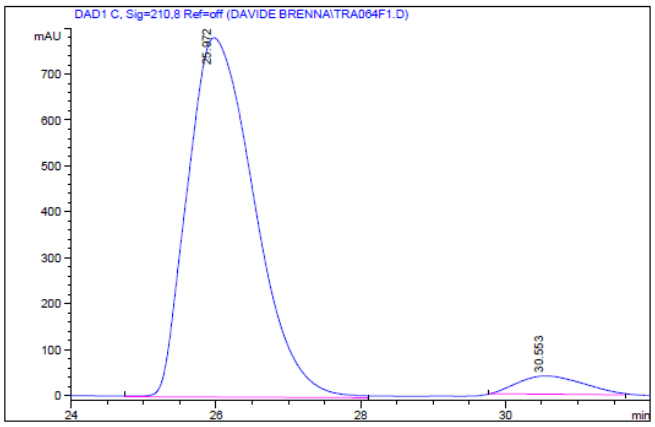

Signal 1: DAD1 C, Sig=210,8 Ref=off

Peak #	RT [min]	Type	Width [min]	Area	Area %	Name
1	25.972	MM	1.063	49882.402	95.249	
2	30.553	MM	1.043	2487.880	4.751	

(R) 4-methoxy-*N*-(1-(3-(benzyloxy)phenyl)ethyl)-aniline (**1-64**)

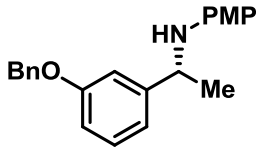

Prepared according to the general procedure. The crude mixture was purified by column chromatography on silica gel eluting with hexane/ethyl acetate 95:5 afford the title product as a yellowish solid. All analytical data are in agreement with literature. [70c]

^{1}H-NMR (300 MHz, $CDCl_3$) δ_H 7.5-7.0 (m, 9H), 6.72 (d, 2H), 6.51 (d, 2H), 5.06 (s, 2H), 4.40 (q, 1H) 3.73 (s, 3H), 1.52 (d, 3H). **MS** (ESI+) m/z for $C_{22}H_{23}NO_2$(+1): 333.8; **$[\alpha_D]^{23}$** = + 4.2 (c: 0.9 $CHCl_3$).

The enantiomeric excess was determined by HPLC on chiral stationary phase with Daicel Chiralcel OD-H column: eluent Hexane/*i*PrOH = 98/2, flow rate 1.0 mL/min, λ=254 nm, τ_{major} = 31.8 min, τ_{minor} = 46.7 min.

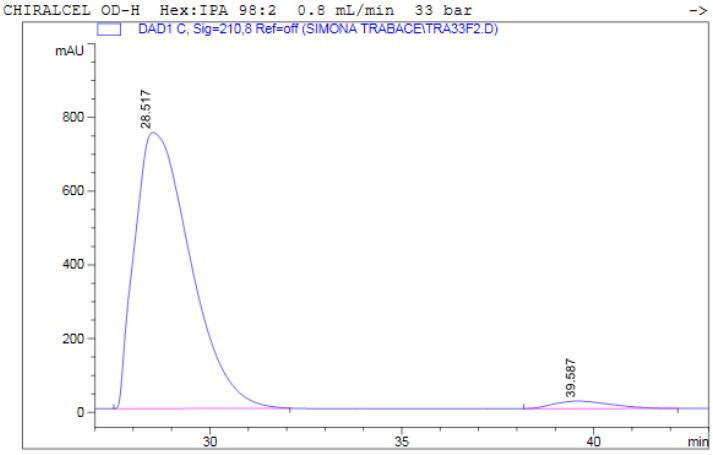

Signal 1: DAD1 C, Sig=210,8 Ref=off

Peak #	RT [min]	Type	Width [min]	Area	Area %	Name
1	28.517	BB	1.299	75291.953	97.264	
2	39.587	BB	1.228	2117.790	2.736	

(*R*)-*N*-benzyl-1-(3-(benzyloxy)phenyl)ethanamine (**1-65**)

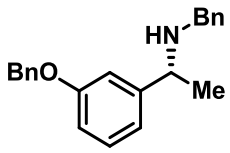

Prepared according to the general procedure. The crude mixture was purified by column chromatography on silica gel eluting with hexane/ethyl acetate 8:2 afford the title product as a white liquid. All analytical data are in agreement with literature.ref

^{1}H-NMR (300 MHz, $CDCl_3$) δ_H 7.5-7.30 (m, 10H), 7.00 (m, 1H) 6.98 (d, 1H), 6.93 (dd, 1H), 5.12 (s, 2H), 3.85 (q, 1H) 3.72-3.60 (AB sytem, 2H), 1.42 (d, 3H).

The enantiomeric excess was determined by HPLC on chiral stationary phase with Daicel Chiralcel OD-H column: eluent Hexane/*i*PrOH = 98/2, flow rate 1.0 mL/min, λ=254 nm, τ_{major} = 31.8 min, τ_{minor} = 46.7 min.

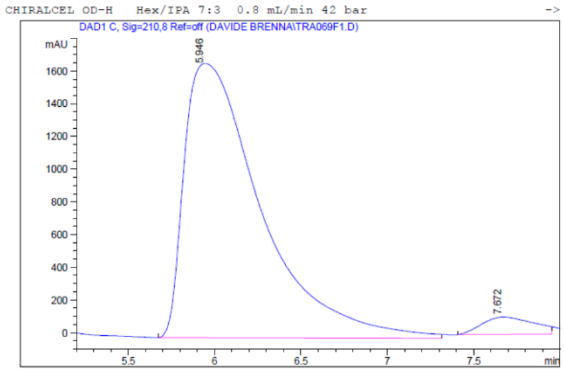

Signal 1: DAD1 C, Sig=210,8 Ref=off

Peak #	RT [min]	Type	Width [min]	Area	Area %	Name
1	5.946	MM	0.514	51784.734	95.846	
2	7.672	MM	0.350	2244.541	4.154	

(*R*)-3-phenyl-N-(1-phenylethyl)propan-1-amine (**1-66**)

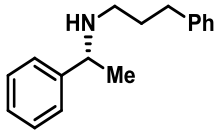

Prepared according to the general procedure. The crude mixture was purified by column chromatography on silica gel eluting with hexane/ethyl acetate 95:5 afford the title product as a white liquid. All analytical data are in agreement with literature.[129]

^{1}H-NMR (300 MHz, $CDCl_3$) δ_H 7.35-7.15 (m, 10H), 3.77 (q, 1H),2.72-2.46 (m, 4H) 1.86-1.76 (m, 2H) 1.53 (br, 1H), 1.37 (d, 3H).

Enantiomeric excess was determined by comparison of the integrals in the **^{1}H NMR** spectrum in $CDCl_3$ of the diastereomeric salts formed by addition of excess L-Mandelic acid.

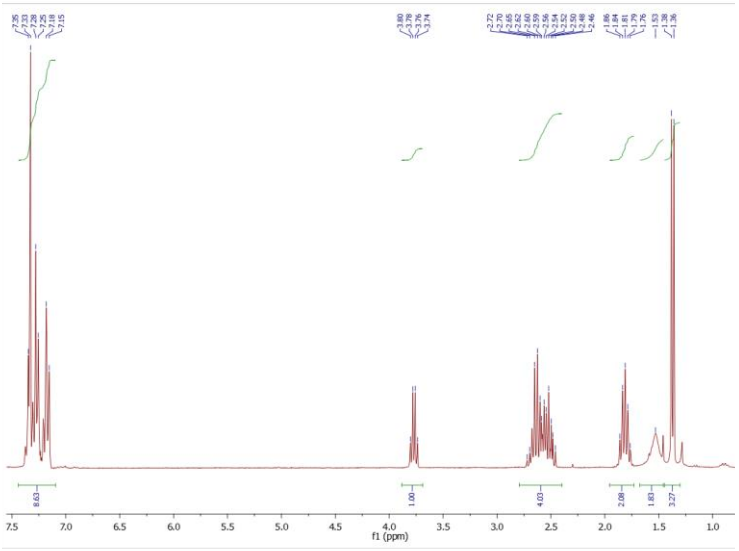

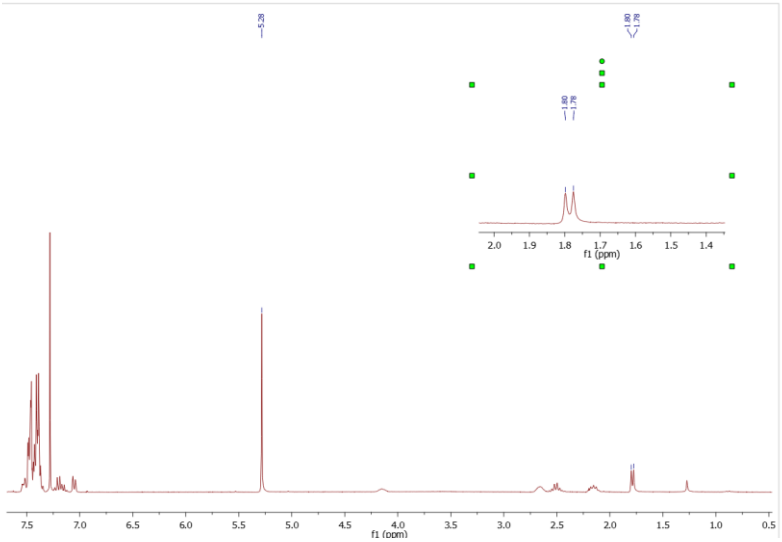

(*R*)-N-(1-phenylethyl)butan-1-amine (**1-67**)

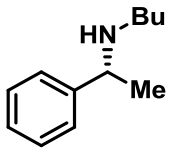

Prepared according to the general procedure. The crude mixture was purified by column chromatography on silica gel eluting with hexane/ethyl acetate 90:10 afford the title product as a white liquid. All analytical data are in agreement with literature.[63c]

^{1}H-NMR (300 MHz, $CDCl_3$) δ_H 7.3-7.1 (m, 5H), 3.73 (q, 1H), 2.45-2.35 (m, 2H), 1.4-1.3 (m, 2H), 1.32 (d, 3H), 1.22-1.15 (m, 2H), 0.79 (t, 3H).

The enantiomeric excess was determined by analysis of the acetamide obtained by reaction of the isolated amine with aceticanhydride at room temperature for 12 The enantiomeric excess was determined on the acetylated product by HPLC on chiral stationary phase with Daicel Chiralcel IB column: eluent Hexane/*i*PrOH = 85/15, flow rate 0.8 mL/min, λ=210 nm, τ_{minor} = 5.7 min, τ_{major} = 6.33 min.

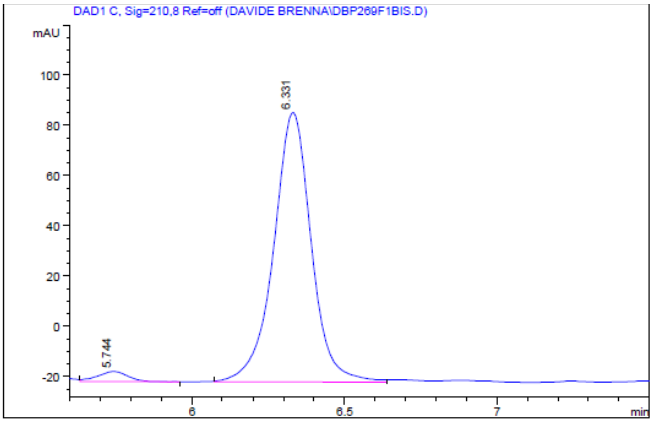

Signal 1: DAD1 C, Sig=210,8 Ref=off

Peak #	RT [min]	Type	Width [min]	Area	Area %	Name
1	5.744	VB	0.104	26.859	2.832	
2	6.331	BB	0.130	921.632	97.168	

Methyl (*S*)-2-((4-methoxyphenyl)amino)-2-phenylacetate (**1-68**)

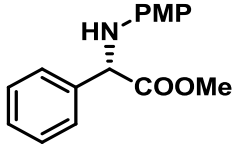

Prepared according to the general procedure. The crude mixture was purified by column chromatography on silica gel eluting with hexane/ethyl acetate 8:2 afford the title product as a yellowish solid. All analytical data are in agreement with literature.

^{1}H-NMR (300 MHz, $CDCl_3$) δ_H 7.53-7.51 (m, 2H), 7.39-7.36 (m, 3H), 6.75 (d, 2H), 6.56 (d, 2H), 5.03 (s, 1H), 4.70 (br s, 1H), 3.73 (s, 3H), 3.71 (s, 3H). ppm.

The enantiomeric excess was determined by HPLC on chiral stationary phase with Daicel Chiralcel OJ-H column: eluent Hexane/*i*PrOH = 7/3, flow rate 0.8 mL/min, λ=210 nm, τ_{minor} = 50.3 min, τ_{major} = 54.2 min.

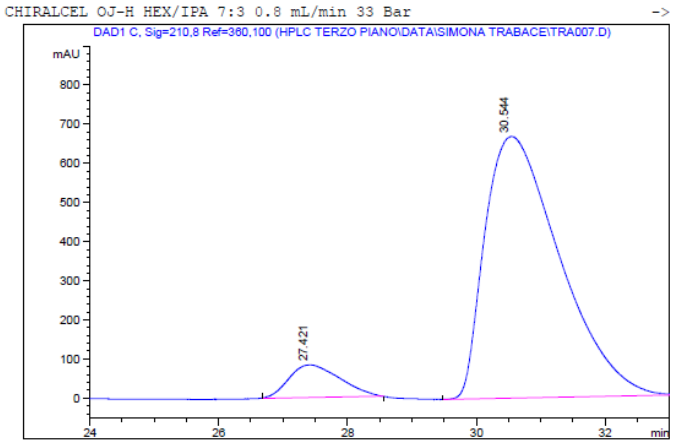

Signal 1: DAD1 C, Sig=210,8 Ref=360,100

Peak #	RT [min]	Type	Width [min]	Area	Area %	Name
1	27.421	MM	0.908	4535.762	7.744	
2	30.544	BB	0.953	54036.539	92.256	

Methyl (*R*)-3-((4-methoxyphenyl)amino)-3-phenylpropanoate (**1-69**)

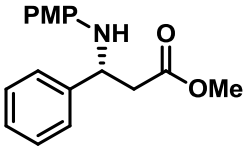

Prepared according to the general procedure. The crude mixture was purified by column chromatography on silica gel eluting with hexane/ethyl acetate 95:5 afford the title product as a white solid. All analytical data are in agreement with literature.

^{1}H-NMR (300 MHz, $CDCl_3$) δ_H 7.32-7.20 (m, 5H), 6.70 (d, 2H), 6.50 (d, 2H), 4.78 (m, 1H), 3.70 (s, 3H), 3.60 (s, 3H), 2.75 (d, 2H) ppm.

The enantiomeric excess was determined by HPLC on chiral stationary phase with Chiralcel cellulose 1 3 micron column: eluent Hexane/*i*PrOH = 95/5, flow rate 0.8 mL/min, λ=210 nm, τ_{major} = 22.7 min, τ_{minor} = 31.0 min.

CHIRALCEL CELLULOSA 1 3 MICRON Hex/iPrOH 95:5 0.8 mL/mi ->

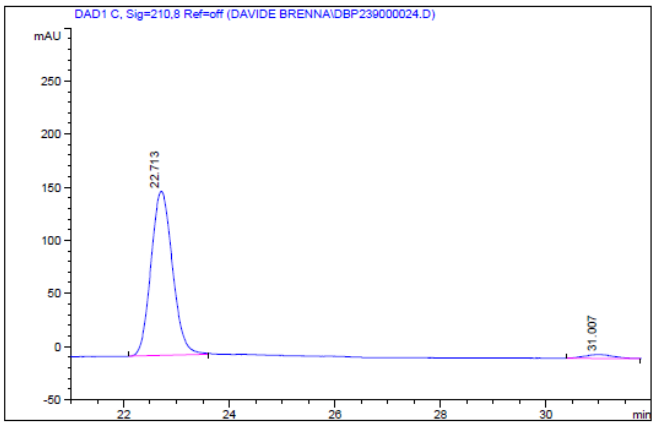

Signal 1: DAD1 C, Sig=210,8 Ref=off

Peak #	RT [min]	Type	Width [min]	Area	Area %	Name
1	22.713	BB	0.438	4367.251	97.122	
2	31.007	BBA	0.447	129.429	2.878	

(*S*)-4-methoxy-N-(2-nitro-1-phenylethyl)aniline (**1-70**)

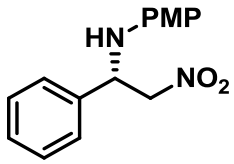

Prepared according to the general procedure. The crude mixture was purified by column chromatography on silica gel eluting with hexane/ethyl acetate 9:1 and then 8:2 afford the title product as a yellowish solid. All analytical data are in agreement with literature.

^{1}H-NMR (300 MHz, $CDCl_3$) δ 7.40 (m, 5H), 6.75(d, 2H), 6.62 (d 2H), 5.11 (t, 1H), 4.74 (m, 2H), 3.73 (s, 3H).

The enantiomeric excess was determined by HPLC on chiral stationary phase with Daicel Chiralcel AD column: eluent Hexane/*i*PrOH = 9/1, flow rate 0.8 mL/min, λ=210 nm, τ_{minor} = 50.3 min, τ_{major} = 54.2 min.

CHIRALCEL AD Hex/iPrOH 9:1 0.8 mL/min 20 Bar ->

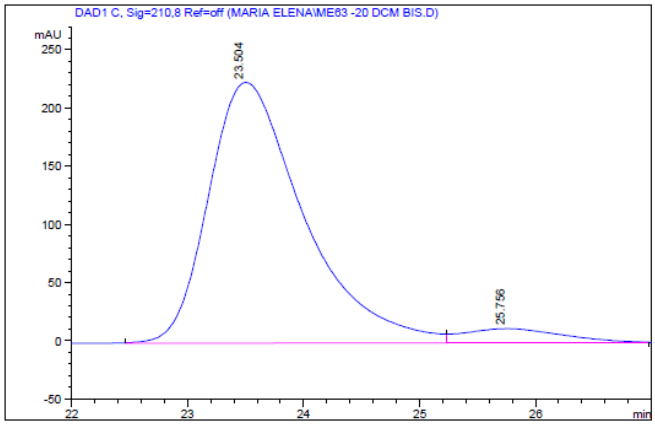

Signal 1: DAD1 C, Sig=210,8 Ref=off

Peak #	RT [min]	Type	Width [min]	Area	Area %	Name
1	23.504	BB	0.816	12800.857	94.630	
2	25.756	BB	0.700	726.360	5.370	

Chapter 2

Stereoselective catalytic reactions in 3D-printed mesoreactors

Introduction to 3D-printing

3D-printing is a technology that allows to prepare and craft customized object. In general, there are the different options available to prepare an object; the four processes are here described.

1) **Subtractive processes**: the starting raw material is transformed and manufactured by removing the excess material. One example of this are Greek statues were created using this process. The starting piece of marble is chiseled, and the final statue is obtained.
2) **Forming**: in forming process a selected amount of material is subjected to an external force and its shape is modified, until the desired object is created. In this process in principle no material is lost.
3) **Casting**: in this process, the material is taken in its starting solid state, and then melted; the melted material is charged into a different shape and is cooled down, obtaining the final object. An example is the preparation of chocolate bars.
4) **Additive**: there is nothing in the beginning, however, the material is put in the right position and the object is created. This particular type of manufacturing is called three-dimensional (3D), printing.

3D printing is a technology capable of transforming ideas in: low cost, flexible and bespoke devices. The production of extremely customized object was also possible before the raising of the 3D printers, however, higher cost are related to this type of realization. Using this simple additive manufacturing process, the selected object could be created “layer after layer”. The desired object is projected using a design software (e.g. CAD), stored in a virtual file in a Stereo-lithography format (usually a STL file) and finally transformed into a G-code file. The G code file, a cartesian description of the object, could be read by a 3D printer. (Figure 2-1)

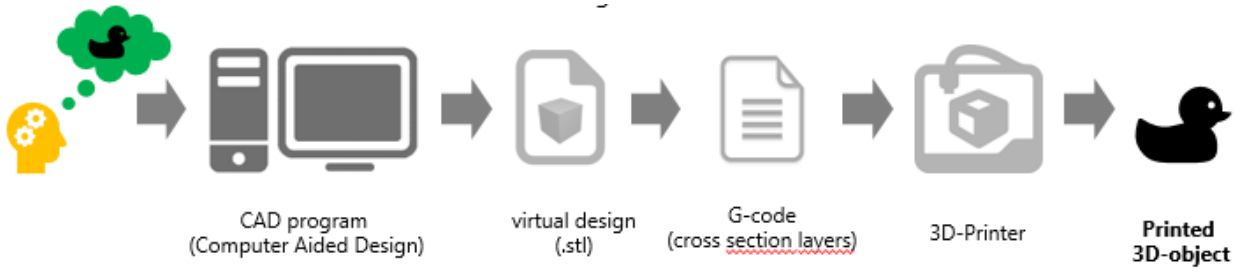

Figure 2-1: procedure for the printing of an object.

3D printers could use different technologies for the realization of the projected object, hence the definition of the 3D printing process is hard to outline. However, the most spread 3D printers are based on Fused Deposition Modeling (FDM) or Fused Filament Fabrication (FFF); these printers work with filaments made of different materials (plastic, metal or composite materials), that are

unwound from a coil, melted and press through a nozzle that is moved by numerically controlled mechanism. (Figure 2-2)

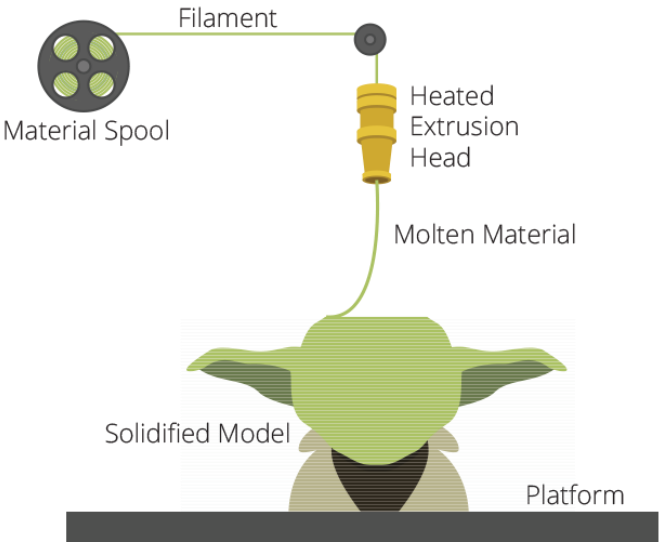

Figure 2-2

The FDM/FFF technology was invented and patented by Scott Crump in 1987[130], however until the expiration of the patents, remains an expansive, close, and niche market. In the last 10 years a new, large, and open source community has started to improve and develop cheap 3D printers base on FDM/FFF tech. Nowadays the FDM 3D printers are affordable also with low budgets and available in many electronic stores[131].

In addition, 3D printers based on different technologies are also available such as, stereolithography (SLA), firstly discovered in 1974[132] by D. Jones and then, successfully developed by W. K. Swainson[133] and C. W. Hull I[134], however these ones are more expansive and more difficult to use compared with the FFF one.

The raising and spreading of 3D printing devices and technologies related, it has been indicated as a possible new industrial revolution. This “label” could be explained because it allows the realization faster, cheaper and customizer of “real-life Object” compared to standard manufacturing process. Another important advantage is the shorter “chain” (construction, packing, shipping) between the producers and the users, since the 3D printed object could be produced in situ; extremes examples of the use of 3D printers are the international space station[135] and in disasters zone[136] (e.g. Nepal after earthquake).

Furthermore, the low-cost production, the easy modification of prototypes, and the development of new printable material (plastic, metals, ceramics, resins and polymers) make possible new applications (biomedical supplies, spare parts of out of production machinery and so on).

An application of 3D printing close to our field of research is the possibility of making the research equipment used every day in a chemistry laboratory [137]. Different objects could be printed[138] such

as, Buchner funnels, lab jack, filter bracket, vial racks microtiter plates, customizable filter wheel, holders, and so on.

L. Cronin, one of the first pioneer scientist that used 3D printers for the preparation of inorganic clusters' models, declared: "I do not want chemistry reduced to plastic trinkets, I want new science to occur because of use of ubiquitous 3-D printing and molecular design".[139] After these words, in the last few years, a huge number of different application of 3D printing were reported by the chemistry community. Device for DNA-extraction, mini-preparative columns, rotors for centrifuging standard tube and orbital shaker were successfully 3D-printed.

Recently, the preparation of a 3D-printed syringe pump has been reported by the group of J. M. Pearce[140]. The printed syringe pump shows similar performance to the commercially available one, however the price of the printed device is lower. In addition, reaction ware used in chemical synthesis and purification[141], flow plates for the water electrolysis[142], and continuous ESI-MS analysis of metal complexes[143] have been produced using the 3D printing technology.

Other examples involve the use of 3D printed devices as reusable electrodes for electrochemical detection.[144]

3D printed devices have been also utilized in biomedical applications[145], the possibility of using polymers compatible with human tissue[146] open the way to different solutions, such as the realization of biodegradable tissue, bones tissue[147] and, cell-culture[148]. .

Furthermore, the potential of 3D printing technology has been having a significantly impact in the field of microfluidics devices,[149] that could incorporate also membranes in order to study drug transport and effect through the cells,[150] or could quantitatively investigate the properties of stored red blood cells for transfusion in medicine.[151] Recently, more complexes devices has been realized by Filippini where with a commercial micro-stereo lithography 3D printer, they were able to realized conventional PDMS (polydimethylsiloxane) glass lab-on-a-chip devices for glucose concentration diagnostics.[152]

An interesting application of 3D printed flow plates was reported by Cronin et all[153]; the authors performed the synthesis and the following reduction of aldimines, under continuous flow conditions using 3D printed reactors. (Scheme 2-1)

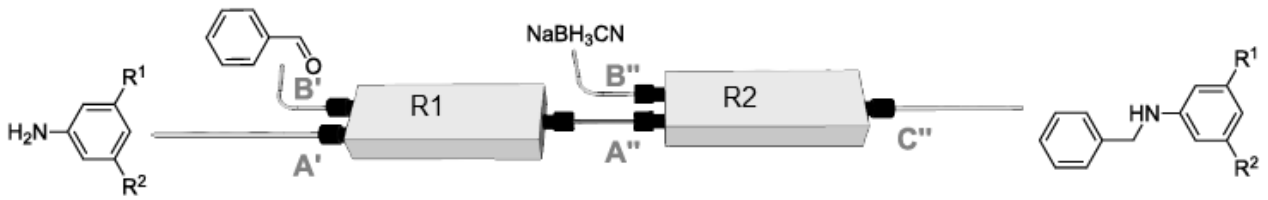

Scheme 2-1: all in flow reductive amination of benzaldehyde in 3D-Printed devices

The reductive amination of benzaldehyde in combination with different aromatic amines, was successfully performed. The two step all in flow process was carried out in two 3D printed reactors made of polypropylene. In the first reactor (Scheme 2-1, R1), the complete condensation (followed by in line IR analysis) of the aldehyde with the amines was successfully achieved using methanol as solvent, with 14 minutes residence time. The imines intermediates were not isolated and directly injected into the second reactor (Scheme 2-1, R2), that was fed with a solution of $NaBH_3CN$. Notably, also the second step of the reaction was followed by in line IR measurement and the complete reduction of the imine was achieved in 14 minutes residence time only. The desired secondary amines were obtained in the process with very good yields up to 99%.

In this chapter the design and preparation of 3D printed reactor, employing different materials will be presented. These reactors will be used for the preparations of key and chiral intermediates for the synthesis of different APIs, in particular using stereoselective Henry reactions. Different reactor set-ups will be explored and compared, thanks to the extremely versatility of the 3D printing technology.

Continuous Flow Henry reaction

The reaction of a nitroalkane with a carbonyl compound is an efficient solution for the formation of C-C bond[154] and it is known as Henry reaction.

The formed β-nitroalcohols are an important synthetic intermediate; they, could be transformed, for examples, in 1-2 amino alcohols, after the reduction of the nitro group. The development of stereoselective methodologies for the preparation of these valuable chiral building blocks was investigated since the first years of the '90.

In 1992, Shibasaki[155] et al reported the first catalytic and stereoselective Henry reaction; after this breakthrough numerous examples were published in the literature, reporting the use of metal based catalysis[156] or organocatalysis[157]. Using the Henry reaction, it is possible to generate up to two different stereocenters, hence a powerful control on the stereochemical outcome is necessary. However, the high acidity of the proton, in alpha position to the NO_2 group, lead to the reversibility of the reaction and an easy epimerization of the substituent in the alpha position. A complete control of the reaction conditions is necessary to avoid the racemization of the final product.

The metal of choice for this transformation is copper(II) [158], and different complexes have been extensively used in literature. One of the milestone work in the field is the enantioselective, copper-catalyzed Henry reaction reported by the group of Jørgensen[159]. The stereoselective attack of nitromethane towards α-keto esters was carried out using a catalytic amount of a copper bis oxazolidine complex, in the presence of TEA as organic base. The α-hydroxy-β- nitro esters were obtained with yields and enantioselectivities, up to 94%. (Scheme 2-2)

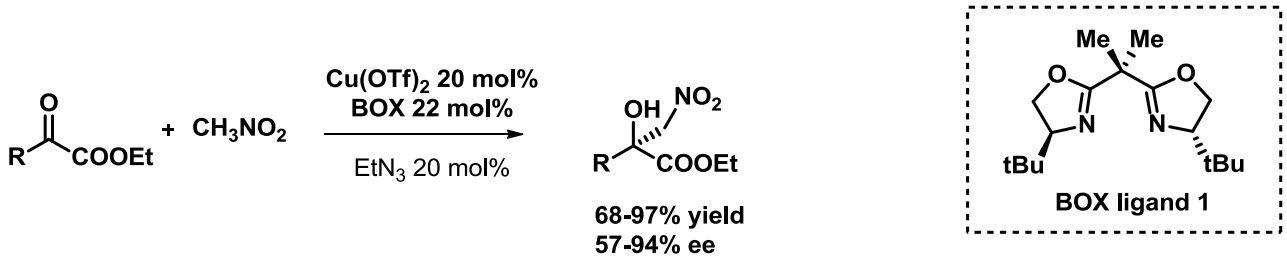

Scheme 2-2: stereoselective copper catalyzed Henry reaction

The use of BOX ligands in combination with Cu(II) in the Henry reaction was also explored by the group of Evans[160]. In this case simple aldehydes were employed, and the reaction was carried out using $Cu(OAc)_2$ but in absence of an external base, indeed the acetate ions could act as base in the formation of the nitronate. The best ligand was BOX derived from cis-1-aminoindan-2-ol (Scheme 2-3), high yields and enantioselectivity were achieved (up to 94 ee).

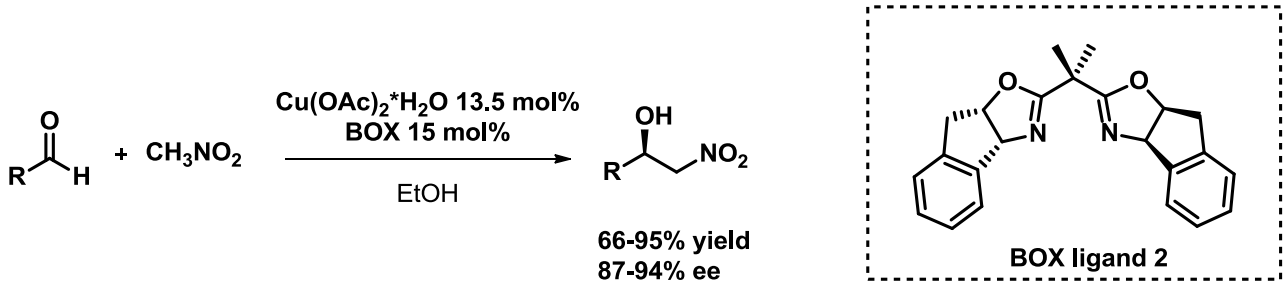

Scheme 2-3

The Henry reaction between aldehydes and nitromethane have been extensively studied in the literature and different systems able to achieve high performance in terms of yield and stereoselection have been reported. However, the condensation using other nitroalkanes is challenging and suffer from low selectivity and low reactivity. The control of the formation of two different stereocenters is very difficult, and only a limited number of catalyst showed good control of diastero and enantio selectivity.

The use of amino pyridine, as chiral ligand, was successfully reported by Pedro and co-workers in 2008[161]. Different aldehydes were attacked by nitroethane, obtaining the desired nitro alcohols in high yields and selectivity, employing a Cu(II) complex derived from aminopyridine. (Scheme 2-4)

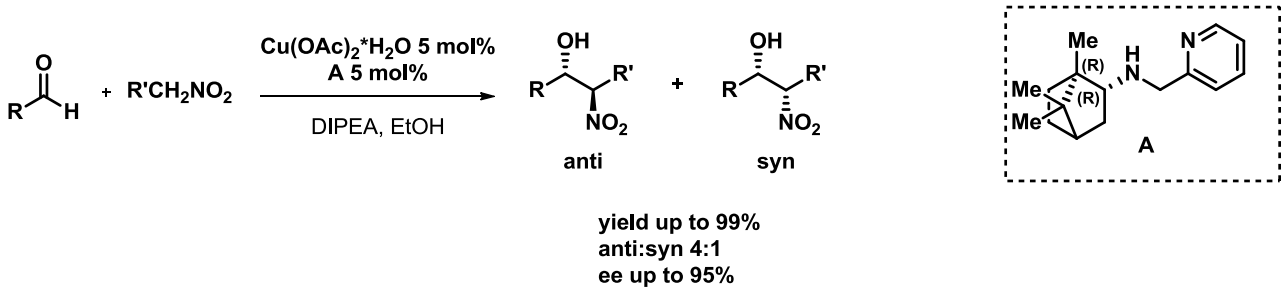

Scheme 2-4. Cu-catalyzed Henry reaction between aldehydes and nitroalkanes using camphor derived complexes.

The rationalization of these results could be explained because the aminopyridine ligand coordinates the copper ion with a strongly basic amine nitrogen (sp^3) and a weakly basic pyridine nitrogen (sp^2) to form a complex in which both equatorial coordination positions of the hypothetical square planar complex would be electronically differentiated. Furthermore, the free rotation around the carbon-nitrogen bond would allow better accommodation of the camphor skeleton in the metal complex compared to the one obtained with previously reported iminopyridine ligand. (Figure 2-3).

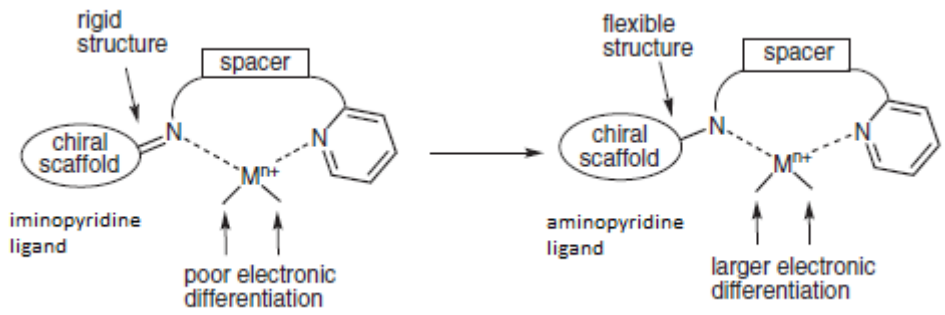

Figure 2-3. Different properties of amino- and imino-pyridine ligands.

In this project developed during my PhD thesis we wanted to explore the possibility of using a 3D printer reactors with different, shape, size of the channels and geometry, focusing our attention on the preparations of 4 targeted amino alcohols. The synthesis of these compounds is straightforward and an all in flow methodology for their preparation was planned (Figure 2-4). The first stereoselective Henry reaction will take place in a 3D printed reactor, subsequently the obtained nitroalcohol will be reduced under continuous flow conditions using an H-Cube apparatus. We decided to study the influence of different parameters on the Henry reaction, taking advantage of the wide range of solutions offered by the 3D printing.

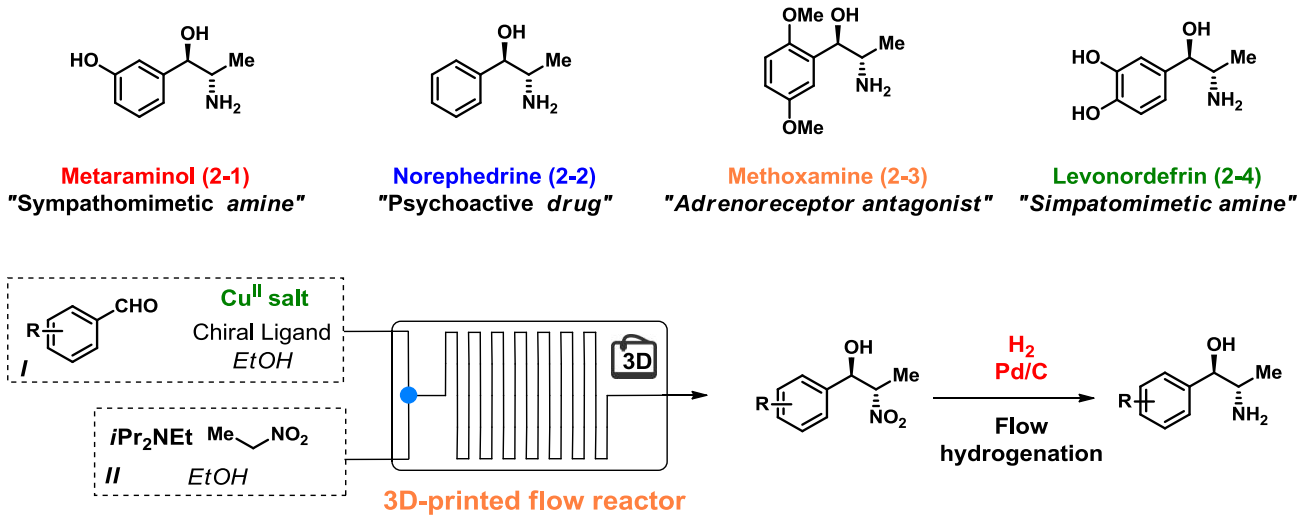

Figure 2-4: API based on chiral aminoalcohols

The first target is Metaraminol (**2-1**), is a sympathomimetic amine, it is used for the prevention and/or the treatment of hypotension[162] when it is a complication of anesthesia. Recently has been used for the treatment of priapism, however, until now, FDA did not approve the amine for this use. Norephedrine (2-2), is a psychoactive drug, obviously belongs to the class of phenethylamine and amphetamine. It is also used as stimulant, anorectic agent and decongestant. It is also used in veterinary medicine for dog's urinary incontinence.

Methoxamine and Levonorephedrine are both biologically active substances and in particular, are alpha-adrenergic agonist, their used for the human treatment is currently under investigation

All these four molecules could be prepared using a stereoselective, copper catalyzed Henry reaction, followed by the nitro group reduction. For safety reason, running the nitro aldol reaction required a particular attention, since the use of explosive nitro derivatives is strictly regulated, the use of continuous flow apparatus for their preparation could be very interesting. Indeed, as already discuss in the introduction the use of flow chemistry could allow the employment and the handling of hazardous chemical substances, reducing volume and the amount of material during the reaction. (Figure 2-4).

In order to find a suitable complex for the stereoselective Henry reaction, the reaction between 3-benzyloxy benzaldehyde and nitroethane was studied as model reaction. Moreover, the nitroalcohol **2-5** was the direct precursor of metaraminol (Table 2-1).

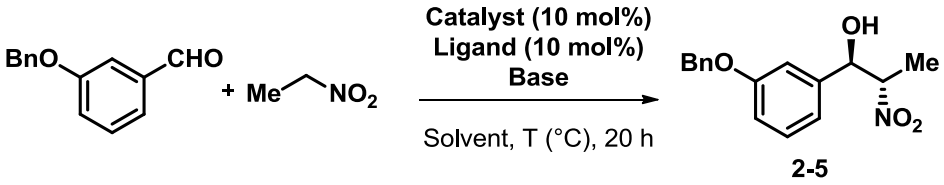

Table 2-1. Screening of catalysts and chiral ligands.

Entry	Ligand	Catalyst	Base	Solvent	T (°C)	Conv.(%)	*anti/syn*[a]	ee_{anti} *(%)*[b]
1	**A**	$Cu(OAc)_2*H_2O$	DIPEA	EtOH	-45	91	7:3	92
2	**B**	$Cu(OAc)_2*H_2O$	DIPEA	EtOH	-45	10	nd	nd
3	**C**	$Cu(OAc)_2*H_2O$	DIPEA	EtOH	-45	21	1:1	10
4	**D**	$Cu(OAc)_2*H_2O$	DIPEA	EtOH	-45	22	1:1	10
5	**E**	$Cu(OAc)_2*H_2O$	DIPEA	EtOH	-45	40	6:4	10
6	**F**	$Cu(OAc)_2*H_2O$	DIPEA	EtOH	-45	24	6:4	15
7	**B**	$Cu(OTf)_2$	DIPEA	EtOH	-45	16	1:1	rac
8	**C**	$Cu(OTf)_2$	DIPEA	EtOH	-45	16	1:1	rac
9	**D**	$Cu(OTf)_2$	DIPEA	EtOH	-45	33	4:6	rac
10	**E**	$Cu(OTf)_2$	DIPEA	EtOH	-45	53	1:1	62
11	**F**	$Cu(OTf)_2$	DIPEA	EtOH	-45	18	7:3	50
13	**G**	$CuBr_2$	Cs_2CO_3	THF	0	69	3:7	rac
12	**H**	$Cu(OAc)_2*H_2O$	DIPEA	Dioxane	0	51	3:7	16
14	**A**	$Cu(OTf)_2$	TEA	MeOH	-45	45	1:2	6
15	**G**	$CuBr_2$	Cs_2CO_3	THF	-15	85	1:1	22

[a]Determined by H-NMR of the crude; [b]determined by HPLC on chiral stationary phase.

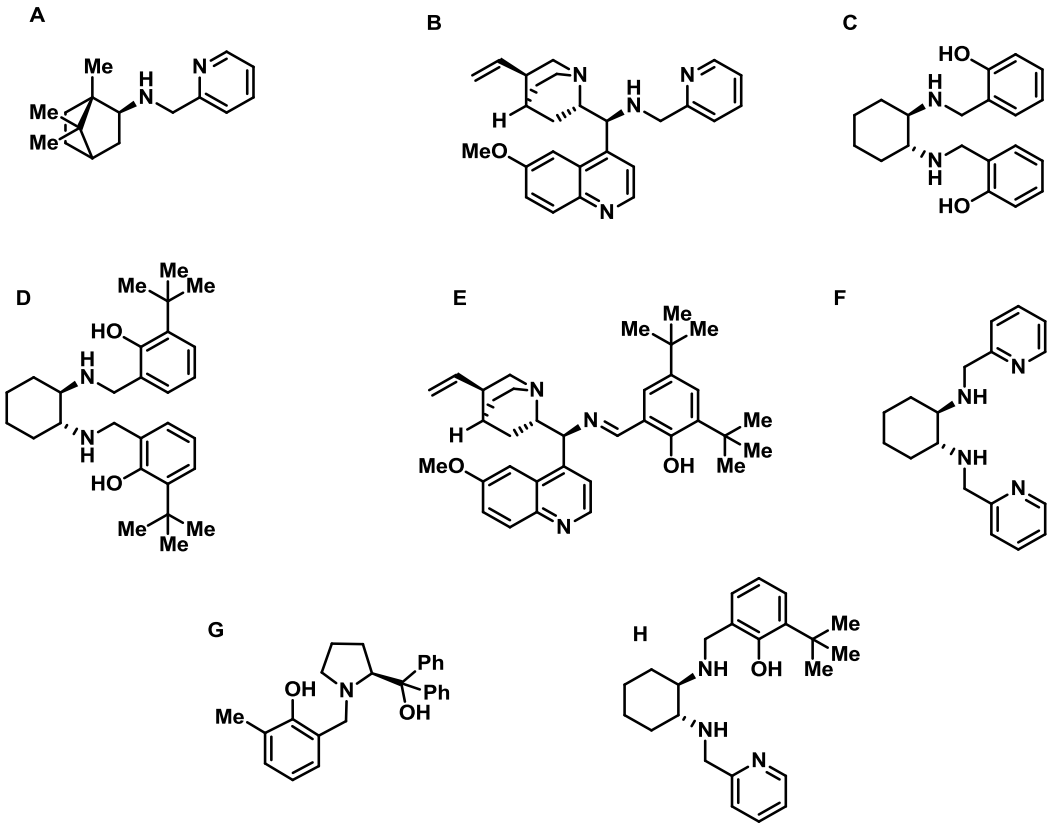

Figure 2-5: chiral ligands for stereoselective Henry reactions

A small library of ligands (Figure 2-5) was tested for the Henry reactions in combination with different Cu source.

The first copper source that was investigated was $Cu(OAc)_2*H_2O$ (Table 2-1, entries 1-6), in the presence of Hünnings base and ethanol as solvent and different chiral ligands. The best results were achieved using the chiral amino pyridine ligand **A**, conversion up to 91 %, d.r. up to 7:3, and ee up to 92 were observed. Using other ligands low conversion, and in most of the cases no enantioselection was observed. Also, $Cu(OTf)_2$ was tested, in combination with the chiral ligands, (Table 2-1, entries 7-11) the best results in this case were achieved using chiral ligand E (Table 2-1, entry 10), however, lower yield (only up to 53) and lower stereoselectivity was observed.

With these preliminary results, the optimization of the reaction condition was performed using chiral ligand A.

The preparation of this amino based chiral ligand is straightforward (Scheme 2-5), the selected enantiomer of Camphor is condensed with 2-Picolylamine, using BF_3 as catalyst and the obtained chiral imine is then stereoselectively reduce using $NaBH_4$ in the presence of $NiCl_{2.}$ (for experimental details see the experimental section of the thesis) This chiral ligand, is a good compromise in terms of availability, low cost, and easy preparation, even if not complete diasterocontrol is reached. .

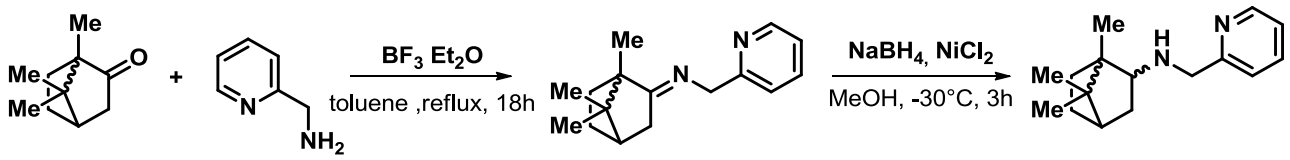

(*R*)(+)-Camphor
(*L*)(-)-Camphor

2-6: (*R*)
2-7: (*S*)

2-8: (*R,R*)
2-9: (*S,S*)

Scheme: 2-5 Synthesis of chiral ligands 81 and 83.

The reaction conditions were optimized using chiral ligand **2-8** and **2-9**. First the influence of the temperature on the reaction outcome was analyzed. (Table 2-2)

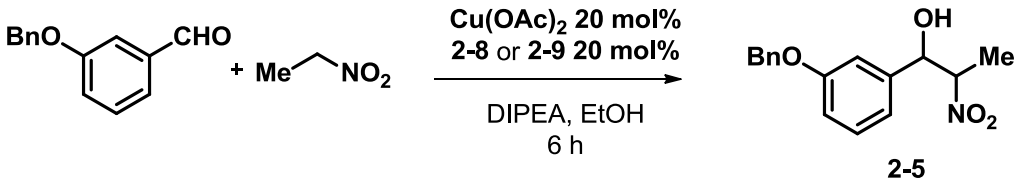

Table2-2. **Screening of reaction conditions.**

entry	Ligand	T (°C)	yield (%)	dr (*anti/syn*)[a]	ee$_{anti}$ (%)[b]
1	**2-8**	0	94	1/1	51 (*S,R*)
2	**2-9**	0	98	1/1	36 (*R,S*)
3	**2-8**	-45	89	7/3	84 (*S,R*)
4	**2-9**	-45	90	7/3	86 (*R,S*)
5[c]	**2-9**	-45	91	65/35	92 (*R,S*)

[a]Determined by H-NMR of the crude; [b]determined by HPLC on chiral stationary phase; [c]*i*PrOH as solvent.

Running the nitro aldol reaction using the two enantiomeric chiral ligands, obviously led to the two-different enantiomer of the product. Working at 0°C the reaction proceeded with high yield, however, no diasteroselectivity was observed, moreover low enantiomeric excess was reached. (Table 2-2)

In order to achieved high stereoselection was necessary to lowering down the reaction temperature to -45°C. In these conditions was possible to obtain the final nitro alcohol 2-5 in the anti-configuration in good yield, and with good enantioselection (Table 2-2).

After the batch chemistry was set up, the possibility of running the reaction under continuous flow was explored. The first reactor tested (1mL of internal volume), was printed using High Impact Poly Styrene(HIPS), and had a squared internal channel of 1-41 x 1.41 mm. The flow set up (scheme 2-6), was composed by two syringes, in the first one (Scheme 2-6, I) the aldehyde(0.25mmol), the copper salt (0.05 mmol) and the chiral ligand **2-8** (0.0065) were dissolved in ethanol; the second one was filled with nitroethane (2.5 mmol), Hünning's base (0.25 mmol) and, ethanol (0.75 mL) as solvent.

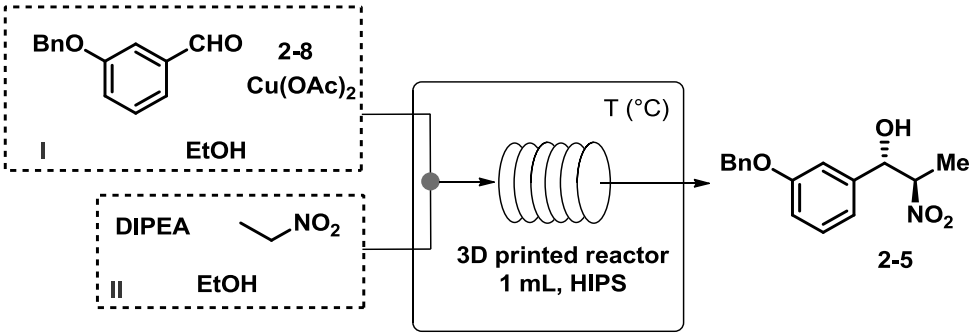

Scheme 2-6. Continuous flow synthesis of 2-5

Syringe I and Syringe II, were connected to a syringe pump and flushed trough the 3D printed reactor. The outcome of the reaction was collected at -78° C, for quenching the reaction. At the end of the reaction, the crude mixture was treated with a 10 % solution of HCl/water and the final product purified using column chromatography (for further details see the experimental section).

Table2-3. Screening of reaction conditions under continuous flow.

entry	T (°C)	Flow rate (mL/min)	Res. Time (min)	yield (%)	dr (*anti/syn*)[a]	ee$_{anti}$ (%)[b]
1	25	0.2	5	61	6/4	70
2	25	0.1	10	87	1/1	49
3	0	0.1	10	73	65/35	85
4	0	0.05	20	91	63/37	78
5	-20	0.1	10	20	75/25	81
6	-20	0.033	30	72	73/27	87
7[c]	-20	0.033	30	75	71/29	86[d]

[a] Determined by H-NMR of the crude; [b] determined by HPLC on chiral stationary phase; (*S*,*R*) enantiomer; [c] **2-9** as chiral ligand; [d] (*R*,*S*) enantiomer.

Running the reaction at room temperature, in only 5 minutes of residence time (Table 2-3, entry 1), yield up to 61% was observed, moreover, compared to the batch experiment, the enantiomeric excess (70%) was excellent (in the case of batch reaction at rt only racemic product was obtained), the d.r. was only up to 6:4 in favor of the anti diasteroisomer. Doubling the residence time, (Table 2-3, entry 2), obviously increase the yield up to 87%, but lower stereoselection was observed, indeed the d.r. was 1:1 and the *ee* was only 49%.

Lowering the reaction temperature down to 0°C led to better stereochemical outcome, (Table 2-3, entries 3-4), however, in order to obtain good level of diasteroselection and enantioselection was necessary to work at -20°C with a residence time of 30 minutes (Table 2-3, entries 6-7). Notably working under continuous flow condition brought some important advantages in terms of stereoselectivity, it was indeed possible to work at higher temperature reaching the same level of stereocontrol.

Using the best reaction conditions, different reactors were tested. In particular the comparison between 3D printed PLA reactors and PTFE coiled tube was studied (Scheme 2-7).

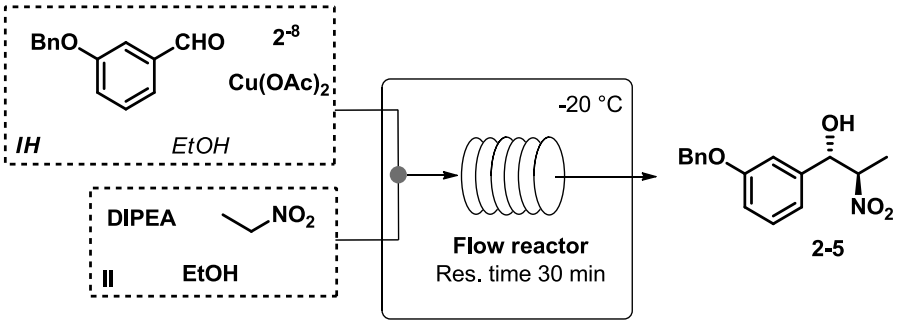

Scheme 2-7. Continuous flow synthesis of 2-5.

Running the reaction in a 1mL 3D-printed reactor, made of Poly-Lactic-Acid(PLA), having square channel with 1.41 x 1.41 mm, compound **2-5** was obtained in 87% yield, 65:35 anti/syn ration and 79% of ee (Table 2-4, entry 1). Interestingly running the Henry reaction in a rector made of PTFE coiled tube, similar results were achieved in terms of yield and selectivity. (Table 2-4, entry 2).

Table2-4. Continuous flow synthesis of 2-5

entry	Flow reactor	yield (%)	dr (*anti/syn*)[a]	ee_{anti} (%)[b]
1	3D-printed PLA **1 mL** (squared channel: 1.41 x 1.41mm)	87	65/35	79
2	PTFE coiled tube **0.5 mL** (circular channel: *id*: 0.58 mm)	90	70/30	80

[a]Determined by H-NMR of the crude; [b] determined by HPLC on chiral stationary phase.

Comparing the results of table 2-3 and 2-4, is possible to notice that the 3D printed reactors made of HIPS offered better performance, as for stereochemical outcome (Table 2-3, entry 6, table 2-4 entry 1). However, PLA printing is easier and more reproducible (for printing parameters see the experimental section); moreover, the PLA reactors are more compatible with the solvent and the reagents employed in the Henry reaction. The performance of the 3D printed reactors and the PFTE coiled one were comparable, furthermore the possibility to design and build completely customize reactors for overcoming different reactions' problems (Figure 2-6), was considered a strong advantage and further test were run using the 3D printed flow reactors.

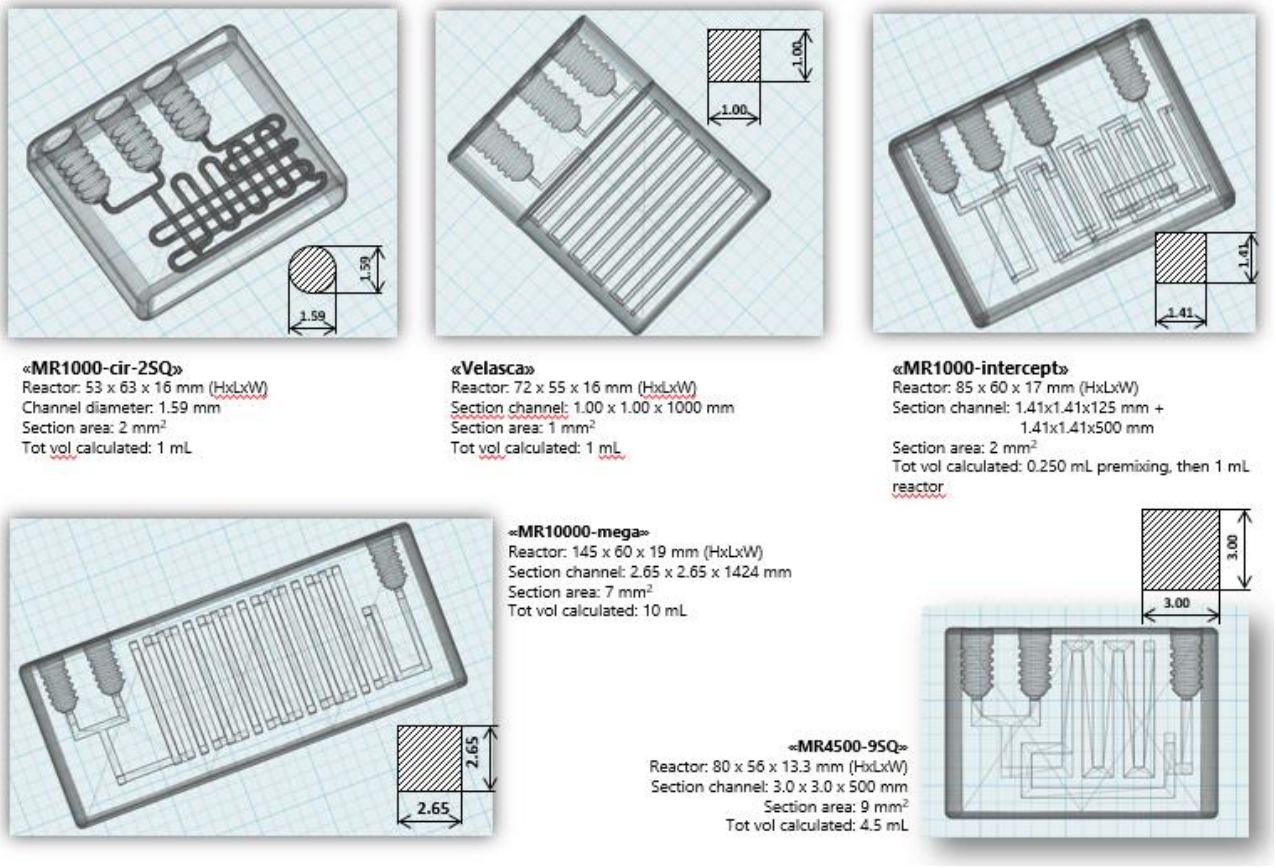

«MR1000-cir-2SQ»
Reactor: 53 x 63 x 16 mm (HxLxW)
Channel diameter: 1.59 mm
Section area: 2 mm^2
Tot vol calculated: 1 mL

«Velasca»
Reactor: 72 x 55 x 16 mm (HxLxW)
Section channel: 1.00 x 1.00 x 1000 mm
Section area: 1 mm^2
Tot vol calculated: 1 mL

«MR1000-intercept»
Reactor: 85 x 60 x 17 mm (HxLxW)
Section channel: 1.41x1.41x125 mm +
1.41x1.41x500 mm
Section area: 2 mm^2
Tot vol calculated: 0.250 mL premixing, then 1 mL reactor

«MR10000-mega»
Reactor: 145 x 60 x 19 mm (HxLxW)
Section channel: 2.65 x 2.65 x 1424 mm
Section area: 7 mm^2
Tot vol calculated: 10 mL

«MR4500-9SQ»
Reactor: 80 x 56 x 13.3 mm (HxLxW)
Section channel: 3.0 x 3.0 x 500 mm
Section area: 9 mm^2
Tot vol calculated: 4.5 mL

Figure 2-6

After the preliminary screening of the Henry reaction using the aldehyde precursor of the metaraminol the attention was focused on the preparation of other precursors of the amino alcohols **2-2**, **2-3** and **2-4** using the same chiral ligand **2-8**.

Firstly, the nitro alcohol precursor of norephedrine, was synthetized in batch. The desired compound **2-10** was obtained in 85% yield, 3:1 in favor of the *anti*-isomer and in 88% of ee. (Scheme 2-8)

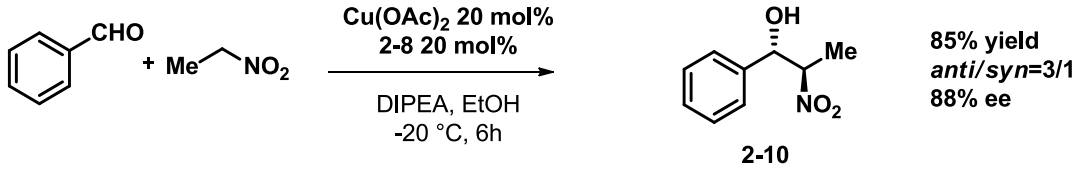

Scheme 2-8. Batch synthesis of 2-10.

The Henry reaction, between benzaldehyde and nitroethane was then run in flow, using the previously optimized reaction conditions (30 minutes of residence time at -20°C). (Scheme 2-9)

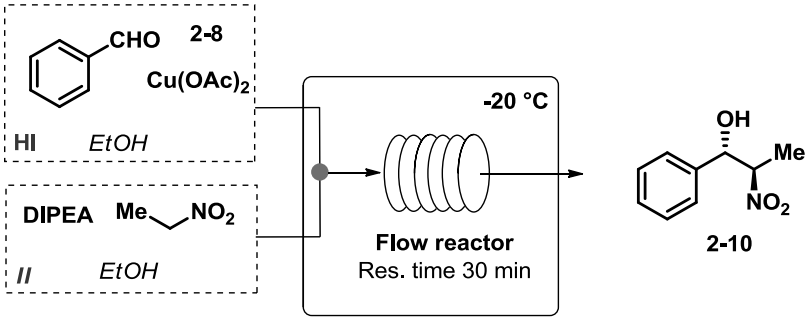

Scheme 2-9. Continuous flow synthesis of 2-10.

The reaction conditions and concentration were the same of the previously reported synthesis of 2-5. Using this standard reaction condition a screening of different reactors was performed. (Table 2-5)

Table 2-5. Screening of different flow reactors.

entry	Flow reactor	conversion (%)	dr (*anti/syn*)[a]	ee$_{anti}$ (%)[b]
1	PTFE coiled tube **0.5 mL** (circular channel: *id*: 0.58 mm)	98	67:33	81
2	3D-printed PLA **1 mL** (squared channel: 1.41 x 1.41mm)	96	67:33	79
3	3D-printed NYLON **1 mL** (squared channel: 1.41 x 1.41mm)	97	68:32	80

4	3D-printed PLA **1 mL** (circular channel: *id*: 1.59 mm)	98	67:33	84
5	3D-printed PLA **1 mL** (squared channel: 1.0 x 1.0mm)	98	67:33	80
6	3D-printed PLA **10 mL** (squared channel: 2.65 x 2.65mm)	96 (78 isolated)	74:26	89

[a]Determined by H-NMR of the crude; [b]determined by HPLC on chiral stationary phase.

Running the reaction in a coiled tube of PTFE (circular channel: id 0.58mm), led to the desired product **2-10** with full conversion, 67:33 as d.r and 81% of ee for the anti-isomer (Table 2-5, entry 1). Using a 1 mL 3D printed reactor, made of PLA or Nylon(squared channels: 1.41x1.41 mm), nitro alcohol **2-10**, was obtained in both cases with the same yield and stereoselectivity(Table 2-5, entries 2-3). When the shape and the size of the channels of 3D printed PLA reactors were changed, no relevant difference was noticed. (Table 2-5, entries 4-5). As final test the reaction was performed using a 10 mL PLA reactor (Table 2-5, entry 6), however, also in this case the outcome of the reaction was even better compared to the 1 mL reactor, reaching 89% of enantioselectivity and 96% of conversion.

For the batch preparation of compound **2-11** the condensation between 2,5 dimethoxy benzaldehyde and nitroethane was studied. Using the standard reaction condition the nitro alcohol **2-11** was obtained in good yield and in a *d.r.* 3:1, an ee of 91% was observed on the *anti*-isomer. (Scheme 2-10).

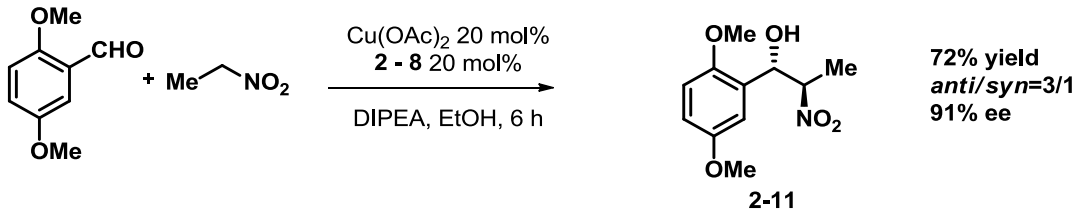

Scheme 2-10. Batch synthesis of 2-11.

In addition, the flow version (Scheme 2-11) of the reaction was explored, using the same experimental set up and reaction conditions describe in scheme 2-7.

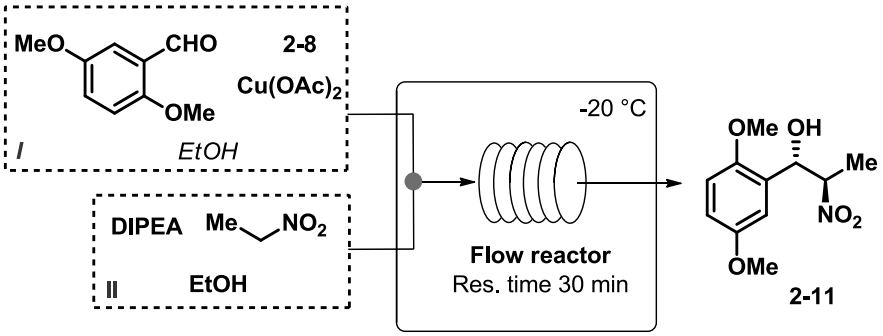

Scheme 2-11. Continuous flow synthesis of 2-12.

The standard comparison between the 3D printed (1mL, PLA, square channel 1.41x1.41) reactor and the PTFE coiled tube was, also in this case, performed. (Table 2-6)

Table 2-6. **Continuous flow synthesis of** 2-12**.**

entry	Flow reactor	yield (%)	dr (*anti/syn*)[a]	ee$_{anti}$ (%)[b]
1	3D-printed PLA **1 mL** (squared channel: 1.41 x 1.41mm)	89	73/27	85
2	PTFE coiled tube **0.5 mL** (circular channel: *id*: 0.58 mm)	67	70/30	82

[a]Determined by H-NMR of the crude; [b]determined by HPLC on chiral stationary phase

Working with the 3D printed reactors compound **2-11** was obtained in better yield, compared to the PTFE tube and also few points more of enantiomeric excess were obtained.

The last precursor studied was chiral nitroalcohol 2-12 (Scheme 2-12), the batch synthesis, run in the standard reaction conditions, produce the desired compound in 53% yield, 65:35 *d.r.* and 84% of *ee*.

Scheme 2-12. Batch synthesis of 2-12.

In this case the addition of THF as co-solvent was crucial because of the poor solubility of starting aldehyde in EtOH.

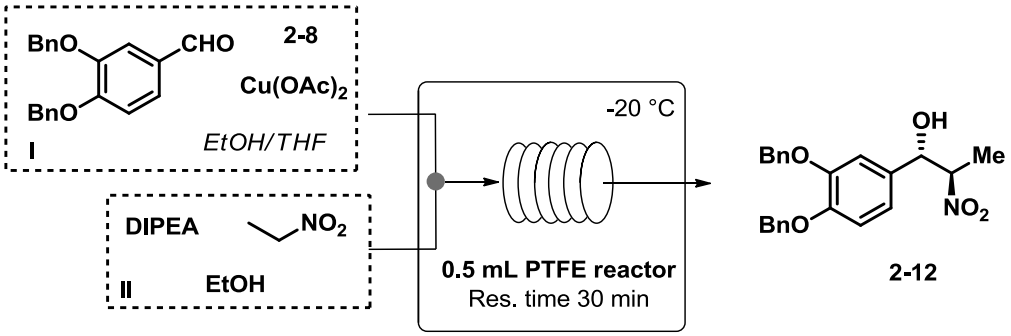

Scheme 2-13. Continuous flow synthesis of 87.

Unfortunately, the flow process in this case was not reproducible, due to the precipitation of the starting material into the reactor channel. Nitroalcohol was obtained one time in 67% of yield, 61:39 *d.r.* and 74% *ee*.

Since the comparison between the 3D printed reactor and the one made of PTFE were not always conclusive, probably due to the speed of the reaction compared with the residence time another test were carried out stopping the reaction at lower level of conversion. A direct comparison , stressing the reaction condition was performed, in 5 minutes of residence time at -20°C, using zig-zag channel in 3D printed reactor for optimizing the mixing was possible to notice the difference in the performance, the yield, using an ad-hoc printed reactor was double compared to the PLA, and also the *d.r* was improved.

Table 2-7, 3D printed reactors and PTFE based one

entry	ArCHO	Flow reactor	Conv. (%)	dr (anti/syn)
1	PhCHO	PTFE coiled tube 1 mL (circular ch.: id: 1.69 mm)	8%	74:26
2	PhCHO	3D-printed PLA 1 mL (rect. Zigzag ch.: 1.1 x 1.7mm)	15%	80:20
3	3OBnPhCHO	3D-printed PLA 1 mL (circular ch. id: 1.59 mm)	10%	61:39
4	3OBnPhCHO	3D-printed PLA 1 mL (rect. Zigzag ch.: 1.1 x 1.7mm)	21%	71:29
5	3OBnPhCHO	3D-printed PLA 1 mL circular ch. Zigzag id:1.59 mm	18%	60/40

Continuous flow hydrogenation of nitroalcohols

To obtain the target chiral aminoalcohols, the second step after the stereoselective Henry reaction, is the reduction of the nitro group. For the nitro group hydrogenation an Thales Nano H-Cube mini, equipped with a Pd/C cartridge (10% wt.) as catalyst was used.

The optimization of the reaction conditions was performed using nitroalcohol **2-10** (Scheme 2-14)

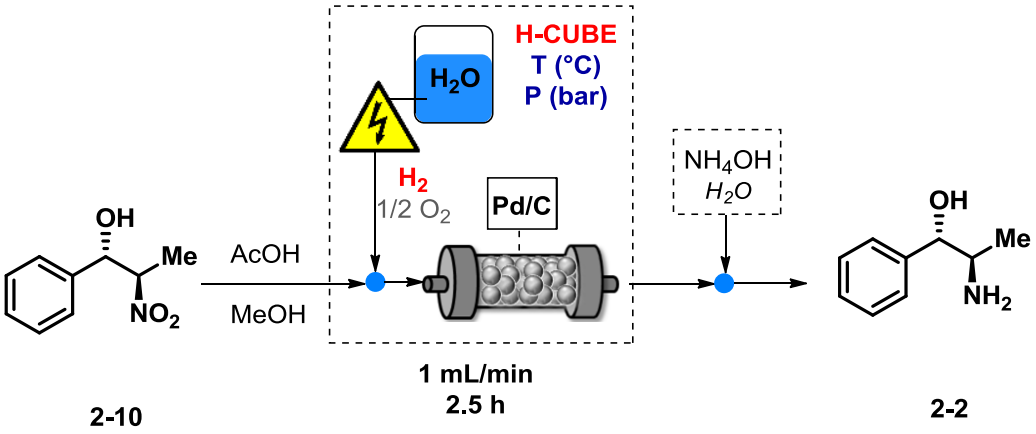

Scheme2-14. Continuous flow synthesis of 2-2.

The nitroalcohol was dissolved in methanol (0.1M), and then pumped through the H-Cube mini. Temperature and pressure were set as indicated (Table 2-8) and the continuous flow reduction was run with 1 mL/min. The outcome of the reactor was recirculated for a reaction time of 2.5 hours (for further details see the experimental section). After preliminary experiment AcOH was added in order to increase the conversion of the starting material. (Table 2-8)

Table 2-8. Screening of reaction conditions.

entry	Solvent [M]	T (°C)	P H_2 (bar)	conversion (%)
1	MeOH (0.1)	25	10	90
2	MeOH (0.1)	30	15	98
3	EtOH (0.1)	30	15	80
4	EtOH (0.03)	30	15	98
5	AcOEt (0.1)	30	15	10
6	AcOEt/EtOH 1/1 (0.1)	30	15	40

Running the reaction in MeOH at 25°C, 10 bars of H_2, the desired compound was obtained in 90% conversion, reaching 30°C and 15 bar of pressure the final aminoalcohol was obtained in 98% of conversion (Table 2-8, entries 1-2). In order to not switch the solvent between the two reactions, also the use of ethanol was investigated. To obtain complete conversion towards the aminoalcohol 2-2, was necessary to work in diluted conditions (0.03M), table 2-8 entry 4. The use of other solvents, such as AcOEt was not compatible with the reduction, indeed in the presence of AcOEt start the precipitation of salts led to the blockage of the system. During the NO_2 reduction, no

epimerization at the benzylic stereocenter was observed. (the enantiomeric excess of the final amino alcohol was evaluated on the bis-acetilated derivative, see the experimental section).
After the identification of the best conditions for the nitro reduction, the transformation of nitroalcohols **2-5** and **2-11** was performed.

The continuous flow hydrogenation of **2-11** using the H-CUBE Mini was performed at 30 °C and 15 bars of H_2 for 2.5 hours. The complete conversion of product **2-11** (Scheme 2-15) into the desired aminoalcohol **2-3** (as acetate salt) was observed. The free aminoalcohol was obtained after the treatment of the acetate salt with a solution of NH_4OH (for further details see the experimental section). Also in this case no epimerization of the final compound was observed

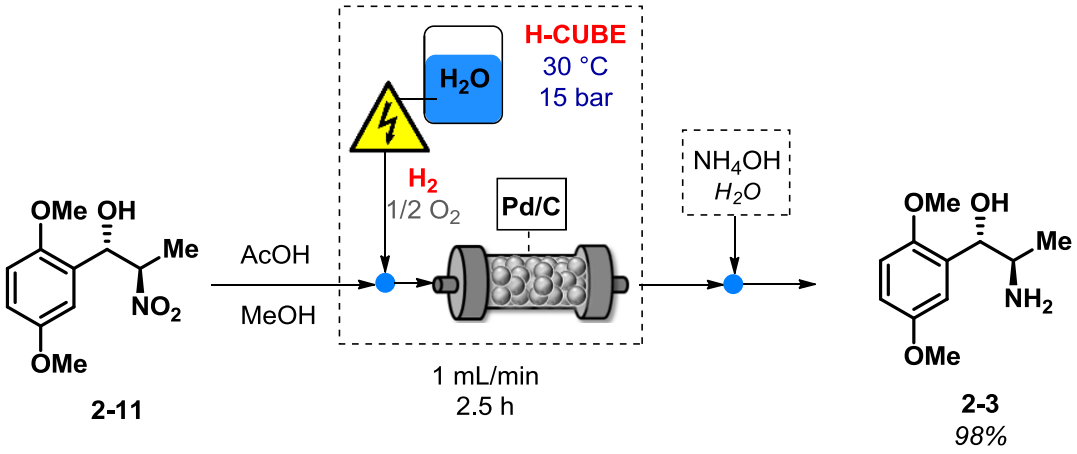

Scheme 2-15. Continuous flow synthesis of 2-3.

The same methodology was applied for the preparation of Metaraminol. Nitroalcohol **2-5** was reduced using the same reaction conditions. Pd/C as catalyst allowed both the nitro reduction and the oxygen debenzylation in one step only. (Scheme 2-16)

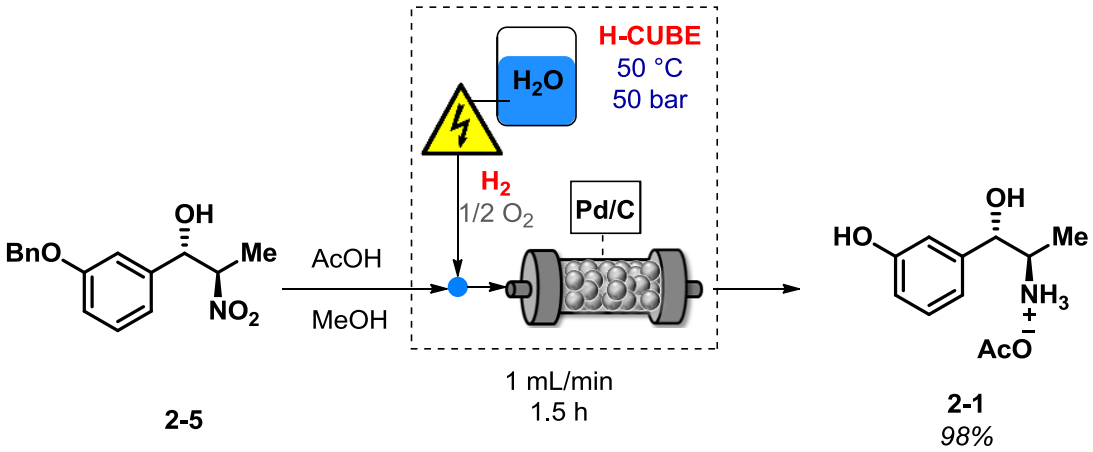

Scheme 2-16. Continuous flow synthesis of 88.

A 0.1 M solution of **2-5** in EtOH in the presence of 30 equivalents of AcOH was loaded in the H-CUBE Mini at 1 mL/min. After 2.5 hours of recirculating process at 50 °C and 50 bar of H_2 amino alcohol **88** (in its acetate salt form) was obtained with a complete conversion. The enantiomeric excess was maintained during the reaction (ee determined by HPLC on chiral stationary phase).

Multistep process

With the best conditions for the Henry and the following reduction, the efforts were focused on the preparation of all in flow step up for the preparation of the final amino alcohol without solvent switching and product isolation. (Scheme 2-17)

This procedure would be appealing for the stereoselective synthesis of chiral 1,2-amino alcohols on a preparative scale.

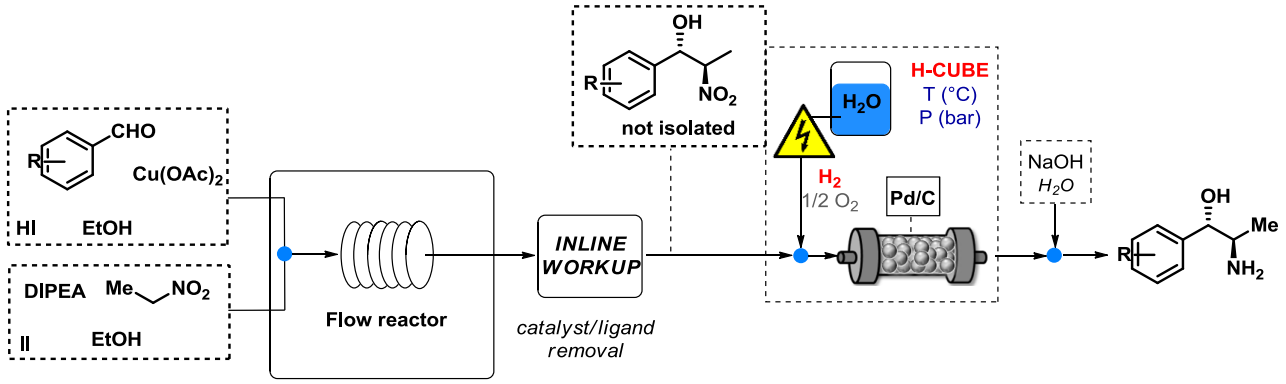

Scheme 2-17. **Multistep synthesis of** amino alcohols.

After the nitroaldol reaction, performed into the 3D printed reactor, was crucial to remove in continuo the copper catalyst and the chiral ligand, in order to avoid interference in the following, Pd catalyzed hydrogenation. The target molecule for the all-in flow preparation was the aminoalcohol **2-2**.

Two different solutions were tested: in the first case, after the inline workup with HCl, the nitroalcohol was extracted using AcOEt, however, the large quantities of AcOEt needed and the non-compatibility of this solvent with the following nitro reduction exclude this way (Table 2-8, entry 5-6). The second solution was a direct filtration of the crude mixture on a pad of silica gel, followed by the elution of the nitroalcohol with EtOH/MeOH. The compatibility of ethanol with the hydrogenation conditions was already proved (Table 2-8, entries 3-4), and it was also possible to recover the valuable chiral catalyst by treating the silica gel with a solution of HCl in ethanol. (Scheme 2-18)

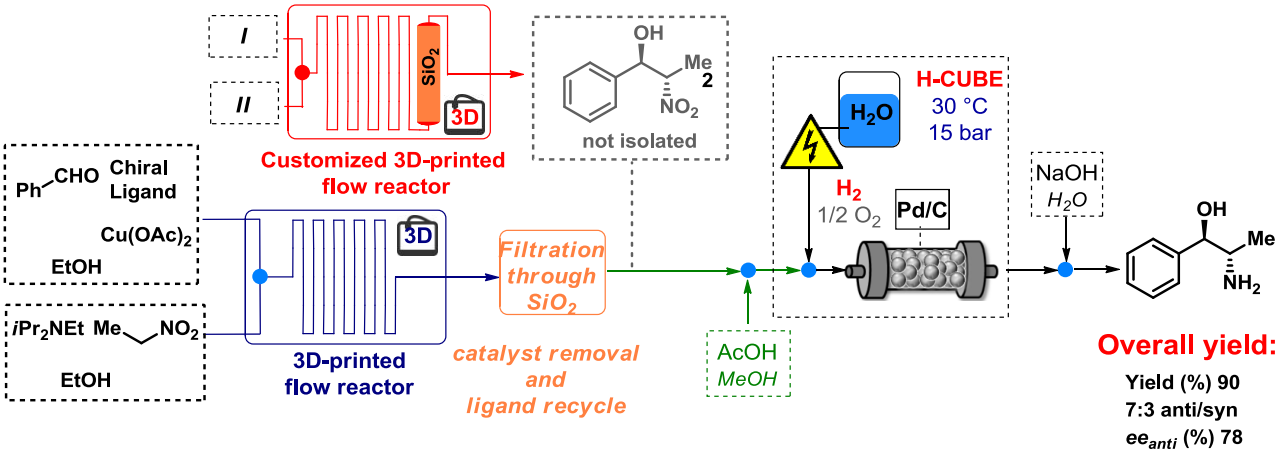

Scheme 2-18. Multistep synthesis of 2-2.

Syringe ***I*** was charged with a preformed mixture of benzaldehyde, (0.375mmol) and $Cu(OAc)_2$ (0.075 mmol) in EtOH (1.5 mL, 0.250 M). Syringe ***II*** was charged with nitroethane (0.270 mL, 3.75 mmol), DIPEA (65 µL, 0.375 mmol) and EtOH (1.26 mL). The two syringes were connected to a syringe pump and the reagents directed to the flow reactor at -20 °C for a residence time of 30 minutes. The outcome of the reactor (dark blue solution, 3 mL) was filtered over a short pad of silica (*h*: 1 cm, *d*: 2 cm) by elution with EtOH (6 mL). To the resulting mixture (light yellow) 30 equivalents of AcOH were added and the resulting mixture was subjected to continuous flow hydrogenation with H CUBE (T: 30 °C, P: 1 bar, flow rate 1 mL/min, t: 2.5 h). The solvent was then evaporated, treated with NH_4OH 33% wt. and extracted five times with AcOEt. Amino alcohol **2-2** was obtained in 90% yield (over 2 steps), 7/3 *dr* and 78% ee as a pure withe solid (*dr* and ee were determined after derivatization of **2-2** into the corresponding bis-acetylamide). Also, a 3D printed reactors containing directly the SiO_2 cartridge was printed and used in the continuous flow production of amino alcohols, demonstrating once more the amazing possibilities of this technology in terms of ad hoc reactors realization.

In conclusion, a new continuous flow process for the stereoselective synthesis of chiral 1,2-amino alcohols has been developed. Three targets displaying biological activities (Norephedrine, Metaraminol and Methoxamine) have been prepared through a two-step sequence:
In the first one an efficient stereoselective Henry reaction was performed under continuous flow conditions in different ad-hoc printed meso and micro reactors. Using the 3D printing technology was possible to fast screen different reactor parameters such as such shape sizes of the channel. The reaction proceeded with good yields and stereoselectivities to give the desired nitro alcohols. Notably the process was easily scaled up using a 10mL printed reactor without any additional study, demonstrating once again the easier scalability of the flow process.

The second step was the nitro reduction, under continuous flow conditions using an H CUBE mini apparatus, in this way was possible to obtain pure 1,2 amino alcohols with no need of further purifications. In order to develop a fully automatic process, the synthesis of Norephedrine was accomplished using the best reaction conditions for each step and with an in line removal of the Cu catalysts and the precious chiral ligand.

Experimental section Chapter 2

Stereoselective catalytic APIs synthesis in home-made 3D-printed mesoreactors.

3D Printing:

3D printing was achieved on a monoextruder Sharebot NG 3D printer. This 3D printer heats a 1.75 mm thermopolymer filament through the extruder, depositing the material in a layer-by-layer fashion. The thermoplastics employed to fabricate the devices presented herein are:

- **PLA**: Polylactic acid purchased from 3D filo supply (www.3dfilo.com)
- **HIPS:** High Impact Polystyrene purchased form Reprapper supply (www.reprappertech.com)
- **NYLON:** Nylon taulman 645 - TAU-002 (Nylon 6,6) purchased from 3Dprima supply (www.3dprima.com)

Synthesis of chiral aminopyridine **2-8/2-9**

Synthesis of compound **2-6, and 2-7**

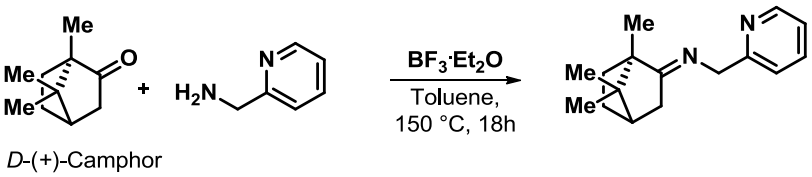

D-(+)-Camphor

In a two-necked flask, with addition of Dean-Stark and dropping funnel, *D*-(+)-Camphor (6.6 mmol), was placed under N_2 atmosphere then amine **8** (6.6 mmol) and BF_3Et_2O (0.4 mmol) were added and dissolved in toluene (16 mL). Reaction mixture was heated at 150 °C with a Dean Stark apparatus and stirred for 24 hours. After reaction time the crude was cooled to room temperature, diluted with ethyl acetate and washed with $NaHCO_3$ s.s.; the organic phase was extracted three times with AcOEt, dried over Na_2SO_4 and concentrated under vacuum. Imine **9** was obtained as dark yellow oil and was used in the following step without any further purification. Full conversion was demonstrated by NMR analysis of the crude.

^{1}H-NMR (300 MHz, $CDCl_3$) δ_H 8.50 (d, J = 4.82 Hz, 1H), 7.65 (dt, J = 7.70, 1.86 Hz, 1H), 7.48 (d, J = 7.83 Hz, 1H), 7.13 (m, 1H), 4.63 (d, J = 16.46 Hz, 1H), 4.55 (d, J = 16.3 Hz, 1H), 2.45 (m, 1H), 1.98 (m, 1H), 1.85 (m, 1H), 1.73 (m, 1H), 1.44 (m, 2H), 1.26 (m, 1H), 1.07 (s, 3H), 0.96 (s, 3H), 0.78 (s, 3H) ppm.

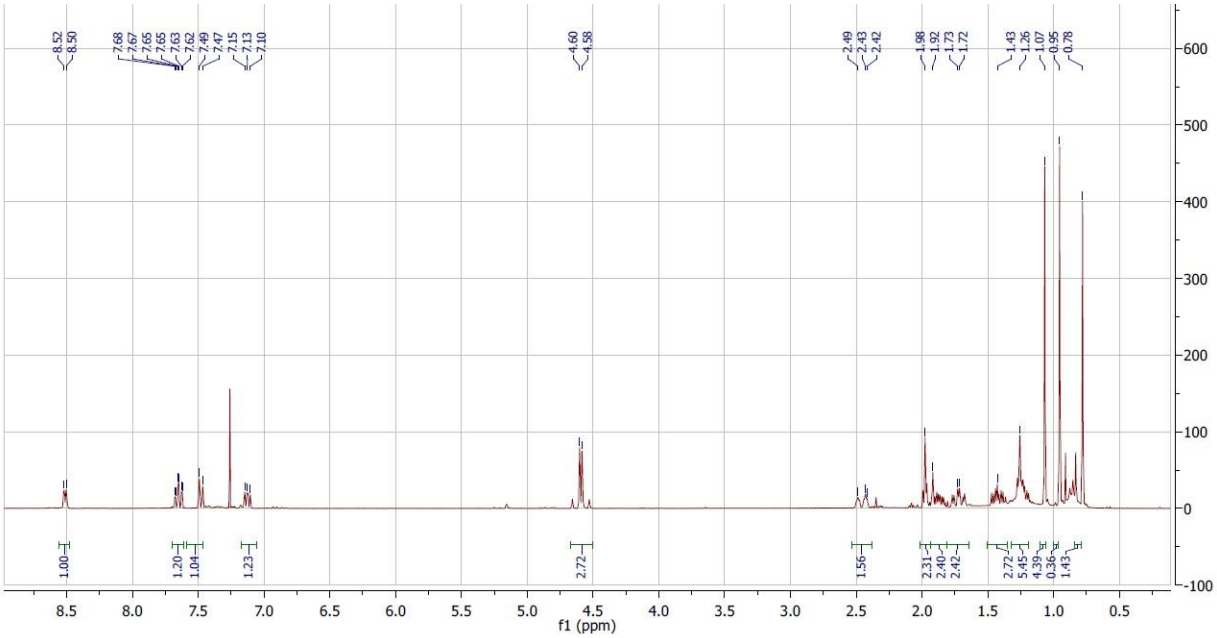

Synthesis of chiral aminopyridine **2-8, and 2-9**

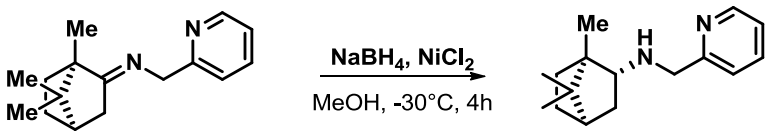

In a two-necked flask a solution of **2-6** (5.9 mmol) in methanol (60 mL) was prepared under N_2 atmosphere and cooled to -30 °C. $NiCl_2$ (11.8 mmol) was added and then $NaBH_4$ (5.9 mmol) was slowly introduced under stirring. Reaction progress was monitored by thin layer chromatography.

After 24 hours no more starting material was detected; reaction mixture was concentrated, diluted with dichloromethane washed with an aqueous solution of NH_4Cl and extracted with dichloromethane; combined organic phases were dried over Na_2SO_4 and concentrated under vacuum. The crude mixture was purified by column chromatography on silica gel eluting with ethyl acetate affording **A** as a yellowish oil with (3.5 mmol, 60% yield). All analytical data are in agreement with literature.[161]

^{1}H-NMR (300 MHz, $CDCl_3$) δ_H 8.55 (d, J = 4.39 Hz, 1H), 7.66 (dt, J = 7.66, 0.76 Hz, 1H), 7.37 (d, J = 6.79 Hz, 1H), 7.17 (m, 1H), 3.95 (d, J = 14.2 Hz, 1H), 3.88 (d, J = 14.18 Hz, 1H), 2.68 (m, 1H), 1.72-1.51 (m, 6H), 1.28 (m, 1H), 1.12 (s, 3H), 0.99 (s, 3H), 0.85 (s, 3H) ppm.

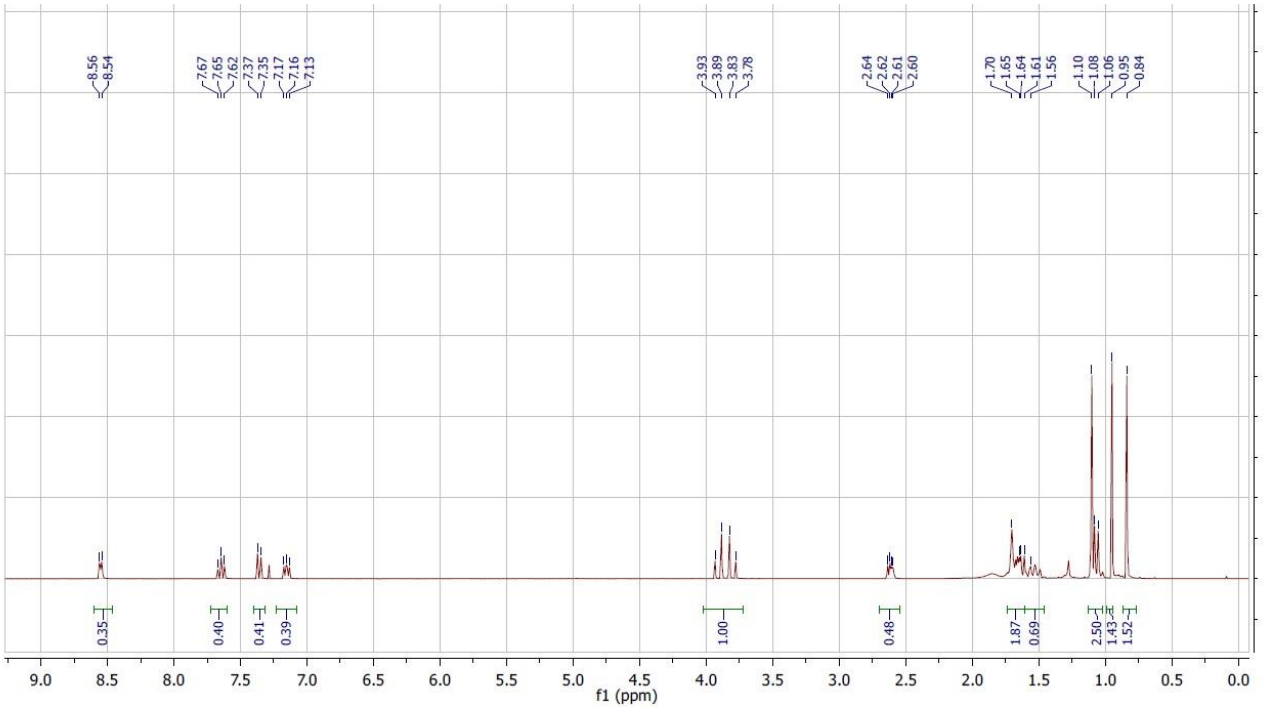

^{13}C-NMR (75 MHz, $CDCl_3$): 160.85, 149.04, 136.19, 122.19, 121.60, 66.52, 54.22, 48.46, 46.72, 45.28, 38.74, 36.84, 27.33, 20.59, 12.17 ppm.

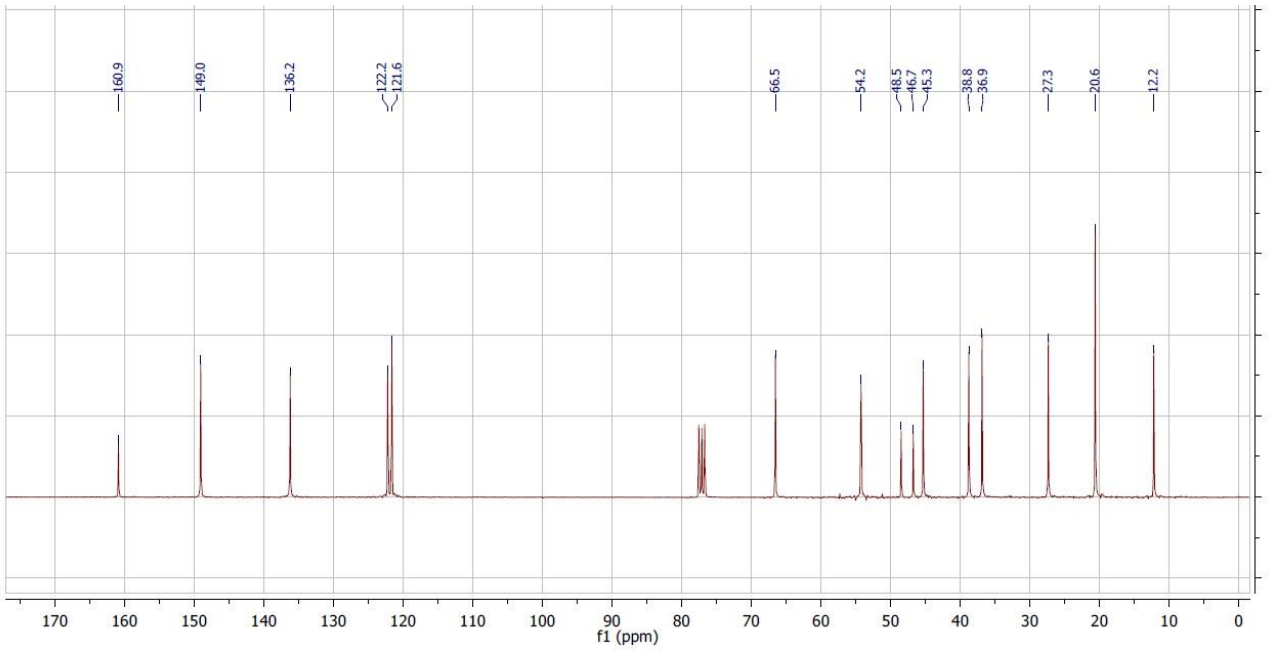

MS (ESI): 245.3.

General procedure for stereoselective Henry reaction

Batch reaction

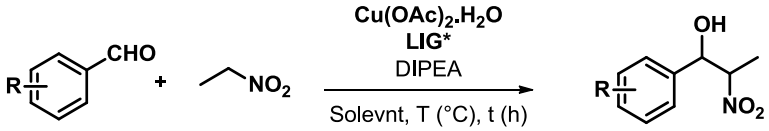

In a round-bottom flask, chiral aminopyridine **A** (or **B**) (15 mg, 0.0625 mmol) and $Cu(OAc)_2$ (10 mg, 0.05 mmol) were dissolved in the indicated solvent (1.75 mL) and the solution was stirred for 10 minutes; then aldehyde (0.25 mmol, 25 µL) was added and mixture was stirred for 30 minutes. After this period the mixture was cooled to the desired temperature and nitroethane (2.5 mmol, 179 µL) and DIPEA (0.25 mmol, 44 µL) were added. The mixture was stirred at the same temperature for the indicated temperature. After reaction time the crude mixture was diluted with ethyl acetate (5 mL), quenched with HCl 10% (1 mL) and rapidly extracted with ethyl acetate (3x5 mL); the combined organic layers were then washed with brine, dried over Na_2SO_4 and concentrated under vacuum conditions. The crude product was purified by column chromatography on silica gel.

Flow reaction

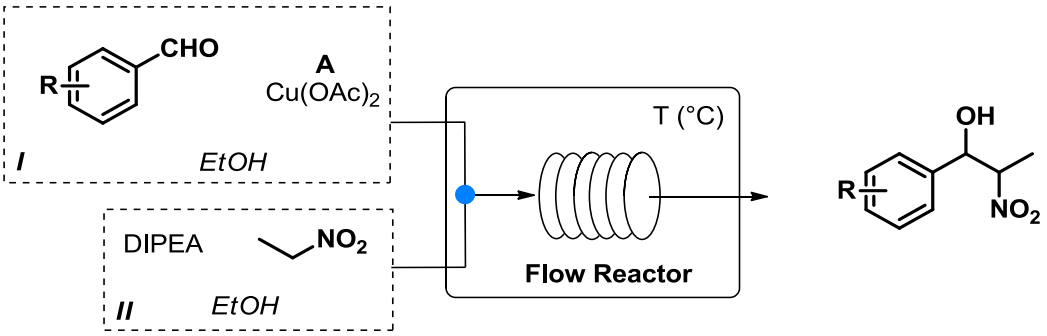

In a round-bottom flask, ligand **A** (or **B**) (0.125 mmol) and $Cu(OAc)_2$ (0.1 mmol) were dissolved in ethanol (2 mL) and the solution was stirred for 10 minutes. The desired aldehyde (0.5 mmol) was then added and mixture was again stirred for 30 minutes. In another flask, nitroethane (5 mmol) and DIPEA (0.5 mmol) were added in ethanol (the final mixture is 2.5 M in nitroethane). The solutions were charged into two different syringes, placed on a syringe-pump and injected into the indicate flow reactor at the indicated flow rate and temperature. The outcome of the reactor was collected at -78 °C. After reaction time, the crude mixture was diluted with ethyl acetate (5 mL), quenched with HCl 10% (1 mL) and rapidly extracted with ethyl acetate three times (5 mL); the combined organic layers were then washed with brine, dried over Na_2SO_4 and concentrated under vacuum conditions. The crude mixture was purified by column chromatography on silica gel.

1-(3-(benzyloxy)phenyl)-2-nitropropan-1-ol **(2-5)**

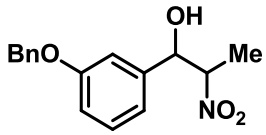

Prepared according to the general procedure. The crude mixture was purified by column chromatography on silica gel eluting with hexane/ethyl acetate 9:1. The title product was obtained as a yellowish oil as mixture of *syn* and *anti* diastereoisomers. All analytical data are in agreement with literature.

^{1}H-NMR (300 MHz, $CDCl_3$) *anti* δ_H 7.48-6.93 (m, 9H), 5.38 (d, J = 3.03 Hz, 1H), 5.08 (s, 2H), 4.73-4.63 (m, 1H), 1.48 (d, J = 6.83 Hz, 3H); *syn* δ_H 7.48-6.93 (m, 9H), 5.13 (s, 2H), 4.98 (d, J = 8.86 Hz, 1H), 4.76 (m, 1H), 1.31 (d, J = 6.83 Hz, 3H) ppm.

^{13}C-NMR (75 MHz, $CDCl_3$): 159.05, 140.24, 139.94, 136.72, 129.87, 128.64, 128.09, 127.55, 119.50, 118.45, 115.61, 114.85, 113.44, 112.67, 88.38, 87.36, 76.18, 73.73, 70.09, 16.43, 11.95 ppm.

The enantiomeric excess was determined by HPLC on chiral stationary phase with Phenomenex Lux Cellulose-1 column: eluent Hexane/*i*PrOH = 90/10, flow rate 0.8 mL/min, λ=210 nm, anti τ_{1S2R} = 39.3 min, anti τ_{1R2S} = 21.2 min, syn τ_{1S2S} = 32.9 min, syn τ_{1R2R} = 24.6 min.

2-nitro-1-phenylpropan-1-ol **(2-10)**

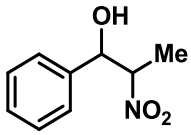

Prepared according to the general procedure. The crude mixture was purified by column chromatography on silica gel eluting with hexane/ethyl acetate 9:1. The title product was obtained as a yellowish oil as mixture of *syn* and *anti* diasteroisomers. All analytical data are in agreement with literature.

^{1}H-NMR (300 MHz, $CDCl_3$) *anti*: δ_H 7.41-7.38 (m, 5H), 5.43 (d, J = 3.52 Hz, 1H), 4.74-4.70 (m, 1H), 2.68 (bs, 1H), 1.53 (d, J = 6.82 Hz, 3H); *syn*: 7.41-7.38 (m, 5H), 5.05 (d, J = 9.01 Hz, 1H), 4.83-4.79 (m, 1H), 2.68 (bs, 1H), 1.34 (d, J = 6.8 Hz, 3H) ppm.

The enantiomeric excess was determined by HPLC on chiral stationary phase with Phenomenex Lux Cellulose-1 column: eluent Hexane/*i*PrOH = 95/5, flow rate 0.8 mL/min, λ=230 nm, anti τ_{1S2R} = 25.9 min, anti τ_{1R2S} = 16.9 min, syn τ_{1S2S} = 24.3 min, syn τ_{1R2R} = 18.9 min

1-(2,5-dimethoxyphenyl)-2-nitropropan-1-ol **(2-11)**

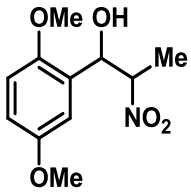

Prepared according to the general procedure. The crude mixture was purified by column chromatography on silica gel eluting with hexane/ethyl acetate 9:1. The title product was obtained as a yellowish oil as mixture of *syn* and *anti* diasteroisomers. All analytical data are in agreement with literature.

^{1}H-NMR (300 MHz, $CDCl_3$) *anti* δ_H 7.02 (s, 1H), 6.82 (d, J = 1.54 Hz, 2H), 5.51 (d, J = 2 Hz, 1H), 4.90 (m, 1 H), 3.83 (s, 3H), 3.78 (s, 3H), 1.49 (d, J = 6.89 Hz, 3H); *syn* δ_H 6.85 (m, 3H), 5.11 (d, J = 8.9 Hz, 1H), 4.96 (m, 1H), 3.85 (s, 3H), 3.78 (s, 3H), 1.36 (d, J = 6.77 Hz, 3H) ppm.

The enantiomeric excess was determined by HPLC on chiral stationary phase with Daicel Chiralcel AD column: eluent Hexane/*i*PrOH = 9/1, flow rate 0.8 mL/min, λ=210 nm, anti $\tau_{1S,2R}$ = 14.8 min, anti $\tau_{1R,2S}$ = 17.0 min, syn $\tau_{1S,2S}$ = 20.7 min, syn $\tau_{1R,2R}$ = 34.7 min.

1-(3,4-bis(benzyloxy)phenyl)-2-nitropropan-1-ol **(2-12)**

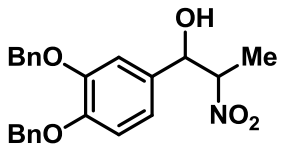

Prepared according to the general procedure. The crude mixture was purified by column chromatography on silica gel eluting with hexane/ethyl acetate 9:1. The title product was obtained as a yellowish oil. All analytical data are in agreement with literature.

^{1}H-NMR (300 MHz, $CDCl_3$) anti δ_H 7.48-6.85 (m, 13H), 5.26 (d, J = 3.78 Hz, 1H), 5.17 (s, 4H), 4.59 (m, 1H), 1.43 (d, J = 6.81 Hz, 3H); syn δ_H 7.48-6.85 (m, 13H), 5.18 (s, 4H), 4.90 (d, J = 9.13 Hz, 1H), 4.66 (m, 1H), 1.22 (d, J = 6.80 Hz, 3H) ppm. **^{13}C-NMR** (75 MHz, $CDCl_3$): 149.5, 148.9, 137.0, 136.9, 131.9, 131.6, 128.5, 128.0, 127.5, 127.3, 120.3, 119.2, 114.8, 113.7, 113.1, 88.5, 87.5, 76.0, 73.7 71.3, 71.2, 16.3, 12.2

The enantiomeric excess was determined by HPLC on chiral stationary phase with Phenomenex Amylose-2 column: eluent Hexane/*i*PrOH/EtOH = 70/25/5, flow rate 0.9 mL/min, λ=210 nm, anti $\tau_{1S,2R}$ = 11.6 min, anti $\tau_{1R,2S}$ = 10.1 min, syn $\tau_{1S,2S}$ = 20.2 min, syn $\tau_{1R,2R}$ = 12.8 min

General procedure for continuous flow hydrogenation

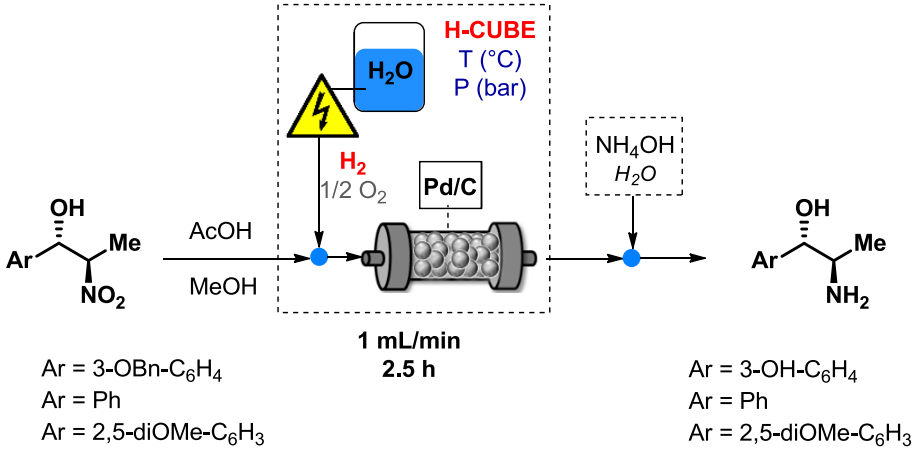

Nitroalcohol (1 mmol) was placed into a beaker and dissolved in methanol (10 mL) and AcOH was added (30 mmol, 500 µL). The reaction mixture was pumped into H-Cube Mini containing a cartridge of Pd/C (l = 3.5 cm) at the indicated pressure of H_2 and temperature. Reaction progress was monitored by TLC. After 2.5 hours, no more starting material was detected. The crude was concentrated under vacuum.

1-(3-(benzyloxy)phenyl)-2-nitropropan-1-ol **(2-1)**

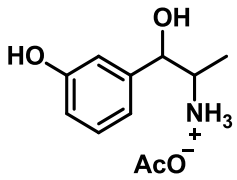

Prepared according to the general procedure at 50 bar and 50 °C. The crude mixture was concentrated and dried under vacuum. No further purification was required. The product was obtained in the form of acetate salt as withe solid as mixture of *syn* and *anti* diasteroisomers. All analytical data are in agreement with literature.

^{1}H-NMR (300 MHz, CD_3OD) *anti* δ_H 7.23-6.73 (m, 4H), 4.90 (d, J = 3.03 Hz, 1H), 3.49 (m, 1H), 1.96 (s, 3H), 1.11 (d, J = 6.63 Hz, 3H); *syn* δ_H 7.23-6.73 (m, 4H), 4.42 (d, J = 8.53 Hz, 1H), 3.34 (m, 1H), 1.96 (s, 3H), 1.12 (d, J = 6.65 Hz, 3H) ppm.

The enantiomeric excess was determined by HPLC on chiral stationary phase (reverse phase).

2-nitro-1-phenylpropan-1-ol **(2-2)**

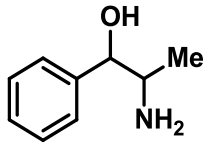

Prepared according to the general procedure at 15 bar and 30 °C. The crude mixture was purified by treatment with NH_4OH (33% wt.) and extraction with AcOEt (5 times). The title product was obtained as a yellowish solid as mixture of *syn* and *anti* diasteroisomers. All analytical data are in agreement with literature.

^{1}H-NMR (300 MHz, $CDCl_3$) *anti* δ_H 7.34-7.25 (m, 5H), 4.45 (d, J = 5.47 Hz, 1H), 3.06-2.97 (m, 1H), 1.03 (d, J = 6.54 Hz, 3H); *syn* δ_H 7.34-7.25 (m, 5H), 4.23 (d, J = 6.52 Hz, 1H), 3.06-2.97 (m, 1H), 0.88 (d, J = 6.56 Hz, 3H) ppm.

1-(2,5-dimethoxyphenyl)-2-nitropropan-1-ol **(2-3)**

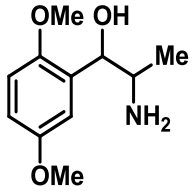

Prepared according to the general procedure at 20 bar and 30 °C. The crude mixture was purified by treatment with NH_4OH (33% wt.) and extraction with AcOEt (5 times). The title product was obtained as a yellowish solid as mixture of *syn* and *anti* diasteroisomers. All analytical data are in agreement with literature.

^{1}H-NMR (300 MHz, $CDCl_3$) *anti* δ_H 7.01-6.74 (m, 3H), 4.77 (d, J = 4.63 Hz, 1H), 3.78 (s, 6H), 3.30 (m, 1H), 1.00 (d, J = 6.52 Hz, 3H); *syn* δ_H 7.01-6.74 (m, 3H), 4.56 (d, J = 5.83 Hz, 1H), 3.14 (m, 1H), 1.06 (d, J = 6.49 Hz, 3H) ppm.

General procedure for derivatization of aminoalcohols

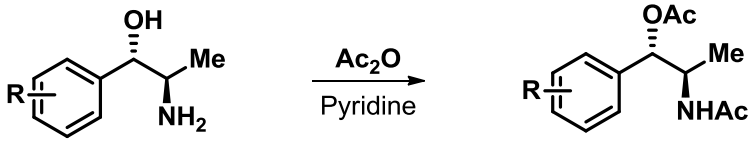

1,2-Amino alcohol was dissolved in pyridine and Ac_2O was slowly added. The reaction was stirred at rt for 24 hours. After reaction time a small portion of ice was added, and the crude was treated with HCl 37%. The aqueous layer was extracted with dichloromethane. The combined organic phases were treated with NaOH 10%, washed with brine, dried with Na_2SO_4 and concentrated under vacuum. The crude product was purified by column chromatography on silica gel.

2-acetamido-1-phenylpropyl acetate **(2-2a)**

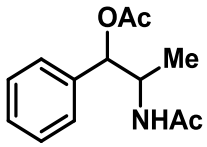

Prepared according to the general procedure. The crude mixture was purified by column chromatography on silica gel eluting with Dichloromethane/ Methanol 98:2. The title product was obtained as a yellowish oil as mixture of *syn* and *anti* diasteroisomers. All analytical data are in agreement with literature.

^{1}H-NMR (300 MHz, $CDCl_3$) *anti* δ_H 7.34-7.26 (m, 5H), 5.83 (d, J = 3.81 Hz, 1H), 4.45 (m, 1H), 2.13 (s, 3H), 1.92 (s, 3H), 1.05 (d, J = 6.84 Hz, 3H); *syn* δ_H 7.34-7.26 (m, 5H), 5.70 (d, J = 6.92 Hz, 1H), 4.42 (m, 1H), 2.09 (s, 3H), 1.91 (s, 3H), 1.03 (d, J = 6.56 Hz, 3H) ppm.

The enantiomeric excess was determined by HPLC on chiral stationary phase with Daicel Chiralcel AD column: eluent Hexane/*i*PrOH = 90/10, flow rate 0.8 mL/min, λ=210 nm, anti τ_{1S2R} = 10.6 min, anti τ_{1R2S} = 13.2 min.

2-acetamido-1-(2,5-dimethoxyphenyl)propyl acetate **(2-3a)**

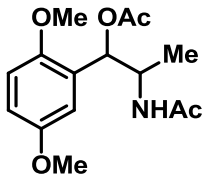

Prepared according to the general procedure. The crude mixture was purified by column chromatography on silica gel eluting with Dichloromethane/ Methanol 98:2. The title product was obtained as a yellowish oil as mixture of *syn* and *anti* diasteroisomers. All analytical data are in agreement with literature.

^{1}H-NMR (300 MHz, $CDCl_3$) *anti:* δ_H 6.85-6.78 (m, 3H), 6.10 (d, J = 4.91 Hz, 1H), 4.42 (m, 1H), 3.82 (s, 3H), 3.76 (s, 3H), 2.13 (s, 3H), 1.90 (s, 3H), 1.08 (d, J = 6.76 Hz, 3H); *syn* δ_H 6.85-6.76 (m, 3H), 6.12 (d, J = 5.69 Hz, 1H), 4.42 (m, 1H), 3.80 (s, 3H), 3.76 (s, 3H), 2.11 (s, 3H), 1.88 (s, 3H), 1.09 (d, J = 6.77 Hz, 3H) ppm. **^{13}C-NMR** (75 MHz, $CDCl_3$): 189.5, 170.2, 169.1, 153.6, 150.4, 127.2, 113.4, 112.8, 111.6, 72.3, 56.2, 56.1, 55.7, 48.1, 23.4, 21.1, 16.0 ppm.

The enantiomeric excess was determined by HPLC on chiral stationary phase with Phenomenex Lux Cellulose-1 3u column: eluent Hexane/*i*PrOH = 9/1, flow rate 0.8 mL/min, λ=210 nm, anti τ_{1R2S} = 18.2 min, anti τ_{1S2R} = 19.7 min.

Multi-step flow synthesis

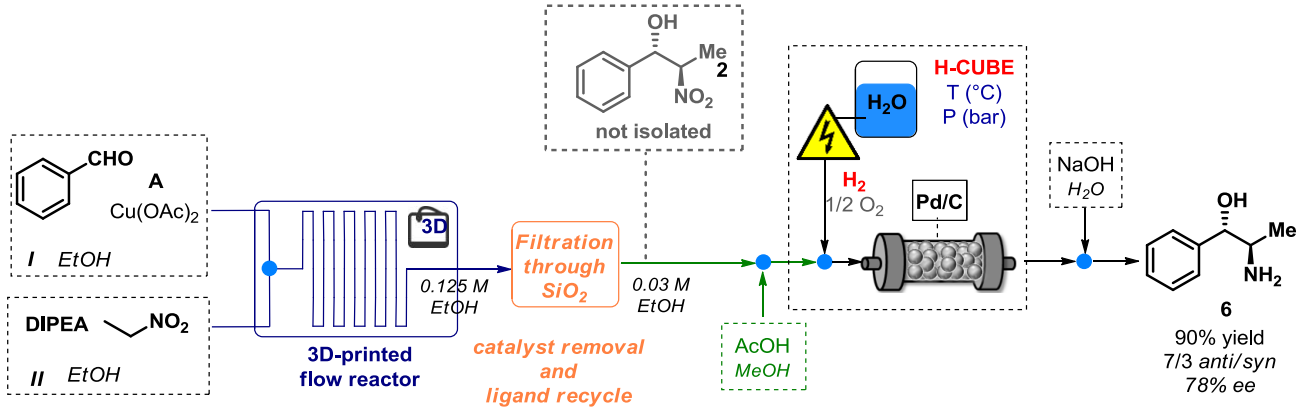

Two syringes of 2.5 mL were taken: ***I*** was charged with a preformed mixture (after 30 min of stirring) of benzaldehyde (0.375 mmol), **A** (0.075 mmol) and $Cu(OAc)_2$ (0.075 mmol) in EtOH (1.46 mL, 0.250 M). Syringe ***II*** was charged with nitroethane (0.270 mL, 3.75 mmol), DIPEA (65 µL, 0.375 mmol) and EtOH (1.26 mL). The two syringes were connected to a syringe pump and the reagents directed to the flow reactor at -20 °C for a residence time of 30 minutes. The collected mixture (dark blue solution, 3 mL) was filtered over a short pad of silica (*h*: 1 cm, *d*: 2 cm) and eluted with EtOH (6 mL). To the crude product (light yellow) 500 µL (30 eq) of AcOH were added and it was subjected to continuous flow hydrogenation with H CUBE (T: 30 °C, P: 1 bar, flow rate 0.1 mL/min). Reaction was followed using TLC and after recirculation for 2.5 hours the solvent was evaporated, treated with NH_4OH 33% wt. and extracted five times with AcOEt. Amino alcohol **6** was obtained in 90% yield (over 2 steps), 7/3 *dr* and 78% ee as pure with solid, with no need for further purification. (*dr* and ee were determined after derivatization of **6** into the corresponding bis-acetylate)**.**

3D-Printed flow reactors

The 3D-printed flow reactors were designed by using a 3D CAD software package (Autodesk123D®), which is freely distributed and produces a *.stl* file. A further optimization of the geometry was performed using Netfabb basic 5.2 free software (Autodesk®) in order to optimize and validate the final design.

Cura 15.02 software was used in order to set-up all the parameters related to the material used for the 3D printing process and to slice the model into thin layers. The final *.gcode* file generated can be directly read by the Sharebot NG 3D-printer and use for printing the device.

Mesoreactors were fabricated in a layer-by-layer fashion by depositing molten polymer in patterns calculated based upon the CAD designs of the reactor being printed. It should be noted that the majority of the printing process can be achieved unattended (for example overnight), requiring attention only to start the process. Once the 3D printer has been correctly calibrated for the printing process, different templates (corresponding to a slice of the desired reactor presenting channel-holes) were printed and analyzed with an optical microscope in order to evaluate the real dimension of the channels. These information were used to re-calibrate the reactor design adjusting the printing scale.

Generally, the shape of the 3D-printed reaction ware devices was chosen in order to combine short design and printing times with the robustness required for a flow system. Details about the different geometry devices and 3d-printing parameters are reported below.

Failure in the device fabrication was rarely observed, consisted mainly in imperfect layer adhesion between two layers. This fact could be avoided working in at constant ambient temperature. Furthermore, all the reactors were printed with the presence of a support in order to increase the adhesion of the first layer to the printer plate.

The presence of one O-ring to the top and one O-ring to the bottom of the 3D-prinded holed-screw connection is required in order to avoid problems related to solution linkage.

General parameters for 3D printing process:

HIPS parameters

QUALITY		Minimun travel (mm)	1.5
Layer height (mm)	0.05	Enable combing	ALL
Shell thickness (mm)	1.6	Minimal extrusion before retracting (mm)	0.02
Initial layer thickness (mm)	0.2	Z hop when retracting (mm)	0
Initial layer width (%)	150		
Cut off object bottom (mm)	0	**SKIRT**	
Dual extrusion overlap (mm)	0.15	Line count (n°)	1
		Start distance (mm)	3.0
RETRACTION		Minimal lenght (mm)	150.0
Enable retraction	YE S		
		FILL	
Retraction speed (mm/s)	50	Bottom/top thickness (mm)	1.6
Retraction distance (mm)	2	Fill density (%)	100

INFILL

solid infill top	YES
solid infill bottom	YES
infill overlap (%)	15

SPEED AND TEMPERATURE

Print speed (mm/s)	40
Travel speed (mm)	150
Bottom layer speed (mm/s)	20
Infill speed (mm/s)	0
Top/bottom speed (mm/s)	20
Outer shell speed (mm/s)	0
Innes shell speed (mm/s)	0
Printing temperature (°C)	240
Bed temperature (°C)	85

FILAMENT

Diameter (mm)	1.75
Flow (%)	100

COOL

Minimal layer time (s)	10
Enable cooling fan	YES
Fan full on at height (mm)	0.5
Fan speed min (%)	0
Fan speed max (%)	0
Minimun speed (mm/s)	15
Cool head lift	NO

SUPPORT

Support type (grid / line)	LINES
Overhang angle for support (deg)	0
Fill amount (%)	30
Distance X/Y (mm)	0.7
Distance Z (mm)	0.15
Platform adhesion type	Brim
Brim line amount	25

RAFT

Extra margin (mm)	20
Line spacing (mm)	3.0
Base thickness (mm)	0.3
Base line width (mm)	1.0
Interface thickness (mm)	0.27
Interface line width (mm)	0.4
Airgap	0
First layer airgap	0.22
Surface layers	0
Surface layers thickness (mm)	0.27
Surface layer line width (mm)	0.4

FIX ORRIBLE

Combine everything (Type-A)	NO
Combine everything (Type-B)	NO
Keep open faces	NO
Extensive stiching	NO

PLA parameters

QUALITY

Layer height (mm)	0.1
Shell thickness (mm)	1.4
Initial layer thickness (mm)	0.2
Initial layer width (%)	150
Cut off object bottom (mm)	0
Dual extrusion overlap (mm)	0.15

RETRACTION

Enable retraction	YES
Retraction speed (mm/s)	50
Retraction distance (mm)	2
Minimun travel (mm)	1
Enable combing	ALL
Minimal extrusion before retracting (mm)	0.02
Z hop when retracting (mm)	0

SKIRT

Line count (n°)	5
Start distance (mm)	5.0
Minimal lenght (mm)	150.0

FILL

Bottom/top thickness (mm)	1.8
Fill density (%)	100

INFILL

solid infill top	YES
solid infill bottom	YES
infill overlap (%)	35

SPEED AND TEMPERATURE

Print speed (mm/s)	60
Travel speed (mm)	150
Bottom layer speed (mm/s)	20
Infill speed (mm/s)	0
Top/bottom speed (mm/s)	20
Outer shell speed (mm/s)	0
Innes shell speed (mm/s)	0
Printing temperature (°C)	220
Bed temperature (°C)	40

FILAMENT

Diameter (mm)	1.75
Flow (%)	100

COOL

Minimal layer time (s)	10
Enable cooling fan	YES
Fan full on at height (mm)	0.4
Fan speed min (%)	0
Fan speed max (%)	0
Minimun speed (mm/s)	10
Cool head lift	NO

SUPPORT

Support type (grid / line)	GRID
Overhang angle for support (deg)	60
Fill amount (%)	15
Distance X/Y (mm)	1
Distance Z (mm)	0.1

Platform adhesion type	NONE
Brim line amount	15

RAFT

Extra margin (mm)	5.0
Line spacing (mm)	3.0
Base thickness (mm)	0.3
Base line width (mm)	1.0
Interface thickness (mm)	0.27
Interface line width (mm)	0.4
Airgap	0
First layer airgap	0.22
Surface layers	2
Surface layers thickness (mm)	0.27
Surface layer line width (mm)	0.4

FIX ORRIBLE

Combine everything (Type-A)	YES
Combine everything (Type-B)	NO
Keep open faces	NO
Extensive stiching	NO

Nylon parameters

QUALITY

Layer height (mm)	0.1
Shell thickness (mm)	1.4
Initial layer thickness (mm)	0.26
Initial layer width (%)	150
Cut off object bottom (mm)	0
Dual extrusion overlap (mm)	0.15

RETRACTION

Enable retraction	YES
Retraction speed (mm/s)	40
Retraction distance (mm)	2
Minimun travel (mm)	5.0
Enable combing	ALL
Minimal extrusion before retracting (mm)	0.02
Z hop when retracting (mm)	0.075

SKIRT

Line count (n°)	1
Start distance (mm)	3.0
Minimal lenght (mm)	150.0

FILL

Bottom/top thickness (mm)	3.2
Fill density (%)	100

INFILL

solid infill top	YES
solid infill bottom	YES
infill overlap (%)	15

SPEED AND TEMPERATURE

Print speed (mm/s)	40
Travel speed (mm)	150
Bottom layer speed (mm/s)	35
Infill speed (mm/s)	0
Top/bottom speed (mm/s)	0
Outer shell speed (mm/s)	0
Innes shell speed (mm/s)	0
Printing temperature (°C)	240
Bed temperature (°C)	60

FILAMENT

Diameter (mm)	1.75
Flow (%)	100

COOL

Minimal layer time (s)	10
Enable cooling fan	YES
Fan full on at height (mm)	0.5
Fan speed min (%)	0
Fan speed max (%)	0
Minimun speed (mm/s)	10
Cool head lift	NO

SUPPORT

Support type (grid / line)	GRID
Overhang angle for support (deg)	90

Fill amount (%)	20
Distance X/Y (mm)	
0.8	
Distance Z (mm)	0.15
Platform adhesion type	Brim
Brim line amount	25

RAFT

Extra margin (mm)	20
Line spacing (mm)	
3.0	
Base thickness (mm)	0.3
Base line width (mm)	1.0
Interface thickness (mm)	0.27
Interface line width (mm)	0.4
Airgap	0
First layer airgap	0.22
Surface layers	0
Surface layers thickness (mm)	0.27
Surface layer line width (mm)	0.4

FIX ORRIBLE

Combine everything (Type-A)	NO
Combine everything (Type-B)	NO
Keep open faces	NO
Extensive stiching	
NO	

Reactors

Reactor-0: 75 ul (circular channel: 1.59 mm ø)

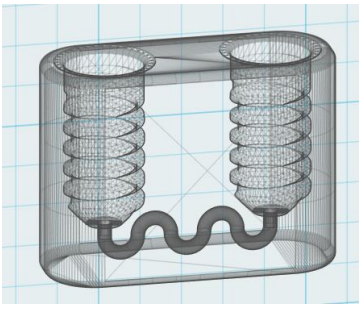

This reactor was realized using three different type of colored PLA filaments (transparent, yellow and green) and used for additive releasing tests.

Each reactor was connected to a HPLC pump, and 20 ml of a 0.125 M mixture of nitroethane in ethanol was circulated *in continuous* for 5 hours. At the end of this time, a UV spectra was collected. All the three mixtures gave the same curve, with a lower signal at 328 nm. All the volatile parts were then removed, and the amount of residue were analyzed using a balance.

PLA: Printing time: 3 hours 13 minutes; Filament used: 4.21m 13.0g

GREEN

Residue after evaporation:

2.8 mg

YELLOW

Residue after evaporation:

0.9 mg

NATURAL

Residue after evaporation:

2.7 mg

UV spectra

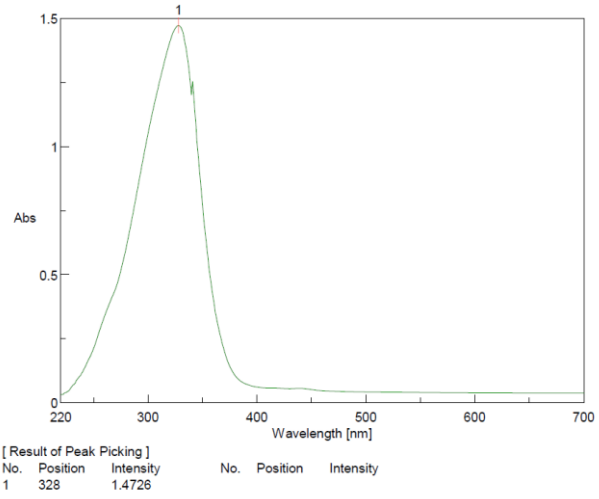

Reactor-1: 1 mL (squared channel: 1.41 x 1.41 mm)

VIRTUAL DESIGN

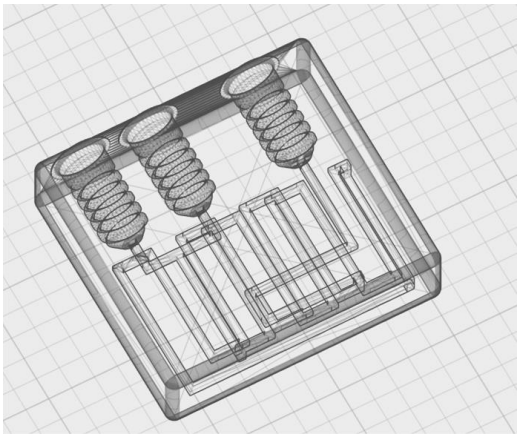

FINAL REALIZATION - (HIPS version)

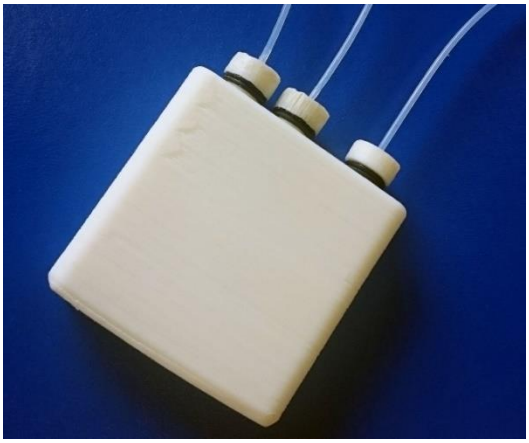

Schematic representation of the 1 ml reactionware device employed in this work showing the internal channels (virtual design) and the final 3D printed reactors with connections. This reactor present two inputs (A and B) and one output (C).

Squared section channel: 1.41 x 1.41 x 500 mm

Section area: 2 mm^2

Total volume (calculated): 1 mL

HIPS: Printing time: 20 hours 11 minutes; Filament used: 21.15 m 63.0g

PLA: Printing time: 16 hours 54 minutes; Filament used: 21.15m 63.0g

NYLON: Printing time: 17 hours 33 minutes; Filament used: 21.15m 63.0g

Reactor-2: 1 ml (circular channel: 1.59 mm ø)

VIRTUAL DESIGN

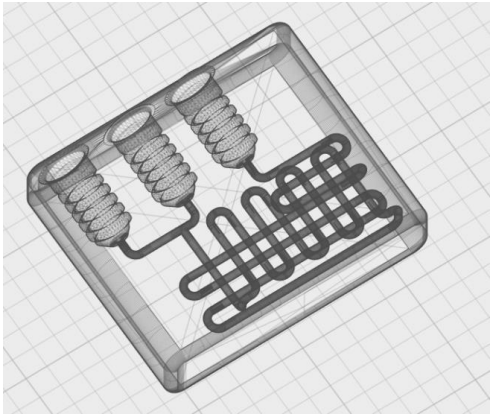

FINAL REALIZATION

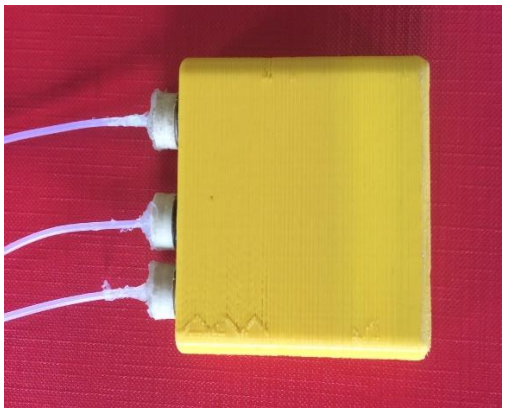

Schematic representation of the 1 ml reactionware device employed in this work showing the internal channels (virtual design) and the final 3D printed reactors with connections. This reactor present two inputs (A and B) and one output (C).

Circular section channel: 1.59 mm diameter

Section area: 2 mm^2

Total volume (calculated): 1 mL

PLA: Printing time: 17 hours 27 minutes; Filament used: 20.69m 62.0g

Reactor-3: 1 ml (squared channel: 1.0 x 1.0 mm)

VIRTUAL DESIGN **FINAL REALIZATION -** (PLA version)

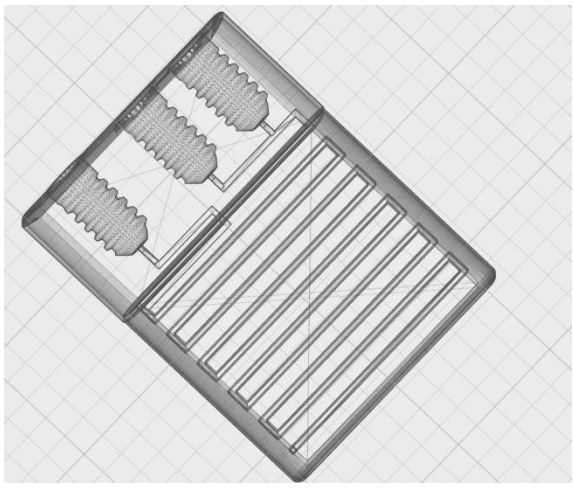

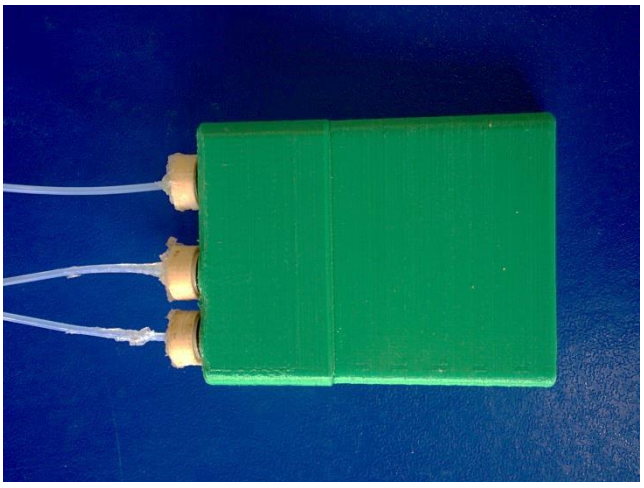

Schematic representation of the 1 ml reactionware device employed in this work showing the internal channels (virtual design) and the final 3D printed reactors with connections. This reactor present two inputs (A and B) and one output (C).

Squared section channel: 1.00 x 1.00 x 1000 mm

Section area: 1 mm^2

Total volume (calculated): 1 mL

PLA: Printing time: 27 hours 32 minutes; Filament used: 16.94m 51.0g (in this case, layer height value was set to 0.05 mm with a print speed of 40 mm/s).

Reactor-4: 1 ml (rectangular channel: 1.42 x 1.67 mm)

VIRTUAL DESIGN **FINAL REALIZATION -** (PLA version)

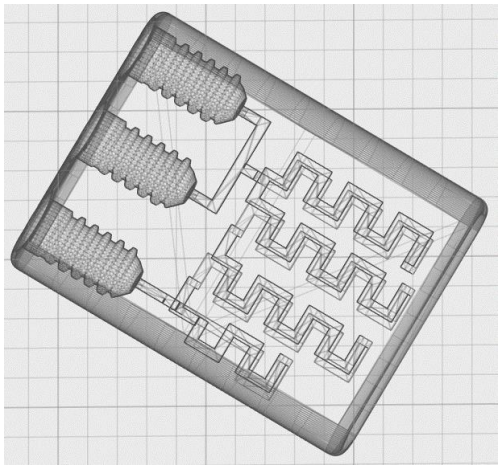

Schematic representation of the 1 ml reactionware device employed in this work showing the internal channels (virtual design) and the final 3D printed reactors with connections. This reactor present two inputs (A and B) and one output (C).

Rectangular section channel: 1.42 x 1.67 x 500 mm

Section area: 2 mm^2

Total volume (calculated): 1 mL

PLA: Printing time: 13 hours 32 minutes; Filament used: 17.11m 51.0g

Reactor-5: 10 ml (squared channel: 2.65 x 2.65 mm)

VIRTUAL DESIGN **FINAL REALIZATION -** (PLA version)

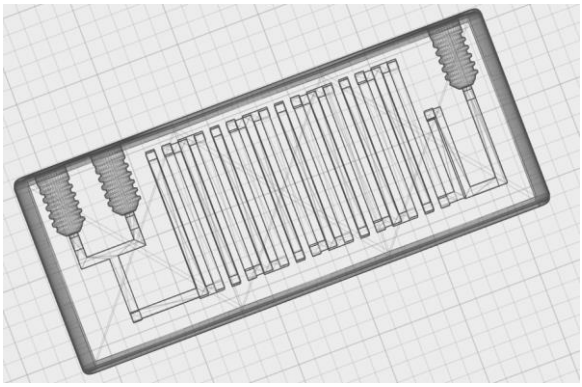

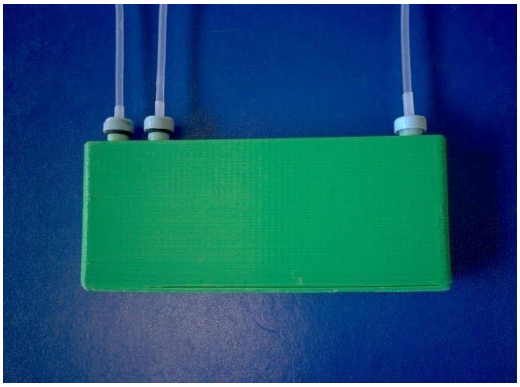

Schematic representation of the 10 ml reactionware device employed in this work showing the internal channels (virtual design) and the final 3D printed reactors with connections. This reactor present two inputs (A and B) and one output (C).

Squared section channel: 2.65 x 2.65 x 1424 mm

Section area: 7 mm^2

Total volume (calculated): 10 mL

PLA: Printing time: 52 hours 14 minutes; Filament used: 64.21 m 192.0 g

Reactor-6: 1 ml + SiO_2 column (circular channel: 1.59 mm ø)

VIRTUAL DESIGN **FINAL REALIZATION -** (PLA version)

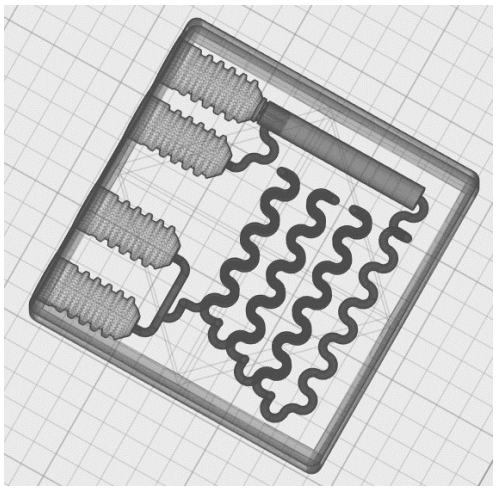

Schematic representation of the 1 ml reactionware device employed in this work showing the internal channels (virtual design) and the final 3D printed reactors with connections. This reactor present two inputs (A and B) and one output (C) and an additional input (D) for the addition/removal of silica that can be closed with a cap.

Circular section channel: 1.59 mm diameter

Section area: 2 mm^2

Total volume (calculated): 1 mL (channels) + 0.650 ml (silica column: 5 mm ø, 35 mm h)

PLA: Printing time: 22 hours 57 minutes; Filament used: 27.21 m 81.0 g

N.B. A small amount of glass fiber was added on the top and on the bottom of the silica column in order to prevent channels occlusion.

Other 3D-printer reactors have been also realized and screened:

Reactor-7

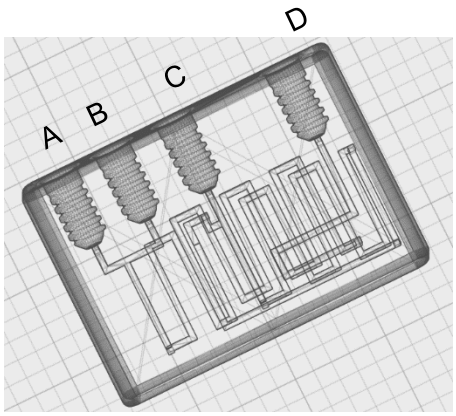

Schematic representation of a 1.25 ml reaction ware device. This reactor present three inputs (A, B and C) and one output (D). After a 250 μL premixing section where A and B are mixed, the resulting solution is mixed with C solution in a 1 mL section.

Squared Section channel: 1.41x1.41x125 mm +

1.41x1.41x500 mm

Section area: 2 mm^2

Total volume (calculated): 1 mL

Reactor-8

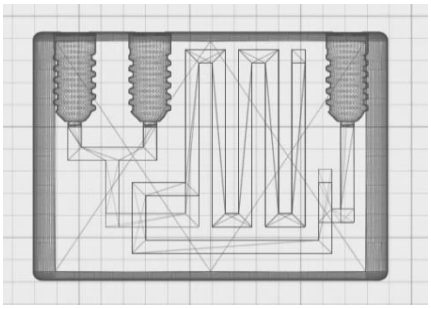

Schematic representation of a 1.25 ml reaction ware device

Squared Section channel: 3 x 3 x 500 mm +

Section area: 9 mm^2

Total volume (calculated): 4.5 mL

General Set-Up of Continuous Flow Reactions with 3D Printed Reactors

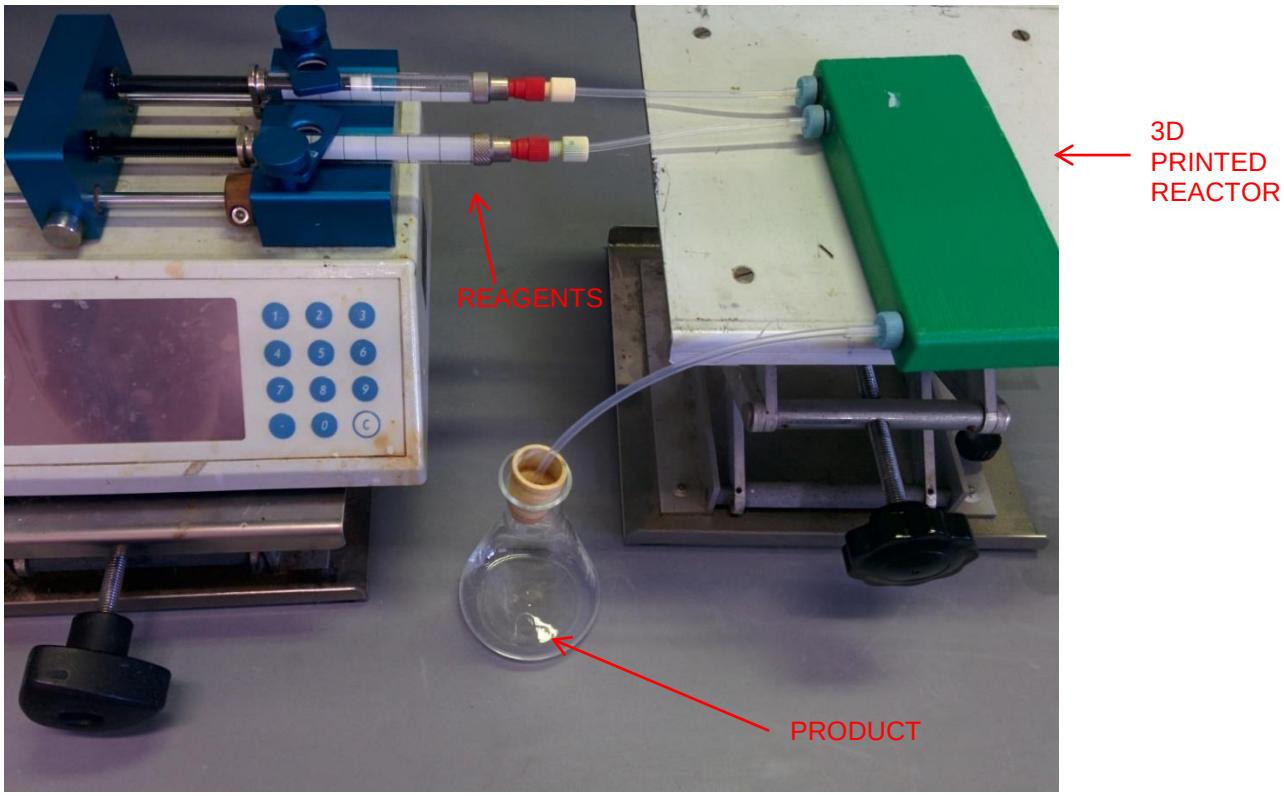

NMR Spectra

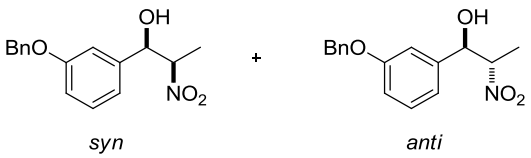

syn *anti*

1

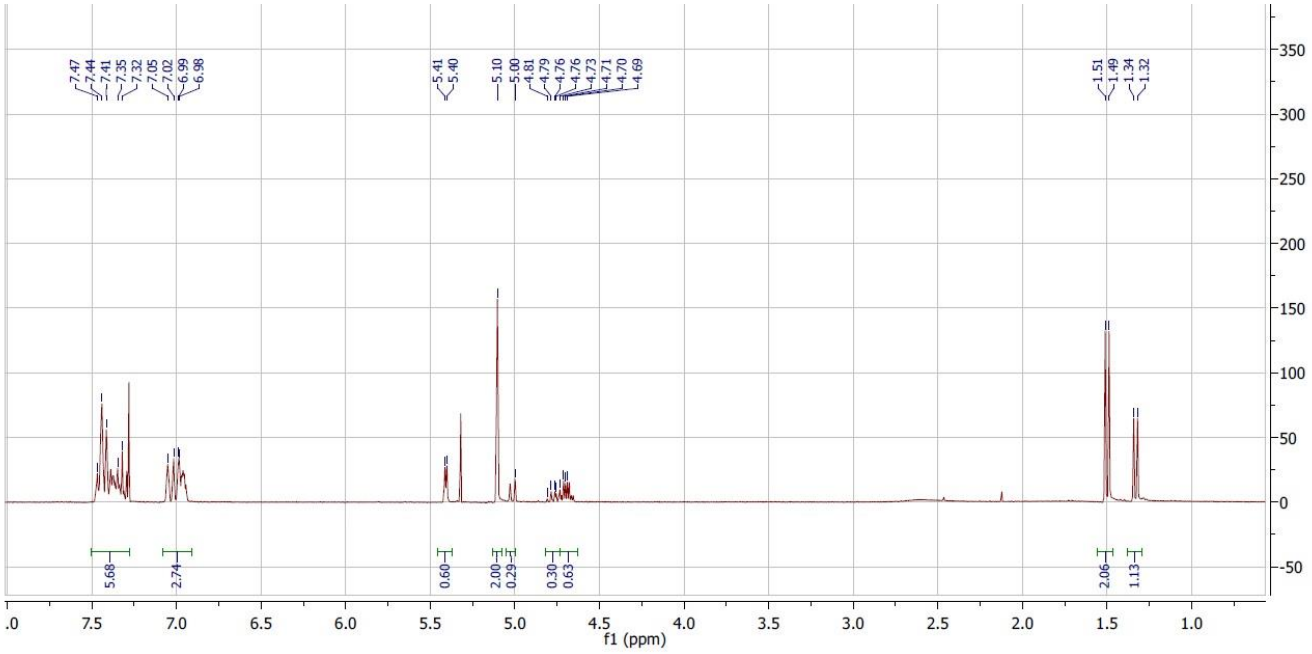

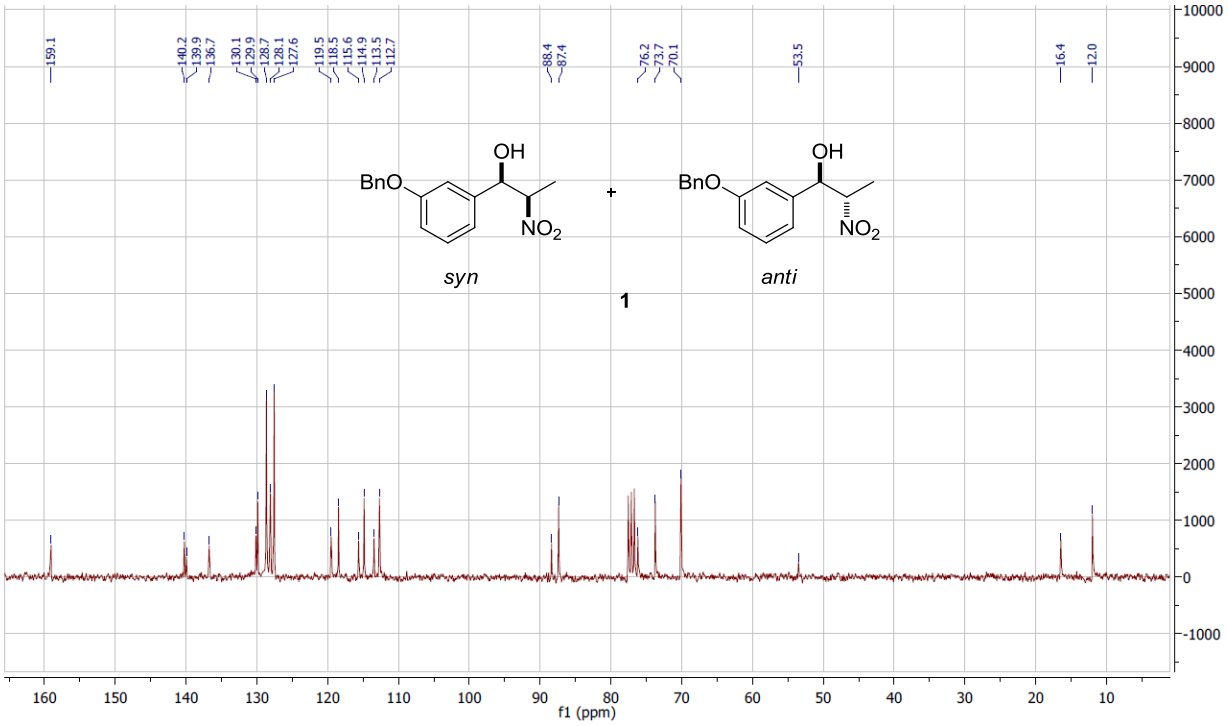
159.1
140.2
139.9
136.7
130.1
129.9
128.7
128.1
127.6
119.5
118.5
115.6
114.9
113.5
112.7
88.4
87.4
76.2
73.7
70.1
53.5
16.4
12.0
OH
BnO
NO2
syn
anti
1
f1 (ppm)

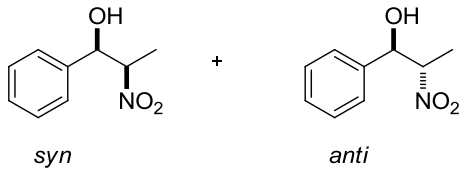
OH
NO2
syn
anti
2

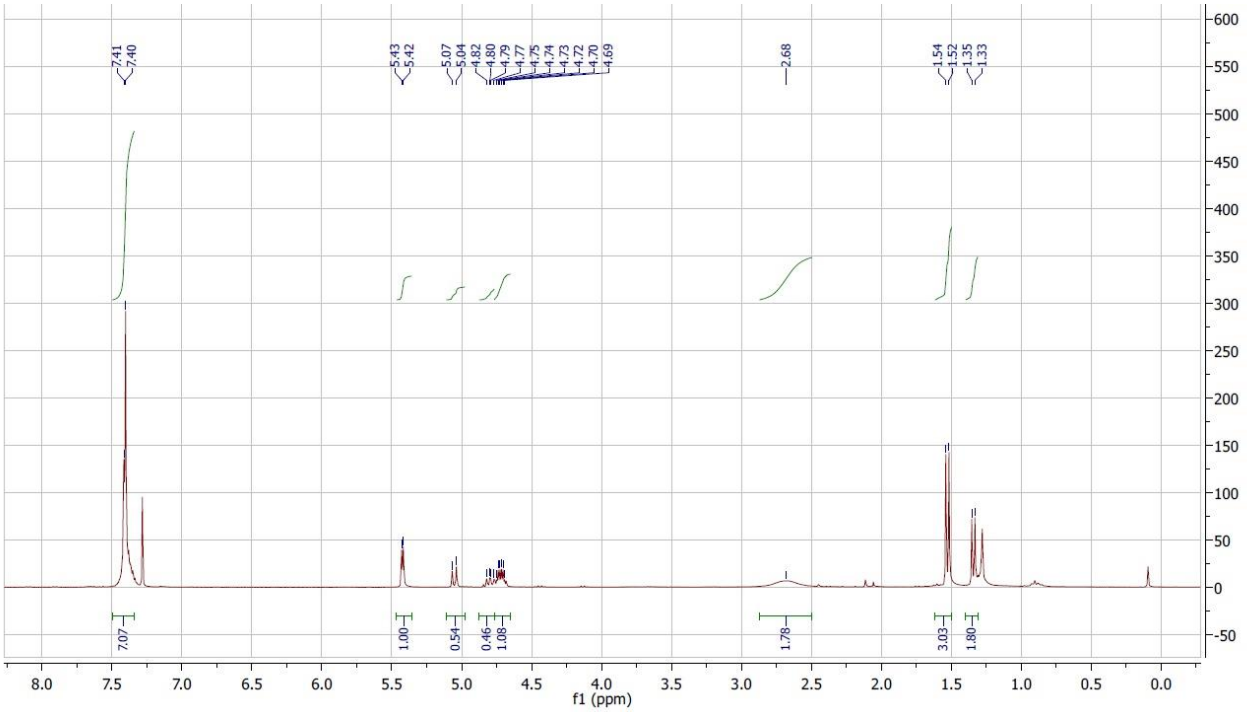
7.41
7.40
5.43
5.42
5.07
5.04
4.82
4.80
4.79
4.77
4.75
4.74
4.73
4.72
4.70
4.69
2.68
1.54
1.52
1.35
1.33
7.07
1.00
0.54
0.46
1.08
1.78
3.03
1.80
f1 (ppm)

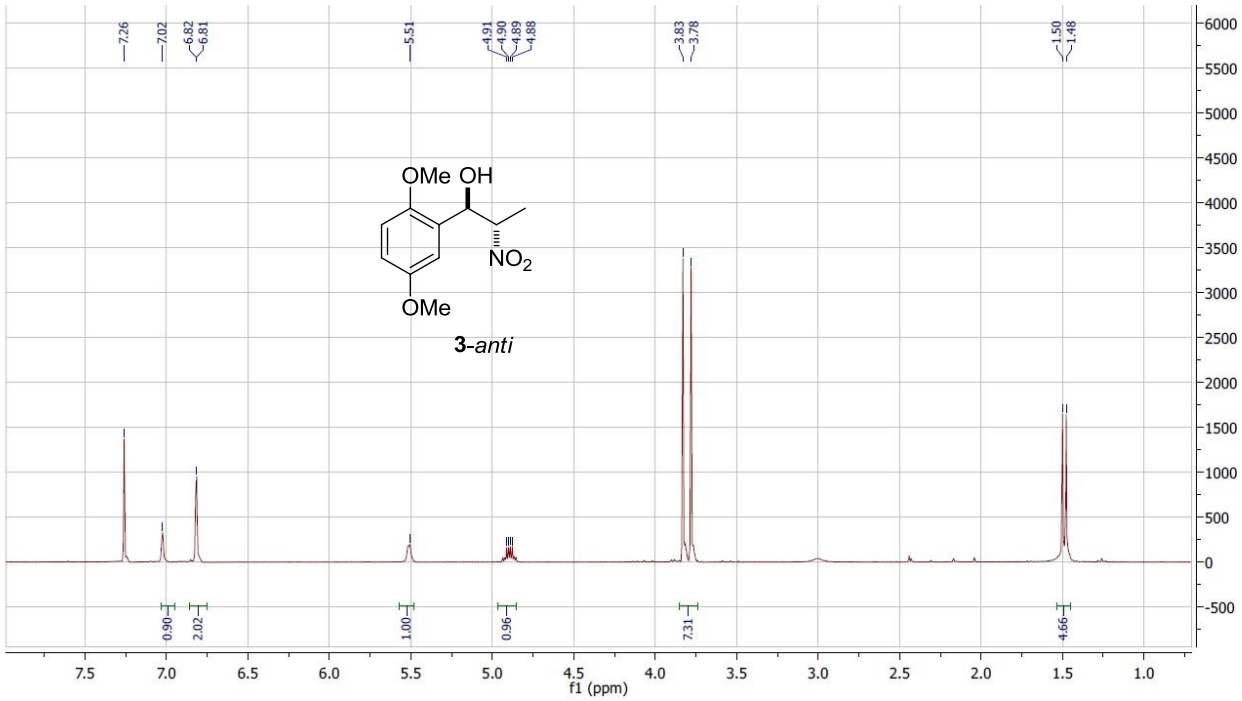
7.26
7.02
6.82
6.81
5.51
4.91
4.90
4.89
4.88
3.83
3.78
1.50
1.48
OMe OH
NO2
OMe
3-anti
0.90
2.02
1.00
0.96
7.31
4.66
f1 (ppm)

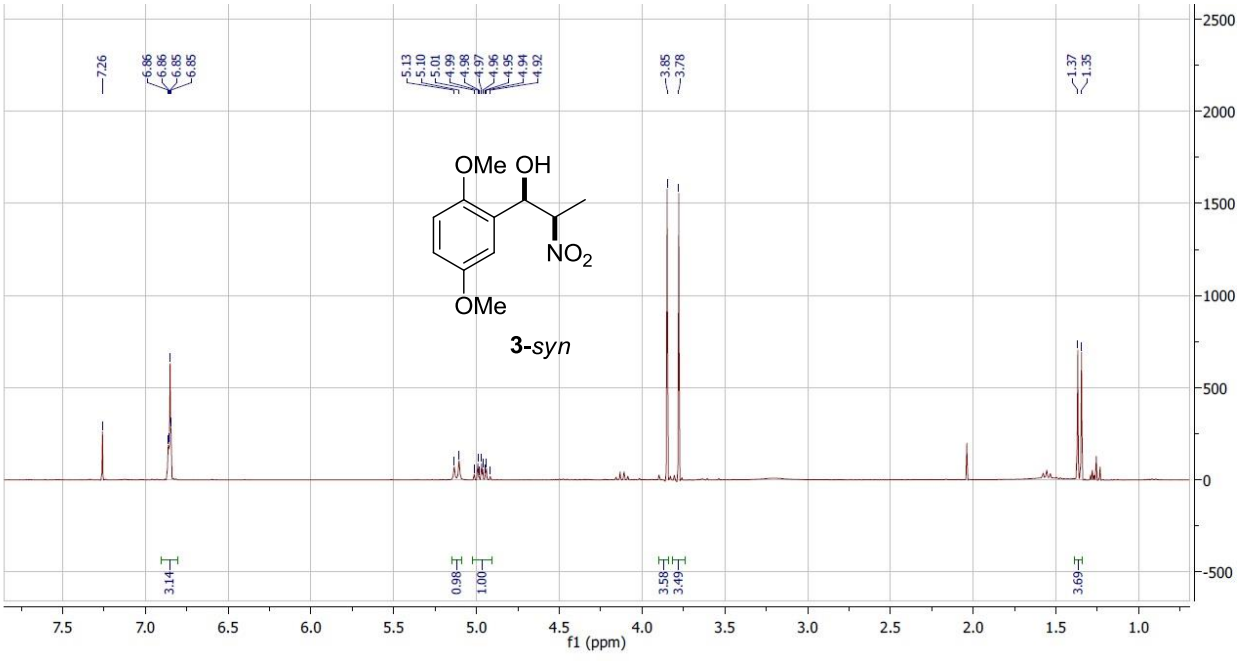
7.26
6.86
6.86
6.85
6.85
5.13
5.10
5.01
4.99
4.98
4.97
4.96
4.95
4.94
4.92
3.85
3.78
1.37
1.35
OMe OH
NO2
OMe
3-syn
3.14
0.98
1.00
3.58
3.49
3.69
f1 (ppm)

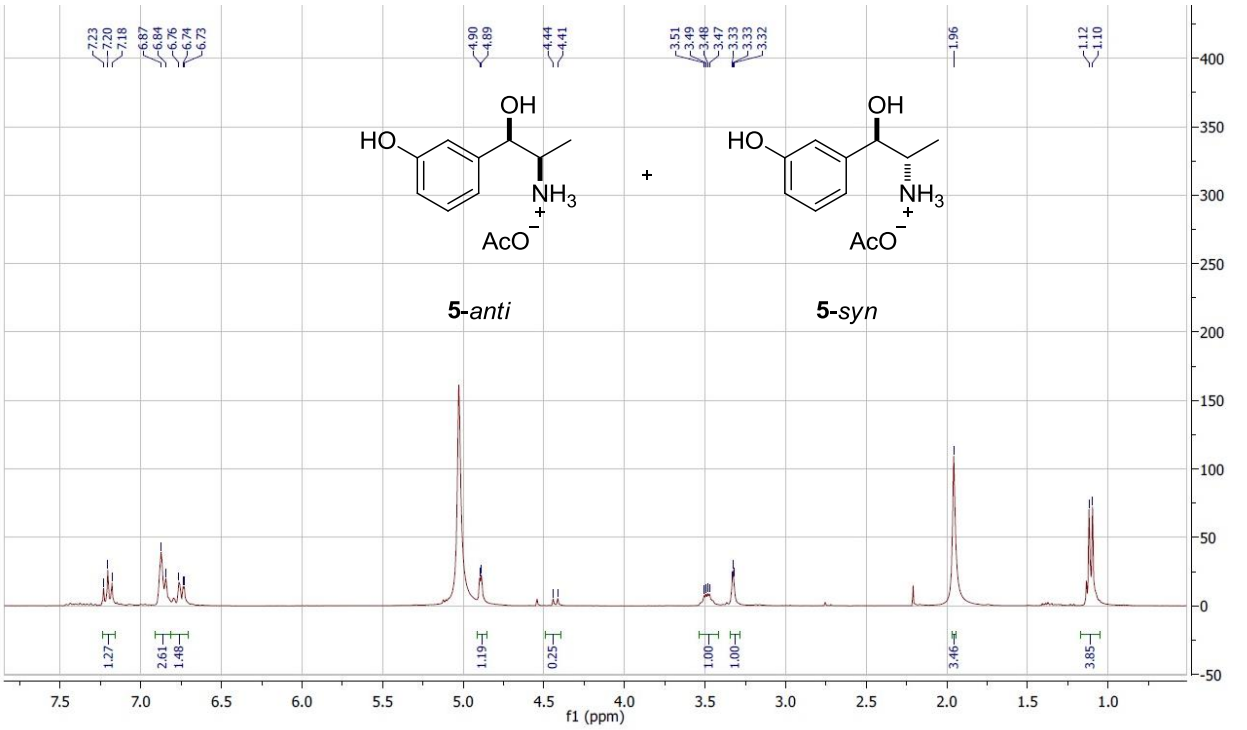
OH
HO
NH3
AcO
5-anti
5-syn
f1 (ppm)

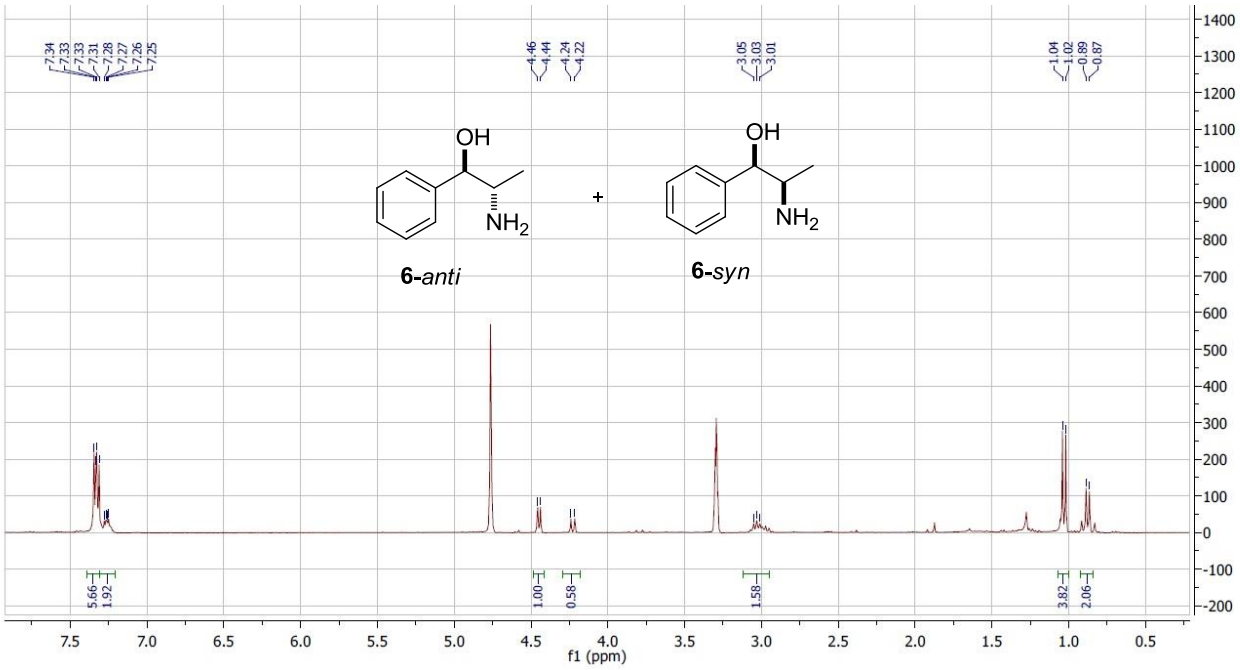
OH
NH2
6-anti
6-syn
f1 (ppm)

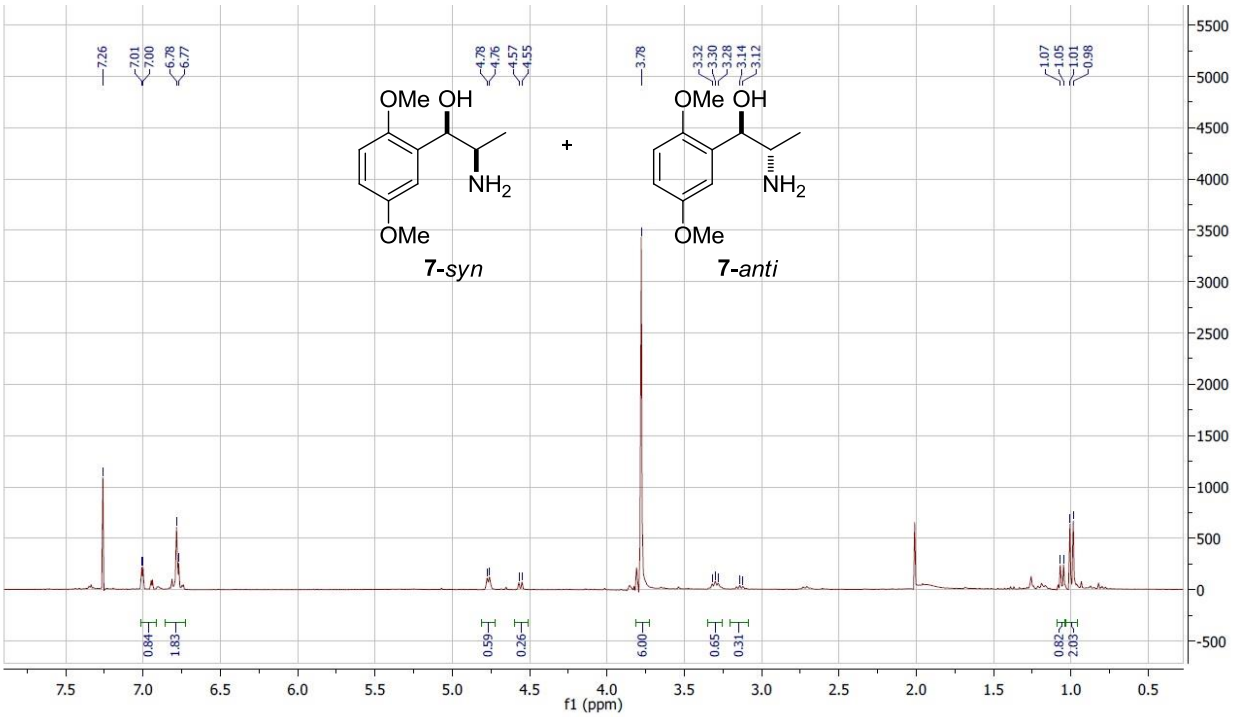
OMe OH
NH2
OMe
7-syn
+
OMe OH
NH2
OMe
7-anti
f1 (ppm)

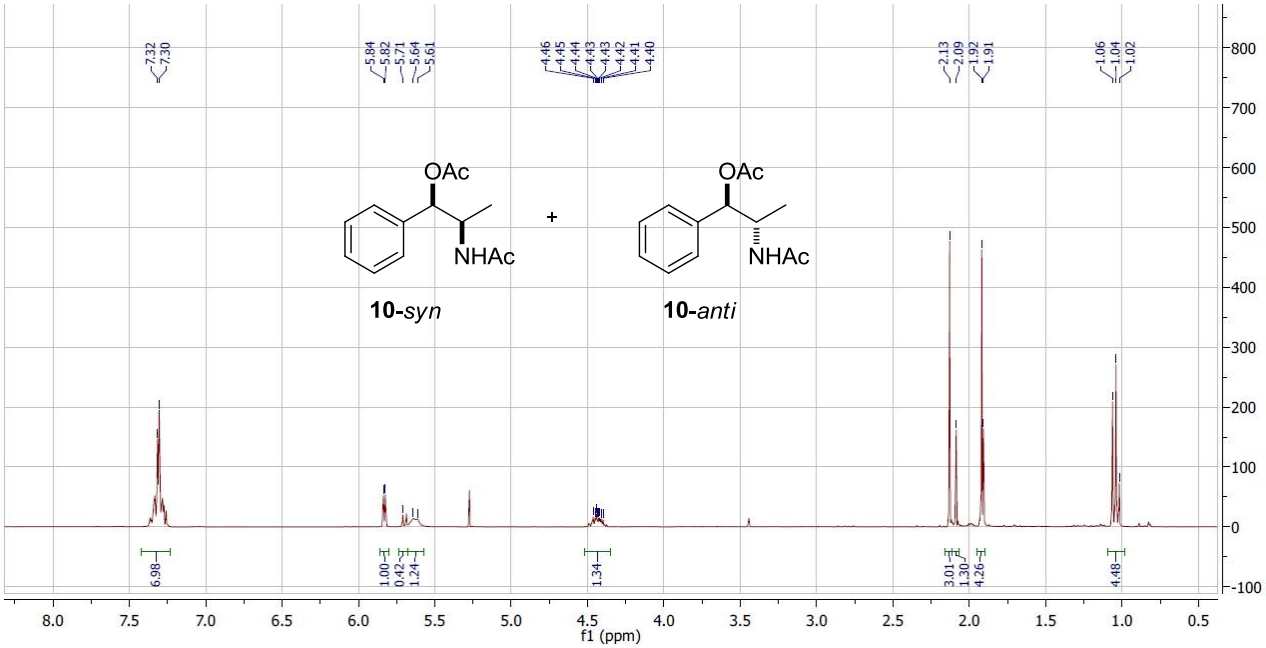
OAc
NHAc
10-syn
+
OAc
NHAc
10-anti
f1 (ppm)

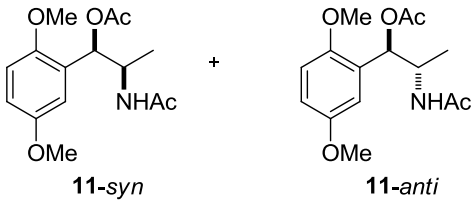
OMe OAc
NHAc
OMe
11-syn
+
OMe OAc
NHAc
OMe
11-anti

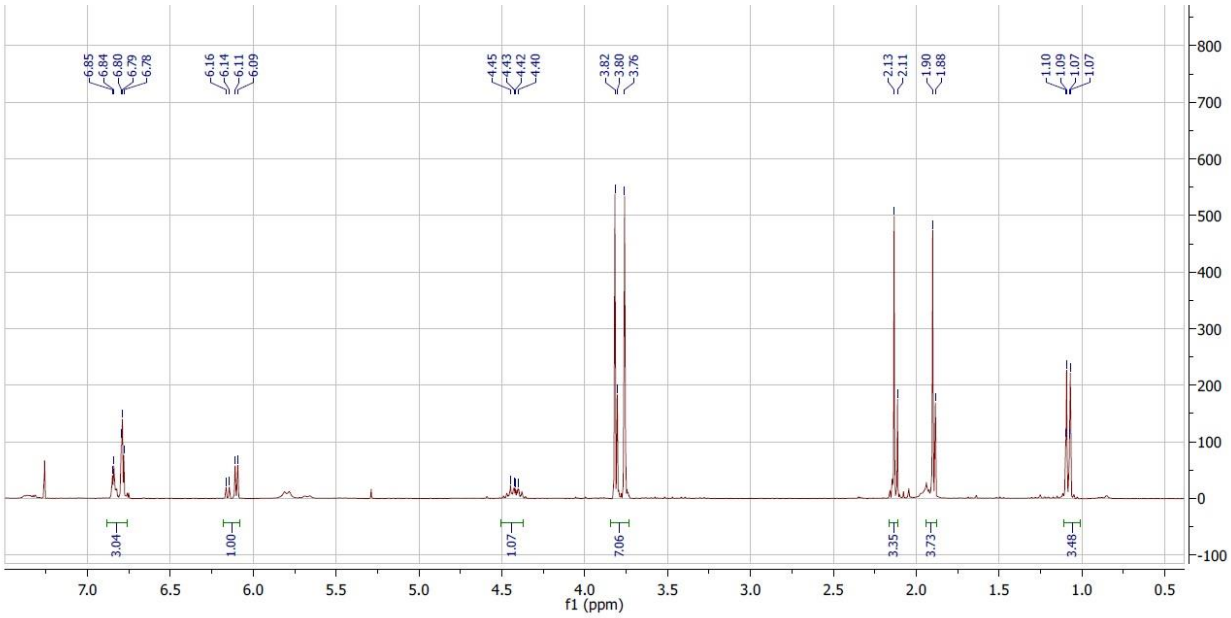
6.85
6.84
6.80
6.79
6.78
6.16
6.14
6.11
6.09
4.45
4.43
4.42
4.40
3.82
3.80
3.76
2.13
2.11
1.90
1.88
1.10
1.09
1.07
1.07
3.04
1.00
1.07
7.06
3.35
3.73
3.48
f1 (ppm)

HPLC traces

CHIRALPAK CELLULOSA1 Hex:IPA 9:1 1 mL/min 65 bar ->

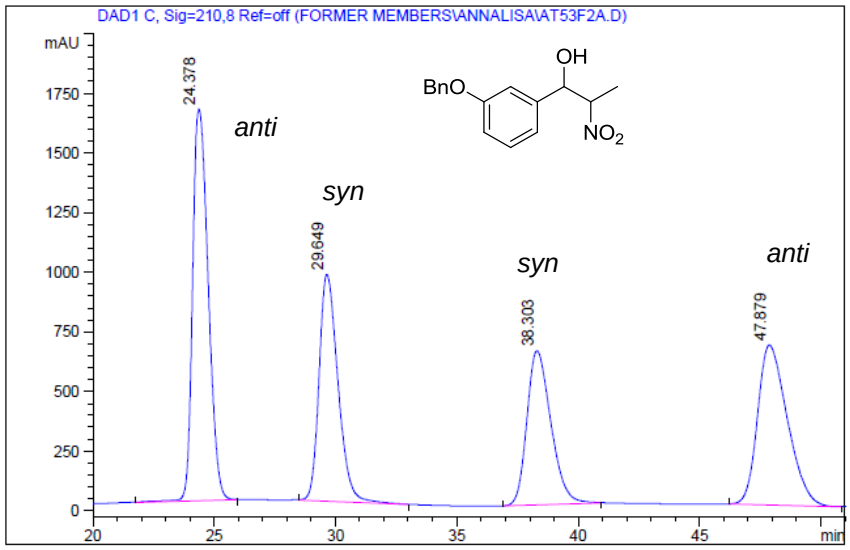

Signal 1: DAD1 C, Sig=210,8 Ref=off

Peak #	RT [min]	Type	Width [min]	Area	Area %	Name
1	24.378	BB	0.702	73425.625	32.392	
2	29.649	BB	0.836	51475.719	22.709	
3	38.303	BB	1.057	44461.184	19.614	
4	47.879	BB	1.274	57313.043	25.284	

CHIRALPAK CELLULOSA1 Hex:IPA 9:1 1 mL/min 65 bar ->

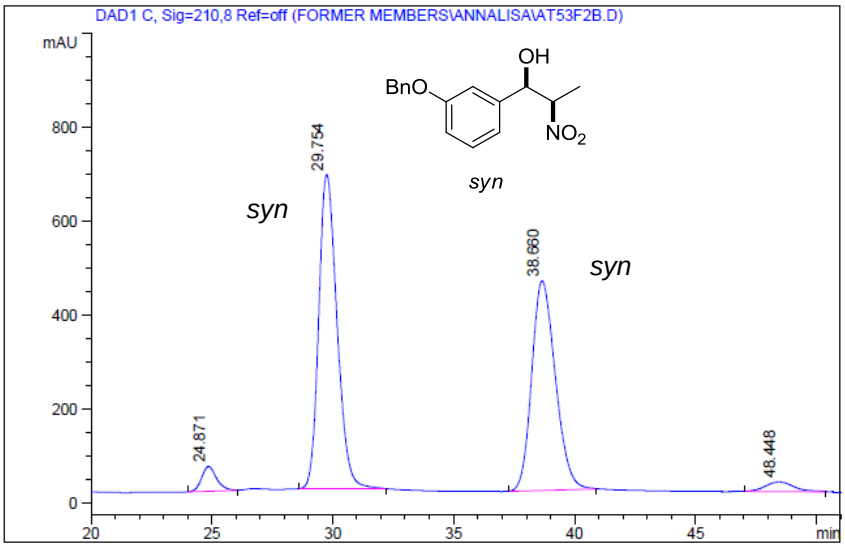

Signal 1: DAD1 C, Sig=210,8 Ref=off

Peak #	RT [min]	Type	Width [min]	Area	Area %	Name
1	24.871	BB	0.644	2309.475	3.312	
2	29.754	BB	0.811	35295.648	50.615	
3	38.660	BB	1.046	30387.883	43.577	
4	48.448	BB	0.996	1740.408	2.496	

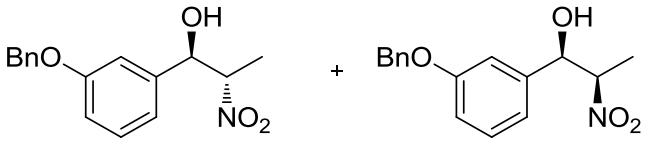

anti *syn*

LUX 3U CELLULOSA 1 Hex:IPA 9:1 0.8mL/min 36 bar COLONNA ->

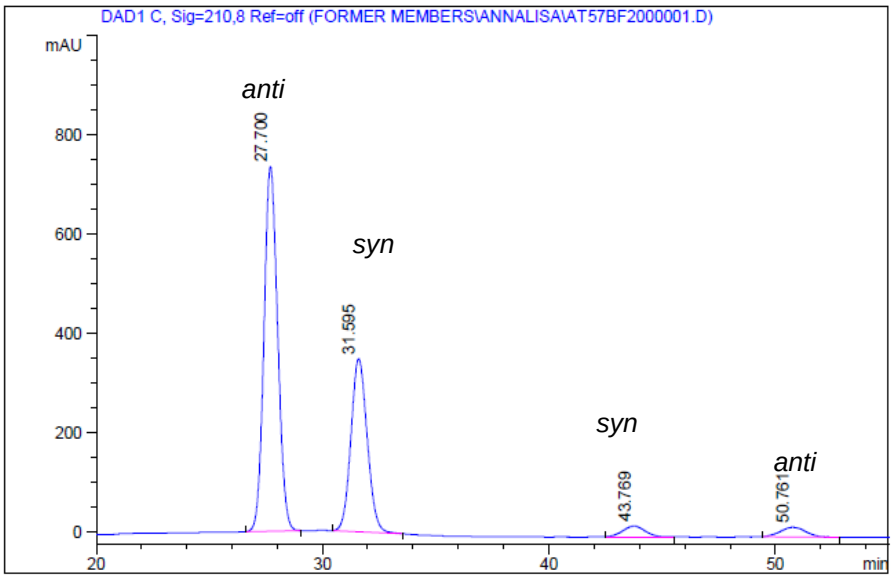

Signal 1: DAD1 C, Sig=210,8 Ref=off

Peak #	RT [min]	Type	Width [min]	Area	Area %	Name
1	27.700	BB	0.652	30834.475	60.032	
2	31.595	BB	0.781	17512.830	34.096	
3	43.769	BB	0.881	1484.848	2.891	
4	50.761	BB	0.933	1531.499	2.982	

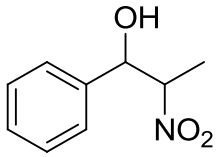

LUX 5 um CELLULOSE 1 Hex/IPA 9:1 0.8 mL/min 47 bar ->

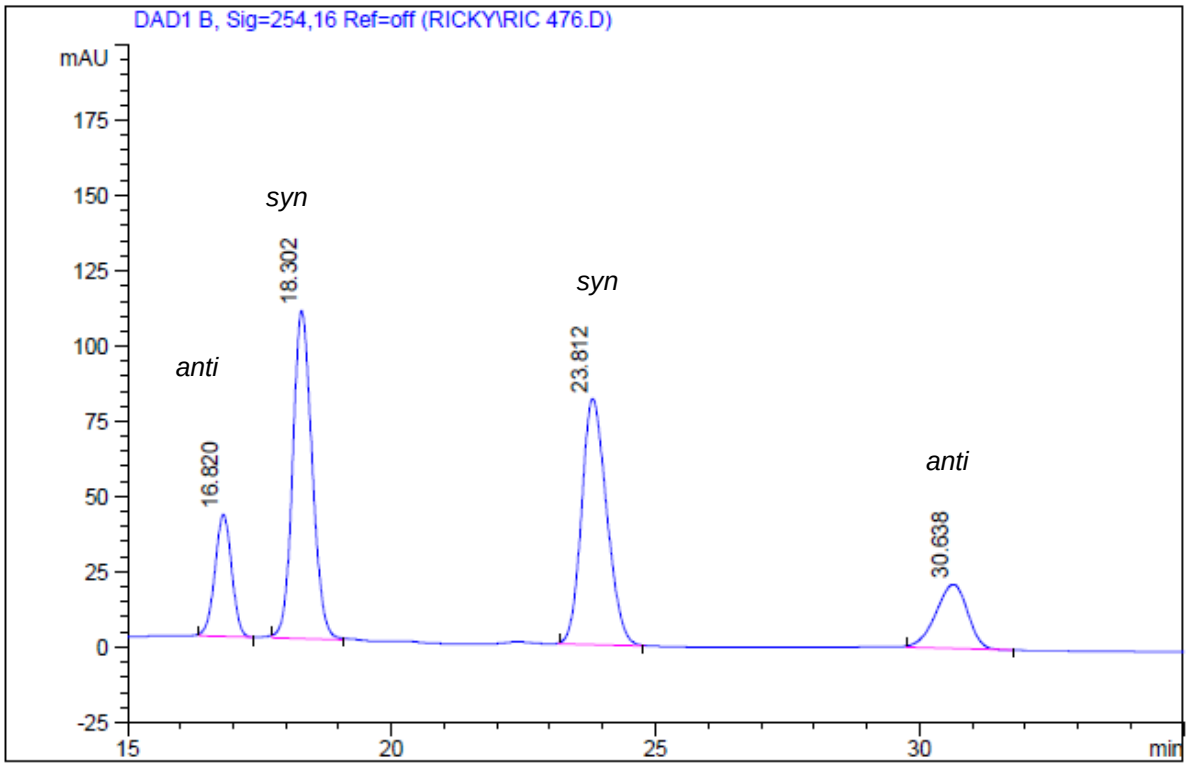

Signal 1: DAD1 B, Sig=254,16 Ref=off

Peak #	RT [min]	Type	Width [min]	Area	Area %	Name
1	16.820	BB	0.341	896.667	12.339	
2	18.302	BB	0.393	2774.646	38.182	
3	23.812	BB	0.510	2705.622	37.232	
4	30.638	BB	0.660	890.000	12.247	

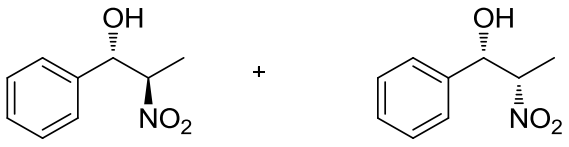

anti *syn*

LUX CELLULOSE 1HEX/IPA 95:5 0.8 mL/min 29 bar ->

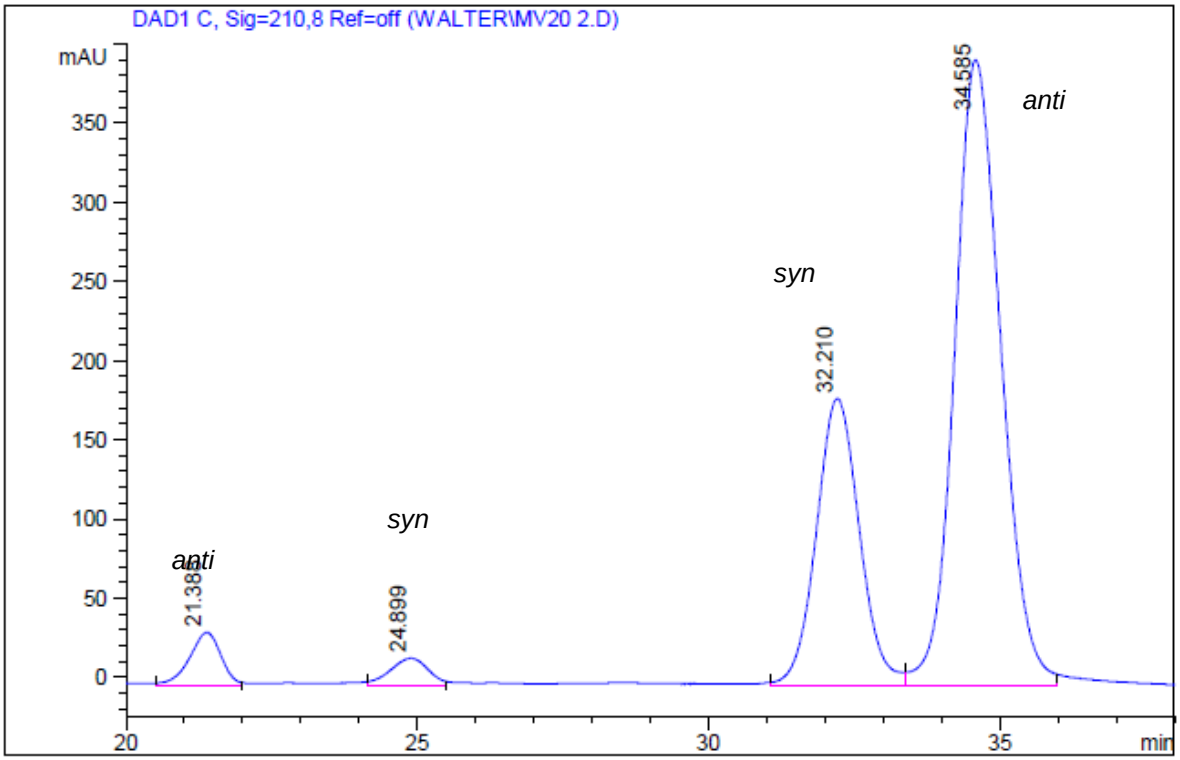

Signal 1: DAD1 C, Sig=210,8 Ref=off

Peak #	RT [min]	Type	Width [min]	Area	Area %	Name
1	21.388	MF	0.637	1284.092	3.849	
2	24.899	FM	0.763	799.912	2.398	
3	32.210	MF	0.862	9383.594	28.128	
4	34.585	FM	0.923	21893.250	65.626	

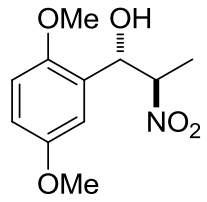

anti

CHIRALCEL AD Hex/IPA 9:1 0.8 mL/min 35 bar ->

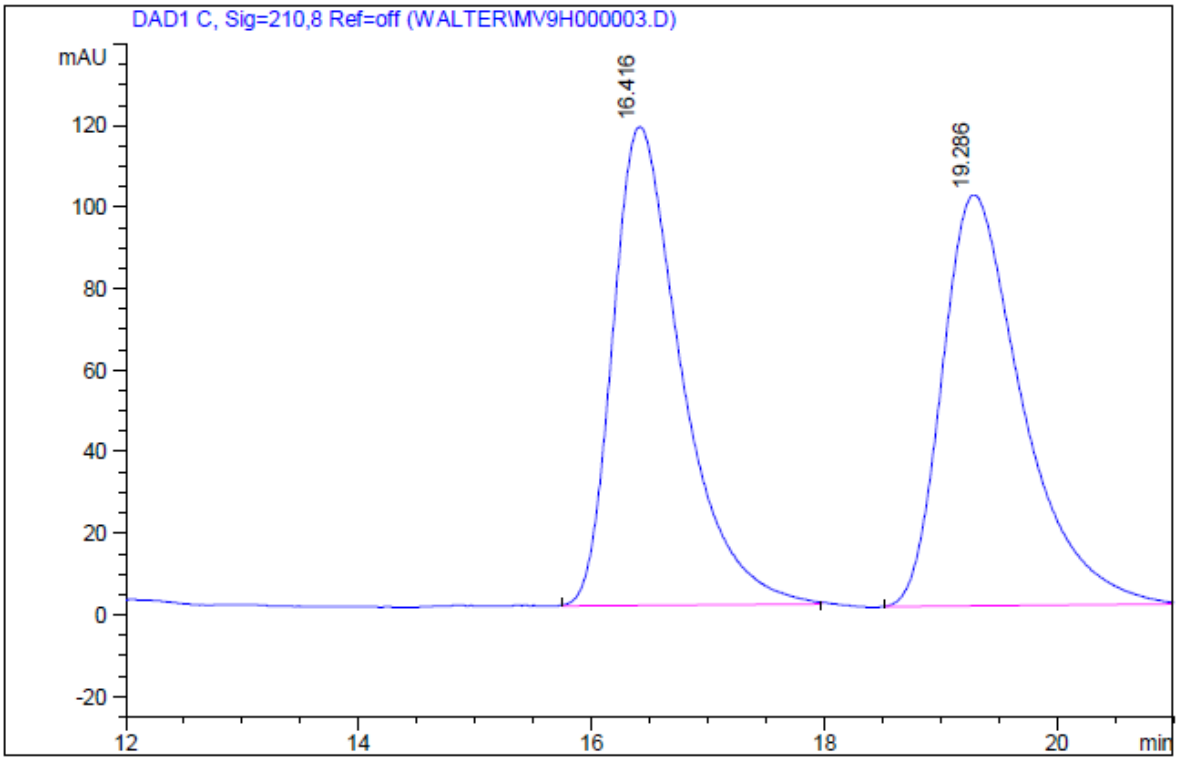

Signal 1: DAD1 C, Sig=210,8 Ref=off

Peak #	RT [min]	Type	Width [min]	Area	Area %	Name
1	16.416	BB	0.610	4812.853	49.892	
2	19.286	BB	0.699	4833.683	50.108	

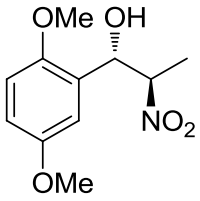

anti

CHIRALCEL AD Hex/IPA 9:1 0.8 mL/min 30 bar ->

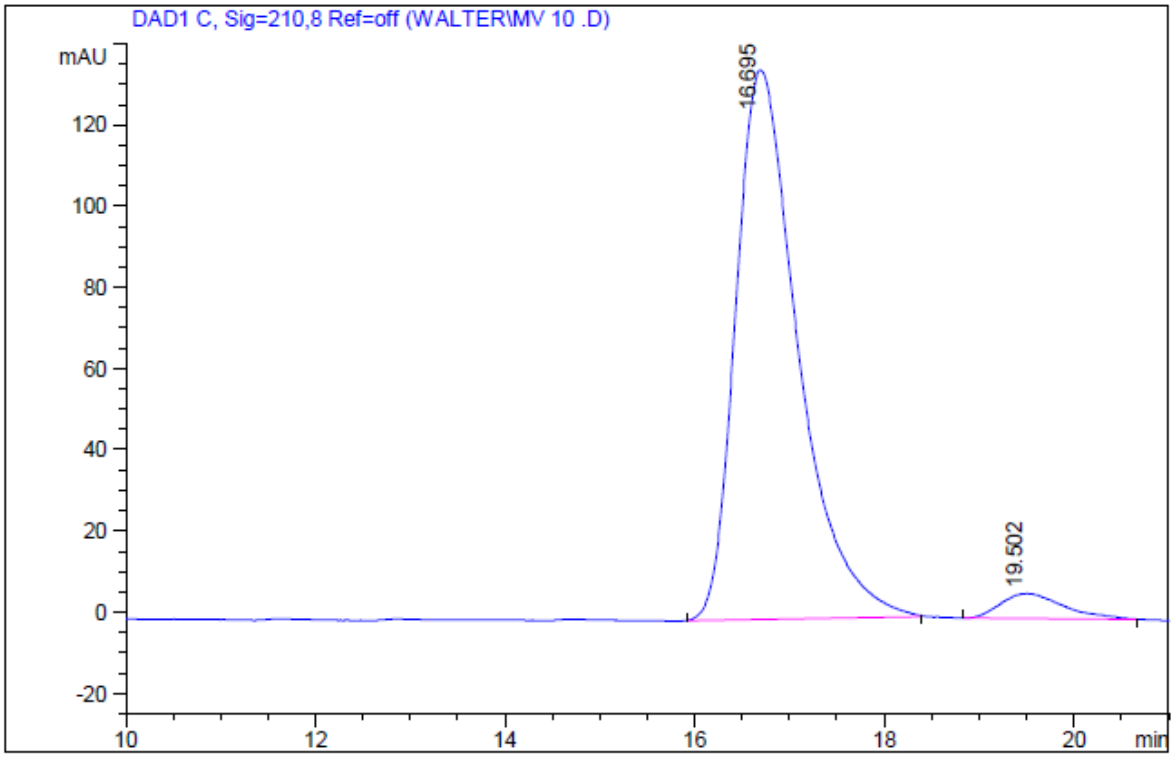

Signal 1: DAD1 C, Sig=210,8 Ref=off

Peak #	RT [min]	Type	Width [min]	Area	Area %	Name
1	16.695	BB	0.667	6193.234	95.540	
2	19.502	BB	0.558	289.108	4.460	

Sample Name : Campione_4
Acquisition Method: C:\CHEM32\1\DATA\ALCHEMIA\RICERCA\MET 2015-04-02 16-54-08\ME->
Data File : C:\CHEM32\1\DATA\ALCHEMIA\RICERCA\MET 2015-04-02 16-54-08\ ->
Injection Date : 02/04/2015
Column Temperature: 20.0°C
Comments : Campioni università

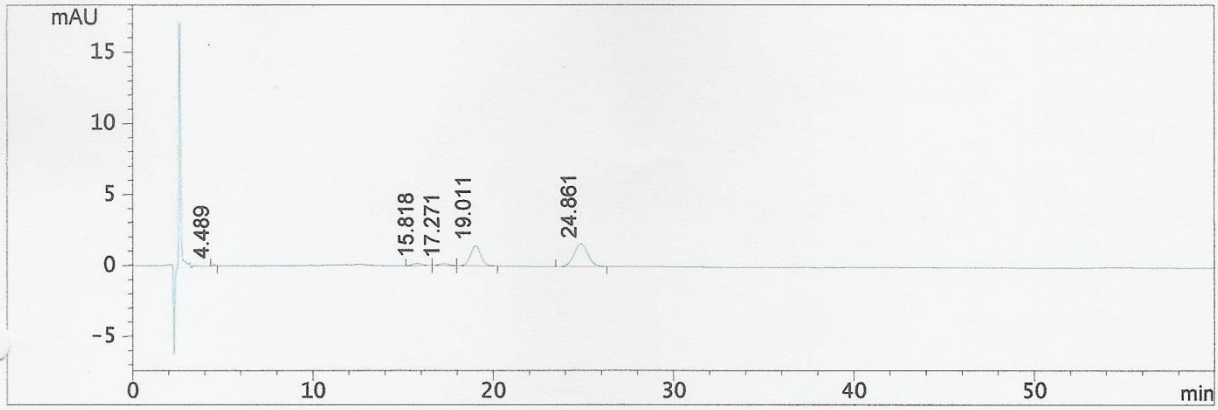

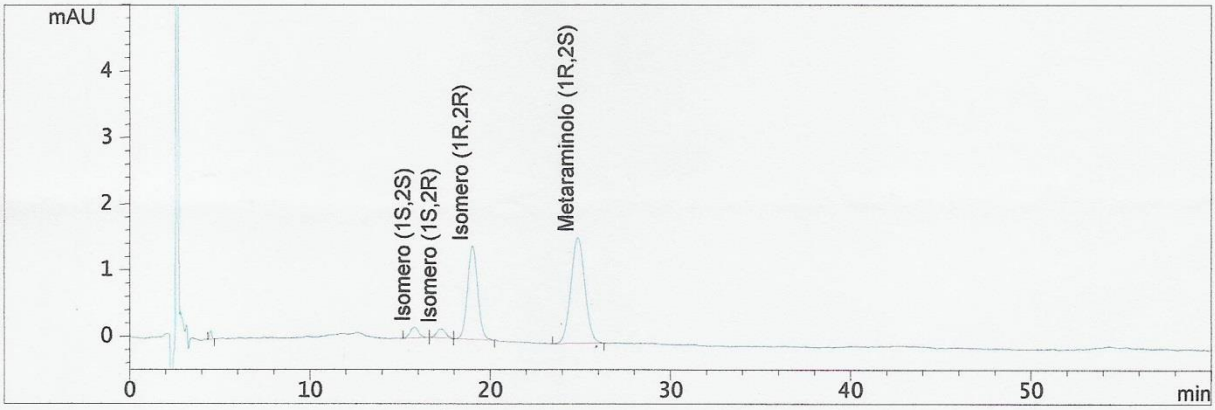

Signal 1: VWD1 A, Wavelength=210 nm

Peak #	Name	RT [min]	Width [min]	Height [mAU]	Area [mAU*s]	Area %
1		4.49	0.12	0.13	0.97386	0.640
2	Isomero (1S,2S)	15.82	0.55	0.16	5.31770	3.496
3	Isomero (1S,2R)	17.27	0.58	0.14	4.77746	3.141
4	Isomero (1R,2R)	19.01	0.66	1.40	55.24473	36.319
5	Metaraminolo (1R,2S)	24.86	0.90	1.59	85.79666	56.404
Total:					152.11040	100.000

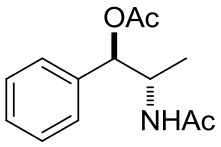

Chiralcell AD 9:1 Hex/iPrOH 0.8 mL/min 20 Bar ->

anti

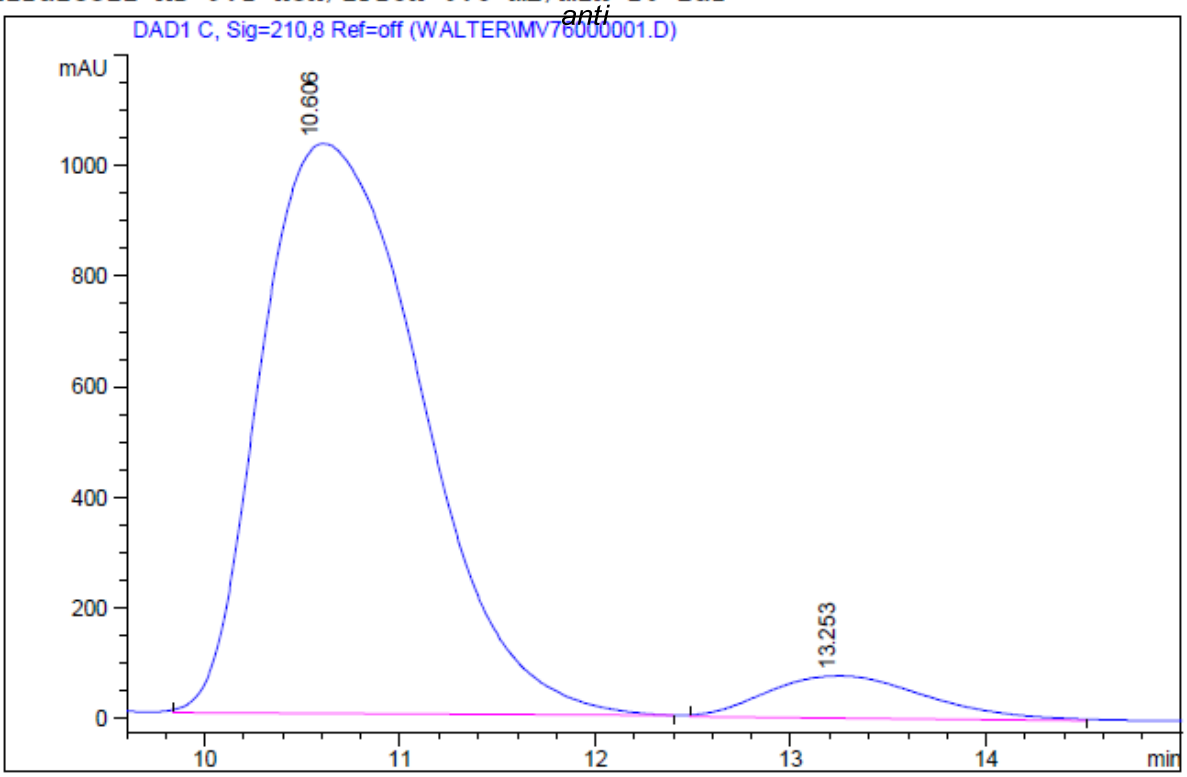

Signal 1: DAD1 C, Sig=210,8 Ref=off

Peak #	RT [min]	Type	Width [min]	Area	Area %	Name
1	10.606	MM	0.948	58623.352	93.123	
2	13.253	MM	0.944	4329.023	6.877	

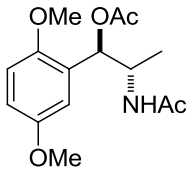

anti

LUX CELLULOSE 1 3u 9:1 Hex/iPrOH 1 mL/min 70 Bar ->

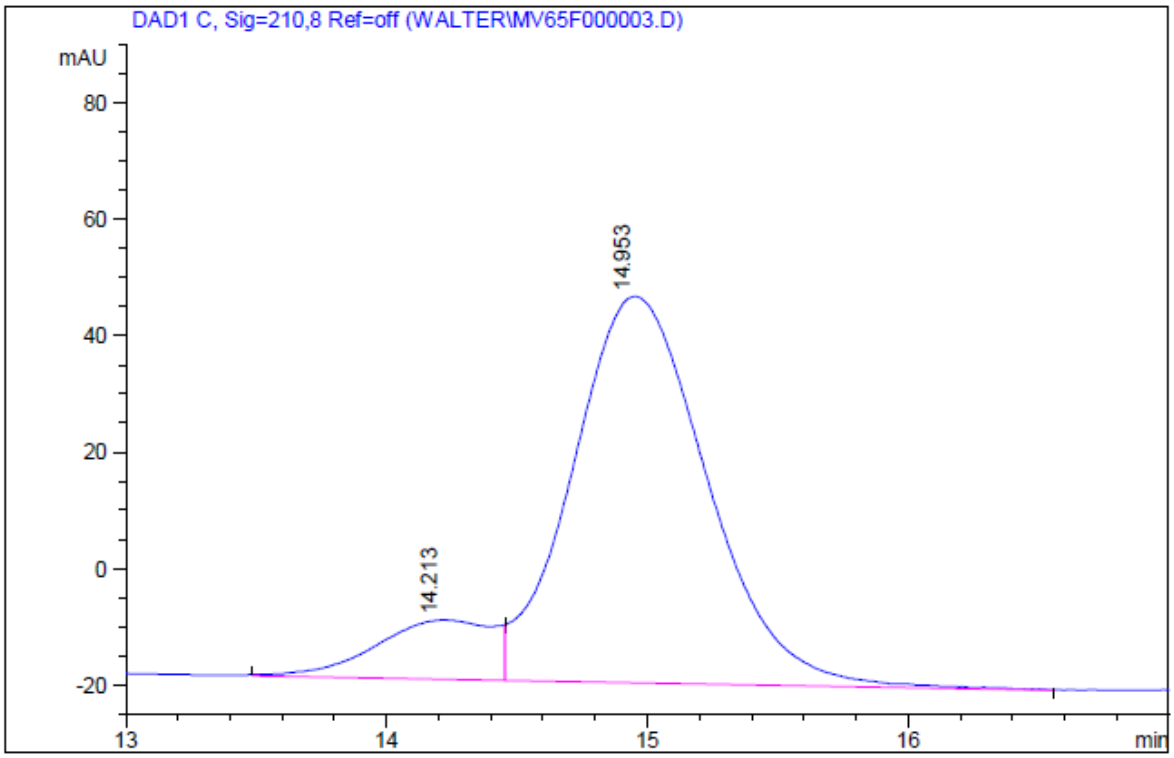

Signal 1: DAD1 C, Sig=210,8 Ref=off

Peak #	RT [min]	Type	Width [min]	Area	Area %	Name
1	14.213	MF	0.527	322.350	11.898	
2	14.953	FM	0.599	2386.934	88.102	

Chapter 3: Iron catalyzed transformations

Introduction to Iron chemistry

Hydrogenation and, more generally speaking, metal catalyzed redox processes, have played a crucial role in organic synthesis. Nowadays metal based catalysis is wildly used in industrial processes, indeed, almost 80% of all chemical and pharmaceutical products are prepared using catalytic approach[163]. The catalysts used in these transformations must meet stringent requirements, such as: functional group tolerance, chemoselectivity and should be able to control the stereochemical outcome of the reaction.

In the last two decades, a large number of homogeneous catalysts based on precious metals (Pd, Rh, Ir and Ru) were discovered. These complexes were prepared using rational design, and expensive chiral ligands; the importance of these discoveries was acknowledged with the Nobel prize to W. S. Knowles and R. Noyori in 2001 (Figure3-1).

Figure3-1: William S. Knowles and Ryoji Noyori, Nobel prize winner 2001, “for their work on chirally catalyzed hydrogenation reactions”.

These catalysts showed high activity and high selectivity, however the low abundance of the metals employed result in high operation cost; for example, the price of Pd has skyrocketed in the last 10 years[164]. Moreover, these metals are toxic and their replacement with hearth abundant and atoxic counterparts is highly recommended. A huge effort has been done from the scientific community for the developing of active metal complexes, based on abundant metals (Fe, Mn, Co) that showed the same reactivity compared to the noble-based ones.

In particular, in the last two decades, the attention towards iron catalyzed transformations has dramatically increased. Iron is industrially used as heterogeneous catalyst since 1910 in the ammonia production (Haber- Bosch process); also, the Fischer-Tropsch process (carbon monoxide reduction) is based on an iron catalyst and it is used since 1934; however, there are no reports in the use of homogeneous iron catalyzed processes to produce fine chemicals intermediates.

Iron catalyzed transformations

The raising interest in Iron based chemistry could be explained taking into consideration its unique characteristics:

1) 5.6% of the heart crust is composed by Iron; hence it is cheap, widespread and readily available (Figure 3-2).

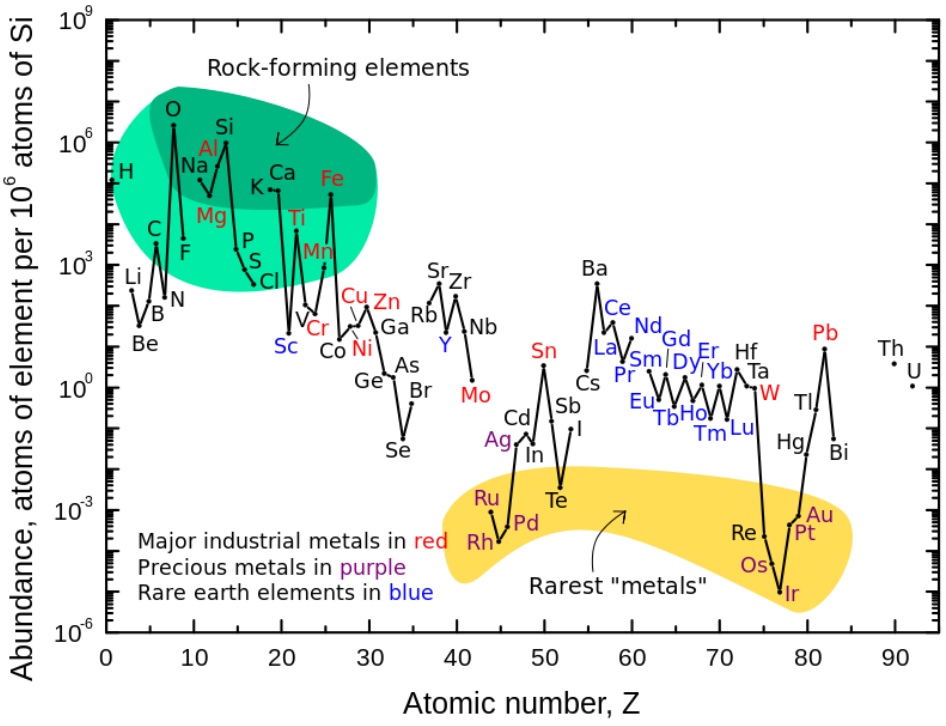

Figure 3-2: Abundance of the chemical elements in Earth's upper continental crust as a function of atomic number

2) Iron is present in different biological systems, the so called heme proteins (cytochrome P450, hemoglobin, and myoglobin); hence it shows a low toxicity profile compared to other metals. This aspect is very important for food, pharmaceutical and cosmetic industry.

3) historically it was often used as a Lewis acid, in particular Fe(III) [165] to catalyze Diels-Alder reaction and Friedel-Crafts acylation or alkylation.

4) A plethora of oxidation states (from -2 to +6) are available when iron is used as catalyst, hence it could be successfully used both for reduction and for oxidation processes.

A variety of reactions can be catalyzed using iron: C-C bonds formations, C=X reduction substitution and oxidations.

In this thesis project two different aspects of iron catalysis were studied: the use of a non-innocent ligand for the stabilization of the oxidation state of iron atom and the use of in situ generated iron nanoparticles.

Heterogeneous Iron Catalysts

The use of heterogeneous iron catalytic systems, offers some practical advantages, such as an easy separation between the catalyst and the final product and easy recoverability and re-use of the catalyst. Recently findings in the synthesis and characterization[166] of **low valent** iron nanoparticles led to the development of new catalytic systems. Usually the catalysts based on Fe-NPs, showed a similar activity compared to the homogeneous one and the typical characteristics of the heterogeneous one (easier recovery compared to homogeneous ones, and easier purification). There are four different methods for the generation of iron nanoparticles (Scheme 3-1): the thermal decomposition of iron carbonyls compounds[167], the reduction of iron oxides[168], and the reduction of iron salts using wet reducing agents.

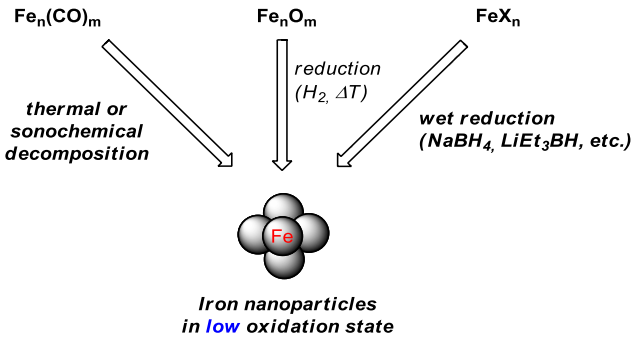

Scheme 3-1 – Classical approaches for iron-nanoparticles generation.

Low valent FeNPs were successfully employed in olefin hydrogenations; in 2009 de Vries[169] and the R&D department of DSM reported the reduction of alkyne and alkenes. The treatment of $FeCl_3$ with a Grignard reagent led to the *in-situ* generation of iron NPs active in the hydrogenation of C-C double and triple bonds. The hydrogenation (Scheme 3-2) of Norbornene, 1-Hexene, *cis*-2-Henzene and 1-Hexyne proceeded with complete conversion in very mild conditions (25 °C, 20 bars of H_2); for the complete hydrogenation of trans-stilbene and cyclohexene it was necessary to run the reduction at 100°C.

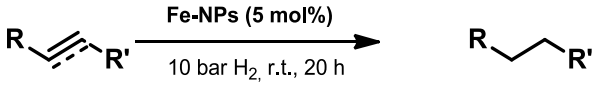

Scheme 3-2: hydrogenations of alkene and alkynes with in situ generated iron nanoparticles

This type of catalyst was also studied in detailed by the group of professor Jacobi[170] in 2012, with demonstrate the composition of the Fe(0) NPs, using Xanes (X-ray absorption near edge) and EXAFS (extended X-ray absorption fine structure) spectroscopy. The major drawback of these two examples was the poor funcitonal group tollerance of the catalyst and the degradation of the

nanoparticles during the work up procedures. In oxigen and acqueous media large nanoparticles are formed, and they are not active in catalysis. The possibility of recovery the NPs under anaerobic environment was studied, however the fine disperison of the particles in solution make the magnetic recovery very difficult. The problem of the NPs recovery was tackled by the group of Breit and Mülhaupt[171], they reported the formation of NPs after the sonication of $Fe(CO)_5$ in the presence of chemically derived graphene sheets. The NPs were active in catalysis in the hydrogenation of terminal olefines; notably the addition of Grignard reagents increased the catalysts activity (probably reducing residual oxidation site present on the graphene), low converison were observed using internal alkyne and substitued alkene. However, the easy magnetic recovery of the catalyst and the possiblity of recycle of the NPs was a big achievement in these field. (Scheme 3-3)

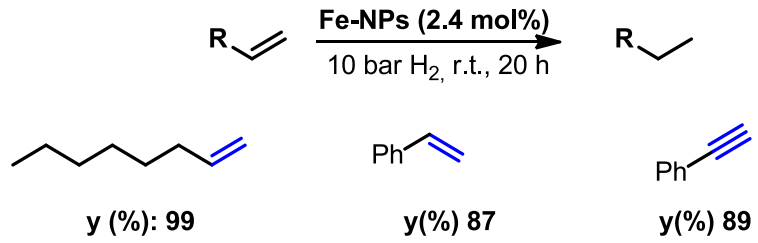

Scheme 3-3:

Iron NPs were also sucesfully used in ketones transfert hydrogenations.The stereoselective ketones reduction was reported by Morris[172] and co workers in 2012, using a imino phosphine ligand, ee up to 64% were achived. (Scheme 3-4)

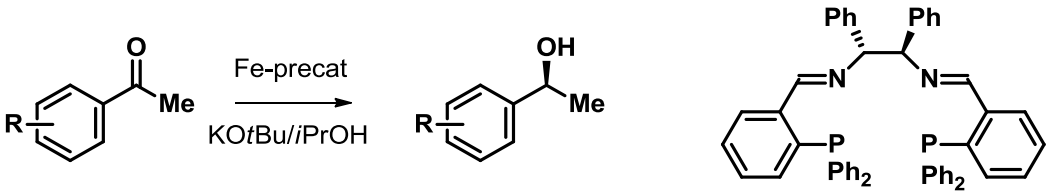

Scheme 3-4: stereoselective ketones reduction using in situ generated iron NPs.

The reduction of nitro group using the NPs and water was succesfully reported by Ranu and co-workers[173] in 2012. High yields were obtained with different aromatic groups; also nitro group in heterocyclic compounds were reduced to the corresponding amine with high yields. Different substiteunts were tolerated, such as aldehydes, acid, cyano, Benzyloxy ether, alogens, vinyl and allyl residue. (Scheme 3-5)

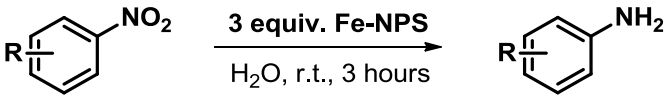

Scheme 3-5: -NO_2 reduction using stoichiometic amount of iron NPs.

Low valent FeNPs were also used in coupling reactions, as reported by Bedford[174]. Fe(III) is in situ reduced using an excess of Grignard reagent, that is also reacting in the followed FeNPs catalyzed cross coupling. Both the presence of PEG and ethylene Glycol are necessary for the stabilization of the nanoparticles, and in particular PEG 14000 showed the best performance.

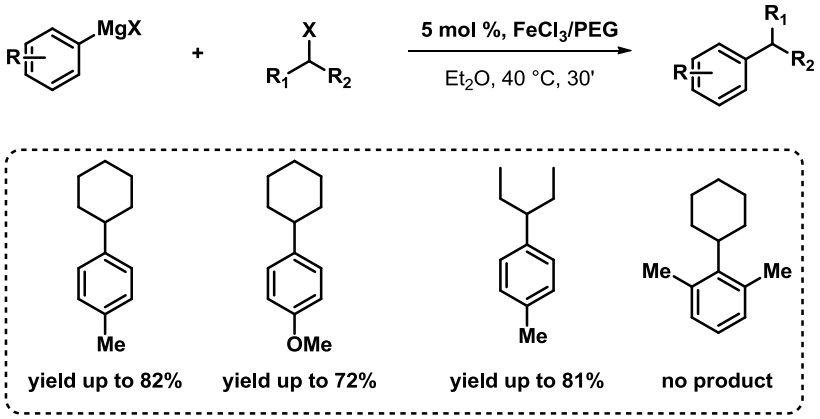

Scheme 3-6

Regarding the generation of Iron NPs is necessary to report the possibility of using $Fe(hmds)_2$ as precursor. In 2008 Lacroix and co-workers[175] reported the treatment of the Fe(II) salt under reducing conditions (H_2) to obtain the NPs, probably stabilized by the hexamethyldisilazane. Chaudret and his group reported in 2011[176] the use of a sacrificial amine for trigging the $Fe(hmds)_2$ NPs formation. Hexadecylamine at high temperatures acts as a surfactant and a reducing agent, generating Fe(0) species and the corresponding imine. The generation of NPs, starting from $Fe(hmds)_2$ could be also possible in milder conditions as reported by Clemete et all[177] using 2 bar of H_2 and room temperature in 24 hours.

Homogeneous Iron Catalysts

The redox properties of Iron, compared to noble metals, are very different. Pd, Pt, Rh, Ru, Ir are able to perform two-electron oxidative and reductive processes, largely applied in organometallic chemistry. However, in the case of Fe, single electron transfer (SET) events, are often present and could interfere with the catalytic cycle. This is the main reason why iron based catalytic transformations were developed with a delay compared to noble metals.

In order to stabilize Fe oxidation state, the use of a non-innocent ligand able to cooperate with Iron redox process was explored. A huge number of review have been published recently on this topic in the last three years[178].

The role of these ligands in catalysis could be classified in two different pathways: in the first case, the ligand plays a spectator role, and does not interfere directly with the substrate, it is used as electron reservoir, and the catalytic activity is concentrated on the metal. In the second case, the ligands actively participate in the catalytic cycle and is helping the bonds breaking and formation. (Scheme 3-7)

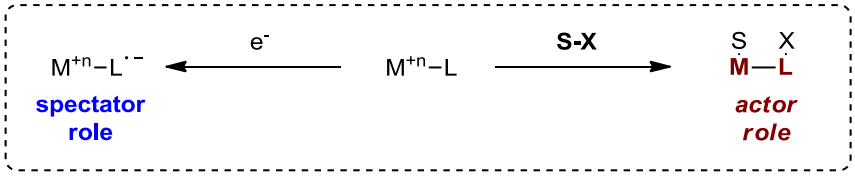

Scheme 3-7

To the first class belongs the ligands based on bis(imino)pyridine (PDI); these ligands are easily prepared by the condensation of 2,6-pyridine carboxy aldehyde with different amines. The first synthesis was reported in 1974 by [179] Merrel and co-workers. (Scheme 3-8)

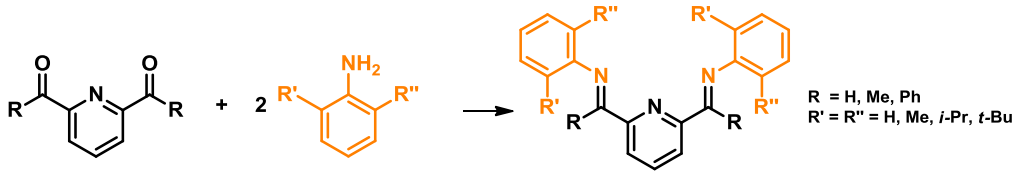

Scheme 3-8

Recently these PDI ligands used in combination with Fe were applied in pletora of possilbe reactions, such as polymerizations, hydroboration and hydrosililations. [180] This type of ligands were also succesfully used in hydrogenations of alkenes by Chirick *et al.*[181], they reported the hydrogenations of mono and di substituted alkenes, in few minutes with high yield and selectivity.

The active catalytic species is generated in situ after the reduction of the (PDI)$FeBr_2$, performed by two equivalents of $NaBH(Et)_3$. Scheme 3-9

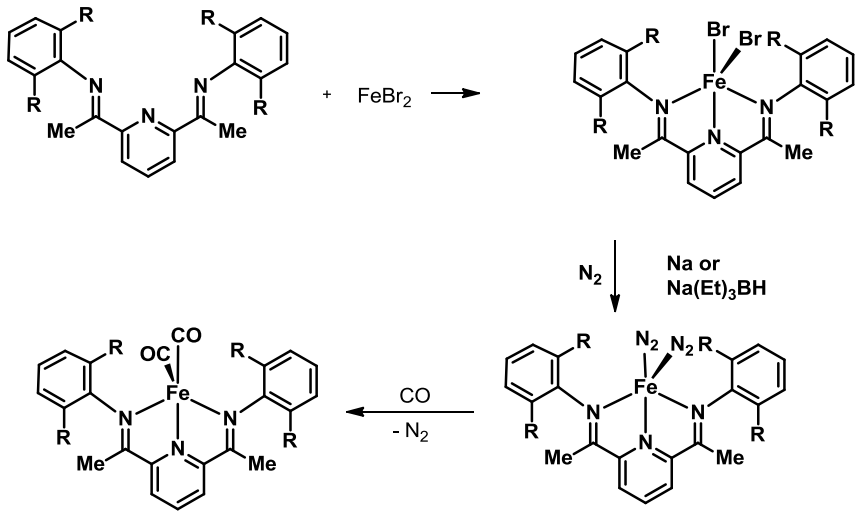

Scheme 3-9 - Synthesis of active (PDI)Fe species according to Chirik *et al.*

The proposed catalytic cycle is illustrated in scheme 3-10; please note the redox activiy of the ligand.

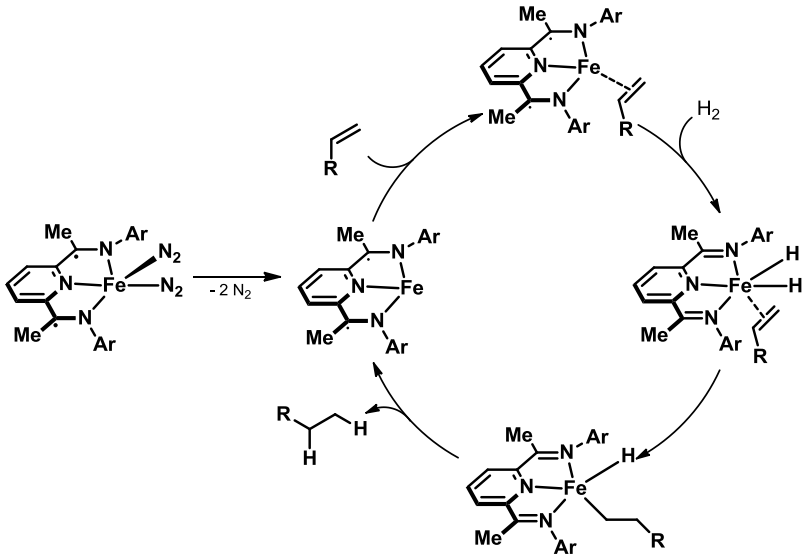

Scheme 3-10 - Catalytic cycle proposed by Chirik *et al.*

Also other redox active ligands have been reported in the literature[182], however the attention will be focused on the one used in the C=O and C=N double bonds reductions.

In 2011 Milstein[183] and co-workers reported one of the first examples of pincer ligand (PNP) in this field. The structure was composed by a pyridine ring with two additional phosphine ligands able to chelate a central metal. (Scheme 3-11) These complexes were used in the reduction of CO_2 and ketones in the presence of H_2 as reducing agent. These catakysts showed very high activity also with low catalyst loading, table 3-1.

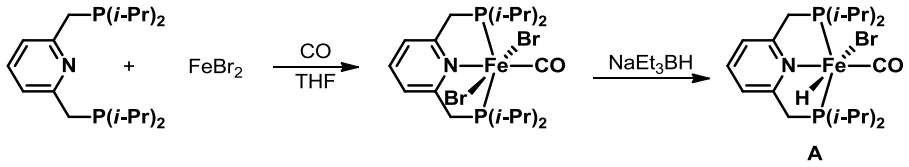

Scheme 3-11 - Synthesis of (PNP)-Fe complexes according to Milstein *et al.*

Table 3-1 Hydrogenation of substituted ketones with A.

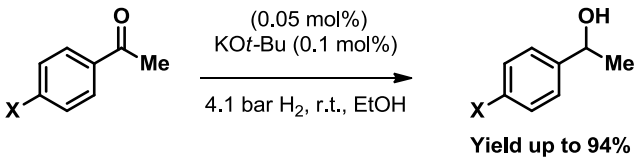

Entry	R	Yield (%)
1	H	94
2	Cl	86
3	Br	78
4	Me	72

The proposed catalytic cycle is reported in scheme 3-12, also in this case the ligand is actively participating into the ketones reductions.

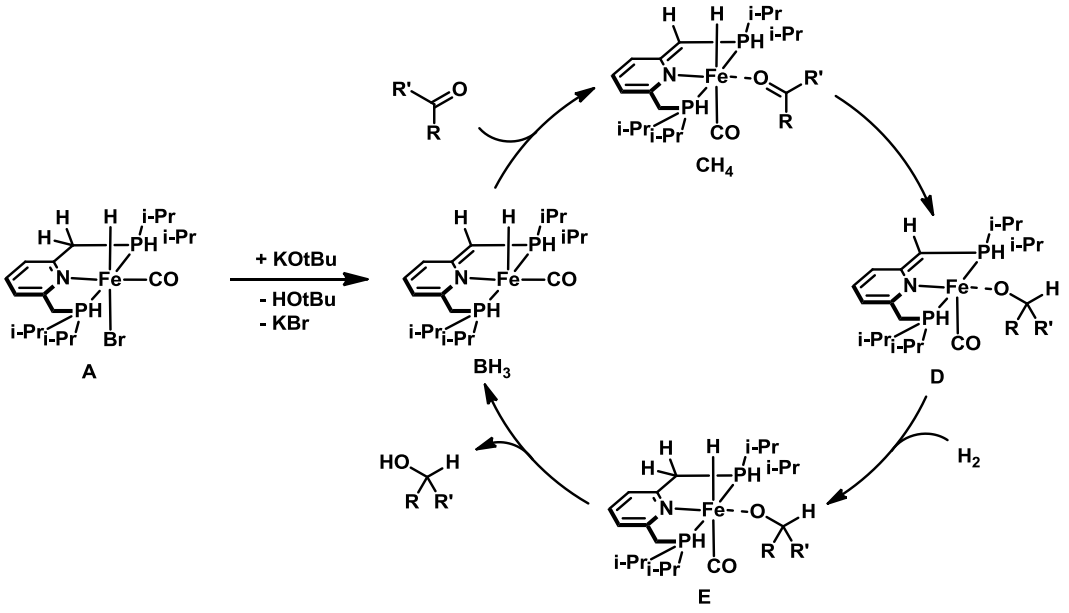

Scheme 3-12- Catalytic cycle for hydrogenation of ketone proposed by Milstein *et al.*

Also, other research group were investigating the same idea. Independently Beller[184], Guan[185] and Jones[186] reported the use of Fe-bis(phosphino)amine complexes (Scheme 1-12) as catalysts for the reduction/oxidation of different functional groups, such as esters, alcohols, and *N*-heterocycles.

In these cases, the authors reported the active participation of the ligand into the redox activity of the catalyst, in particular the ligand was able to abstract a proton from the substrate.

In 2016 the nitrile reduction to obtain primary amine was reported by Lange *et al.*[187]; in the catalyst was prepared by changing the residue on the phosphine ligand. In this case high hydrogen pressure was needed for the reduction. However, excellent yields were obtained, and different functional group were tolerated.

The group of professor Morris[188] had intensively studied the PNP residue and its use in catalysis. Also, chiral ligands were developed and one of the first stereoselective reduction of ketones and imines was reported. Extremely high TOF, up to 25000h^{-1} and enantioselectivity were reported. DFT[189[calculation and Kinetic[190] studies suggested an outer-sphere mechanism, the definite catalytic cycle is reported in scheme 3-13

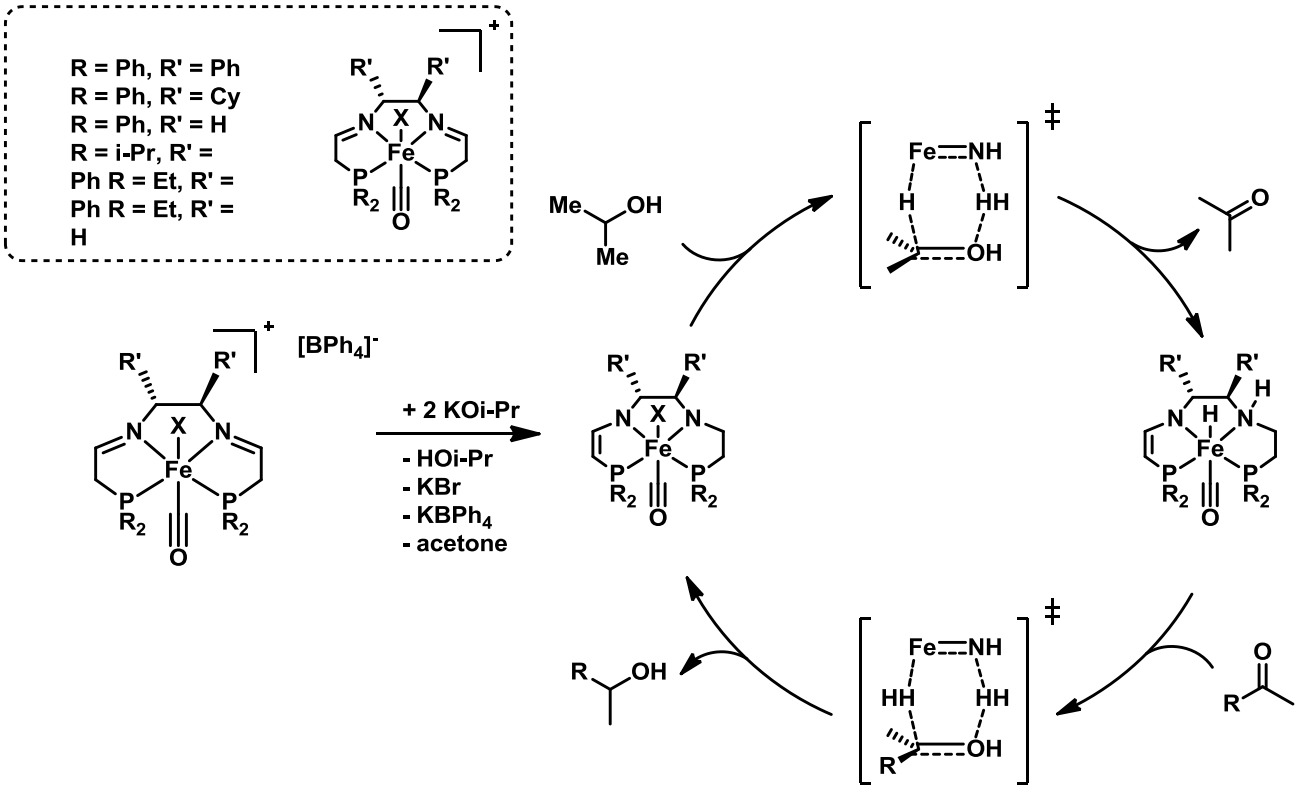

Scheme 3-13 – Catalytic cycle proposed by Morris et al.

Another important class of non-innocent ligands as emerged in the last decades: Iron cyclopentadienone complexes have recently received particular attention in organic chemistry. Thanks to their easy synthesis from simple and cheap materials, air-water stability, and, most importantly, for their unique catalytic features arising from the presence of a non-innocent ligand, triggering powerful redox properties.[191] The first report of iron cyclopentadienone complexes was published by Reppe and Vetter in 1953[192]. The authors described the complexation of alkynes with different iron sources (Fe_2CO_9 and $FeCO_5$). Unfortunately, no structure elucidation was reported, and no crystal structures of the complex were available. Six years later in the 1959 Schrauzer[193]

successfully described the structure of those complexes reporting extensive analytical data and crystal structures. (Scheme 3-14)

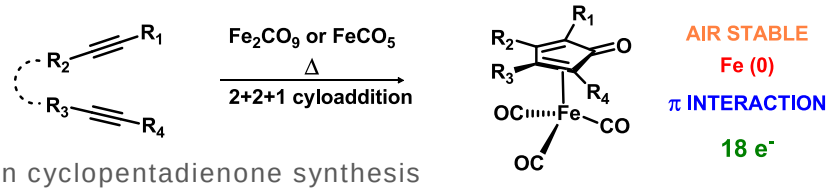

Scheme 3-14 iron cyclopentadienone synthesis

The isolated iron (0) complex was a cyclopentadienone ring bound by π interaction to the metal. The reactivity of the complex is strongly dependent on the ligand; so is possible to tune electronic and steric properties of iron cyclopentadienone complexes by varying the substituents on the alkynes. In these years a lot of variations on the structure of the cyclopentadienone were studied and a large numbers of complexes were prepared.[194] However, the initial use of those complexes was not as catalysts, but they were used for the synthesis of cyclopentadienone obtained by simple oxidative decoordination of the iron, thanks to trimethylamine N-oxide (Me_3NO) (Scheme 3-15).

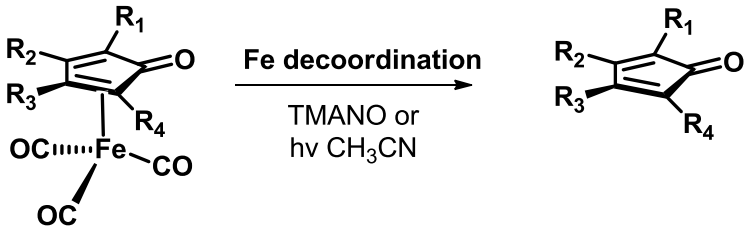

Scheme 3-15: complexes activation

The structure of those systems is very similar to the Shvo[195] complex but their reactivity was reported for the first time only in 1999 by Knölker and co-workers[196]. The authors described the possibility of a selective de-coordination of a CO from the iron center with a Hieber-type reaction. After protonation Knölker obtained a mixture of the hydride form and of the starting complex. The X-ray structure of the unstable hydride form was obtained (Scheme 3-16). In this case the Fe atom changes its formal oxidation state from (0) to (2) and the ligand, existing in its enolic form, leads to a cyclopentadienyl like structure. These results were confirmed by a computational study performed by Chen[197].

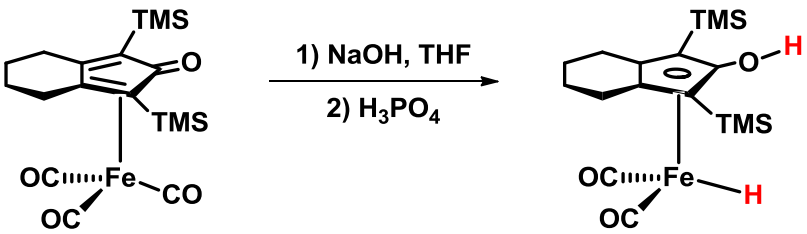

Scheme 3-16: first hydride species observed

At this stage, all the knowledge was set for the application of these complexes in catalytic redox transformations, but eight years were necessary before their successful utilization in catalytic reactions[198]. In 2007[199] the group of Casey at the University of Wisconsin reported the use of the complex in a homogenous reduction of carbonyl compounds and imines using isopropanol as a reducing agent (Scheme 3-17).

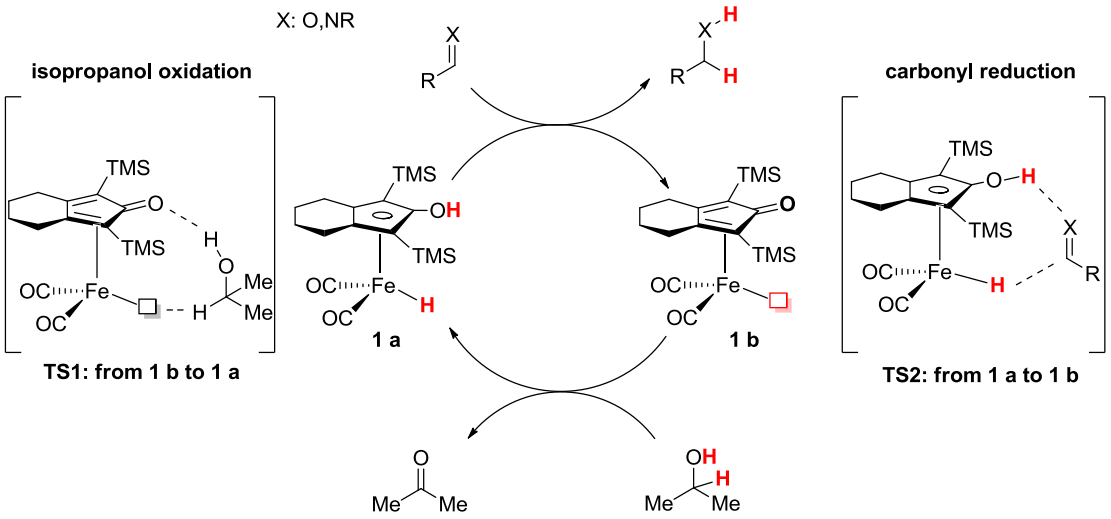

Scheme 3-17

During the isopropanol oxidation (**TS1**) the oxygen of the ketone present on the ligand forms a hydrogen bond that is crucial for the proton extraction, leading to the formation of acetone and hydride specie **1a**. During the reduction (**TS2**) the carbonyl oxygen first coordinates the residual OH acid presents on the ligand, and then the hydride attacks leads to the reduced product and to catalyst **1b**. Definitely this type of complexes works as bifunctional hydrogenation catalysts, with an acid proton on the ligand and with a hydride on the iron.
After the reduction reported by Casey, a huge number of different examples appeared in the literature. Molecular hydrogen was also used as reducing agent in reductive amination[200].

The pre-catalyst, is an 18 electrons air stable complex; for the successful synthetic utilization of its redox properties, the selective mono-decoordination of one of the CO ligand from the Knölker pre-catalyst is a prerequisite. Oxidative decomplexation is possible thanks to Me_3NO. Me_3NO reacts with one CO ligand on the metal center revealing the vacant site and generating a 16 electron oxidizing species (Figure 5) as well as a stoichiometric amount of CO_2 and trimethylamine as side products. The Fe (0) 16 electron complex is an oxidizing agent and is able to activate hydrogen through heterolytic splitting, leading to the hydride 18 electron complex, that acts as reducing agent. (Scheme 3-18) These two iron complexes are in an equilibrium state which depends on the reaction conditions. Theoretically direct displacement of a CO by H_2 followed by an oxidative

addition of the hydrogen to the metal is possible, but this pathway of activation has never been used.

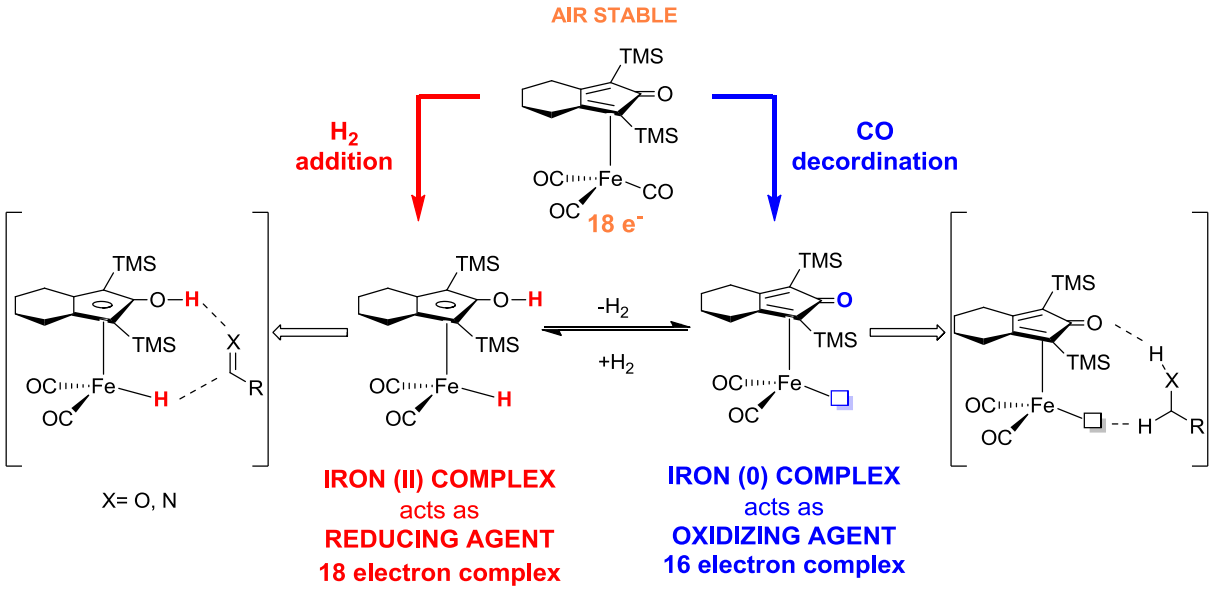

Scheme 3-18: activation of the catalyst

In terms of reactivity profile, the reduction complex gives excellent selectivity for the hydrogenation of polar double bonds, such as C=O and C=N groups. Different carbonyl compounds and imines were reduced under mild conditions, and examples of reductive amination were also reported. A number of possible structural variations on the ligand are possible; these include, the insertion in the backbone of an electron rich heteroatom (N, O Figure 6 a) to improve the reduction ability of the catalyst[201]. Interesting examples were reported using a water-soluble catalyst in order to run the reduction in aqueous media[202] (Figure 3-3 b, c). The reduction of ketones and imines proceeded with good yields using catalyst b, while lower yields were achieved using catalyst c. The author proposed that in the case of c the ammonium is too close to the reaction site in order to that catalyst c is more electron poor than catalyst b and this reduces the hydride character of the proton on the iron atom.

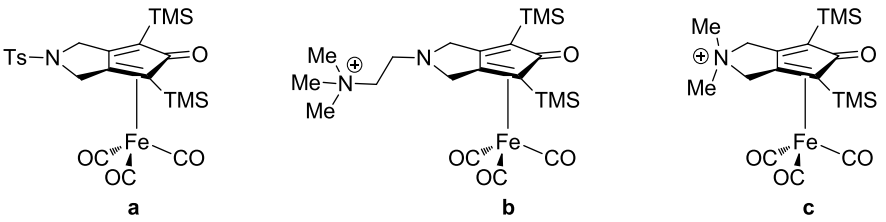

Figure 3-3

Recently the group of Renaud reported the use of a new iron based catalyst for the reduction of imines[203]. In particular the authors found that a more electron rich ring as ligand lead to a better chemical activity, compared to the “classical version” of the Knölker complex, also less hindered substituent of the cyclopentadienone ring increase the chemical activity. (Figure 3-4).

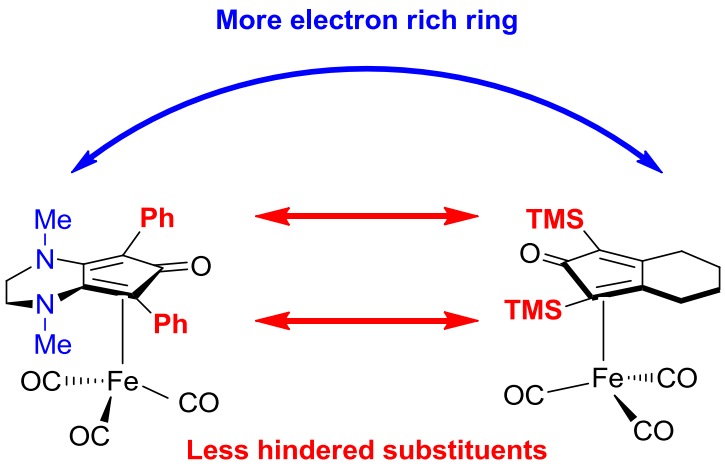
More electron rich ring
Me
Ph
N
O
N
Ph
Me
OC
Fe
CO
OC
TMS
O
TMS
OC
Fe
CO
CO
Less hindered substituents

Figure 3-4

Iron catalyzed diasteroselective imines reductions

In the last years a huge number of synthetic methodologies based on iron catalysis were reported by different research groups[204]. The reasons of this interest in the iron catalysis is due to different factors. Iron is the most abundant element in the heart crust, is cheap and is widespread in a lot of different countries, hence no geo-political problems could afflict its extraction. Iron shows a low toxicity compared to other metals[205]; in fact, it is found in different biological systems, such as cytochrome p450 and hemoglobin. The low toxicity of the metal is very attractive for the pharmaceutical industry, the food industry and the cosmetic one. Since from the raising of the organic chemistry iron played an important role especially as Lewis acid (eg Diels-Alder reaction and Friedel-Crafts acylation and alkylation). More recently iron was used as catalyst taking advantages of its possible oxidations states (from -2 to +5 and in some cases +6). A huge number of different transformations were possible, such as substitution reaction, C-C bonds formations, C=O reductions[206].

Nevertheless, few examples of stereoselective imine reductions were reported in the literature. A pioneering work was reported by Beller and co-workes in 2010, using iron cyclopentadienone catalysts in combination with phosphoric acids, to achieve imine reductions in very high yield and stereoselectivity[207]. More recently Morris et al reported the use of an Iron complex for the very efficient reductions of ketones and also the possibility of reducing an imine, with almost complete stereoselection[208]. Recently the group of Renaud report the use of a new iron based catalyst for the reduction of imines[203], that showed an enhanced reactivity compared to the first cyclopentadienone complexes previously reported in literature. We decided to explore the reduction of chiral imines using different iron complexes (Figure 3-5).

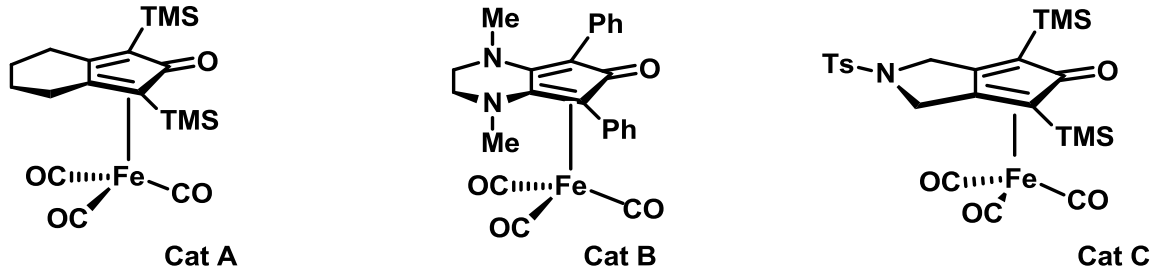

Figure 3-5: Pre-catalysts used

Since the excellent results achieved using the phenyl ethyl amine as chiral auxiliary in combination with $HSiCl_3$, we decided to use again the same chiral auxiliary. (Table 3-2)

Table 3-2: optimization of reaction conditions

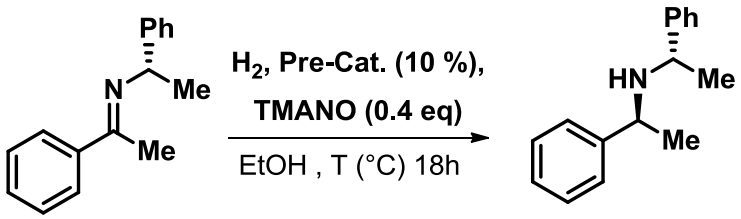

Entry[a]	Pre-Cat.	P (bar) [a]	T (°C)	Conv. (%)[b]	*dr* [b]
1	A	30	70	41	97:3
2	A	30	100	<5	6:4
3	A	80	25	-	-
4	B	30	40	26	93:7
5	B	30	50	41 [c]	92:8
6	B	30	70	96[c]	92:8
7	B	80	25	-	-
8	C	30	70	30	98:2
9	C	30	100	< 5	6:4
10	C	80	25	-	-
11	$Fe(CO)_9$	EtOH	70	14	6:4

Reductions were run in a Parr apparatus; [a] reactions were performed on 0.2 mmol of imines in 2 mL of degassed ethanol; [b] conversion and dr were evaluated on crude mixture; [c] isolated yield.

N-(1-(*S*)-phenylethyl)-ethan-1-(phenyl)-1-imine was selected as a model substrate in order to optimize the reaction conditions and to screen the four different pre-catalysts (Table 3-2). Complex A showed a modest activity (entry 1) giving the desired amine in only 41% yield but with high diastereoselection 97:3; unfortunately rising up the temperature to 100 °C (entry 2) did not improve the conversion and the stereoselectivity drops down. The reduction using pre-catalyst B at 70 °C proceed with excellent yield up to 96 % and with interesting stereoselection (entry 6), in order to increase the stereoselection the reaction was run at lower temperature (entry 4, 5) however no significant improvements were achieved. Pre-catalyst C lead to high stereoselection but low yields working at 70 °C, in order to improve the conversion, we run the reaction at 100 °C (entry 9) no stereoselection was observed. At low temperature and high hydrogen pressure (entries 3, 7 and 10) the reduction did not procced and all the starting imines were recovered unreacted. We noticed that working at high temperature lead to the de-coordination of iron from the cyclopentadienone ligand with the generation of iron nanoparticles. Iron nanoparticles could be active in catalysis, but with no control over the stereochemical outcome of the reaction, to prove this hypothesis, the reaction was run using $Fe_2(CO)_9$ (entry 9), a thermally instable source of iron and we observed a similar conversion and stereoselection to the high temperature experiments with iron de-coordination.

Table 3-3: acid influence

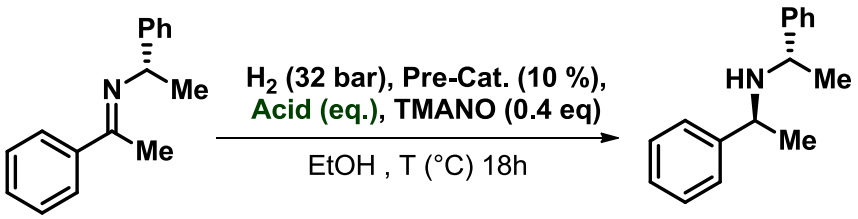

Entry	Pre-cat	Acid (eq) [a]	T (°C)	Conv. (%)[b]	*dr*
1	A	1	50	16	95:5
2	A	0.5	50	19	92:8
3	A	1	70	20	92:8
4	B	1	50	-	nd
5	B	0.5	50	-	nd
6	B	1	70	-	nd

Reductions were run in a Parr apparatus; [a] reactions were performed on 0.2 mmol of imines in 2 mL of degassed ethanol, using salicylic acid as additive; b conversion and dr were evaluated on crude mixture.

In order to pre-form the more electrophilic iminium ion the use of an acid additive was tested. However, the reduction performed using pre-catalyst A showed similar chemical activity but lower stereoselectivity (entries 1,2 and 3) compared to the one without the acid additive. Using complex B no conversion was observed, probably due to the interaction of the acid with the nitrogen moiety on the catalyst.

Table 3-4: reaction scope

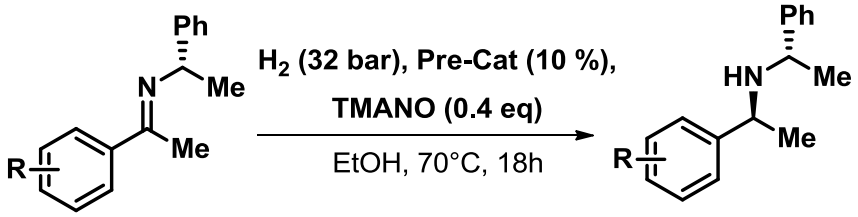

Entry[a]	Product	R:	Pre-cat.	Conv. (%) [b]	*dr*[b]
1	3-2	4 OMe	B	60[c]	92:8
2	3-3	3 OBn	B	50[c]	93:7/ <98:2[d]
3	3-4	3OMe	B	40	92:8
3	3-5	4 Cl	A	16	98:2
4	3-5	4 Cl	B	46	98:2
5	3-5	4Cl	C	10	98:2
6	3-6	4 Me	A	20	95:5
7	3-6	4 Me	B	65[b]	92:8
8	3-6	4 Me	C	36	87:13
9	3-7	4 NO_2	A	5	67:33

10	3-7	4 NO_2	B	26	72:28
11	3-7	4 NO_2	C	6	65:35

Reductions were run in a Parr apparatus; [a] reactions were performed on 0.2 mmol of imines in 2 mL of degassed ethanol; b conversion and dr were evaluated on crude mixture; c isolated yield; d *d.r.* after purifications

With the optimized conditions in our hands(70°C 30 bar of H_2), the scope of the reaction was explored. Different imines bearing electron-withdrawing and electron-donating substituted on the aromatic ring were prepared and then hydrogenated. Catalyst B shown the best activity as already observed. Good yields, up to 65%, were achieved when electron rich imines were reduced (entries 1 and 7). However, when electron poor substrates were hydrogenated lower yields were observed, only up to 46% with the 4 Chlorine substituted one, while in the case of 4 nitro and 4 trifluoromethyl substitution no amine was observed.

High level of diasteroselectivity were observed, up to 98:2 (entries 3,4 and 5).

The unsatisfactory results obtained using electron poor imines, were also reported by Feringa [209] in 2016. To fully understand the difference in reactivity observed with this class of imines, also preliminary theoretical calculations were performed by Dr. Sergio Rossi. Figure 3-6.

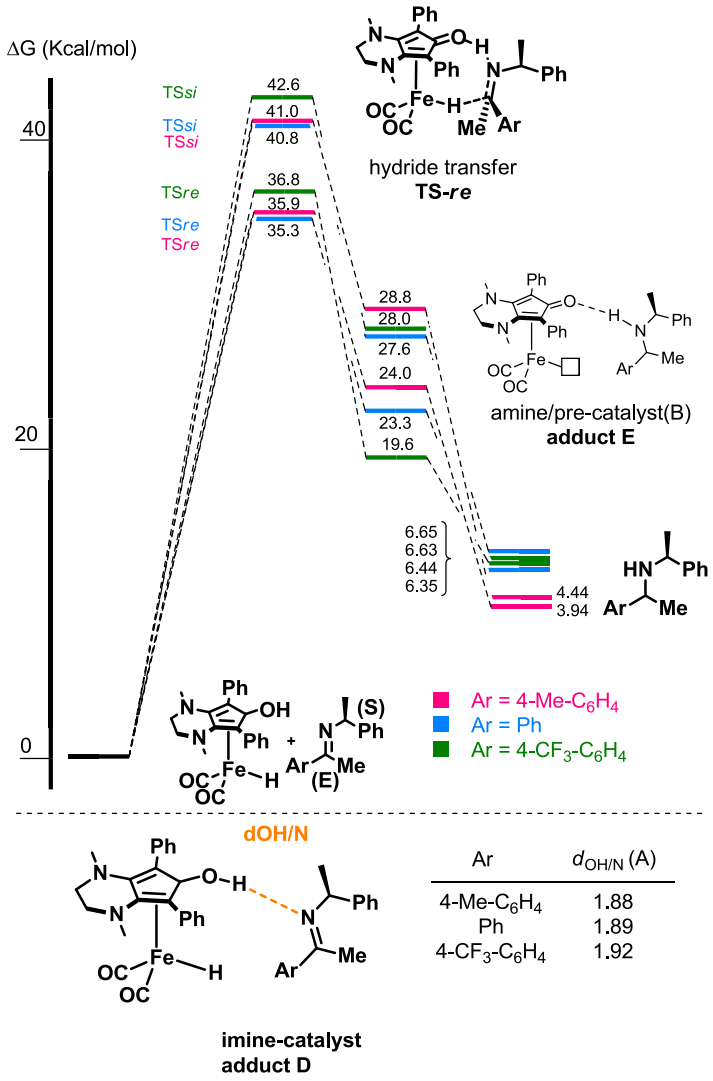

Figure 3-6

The reductions of (*E*) *N*-(1-(*S*)-phenyl)ethyl imines derived from differently substituted acetophenones promoted by precatalyst **B** were studied, and the lowest energy transition states (TSs) leading to the formation of (1R,1'S) and (1S,1'S) amines, respectively, were located. After preliminary Monte Carlo conformational analysis, the lowest energy structures leading to the formation of (1R,1'S) and (1S,1'S) diastereoisomers, were optimized to the relative TSs by DFT calculations performed with GAUSSIAN 09 program, using the hybrid B3LYP functional for all atoms except for iron.¥

A superimposed cross section of the reaction profiles for the reduction of (*E*)-imines derived from acetophenone (**1a**), 4'-methyl acetophenone (**1f**) and 4'-(trifluoromethyl) acetophenone (**1g**) is reported in Figure 3-6.

Our calculation indicates that at the reaction outset, all the imines were coordinated by the hydrogenated form of **B** to give the corresponding adduct **D**. As expected, this substrate/catalyst

coordination is energy demanding and the hydrogen bond is significantly bent out of a linear alignment.

The hydrogenation of imines have been described to proceed according to two different pathways: a synchronous process, where both the hydrogen proton and the hydride are transferred simultaneously (as proposed by Renaud); or a two steps process (formally the protonation of imine nitrogen atom followed by the transfer of the hydride) as reported by Berkessel for *N*-*t*-butyl substituted aromatic keto-imines.

Analysis of the diastereoisomeric TS's involving the *Re* and *Si* faces (**TS*Re*** and **TS*Si***) revealed that the transfer of the hydride from the iron atom to the carbon atom happens when the proton transfer from the hydroxy group of hydrogenated catalyst **B** to the imine nitrogen has already almost completely occurred in a mechanism that we can define concerted but asynchronous. Indeed, a clearly defined two-steps mechanism could be considered as an exception, as already remarked. Finally, after the transfer of both hydrogen atoms to the imine, the resulting adduct **E** is formed and dissociates to afford the free amine and pre-catalyst **B**, which will re-enter the catalytic cycle once that it has taken up a new molecule of hydrogen.

Looking at the energy values in Figure 3-5, the TSs at lower energy are those responsible of the hydride transfer onto the *Re*-face of the (1S')-imines, and lead to the favored (1S,1'S)-isomers, in qualitative agreement with the experimental data. Moreover, electron-rich imines, that are reduced in higher yields, have indeed TSs of lower energy than those of electron poor counterparts (4-CH_3Ph ~ Ph < 4-CF_3Ph). Although the calculations well rationalize the diasteroselectivity and the order of reactivity of the imines, the poor or inexistent reactivity of electron poor imines is not easily accounted for. A possible explanation could be that *N*-protonation to generate a more reactive iminium ion (see adduct **D**), is more facilitated with electron rich imines, due to their nitrogen higher basicity. The observation that the OH-N distance in adduct **D** for the CF_3-substituted imine is longer than in the Me-substituted substrate can tentatively lend support to this interpretation (Figure 3-5).

Scheme3-19 :Chiral auxiliary screening

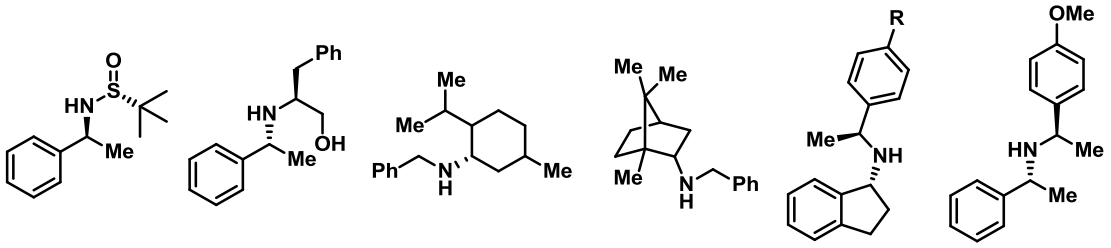

To extend the methodology to other chiral imines different scaffolds were used. (scheme 2) A chiral sulfoxide derivatives showed no reactivity and the starting imine was recovered unreacted. It was not possible to use chiral amino alcohols, also the use of Menthol and camphor was not feasible. Interesting, using the (*R*)-1-(4-Methoxyphenyl)ethylamine as chiral residue, that could be removed without the use of precious transition metals (e.g. the use of phenylethyl amine led to the necessity of using a Pd catalyzed removal of the chiral auxiliary to obtain the primary amine).

The removal of the chiral auxiliary was then performed, first the protection of the secondary amine as amide was performed using AcCl in the presence of triethylamine, the protection led to a mixture of protected and unprotected amine. The crude mixture was then treated with DDQ in the presence of water and DCE at 80 °C; the final product was then obtained, as amide in 60% yield after chromatographic purification. The unprotected secondary amine was recovered, and the 4-methoxy acetophenone derived from the chiral auxiliary was observed(scheme 3-20).

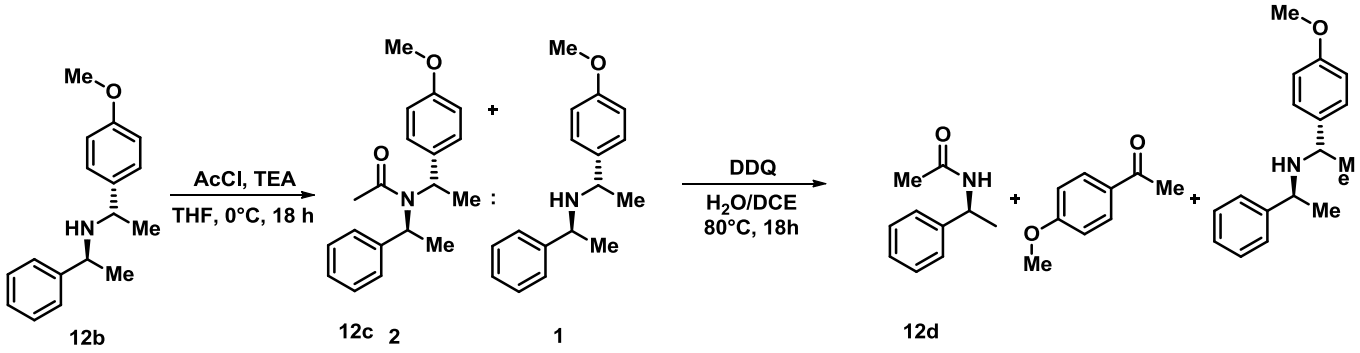

Scheme 3-20: metal free deprotection

We also applied this methodology to the preparation of different compounds direct precursors of APIs. Amine (x) a direct precursor of Rasagiline was obtained with 70 % conversion and high diasteroisomeric ratio (95:5), the pure amine was isolated in 60 % yield as a single diasteroisomer. Reducing the imine derived from the condensation of acetophenone and (*R*)-1-(4-Methoxyphenyl)ethylamine lead to a conversion up to 70 % with a diasteroisomeric ratio of 96:4.

Scheme 3-21: API's chiral amine precursor

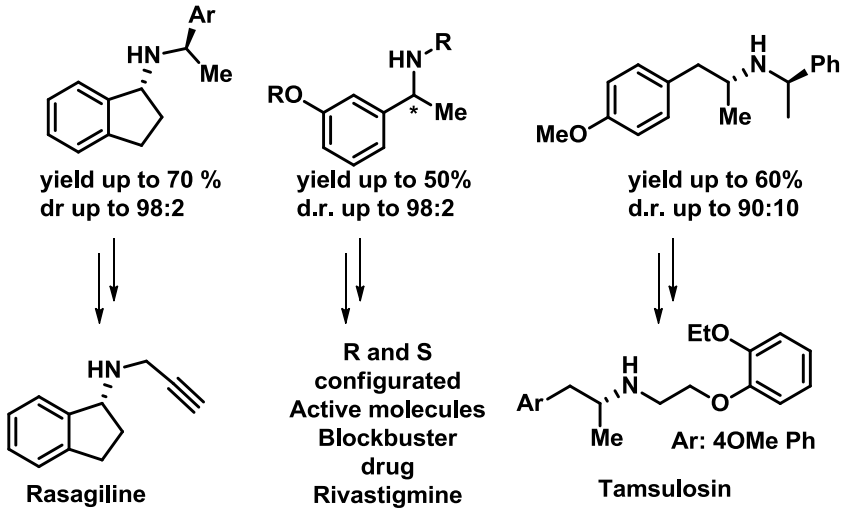

Scheme 3-21

In conclusion, we have reported the first iron-catalyzed diastereoselective reduction of chiral imines; the method leads to the formation of chiral amines, often isolated as enantiomerically pure products. The removal of a chiral auxiliary without the use of precious metal was successfully studied; in addition, the synthesis of advanced intermediates of highly valuable APIs demonstrates the possibility to apply iron catalysis also in the fine chemical industry.

Iron catalyzed alkyne trimerizations

Metal catalyzed 2+2+2 cycloadditions of alkynes are one of the most useful synthetic tool for the preparation of substituted aromatic rings[13210]. Different transition metals could be used to catalyze alkynes trimerization (e.g. Ru[14211], Rh[15212], Co[16213], Ir[17214], Ni[18215], Pd[19216], Ti[20217], Mn[21218] and Fe). The development of such synthetic methodology using earth abundant and non-toxic transition metals (Fe[204] and Mn) is a crucial goal in academic field. Different examples of iron catalyzed trimerization of alkynes have already been reported, however these systems are usually characterized by the presence of a stoichiometric reducing agent for the initial reduction of Fe(II) to Fe(0) or/and harsh reaction conditions (high temperature, long reaction time, high catalyst loading). The first iron (carbonyl) catalyst active in alkynes trimerization was reported by Hübel in 1960[219]; the reaction led to the unsymmetrical substituted benzene ring at very high temperature. Okamoto and co-workers[220] developed a system, for the intramolecular 2+2+2 cyclization of alkynes using a catalytic amount of Fe(II) and Fe(III) chloride, NHC as ligand, in the presence of zinc powder as reducing agent. Fürstner and co-workers[221] used a well defined Fe(I) ferrate complex for the alkyne trimerization, using high temperature. Iron bis(imino) pyridine complex were successfully applied in combination with zinc dust and ZnI_2 for the terminal alkynes trimerization by Liu[222]. Also, indole containing molecules could be prepared using this methodology as reported by Goswami[223]. Recently a well defined heteroleptic two-coordinate iron(I) complex was reported by Tilley and co-workers[224] and tested in a model reaction for alkynes trimerization. Moreover, heterocyclic rings could be successfully created using iron catalysts[29225]. Recently the group of professor Jacobi demonstrated the possibility to use iron(II) bis(1,1,1,3,3,3-hexamethyl-disilazan-2-ide), $Fe(hmds)_2$,[30226] activated by various reductants as very active catalyst for alkenes hydrogenations[31227]. There are several reports on the coordination chemistry of $Fe(hmds)_2$ in the presence of various ligands, but only very few catalytic applications have been demonstrated[228].[20] The reactivity of this complex was further explored, in particular its use in alkynes trimerization reactions. (Figure 3-7)

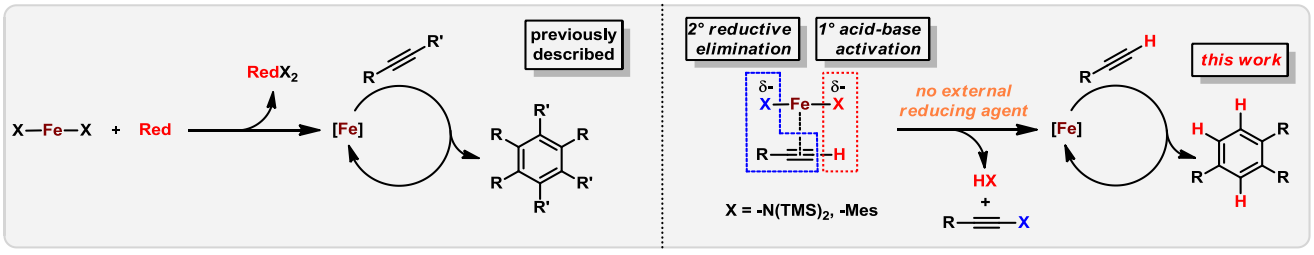

Figure 3-7: Unprecedented, reducing agent free, Iron(II) activation for 2+2+2 alkynes trimerizations

We initially screened different metals generating the active species in situ, starting from the metal chloride and the $LiN(SiMe_3)_2$ and using phenyl acetylene as model substrate. (Table 3-5)

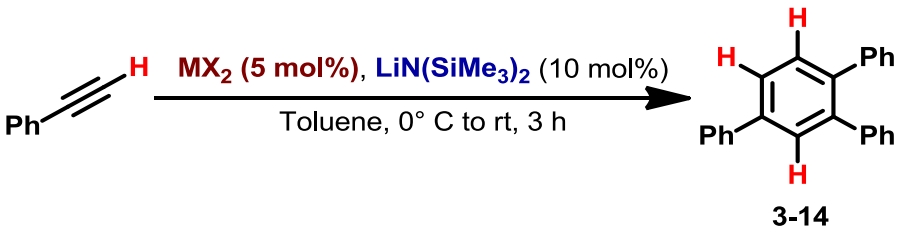

3-14

Table 3-5: metals screening

Entry	MX_2	Yield (%)[a]	Selectivity[b]
1	$PdCl_2$	--	--
2	$MnCl_2$	--	--
3	$CuCl_2$	< 5	--
4	$CoBr_2$	< 5	--
5	$ZnCl_2$	--	--
6	$FeCl_2$	98	> 99:1

Conditions: The metal source and the $LiN(SiMe_3)_2$ were suspended in toluene and stirred overnight before the alkyne addition. 0.48 mmol alkyne, 1 M ir toluene. [a] isolated yield, [b]1,2,4:1,3,5 ratio was evaluated using GC-FID

Pd, Mn, Cu,Co and Zn displayed no reactivity.(entries 1 to 5, table 3-5). Only the iron salt was active for the alkyne 2+2+2 trimerization, leading to the desired product in 98 % of isolated yield and with complete selectivity towards the 1,2,4 isomer. Surprisingly the reaction was run in the absence of reducing agents, suggesting the activation of the catalyst by the alkyne itself. At the best of our knowledge this is the first example of a Fe(II) based system that is directly activated by the alkyne. To further explore the reactivity of the system, different iron salts were tested in the trimerization of phenylacetylene (Table 3-6). The starting material was recovered unreacted when non-basic salts were used (entries 1-5, table 3-6), while using $Fe(hdms)_2$ the reaction proceeds with high yield and complete selectivity (entry 6, table 3-6).

Table 3-6: iron salts screening

Entry	Iron salt	Yield (%)[a]	Selectivity[b]
1	$FeCl_2$	--	--
2	$FeCl_2$*THF	--	--

3	$Fe(OAc)_2$	--	--
4	$Fe(OTf)_2$	--	--
5	$Fe(acac)_2$	--	--
6	$Fe(hmds)_2$	96	> 99:1
7	$Fe_2(mes)_4$	90	94:6

Conditions: 0.48 mmol alkyne,1 M in toluene 5% of catalyst loading. [a] isolated yield, [b]1,2,4:1,3,5 ratio was evaluated using GC-FID

When $Fe_2(mes)_4$ was used as catalyst only 90 % of the desired benzene was recovered, and the selectivity towards the 1,2,4 isomer was reduced. From the collected data the best results in term of selectivity and yield were achieved using $Fe(hmds)_2$ that was selected as catalyst and for further optimizations of the reaction conditions. (Table 3-7)

Table 3-7: optimizations of reaction conditions

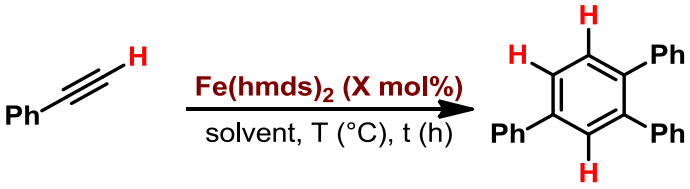

Entry	Cat. (%)	Solvent	T (°C)	t (h)	Yield (%)[a]	Selectivity[b]
1	5	Toluene	0 to rt	3	96	> 99:1
2[c]	5	Toluene	0 to rt	3	97	> 99:1
3	2.5	Toluene	0	1	97	> 99:1
4	2.5	Toluene	rt	1	97	> 99:1
5	2.5	THF	rt	1	97	> 99:1
6	2.5	Et_2O	rt	1	97	> 99:1
7	2.5	Hexane	rt	1	90	95:5
8	2.5	Toluene	rt	1	97	> 99:1
9[d]	1	Toluene	rt	1	98	
10[d]	1	Toluene	rt	0.02	99	
11	0.1	Toluene	rt	1	50	
12	0.1	Toluene	rt	18	55	96:4
13[e]	5	Toluene	rt	3	95	94:6

Conditions: 0.48 mmol alkyne,1 M in toluene; [a] isolated yield, [b]1,2,4:1,3,5 ratio was evaluated using GC-FID, [c]reaction performed using 10 % of DIBAL-H, [d] reaction run on 5 mmol scale; [e] reaction performed using $Fe_2(mes)_4$ as catalyst.

The same high yields and selectivity were observed running the reaction using directly the $Fe(hmds)_2$ or pre-activating the Fe(II) salt with a 10% of reducing agent. (Entries 1 and 2, Table 3-7). Reactions performed at room temperature have shown the same reactivity and selectivity in comparison with the one performed at 0 °C (entry 3, Table 3). The 2+2+2 reaction proceeds with high yields and selectivity in different aprotic solvents, also using 2.5 % of the iron pre-catalyst (entries 4 to 7, Table 3-7). Notably, also reducing the loading of the catalyst to 1 mol% ensured complete conversion (entry 10, Table 3-7) leading to the final aromatic ring with complete selectivity towards the 1,2,4 product. Unfortunately, the reaction run with 0.1 % of catalyst loading lead only to 55 % of yield, with 96:4 as selectivity. With the optimized reaction conditions in our hands the scope of the reaction was further explored.

Table 3-8: scope of the reaction

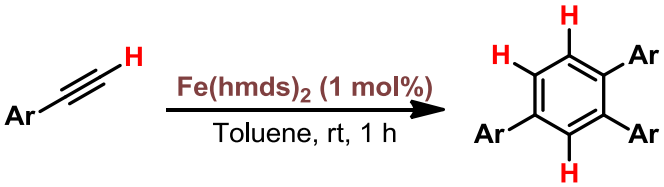

Entry	Product	Ar:	Yield (%)[a]	Selectivity[b]
1	3-15	4-Me	98	> 99:1[b]
2	3-16	2-Me	90	96:4[c]
3	3-17	2,4,6-Me	--	--
4	3-18	2,4,5-Me	98	99:1[b]
5	3-19	4-OPh	94	nd
6	3-20	4-OMe	95	99:1[c]
7	3-21	3-OMe	98	96:4[c]
8	3-22	3-OBn	98	98:2[c]
9	3-23	3,4-OMe	98	98:2[c]
10	3-24	2-Me 4-OMe	95	98:2[c]
11	3-25	6 OMe Nhp	93	98:2[c]
12	3-26	4-NMe_2	95	96:4[c]
13	3-27	4-CF_3	98	99:1[a]
14	3-28	4-F	94	96:4[c]
15	3-29	4-Cl	55	Nd

Conditions: 0.48 mmol alkyne,1 M in toluene; [a] isolated yield, [b]1,2,4:1,3,5 ratio was evaluated using GC-FID, [c]1,2,4:1,3,5 ratio was evaluated using NMR technique.

Different aromatic terminal alkynes were used in the 2+2+2 trimerization, showing the general scope of the reaction. The trimerization is usually complete in 1 hour of reaction time using only 1 % of catalyst loading. The reaction with electron rich rings proceeds with high yields and high

selectivity. (Entries 1-12, table 3-8). Ether and alkyl substituent are compatible with this catalytic system. Tertiary amine substitution is fully compatible with this methodology. The using the bis ortho substitution alkyne led only to traces of product suggesting a strong influence of the steric bulk for this catalyst (entry 3, table 3-8). Halogen-containing substrates are well tolerated, the 4-trifluoro methylated aromatic ring was successfully converted in the desired product with high yield and selectivity. 4-F phenyl acetylene was transformed in the desired product with almost complete yield and selectivity. The presence of the chlorine atom reduced the reactivity of the system leading only to a 55 % of isolated yield. Also, non-aromatic and more electron rich alkynes were tested in the iron catalyzed 2+2+2 cycloadditions with excellent results.

Scheme 3-22: non-aromatic alkynes.

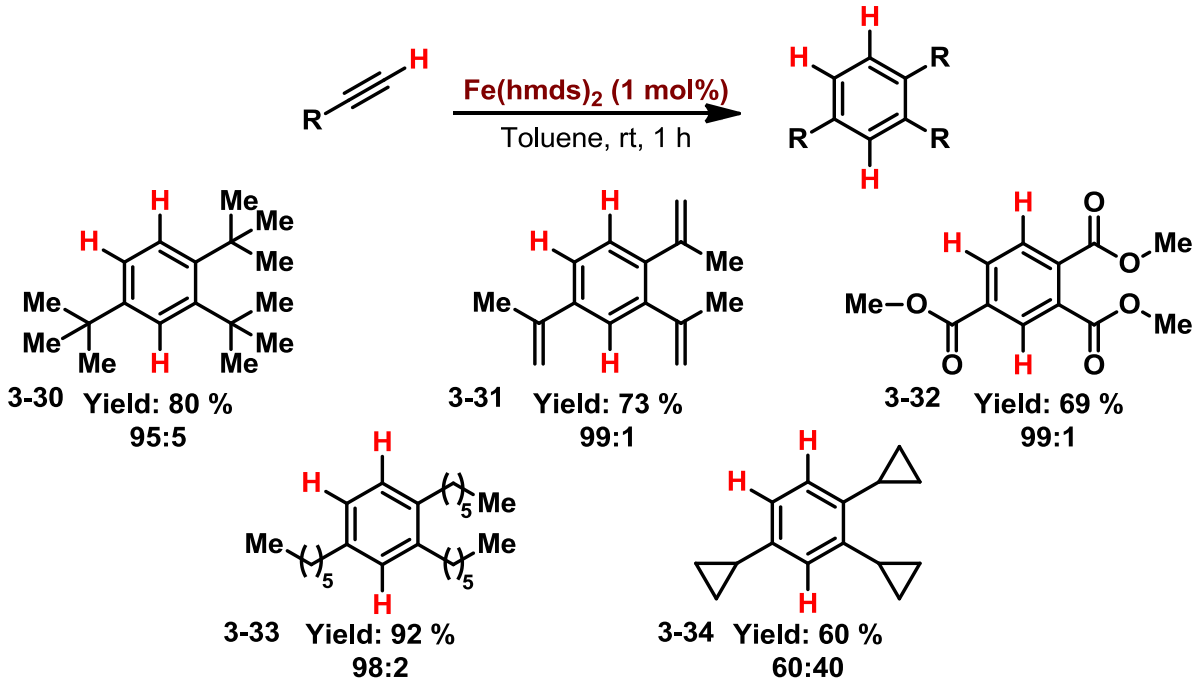

Different functional groups were tolerated, such as alkenes, esters and cyclopropyl residues. In the case of cyclopropyl residues no ring opening was observed. The yield for these non-aromatic alkynes were good and the reactions generally proceeds without the formation of any byproduct and from the analysis of the crude mixture is possible to observe the starting alkyne unreacted. The low selectivity towards the 1,2,4 and 1,3,5 isomer in the case of the cyclopropyl residue could be related to its low steric bulk. To further investigate the reactivity of the system the use of internal alkynes was explored (Table 3-9).

Table 3-9: internal alkyne reactivity

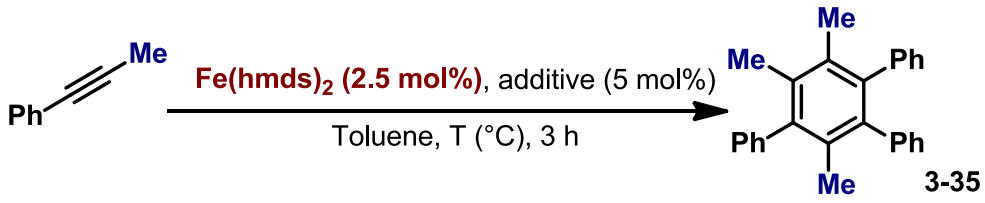

Entry	Additive	T (°C)	Yield (%)[a]	Selectivity[b]
1	none	rt	--	--
2[c]	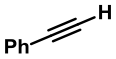	rt	--	--
3	DIBAL-H	rt	--	--
3		90	70	90:10
4	none	90	85	89:11

Conditions : 0.48 mmol alkyne,1 M in toluene; [a] isolated yield, [b]1,2,4 product against 1,3,5 product were evaluated using GC-FID, [c] a solution of the two alkynes was directly added to the catalyst dissolved in toluene.

Running the reaction at room temperature and without any additives led to the recovery of all the starting material completely unreacted (entry 1, table 5). the use of a terminal alkyne and DIBAL-H, as additives, for the activation of the $Fe(hmds)_2$ was unsuccessfull (entries 2 and 3, table 5). The trimerization product of the internal alkyne was finally obtained working at 90 °C in the presence of a 5 % of internal alkyne as activating agent, running the reaction in the presence of a terminal alkyne led to different byproduct produced by the reaction of the terminal alkyne and the internal one, nevertheless the trimerization product was obtained in 70 % of isolated yield and good selectivity (90:10) (entry 3, table 3-9). To increase the yield, the reaction was run in absence of terminal alkyne and surprisingly, the desired product was isolated in 85 % yield with good selectivity towards the 1,2,4 isomer. To further explore the scope of the reaction, selected examples of intra and intermolecular alkyne cyclization were performed. (Scheme 3-23)

Scheme 3-23: intra and intermolecular alkyne cyclization

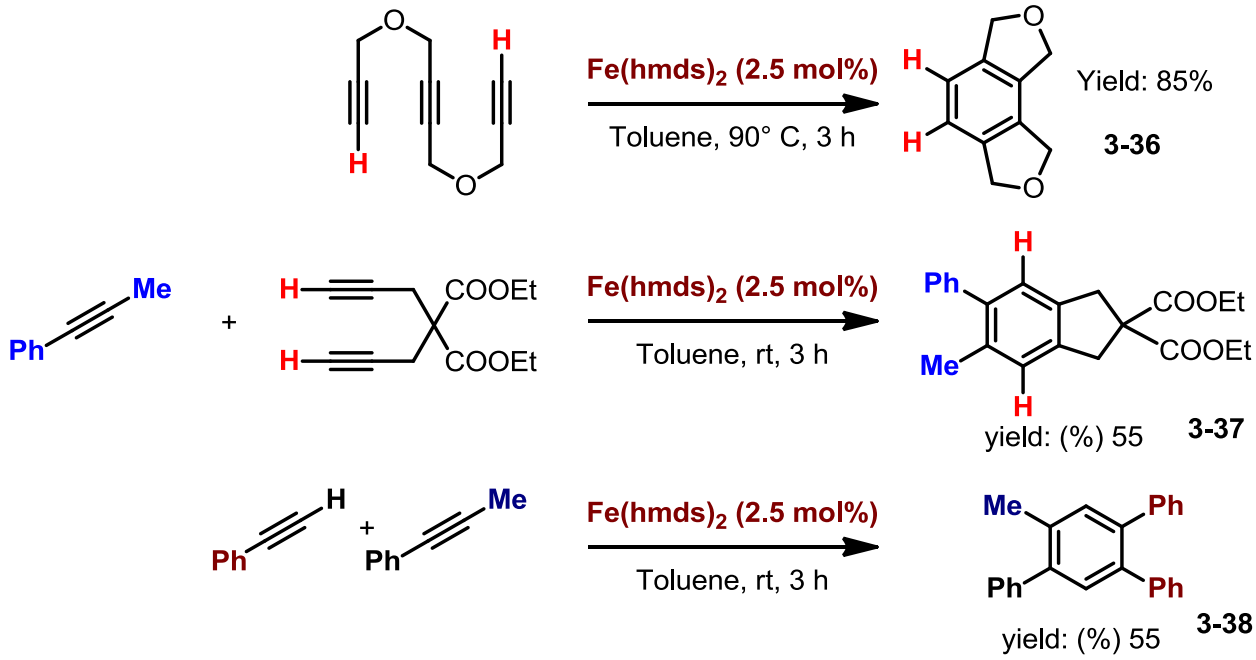

Both intramolecular (eq. 1 Scheme 3-23) and intermolecular (eq. 2 and 3 Scheme 3-23) reactions were successfully performed with good yields, demonstrating the robustness of this catalytic system for the construction aromatic rings with different substituent.

Mechanistic studies on iron catalyzed trimerizations

Poisoning studies with 0.5 equiv. trimethyl-phosphine (PMe_3) per Fe unambiguously resulted in inhibition of catalysis (Figure 3-7). No impact on the catalyst activity was observed upon addition of the selective homotopic poison dibenzo[*a*,*e*]cyclo-octatetraene (dct) to the reaction mixture (Figure 3-7)[229].

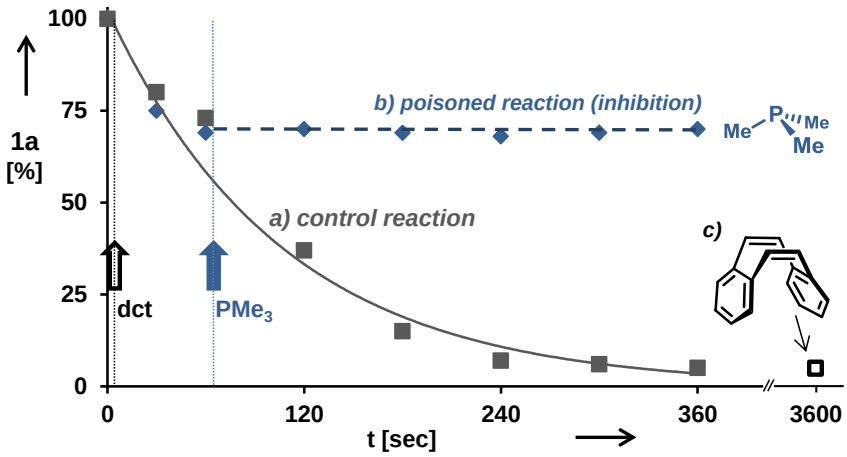

Entry	Agent	Poisoning (mol %)	Temperature (°C)	Time(min)	Yield (%)
1	none	--	rt	10	60
2	PMe_3	0.5	rt	10	10
3	none	--	rt	60	96

4	PMe_3	0.5	rt	60	20
5	PMe_3	0.25	rt	60	27
6	none		rt		98
7	dct	6	rt	60	97
8	PMe_3	0.5	- 30	60	0
9	dct	6	-30	60	95
10	none	--	-30	60	98

In order to study the stability of the catalyst, a stock solution of Fe(hmds)2 was activated with phenyl acetylene, stored under argon and then used after 14 days. Same yields and selectivity were observed in the trimerization of the *p*-tolylacetylene. (Scheme 3-24)

Scheme 3-24: studies on catalysts aging

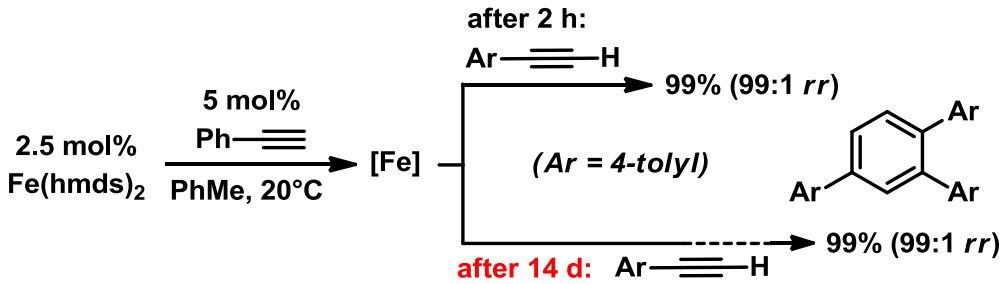

The proposed reaction mechanism (Scheme 3-25) starts with the alkyne-assisted reduction of the Fe(II) species to Fe(0). Probably the first step of the mechanism involved an acid/base reaction between the acid proton of the alkyne and the ligand on the metal, generating a Fe(II) species that could evolve into Fe(0) after reductive elimination of the two ligands. The formation of intermediates D-Y and the reductive elimination product were detected by GC-MS spectroscopy. The Iron (0) species, stabilized by the solvent (Toluene, THF), reacts with two equivalents of alkyne generating a 5 membered metallacycle with a vacant site on the iron, after the coordination a second molecule of alkyne and the formation of a 7 member ring metallacycle; the reductive elimination leads to the desired aromatic product and regenerated the Fe(0) active species. Running the reaction using deuterated phenyl acetylene, the complete incorporation of the deuterium in the final product was observed. The high selectivity of the reaction towards the 1,2,4 product strongly suggests the selective formation of the 5-membered ring with the two substituents on the same side. The activation pathway for the internal alkyne probably involves the coordination of the alkynes to the Fe(II) species and the subsequently reductive elimination of the amide ligands leading to Fe(0) active catalyst.

Scheme 3-25: proposed reaction mechanism

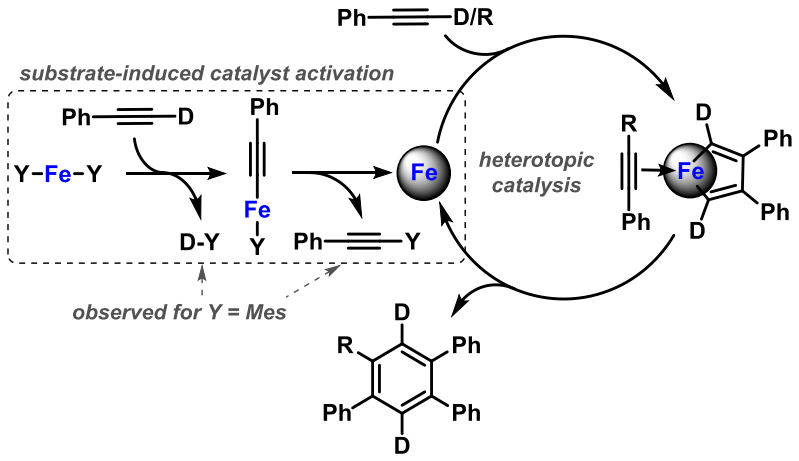

In summary, we have developed an iron(II)-catalysed trimerization protocol that displays unprecedented activity and does not need a reducing agent for the catalyst activation. The reaction proceeds with high yields and selectivity at low temperature and low catalyst loading (1%) in short reaction time. The isolated $Fe(hmds)_2$ is activated in situ by the alkyne, however a most user-friendly procedure involved the preparation of the catalyst in situ from $FeCl_2$ and $LiN(SiMe_3)_2$.

Experimental section chapter 3

Iron catalyzed diastereoselective hydrogenation of chiral imines

NMR spectra: ^{1}H-NMR and ^{13}C-NMR spectra were recorded with instruments at 300 MHz (Bruker AMX 300 and Brucker F300). The chemical shifts are reported in ppm (δ), with the solvent reference relative to tetramethylsilane (TMS).

TLC: Reactions and chromatographic purifications were monitored by analytical thin-layer chromatography (TLC) using silica gel 60 F254 pre-coated glass plates and visualized using UV light, phosphomolybdic acid or ninhydrin.

Chromatographic purification: Purification of the products was performed by column chromatography with flash technique (according to the Still method) using as stationary phase silica gel 230-400 mesh (SIGMA ALDRICH).

Dry solvents: Ethanol was degassed using N2 for 1 h before its use.

Reactions work-up: The organic phases, if necessary, were dried over Na_2SO_4. The solvents were removed under reduced pressure and then at high vacuum pump (0.1-0.005 mmHg).

Batch hydrogenations: The hydrogenations were run in a 450 mL Parr autoclave equipped with a removable aluminum block that can accommodate up to 4 magnetically stirred 20 mL-glass vials, fitted with a Teflon septum.

Gas chromatography with mass-selective detector (GC-MS): Agilent 6890N Network GC-System, mass detector 5975 MS. Column: HP-5MS (30m × 0.25 mm × 0.25 µm, 5% phenylmethylsiloxane, carrier gas: H_2. Standard heating procedure: 50 °C (2 min), 25 °C/min -> 300 °C (5 min)

Optical rotations: Were obtained on a Krüss optic polarimeter P8000 at 589 nm using a 5 mL cell, with a length of 1 dm.

The iron complexes Cat **A,** [230] Cat **B**[203] and Cat **C**[231] were prepared following literature procedures.

Synthesis of Imines

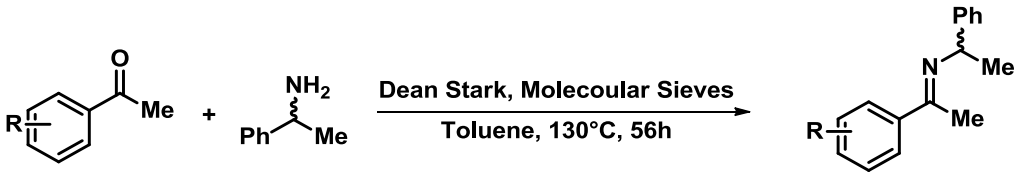

General procedure (A): Toluene (8 mL), 4 Å molecular sieves, amine (6.6 mmol, 1.5 eq.) and ketone (4.4 mmol, 1 eq.) were introduced in a one necks 25 mL round-bottomed flask provided with a condenser and a Dean-Stark apparatus. The reaction mixture was heated to 130 °C and stirred at this temperature for 56 h. After cooling to room temperature, molecular sieves were removed filtering over Na_2SO_4 pad and washed with DCM. The solvent was removed under reduced pressure. The residual starting materials were removed by fractional distillation at P = 3 x 10^{-2} mbar at 150 °C with Glass Oven B-585 Kugelrohr (only terminal round flask inserted). in order to remove the excess of amine.

General procedure (B): Toluene (6 mL), molecular sieves (350 mg), amine (1.5 eq, 6.6 mmol) and ketone (1 eq, 4.4 mmol) were introduced in a 25 mL vial without inert atmosphere. The stirred mixture was subjected to 200 W microwave irradiation and heated to 130 °C for 6 h 30 min. Constant microwave irradiation as well as simultaneous air-cooling (2 bar) were used during the entire reaction time. After cooling to room temperature, the reaction mixture was filtered on Na_2SO_4 , and washed with DCM, the solvent was removed under reduced pressure. The residual starting materials were removed by fractional distillation at P = 3 x 10^{-2} mbar at 150 °C with Glass Oven B-585 Kugelrohr (only terminal round flask inserted).

General procedure (C): The selected ketone was charged in a two round bottomed flask, posed under nitrogen and dissolved in dry Toluene (0.1M). At this solution was added Ti(*i*PrOH)$_4$ (2 eq.), after 5 minutes of mixing the (*R*)-(+)-2-Methyl-2-propanesulfinamide was added. The reaction mixture was stirred for 18 hours at 110 ° C, then poured into a same volume solution of brine. The resulting slurry was filtered over celite and the cake was washed with AcOEt. The two phases were separated and the organic phase was further washed with brine. The organic layer was dried with Na_2SO_4 pad, and the solvent was removed under reduced pressure. The desired imines were obtained pure after chromatographic purification.

N-(1-(*S*)-phenylethyl)-ethan-1-(phenyl)-1-imine **(3-1a)**

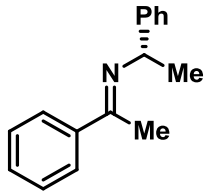

Synthetized according to general procedure A starting from the corresponding ketone and (*S*)-phenylethylamine. The pure product was obtained in 60% yield after purification by fractional distillation at P = 3 x 10^{-2} mbar with Glass Oven B-585 Kugelrohr set to 95 °C. The imine is a 92:8 mixture of the *E* and the *Z* isomers.

Major isomer:

^{1}H NMR (300 MHz, $CDCl_3$) δ: 7.87 (m, 1H), 7.57 – 7.21 (m, 9 H), 4.87 (q, J = 6.5 Hz, 1 H), 2.29 (s, 3 H), 1.57 (d, J = 6.5 Hz, 3H).

Compound **3-1a** is known and all analytical data are in agreement with literature[232]

N-(1-(*S*)-phenylethyl)-ethan-1-(4-(methoxy)phenyl)-1-imine **(3-2a)**

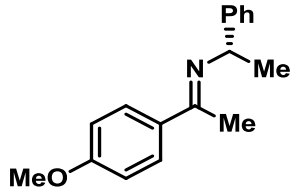

Synthetized according to general procedure B starting from the corresponding ketone and (*S*)-phenylethylamine. The pure product was obtained in 50% yield after purification by fractional distillation at P = 3 x 10^{-2} mbar with Glass Oven B-585 Kugelrohr set to 95 °C. The imine is a 95:5 mixture of the *E* and the *Z* isomers.

Major isomer:

1H NMR (300 MHz, $CDCl_3$), E isomer: δ 7.2-8.0 (m, 9H), 4.90 (q, J=6.50 Hz, 1H), 3.86 (s, 3H), 2.29 (s, 3H), 1.62 (d, J=6.50 Hz, 3H)

Compound **1b** is known and all analytical data are in agreement with literature[233]

N-(1-(*S*)-phenylethyl)-ethan-1-(3-(benzyloxy)phenyl)-1-imine **(3-3c)**

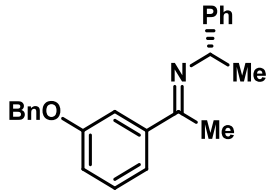

Synthetized according to general procedure A and B starting from the corresponding ketone and (*S*)-phenylethylamine. The pure product was obtained in 45% (Procedure A) and 25% (Procedure B) yield after purification by fractional distillation at P = 3 x 10^{-2} mbar with Glass Oven B-585 Kugelrohr set to 95 °C. The imine is a 91:9 mixture of the *E* and the *Z* isomers.

Major isomer:

^{1}H NMR (300 MHz, $CDCl_3$) *E* δ: 7.99-7.94 (m, 1H), 7.58-7.31 (m, 12H), 5.19 (s, 2H), 4.94 (q, 1H, *J* = 9.0 Hz), 2.25 (s, 3H), 1.66 (d, 3H, *J* = 9.0 Hz).

Compound **3-3c** is known and all analytical data are in agreement with literature.[233]

N-(1-(*R*)-phenylethyl)-ethan-1-(3-(methoxy)phenyl)-1-imine **(3-4d)**

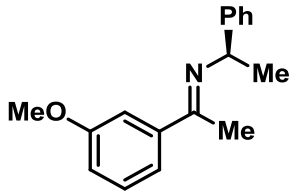

Prepared according to general procedure A and B starting from the corresponding ketone and (*R*)-phenylethylamine. The pure product was obtained in 50% (Procedure A) and 35% (Procedure B) yield after purification by fractional distillation yield after purification by fractional distillation at P = 3 x 10^{-2} mbar with Glass Oven B-585 Kugelrohr set to 95 °C. The imine was a 90:10 mixture of the *E* and the *Z* isomers as reported in literature.

Major isomer:

^{1}H NMR (300 MHz, $CDCl_3$) *E* δ 7.55–7.20 (m, 9H), 4.86 (q, *J* = 6.6 Hz, 1H), 3.88 (s, 3H), 2.28 (s, 3H), 1.56 (d, *J* = 6.6 Hz, 3H).

Compound **3-4a** is known and all analytical data are in agreement with literature.[234]

N-(1-(*S*)-phenylethyl)-ethan-1-(4-(chloro)phenyl)-1-imine **(3-5a)**

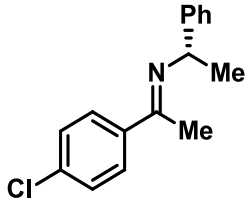

Synthetized according to general procedure B starting from the corresponding ketone and (*S*)-phenylethylamine. The pure product was obtained in 30 % yield after purification by fractional distillation at P = 3 x 10^{-2} mbar with Glass Oven B-585 Kugelrohr set to 95 °C. The imine is a 93:7 mixture of the *E* and the *Z* isomers.

Major isomer:

^{1}H NMR (300 MHz, $CDCl_3$) δ 7.82 (d, J = 8.6 Hz, 2H), 7.44 – 7.31 (m, 7H), 4.85 (q, J = 6.5 Hz, 1H), 2.27 (s, 3H), 1.55 (d, J = 6.5 Hz, 3H).

Compound **1e** is known and all analytical data are in agreement with literature[233

N-(1-(*S*)-phenylethyl)-ethan-1-(4-(Methyl)phenyl)-1-imine **(3-6a)**

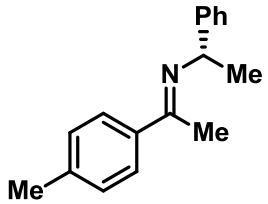

Synthetized according to general procedure B starting from the corresponding ketone and (*S*)-phenylethylamine. The pure product was obtained in 40% yield after purification by fractional distillation at P = 3 x 10^{-2} mbar with Glass Oven B-585 Kugelrohr set to 95 °C. The imine is a 92:8 mixture of the *E* and the *Z* isomers.

Major isomer:

^{1}H NMR (300 MHz, $CDCl_3$) δ 7.76 (d, J = 8.2 Hz, 2H), 7.47-7.20 (m,7H), 4.84 (q, J = 6.6 Hz, 1H), 2.38 (s, 3H), 2.25 (s, 3H), 1.55 (d, J = 6.6 Hz, 3H).
Compound **1f** is known and all analytical data are in agreement with literature.[235]

N-(1-(*S*)-phenylethyl)-ethan-1-(4-(Nitro)phenyl)-1-imine **(3-7a)**

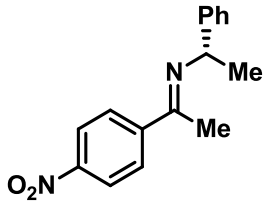

Synthetized according to general procedure B starting from the corresponding ketone and (*S*)-phenylethylamine. The pure product was obtained in 50% yield after purification by fractional distillation at P = 3 x 10^{-2} mbar with Glass Oven B-585 Kugelrohr set to 95 °C. The imine is a 95:5 mixture of the *E* and the *Z* isomers.
^{1}H NMR (300 MHz, $CDCl_3$) δ 8.32 – 8.23 (d, J = 8.89 Hz, 2H), 8.08 (d, J = 8.89 2H), 7.61 – 7.50 (m, 2H), 7.43 (t, J = 7.5 Hz, 2H), 7.38 – 7.25 (m, 1H), 4.95 (q, J = 6.5 Hz, 1H), 2.38 (s, 3H), 1.64 (d, J = 6.5 Hz, 3H).
Compound **3-7a** is known and all analytical data are in agreement with literature.[236]

N-(α-Methylbenzyliden)-α-(4-methoxyphenyl)aethylamine **(3-12a)**

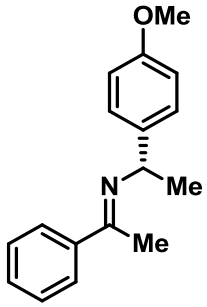

Synthetized according to general procedure B starting from the corresponding ketone and (*R*)-4-Methoxy-α-methylbenzylamine. The pure product was obtained in 50% yield after purification by fractional distillation at P = 3 x 10^{-2} mbar with Glass Oven B-585 Kugelrohr set to 95 °C. The imine is a 95:5 mixture of the *E* and the *Z* isomers.
Major isomer:
1H NMR (300 MHz, CDCl3), E isomer: δ 7.2-8.0 (m, 9H), 4.90 (q, J=6.50 Hz, 1H), 3.86 (s, 3H), 2.29 (s, 3H), 1.62 (d, J=6.50 Hz, 3H)
Compound **3-12a** is known and all analytical data are in agreement with literature.[233]

N-(1-(*R*)-phenylethyl)-propan-1-(4-methoxyphenyl)-1-imine **(3-13a)**

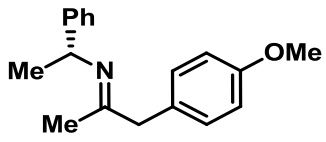

Synthetized according to general procedure B starting from 4-methoxyphenylacetone and (*R*)-phenylethylamine. The pure product was obtained in 85% yield after purification by fractional distillation at P = 3 x 10^{-2} mbar with Glass Oven B-585 Kugelrohr set to 95 °C. The imine was obtained as yellow oil a 7:3 E/Z mixture.

Major isomer: (*E*)

^{1}H NMR (300 MHz, $CDCl_3$) *E:* δ: 7.45 – 7.11 (m, 7H), 6.86-6.84 (m, 2H), 4.63 (q, 1H, J = 6.6 Hz), 3.90 (s, 3H), 3.56 (s, 2H),1,77 (s, 3H), 1.53 (d, 3H, *J* = 6.6 Hz).

Compound **1j** is known and all analytical data are in agreement with literature.[10]

(*R*)-*N*-(4-methoxyphenylethyl)indanimine **(3-10a)**

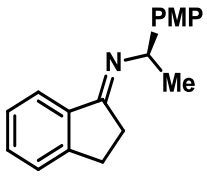

Synthetized according to general procedure A starting from 1-indanone and (*R*)-4-Methoxy-α-methylbenzylamine . The pure product was obtained in 60% yield after purification by crystallization in Et_2O. The imine was a pure *E* isomer.

^{1}H NMR (300 MHz, $CDCl_3$)*:* δ: 7.99 (d, 1H, J = 6.5 Hz), 7.41-7.31 (m, 5H), 6.91 - 6.88 (m, 2H), 4.66 (q, 1H, J = 6.6 Hz), 3.81 (s, 3H), 3.11-3.05 (m, 2H), 2.90-2.83 (m, 1H), 2.72-2.57 (m, 1H), 1.50 (d, 3H, *J* = 6.6 Hz).

Compound **3-10a** is known and all analytical data are in agreement with literature[72.]

Imines reductions

General procedures Iron catalyzed imine hydrogenation: The selected pre-catalyst (0.1 eq.) was dissolved into degassed ethanol (0.1M solution). The imine (1 eq.), and the trimethylamine N-oxide (0.4 equivalent) were charged into a 20 mL-glass vial, equipped with a rubber septum. The mixture was posed under nitrogen atmosphere. The vial was located in the removable aluminum block of a 450 mL Parr autoclave. The solution of the catalyst was added to the vial, the rubber septum was pierced with a nail. The reaction set up was set at the desired hydrogen pressure and the system was purged 3 times. The reaction temperature was then set. After 18 hours the heating system was shut down and the pressure was released. The crude mixture was analyzed by NMR in order to evaluate the dr. For removing the iron particles the crude where filtered over HPLC-filter (CPS-F-NY2545/100), and the solvent was removed under reducing pressure. The desired amine was obtained as pure compounds after chromatographic purification using (hexanes/AcOEt) as eluent.

N-(1-phenylethyl)-(S)-α-methylbenzylamine **(3-1b, 3-1b')**

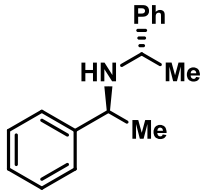

Diasteroisomer B

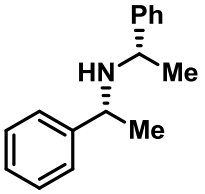

Diasteroisomer B'

^{1}H NMR (300 MHz, $CDCl_3$) δ: Selected signals for the evaluation of the diasteroisomeric ratio: 3.77 (m, 2H, diast. B'), 3.49 (m, 2H diast. B). The major diasteroisomer A was obtained pure after flash column chromatography on silica gel with a 90:10 hexane/ethyl acetate mixture as eluent. Rf = 0.18.

^{1}H NMR (300 MHz, $CDCl_3$) Diast. B δ 7.46 – 7.12 (m, 10H), 3.50 (m, 2H), 1.57 (s, 1H), 1.28 (2d, J = 6.6 Hz, 6H).
^{1}H NMR (300 MHz, $CDCl_3$) Diast. B' δ 7.46 – 7.12 (m, 10H), 3.78 (m, 2H), 1.57 (s, 1H), 1.37 (2d, J = 6.6 Hz, 6H).
Compound **2a** is known and all analytical data are in agreement with literature.[11]

N-(1-(4-methoxyphenyl)ethyl)-(S)-α-methylbenzylamine **(3-2b, 3-2b')**

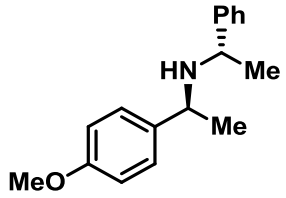

Diasteroisomer B

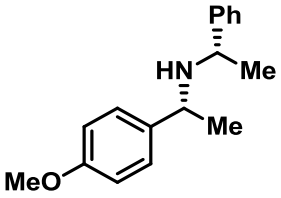

Diasteroisomer B'

^{1}H NMR (300 MHz, $CDCl_3$) δ: Selected signals for the evaluation of the diasteroisomeric ratio: 1.37 (t, J = 6 Hz (2d collapsed) , 6H, diast. B'), 1.29 (t, J = 6 Hz (2d collapsed), 6H diast. B).

^{1}H NMR (300 MHz, $CDCl_3$) Diast. B δ 7.47 – 7.07 (m, 7H), 6.96 – 6.79 (m, 2H), 3.84 (s, 3H), 3.51 (m, 2H), 1.29 (t, J = 6 Hz (2d collapsed), 6H diast. A).
^{1}H NMR (300 MHz, $CDCl_3$) Diast. B' δ 7.47 – 7.07 (m, 7H), 6.96 – 6.79 (m, 2H), 3.84 (s, 3H), 3.81 – 3.70 (m, 2H), (t, J = 6 Hz (2d collapsed) , 6H,).
Compound **3-2b** is known and all analytical data are in agreement with literature.[237]

N-(1-(4-chlorophenyl)ethyl)-(S)-α-methylbenzylamine **(3-5b, 3-5b')**

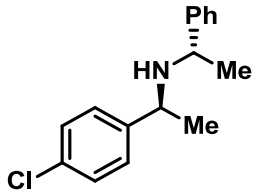

Diasteroisomer B

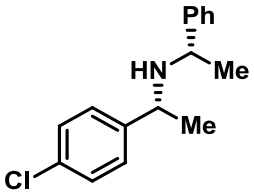

Diasteroisomer B'

^{1}H NMR (300 MHz, $CDCl_3$) δ: Selected signals for the evaluation of the diasteroisomeric ratio: 3.76 (m, 2H, diast. B'), 3.51 (m, 2H diast. B).

^{1}H NMR (300 MHz, $CDCl_3$) δ 7.30-7.18 (m, 9H), 3.55 – 3.42 (m, 2H), 1.57 (s, 1H), 1.26 (2d, J = 6.7 Hz, 6H).
^{1}H NMR (300 MHz, $CDCl_3$) δ 7.30-7.18 (m, 9H), 3.75 (q, J = 6.8 Hz, 2H), 1.57 (s, 1H), 1.35 (2d, J = 6.8 Hz, 6H).
Compound **2e** is known and all analytical data are in agreement with literature.[11]

N-(1-(3-benzyloxyphenyl)ethyl)-(S)-α-methylbenzylamine **(3-3b, 3-3b')**

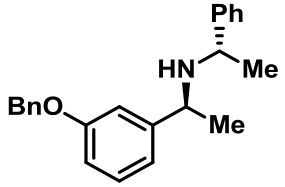

Diastereoisomer B

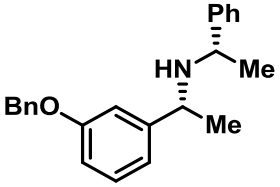

Diastereoisomer B'

^{1}H NMR (300 MHz, $CDCl_3$) δ: Selected signals for the evaluation of the diasteroisomeric ratio: 3.77 (m, 2H, diast. B), 3.49 (m, 2H diast. B'). The major diasteroisomer B was obtained pure after flash column chromatography on silica gel with a 90:10 hexane/ethyl acetate mixture as eluent. Rf = 0.18.

^{1}H NMR (300 MHz, $CDCl_3$) δ: 7.47-7.20 (m, 11H), 6.89-6.87 (m, 2H), 6.81 (d, 1H, *J* = 7.5 Hz), 5.08 (s, 2H), 3.49 (m, 2H), 1.26 (d, 6H, J=6.3 Hz).
Compound **2c** is known and all analytical data are in agreement with literature.[237]

N-(1-(3-methoxyphenyl)ethyl)-(S)-α-methylbenzylamine **(3-4b, 3-4b')**

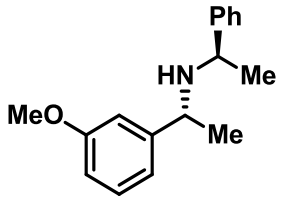

Diastereoisomer B

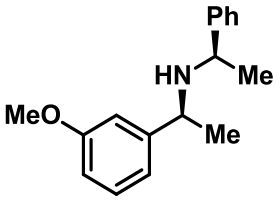

Diastereoisomer B'

^{1}H NMR (300 MHz, $CDCl_3$): Selected signals for the evaluation of the diasteroisomeric ratio: 3.79 (m, 2H, diast. B'), 3.50 (m, 2H, diast. B).

^{1}H NMR (300 MHz, $CDCl_3$) δ 7.39–7.05 (m, 6H), 6.81 (m, 3H), 3.82 (s, 3H), 3.50 (m, 2H), 1.54 (br, 1H), 1.28 (dd, 6H, J=6.5 Hz).

Compound **2d/2d'** is known and all analytical data are in agreement with literature.[238[

N-(1-(4-methylphenyl)ethyl)-(S)-α-methylbenzylamine **(3-4b, 3-4b')**

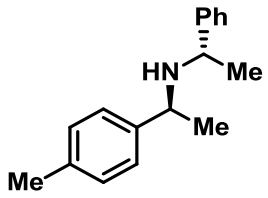

Diasteroisomer B

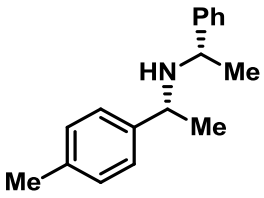

Diasteroisomer B'

^{1}H NMR (300 MHz, $CDCl_3$) δ: Selected signals for the evaluation of the diasteroisomeric ratio: 3.76 (m, 2H, diast. B), 3.51 (m, 2H diast. B').
^{1}H NMR (300 MHz, $CDCl_3$) δ 7.38-7.11 (m, 9H), 3.55 – 3.42 (m, 2H), 2.38 (s, 3H), 1.57 (s, 1H), 1.26 (2d, J = 6.7 Hz, 6H).

^{1}H NMR (300 MHz, $CDCl_3$) δ 7.30-7.18 (m, 9H), 3.75 (q, J = 6.8 Hz, 2H), 2.36 (s, 3H), 1.57 (s, 1H), 1.35 (2d, J = 6.8 Hz, 6H).
Compound **2f** is known and all analytical data are in agreement with literature.[237]

(*R*)-1-(4-methoxyphenyl)-*N*-((*R*)-1-phenylethyl)propan-2-amine **(3-13b, 3-13b')**

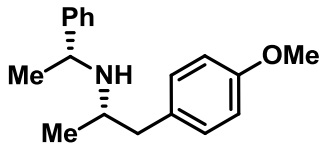

Diastereoisomer B

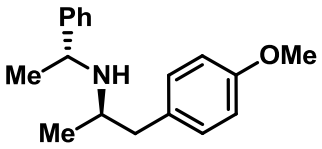

Diastereoisomer B'

The mixtures of the two diasteroisomers is a light-yellow oil. The reaction leaded to a mixture of the two diasteroisomers. Major (B) Minor (A).

^{1}H NMR (300 MHz, $CDCl_3$) δ: Selected signals for the evaluation of the diasteroisomeric ratio: 1.07 (d, 3H, diast. A), 0.95 (d, 3H, diast. B).

After chromatographic purification on silica gel, using a mixture of 9:1 ETP:AcOEt as eluent, a diasteroisomeric mixture (9:1) of amines was obtained in 60% yield.

Major isomer:

^{1}H NMR (300 MHz, CDCl3) δ 7.42 – 7.22 (m, 5H), 7.02 (d, J = 8.6 Hz, 2H), 6.82 (d, J = 8.6 Hz, 2H), 3.98 (m, 1H), 3.80 (s, 3H), 2.93 – 2.73 (m, 2H), 2.54-2.47 (m, 1H), 1.37 (d, J = 6.6 Hz, 3H), 0.97 (d, J = 6.2 Hz, 3H).

Compound **2j** is known and all analytical data are in agreement with literature.**Errore. Il egnalibro non è definito.**

(*R, R*)-*N*-1-indan-(1-*p*-methoxyphenylethyl)amine **(3-10b, 3-10b')**

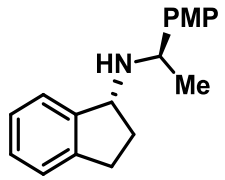

Diastereoisomer B

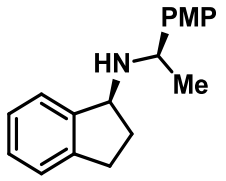

Diastereoisomer B'

The mixtures of the two diasteroisomers is a transparent oil. The reaction leaded to a mixture of the two diasteroisomers. Major (B) Minor (B').

^{1}H NMR (300 MHz, $CDCl_3$) δ: Selected signals for the evaluation of the diasteroisomeric ratio: 2.45 (m, 1H, diast. A), 2.20 (m, 1H, diast. B).

After chromatographic purification on silica gel ,using a mixture of 8:2 (ETP:AcOEt) as eluent, a diasteroisomeric pure amine was obtained with a 55 % of isolated yield.

Major isomer:

^{1}H NMR (300 MHz, $CDCl_3$) δ: 7.38 (d, 2H, J = 8.6 Hz), 7.25-7.19 (m, 4H), 6.92 (d, 2H. J = 8.6 Hz) 4.15-4.22 (m, 2H), 3.84 (s, 3H), 2.98-3.05 (m, 1H), 2.75-2.82 (m, 1H), 2.28-2.22 (m, 1H), 1.74-1.82 (m, 1H), 1.40 (d, 3H, J = 6.5 Hz).
Compound **3-10b** is known and all analytical data are in agreement with literature.[10]

.

General procedure for metal-free deprotection

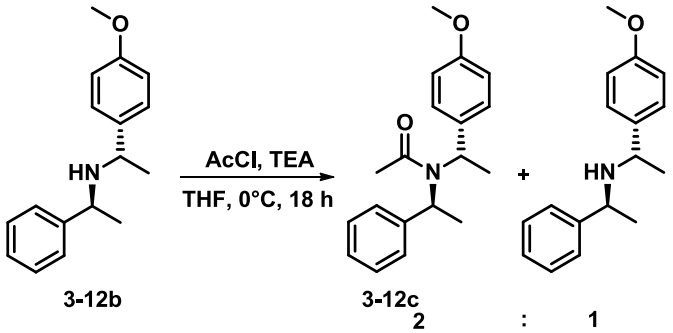

Amine **3-12b** (150 mg, 0.68 mmol, 1 eq) was dissolved in 1 mL of dry THF and the solution was cooled down to 0 °C. Triethyl amine (0.141mL, 1,02 mmol, 1.5 eq) was added to the solution, then AcCl (0.048mL, 0.68mmol, 1 eq), was slowly added to the reaction mixture. The solution was stirred at room temperature for 14 hours. 2 mL of NH_4Cl (sat. sol.) were added, the organic phase was collected and the aqueous one was further extracted with AcOEt (3 * 5mL). The collected organic phase was dried over Na_2SO_4 the solvent was removed under reduced pressure. The crude product was purified using column chromatography (from 9:1 to 7:3 Hexanes/AcOEt), giving the desired compound in a 75% yield. The acetylated compound was not separable from the starting material. The mixture was used without further purification.

^{1}H NMR (300 MHz, $CDCl_3$) δ 7.52 – 6.47 (m, 9H), 3.74 (s, *3*H), 3.42 – 3.20 (m, 2H), 2.23 – 2.01 (m, 3H), 1.72 (m, *6*H).

GC-MS: t_R = 11.419 min and 11.460, (EI, 70 eV): *m/z* = 297 $[M]^+$, 192, 150, 135, 120, 105, 91. 77

Compound **3-12c** is known and all analytical data are in agreement with literature.[239][13]

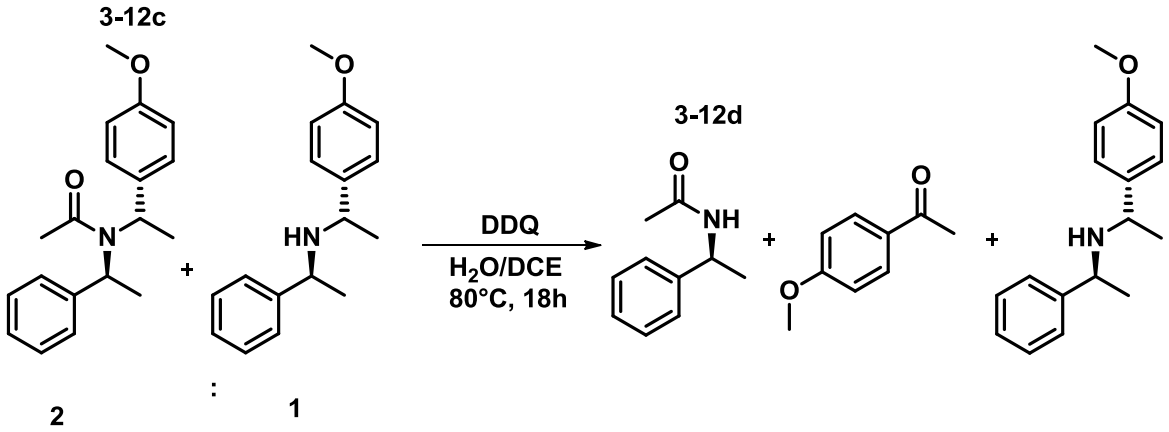

The procedure for the amide deprotection was known in literature[13], and was followed with slightly modification, regarding the purification. Amide **3-12c** (500 mg, 1.68 mmol, 1 eq) was dissolved in 10 mL of DCE, DDQ (1385 mg, 5.05 mmol, 3 eq), was dissolved in 10 mL of H_2O and slowly added to the reaction mixture. The solution was stirred at 70 °C for 14 hours. The reaction was cooled down to room temperature and 10 mL of a saturated solution of $NaHCO_3$ was added, 50 mL of DCM were further added. The organic phase was collected and further washed with a saturated

solution of $NaHCO_3$ (3 * 5mL). The organic phase was dried over Na_2SO_4 the solvent was removed under reduced pressure. The crude product **3-12d** was purified using column chromatography (9:1 pentane/AcOEt), giving the desired compound in 87% yield as white solid. The not acetylated compound was recovered unreacted.

^{1}H NMR (300 MHz, CDCl3) δ 7.42 - 7.18 (m, 5 H), 6.04 (br. s., 1 H), 5.09 (m, 1 H), 1.95 (s, 3 H), 1.47 (d, J = 7.1 Hz, 3 H).
GC-MS: t_R = 7.54 min, (EI, 70 eV): *m/z* = 163 $[M]^+$, 148, 120, 106, 77.
$[\alpha]^{25}_D$ = 106.3 (c: 1g/100mL $CHCl_3$).

Compound **3-12d** is known and all analytical data are in agreement with literature.[240]

DFT data

Calculations were performed with the GAUSSIAN09[15] within the framework of density functional theory (DFT) by using the hybrid B3LYP functional for all atoms except for iron. The SDD-functional with default parameters was used for iron to account for the influence of d-orbitals. The geometry of intermediate complexes and transition states was optimized in the gas phase without geometry constraints using the 6-31G(d,p) basis set for all atoms except for iron, which was described by the SDD basis set. The stationary points localized thereby were verified using frequency-calculations with the same basis set as before.

The free energies in the energy profiles representing two molecules were calculated by summing up the free energies of the two structures derived from separate calculations without taking into account Basis Set Superposition Errors (BSSE) and additional degrees of freedom of translation and rotation.

Iron catalyzed alkyne trimerizations

General procedures:

Synthesis of $\{Fe[N(SiMe_3]_2\}_2$

Synthesis slightly modified from the literature.[241]

A flame-dried *Schlenk*-flask was charged with $LiN(SiMe_3)_2$ (6.37 g, 2.2 equiv., 38.1 mmol) in diethyl ether (60 mL) in a glove box full of argon. $FeCl_2$ (2.24 g, 1.0 equiv., 17.1 mmol, 97%) previously charged in a glove box full of argon in a flame-dried Schlenk was added in portions at 0 °C. The resulting reaction mixture could warm to room temperature and stirred for 24 h. The Et_2O was removed under high vacuum, then the solid residue was suspended in *n*-hexane (25 mL) filtered over a glass frit and washed with *n*-hexane (5× 3 mL). After removing the solvent under reduced pressure, the crude product was purified by distillation under reduced pressure (90 C, 10^{-3} mbar) to obtain a dark green oil which crystallizes upon standing at room temperature.

^{1}H-NMR (400 MHz, C_6D_6) (400 MHz, C_6D_6) δ = 64.10 (bs).

Synthesis of $Fe_2(mes)_4$

Compound prepared following literature procedures[242]

IR (Nujol): υ =470 (str), 572(med), 643(str), 715(str), 748(str), 880(med), 902(wk), 935(str), 1020(med), 1124(med), 1168(med), 1210(med), 1448(str), 1346(str), 1364(str), 1387(str), 1525(med), 1593(med) cm^{-1}.

^{1}H NMR ([D8toluene. 75 C): 6 = 19(s. 18H). 55 (s, 36H), 113 (s. 4H).

General method for [2+2+2]-TOF calculation:

In an argon-filled glovebox, a flame-dried vial was charged with the $Fe(hdms)_2$ (0.0048 mmol) and toluene (0.25 mL) and sealed with a septum cap. After the complete dissolution of the pre-catalyst, a solution of alkyne (0.48 mmol) in toluene (0.25 mL) was slowly added. The solution turned brownish-black immediately and was then stirred at room temperature for 2 seconds. The reaction was quenched following the **general method a.** Analytically pure compounds were obtained after chromatographic purification on SiO_2 using hexanes/ethyl acetate as eluents or pentane/diethylether.

General method for [2+2+2]-cyclotrimerization with different iron salts: (table 1 manuscript entries 1-8). **(a)**

In an argon-filled glovebox, a flame-dried vial was charged with the iron(II) pre-catalyst (0.024 mmol) and toluene (0.25 mL) and sealed with a septum cap. After the complete dissolution of the pre-catalyst, a solution of alkyne (0.48 mmol) in toluene (0.25 mL) was slowly added. The solution turned brownish-black immediately and was then stirred at room temperature for 3 hours. The

reaction was quenched with a saturated aqueous solution of $NaHCO_3$ (1 mL). The resulting slurry was further diluted with 4 mL ethyl acetate. The organic phase was separated and dried with Na_2SO_4, filtered through silica using 5 mL of ethyl acetate as eluent and analyzed with GC-MS and ^{1}H-NMR spectroscopy. Analytically pure compounds were obtained after chromatographic purification on SiO_2 using hexanes and ethyl acetate as eluents.

General method for in situ catalyst preparation with $LiN(SiMe_3)_2$ and various metals salts

In an argon-filled glovebox, a flame-dried vial was charged with the metal(II) pre-catalyst (0.024 mmol) and toluene (0.1 mL), a solution of $LiN(SiMe_3)_2$ in toluene (0.15 mL) was added; the vial was sealed with a septum cap and stirred overnight. In the morning, a solution of alkyne (0.48 mmol) in toluene (0.25 mL) was slowly added. The solution was then stirred at room temperature for 1 hours.

The reaction was quenched following the **general method a.**

General method for optimization of the reaction conditions: In an argon-filled glovebox, a flame-dried vial was charged with the $Fe(hdms)_2$ (**x** mmol%) and the desired solvent (0.25 mL) and sealed with a septum cap. After the complete dissolution of the pre-catalyst, a solution of alkyne (0.48 mmol) in the selected solvent (0.25 mL) was slowly added. The solution turned brownish-black immediately and was then stirred at the selected temperature for the desired time. The reaction was quenched following the **general method a.**

General method for [2+2+2]-cyclotrimerization: In an argon-filled glovebox, a flame-dried vial was charged with the $Fe(hdms)_2$ (0.0048 mmol) and toluene (0.25 mL) and sealed with a septum cap. After the complete dissolution of the pre-catalyst, a solution of alkyne (0.48 mmol) in toluene (0.25 mL) was slowly added. The solution turned brownish-black immediately and was then stirred at room temperature for one hour. The reaction was quenched following the **general method a.** Analytically pure compounds were obtained after chromatographic purification on SiO_2 using hexanes/ethyl acetate as eluents or pentane/diethylether.

General method for [2+2+2]-cyclotrimerization of internal alkyne: In an argon-filled glovebox, a flame-dried vial was charged with the $Fe(hdms)_2$ (0.012 mmol) and toluene (0.25 mL) and sealed with a septum cap. After the complete dissolution of the pre-catalyst, a solution of alkyne (0.48 mmol) in toluene (0.25 mL) was slowly added. The solution turned brownish-black immediately and was then stirred at 90 °C for 3 hours. The reaction was quenched following the **general method a.** Analytically pure compounds were obtained after chromatographic purification on SiO_2 using hexanes/ethyl acetate as eluents or pentane/diethylether.

General method for [2+2+2]-cyclotrimerization of internal alkyne: In an argon-filled glovebox, a flame-dried vial was charged with the $Fe(hdms)_2$ (0.012 mmol) and toluene (0.1 mL) and sealed with a septum cap. After the complete dissolution of the pre-catalyst, a solution of internal alkyne (0.48 mmol) in toluene (0.1 mL) was slowly added, a solution of the terminal alkyne (1 or 2 equivalent) in toluene (0.3 mL) was slowly added over 1 hour, the. The solution turned brownish-black and was then stirred at rt for further 2 hours. The reaction was quenched following the **general method a.** Analytically pure compounds were obtained after chromatographic purification on SiO_2 using hexanes/ethyl acetate as eluents or pentane/diethylether.

General method for catalyst aging experiments: In an argon-filled glovebox a flame-dried vial was charged with the iron catalyst (2.5%, 0.012 mmol) and toluene (0.25 mL) then sealed with a disposable cap. After the complete dissolution of the catalyst, a solution of phenylacetylene (0.024 mmol) in toluene (0.25 mL) was slowly added; The solution turned black immediately and was then stirred at room temperature for the selected aging period. The *p*-tolyl acetylene (0.48 mmol) was added to the reaction mixture and the reaction was stirred at rt for 1 hour. The reaction was quenched using a saturated solution of $NaHCO_3$ (1mL), the resulting slurry was further diluted with 4 mL of ethyl acetate. The phases were separated and the organic one was dried with Na_2SO_4, filtered through silica using 5 mL of ethyl acetate as eluent and analyzed with GC-MS and H^1-NMR spectroscopy. The pure compounds were obtained after chromatographic purification using hexanes and ethyl acetate as eluents.

General method for *kinetic experiments*: In an argon-filled glovebox a flame-dried vial was charged with the iron catalyst (1 mol%, 0.048 mmol) and toluene (2.50 mL) then sealed with a disposable cap and cooled down to the desired temperature. After the complete dissolution of the catalyst, a solution of phenyl acetylene (4.8 mmol dissolved in 2.50 mL of toluene) at the same temperature of the reaction was slowly added, after the desired amount of time also the poisoning agent was added (in the case of PMe_3 0.5 mol%, in the case of dct 6 mol%). The samples (50 µl) were taken every 30 seconds, quenched with a saturated solution a saturated solution of $NaHCO_3$ (1mL), the resulting slurry was further diluted with 1 mL of ethyl acetate. The phases were separated and the organic one was dried with Na_2SO_4, filtered through silica using 5 mL of ethyl acetate as eluent and analyzed with GC-FID to evaluate the ratio between the starting material and the product.

General method for [2+2+2]-TOF calculation:

In an argon-filled glovebox, a flame-dried vial was charged with the $Fe(hdms)_2$ (0.0048 mmol) and toluene (0.25 mL) and sealed with a septum cap. After the complete dissolution of the pre-catalyst, a solution of alkyne (0.48 mmol) in toluene (0.25 mL) was slowly added. The solution turned

brownish-black immediately and was then stirred at room temperature for 2 seconds. The reaction was quenched following the **general method a.** Analytically pure compounds were obtained after chromatographic purification on SiO_2 using hexanes/ethyl acetate as eluents or pentane/diethylether.

General method for *poisoning experiments with PMe_3*: In an argon-filled glovebox a flame-dried vial was charged with the iron catalyst (1 mol%, 0.0048 mmol) and toluene (0.3 mL) then sealed with a disposable cap. After the complete dissolution of the catalyst, a solution of phenyl acetylene (0.0096 mmol) in toluene (0.1 mL) was slowly added; The solution turned black immediately and was then stirred at room temperature for 5 minutes. After that a solution containing the PMe_3 (in different stoichiometry compared to the catalyst using a stock solution 0.5 M in Hexane) was added at the black stirred solution. The solution containing the poisoning agent was stirred for 5 more minutes. *p*-tolyl acetylene (0.48 mmol) dissolved in 0.1 mL of toluene was added to the reaction mixture. The reaction was stirred at rt for the desired reaction time. (Table S2) The reaction was quenched using a saturated solution of $NaHCO_3$ (1mL), the resulting slurry was further diluted with 4 mL of ethyl acetate. The phases were separated and the organic one was dried with Na_2SO_4, filtered through silica using 5 mL of ethyl acetate as eluent and analyzed with GC-MS and H^1-NMR spectroscopy. The pure compounds were obtained after chromatographic purification using hexanes and ethyl acetate as eluents.

General method for *poisoning experiments with DCT*: In an argon-filled glovebox a flame-dried vial was charged with the iron catalyst (1 mol%, 0.0048 mmol) and toluene (0.2 mL) then sealed with a disposable cap. After the complete dissolution of the catalyst, a solution of phenyl acetylene (2 mol%, 0.0096 mmol) in toluene (0.1 mL) was slowly added; the solution turned black immediately and was then stirred at room temperature for 5 minutes. After that a solution containing the DCT (5 mol%, 0.024) in 0.1 mL of toluene was added at the black stirred solution. The solution containing the poisoning agent was stirred for 5 more minutes. *p*-tolyl acetylene (0.48 mmol) dissolved in 0.1 mL of toluene was added to the reaction mixture. The reaction was stirred at room temperature for the desired reaction time. (Table S2) The reaction was quenched using a saturated solution of $NaHCO_3$ (1mL), the resulting slurry was further diluted with 4 mL of ethyl acetate. The phases were separated and the organic one was dried with Na_2SO_4, filtered through silica using 5 mL of ethyl acetate as eluent and analyzed with GC-MS and H^1-NMR spectroscopy. The pure compounds were obtained after chromatographic purification using hexanes and ethyl acetate as eluents.

Different poisoning experiments were performed. The use of PMe_3 in sub-catalytic amount respect to the catalyst inhibit the reaction only 10 % yield after 10 minutes at rt. (entry 1, table s2); in case of longer reaction time (entry 4, table s2) only 20 % of the desired compound was obtained. The presence of dct do not influence the outcome of the reaction, neither at rt or at -30 °C degrees (entries 7 and 8, table s2); on the other hand, running the reaction in the presence of the PMe_3 at –30° C (entry 8, table s2) completely inhibit the reactivity of the system. These data strongly suggest a nanoparticle nature of this catalyst.

Products description:

1,4-bis(prop-2-yn-1-yloxy)but-2-yne

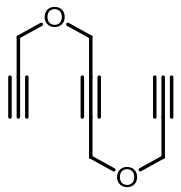

This compound was prepared according to literature procedure.[243]

The triyne was obtained as oily liquid after chromatographic purification using hexanes/ethyl acetate (95:5, R_f = 0.16).

^{1}H-NMR: (300 MHz, $CDCl_3$) δ 4.31 (s, 4H), 4.26 (d, *J* = 2.4 Hz, 4H), 2.46 (t, *J* = 2.4 Hz, 2H).

^{13}C-NMR : (75 MHz, $CDCl_3$) δ 82.09, 78.78, 75.11, 56.73, 56.54.

GC-MS: t_R = 6.54 min, (EI, 70 eV): *m/z* = 162 $[M]^+$, 131, 103, 93, 77, 65, 53.

The analytical data were in agreement with the literature.[243]

Diethyl 2,2-di(prop-2-yn-1-yl)malonate

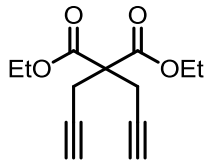

A *Schlenk* flask was charged with sodium hydride (3.20 g, 80.0 mmol, 60% in paraffin) in dry THF (80 mL) and cooled to 0 °C. Diethyl malonate (6.41 g, 40.0 mmol) was added via syringe pump (0.2 mL/min). After complete addition, the reaction mixture was allowed to warm to room temperature and stirred for 2 h. The reaction mixture was cooled to 0 °C and propargylic bromide (14.87 g, 100 mmol, 80% in toluene) was added dropwise. The suspension was allowed to warm temperature and stirred overnight after which it was quenched with H_2O (15 mL). The reaction mixture was extracted with ethyl acetate (3 × 20 mL) and the combined organic layers were dried (Na_2SO_4), concentrated subjected to distillation under reduced pressure, affording the desired compound as colorless liquid in 94% yield. bp. 91 °C at 0.1 mbar.

^{1}H-NMR: (300 MHz, $CDCl_3$) δ 4.23 (q, *J* = 7.1 Hz, 4H), 2.99 (d, *J* = 2.7 Hz, 4H), 2.03 (t, *J* = 2.7 Hz, 2H), 1.26 (t, *J* = 7.1 Hz, 6H).

^{13}C-NMR: (75 MHz, $CDCl_3$) δ 168.60, 78.44, 71.68, 62.09, 56.25, 22.50, 14.03.

GC-MS: t_R = 7.09 min, (EI, 70 eV): m/z = 197 $[M\text{-}C_3H_3]^+$, 162, 151, 133, 123, 105, 89, 77, 63, 51.

All analytical data were in agreement with the literature.[244]

1,2,4-Triphenylbenzene **(3-14)**

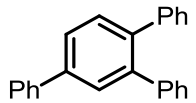

98 % yield, white solid after chromatographic purification using hexanes/ethyl acetate (99.5:0.5).

^{1}H-NMR: (300 MHz, $CDCl_3$) δ 7.77–7.66 (m, 4H), 7.56 (d, J = 7.7 Hz, 1H), 7.50 (t, J = 7.4 Hz, 2H), 7.45–7.36 (m, 1H), 7.34–7.17 (m, 10H).

^{13}C-NMR: (75 MHz, $CDCl_3$) δ 141.54, 141.17, 141.04, 140.64, 140.43, 139.60, 131.18, 129.98, 129.94, 129.50, 128.90, 128.01, 127.98, 127.51, 127.21, 126.67, 126.60, 126.20.

GC-MS: t_R = 12.52 min, (EI, 70 eV): m/z = 306 $[M]^+$, 289, 276, 228, 215, 202, 145, 77, 51.

The analytical data were in agreement with the literature.[245]

1,2,4-tris(*p*-tolyl)benzene (**3-15**)

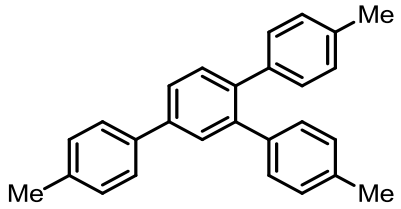

98 % yield, white solid after chromatographic purification using hexanes/ethyl acetate (99.9:0.1).

^{1}H-NMR: (300 MHz, $CDCl_3$) δ 7.66 – 7.53 (m, 5H), 7.47 (dd, J = 7.5, 0.9 Hz, 1H), 7.28 (s, 1H), 7.12- 7.07 (m, 8H), 2.41 (s, 3H), 2.33 (s, 6H).

^{13}C-NMR: (75 MHz, $CDCl_3$) δ 140.83, 140.09, 139.20, 138.79, 138.40, 137.85, 137.19, 136.13 (2C), 131.17, 129.99–129.44 (9C), 129.33, 128.73, 127.01, 125.78, 21.21 (3C).

GC-MS: t_R = 14.08 min, (EI, 70 eV): m/z = 348 $[M]^+$, 333, 318, 303, 256, 239.

The analytical data were in agreement with the literature.[246]

1,2,4-tris(*o*-tolyl)benzene **(3-16)**

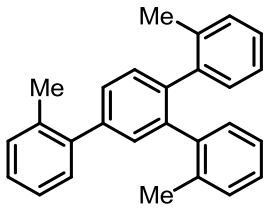

Compound **3** was obtained in 90 % yield as white solid after chromatographic purification using PE:AcOEt 99.9:0.1 as eluent.

^{1}H-NMR: (300 MHz, $CDCl_3$) δ 7.09 – 7.37 (m, 15H), 2.41 (s, 3H), 2.20-2.05 (m, 6H).

^{13}C-NMR: (75 MHz, $CDCl_3$) δ 19.5–20.6 (2C), 20.6, 124.8, 125.8 , 126.8 (2C), 127.3, 127.6 , 129.8 (2C), 129.9 (2C), 130.4 (2C), 131.4 (2C), 135.4, 135.6, 135.7, 139.2, 140.3 (2C), 141.5 .

GC-MS: t_R = 14.08 min, (EI, 70 eV): m/z = 348 $[M]^+$, 333, 318, 303, 256, 239.

The analytical data were in agreement with literature. [246]

1,2,4-tris-(2',4',5'-trimethylphenyl)benzene **(3-17)**

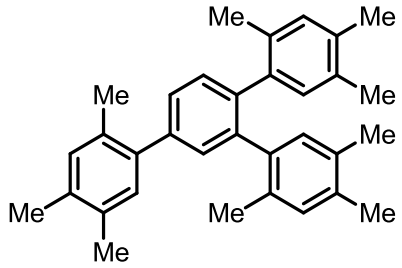

98 % yield, white solid after chromatographic purification using hexanes.

^{1}H-NMR: (300 MHz, $CDCl_3$) δ 7.44 – 6.83 (m, 9H), 2.38 (s, 3H), 2.34 (s, 3H), 2.32 (s, 3H), 2.22 (s, 3H), 2.21 (s, 3H), 2.16 (s, 3H), 2.14 (s, 3H), 2.09 (s, 6H).

^{13}C-NMR: (75 MHz, $CDCl_3$)δ 140.07(2C), 139.13(2C), 137.93, 135.43, 134.68, 133.87, 132.84, 132.70, 132.58 (2C), 131.87 (2C), 131.69, 131.35, 131.09, 130.48 (2C), 129.11, 128.30, 127.44(2C), 125.38, 20.11, 19.64, 19.40(4), 19.26, 19.13, 18.91.

GC-MS: t_R = 15.443 min, (EI, 70 eV): m/z = 432.

HRMS:(EI, m/z): found 432.2811 [M^+] (calculated 432.28115).

The analytical data were in agreement with literature.[248]

1,2,4-tris-(4'-phenyloxyphenyl)benzene **(3-19)**

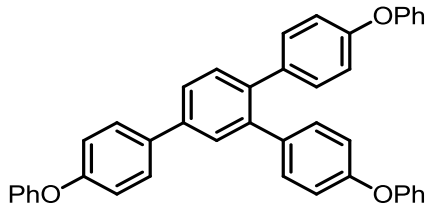

94 % yield, white solid after chromatographic purification using pentane/diethyl ether (99:1).

^{1}H-NMR: (300 MHz, $CDCl_3$) δ 7.69 – 7.57 (m, 4H), 7.50 (m, 1H), 7.41 – 7.29 (m, 7H), 7.21 – 6.98 (m, 14H), 6.90 (dd, J = 8.7, 2.7 Hz, 4H).

^{13}C-NMR: (75 MHz, $CDCl_3$) δ 157.09 (2C), 156.10, 140.37, 139.70, 138.69, 136.48, 136.07, 135.57, 131.25(2C), 131.21, 131.02(2C), 129.85(2C), 129.79(2C), 129.07(2C), 128.67(2C), 128.44(2C), 125.86(2C), 123.48(2C), 123.33(2C), 119.11(2C), 119.08, 118.97, 118.92, 118.41, 118.33.

HRMS:(EI, m/z): found 582.2189 [M^+] (calculated 582.21895).

Melting point: 187-192 °C

IR(neat): υ = 580 (str), 808(str), 1038(str), 1225(str), 1478(med), 1609(med) cm^{-1}.

1,2,4-tris-(4'-methoxyphenyl)benzene **(3-20)**

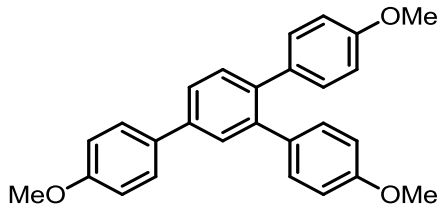

95 % yield, white solid after chromatographic purification using hexanes/ethyl acetate (99:1).

^{1}H-NMR: (300 MHz, $CDCl_3$) δ 7.67 – 7.54 (m, 4H), 7.46 (d, J = 7.8 Hz, 1H), 7.14 (m, 4H), 7.01 (d, J = 8.7 Hz, 2H), 6.81 (m, 4H), 3.87 (s, 3H), 3.81 (s, 6H).

^{13}C-NMR: (75 MHz, $CDCl_3$) 149.22, 148.76, 148.32, 148.25, 147.86, 147.77, 140.60, 140.11, 138.83, 134.37, 133.95, 133.65(2C), 130.82(2C), 128.83, 125.75(2C), 121.86 (2C), 119.43, 113.46, 113.40, 111.51, 110.80 (2C), 110.36.

The analytical data were in agreement with literature. [246]

1,2,4-tris-(3'-methoxyphenyl)benzene **(3-21)**

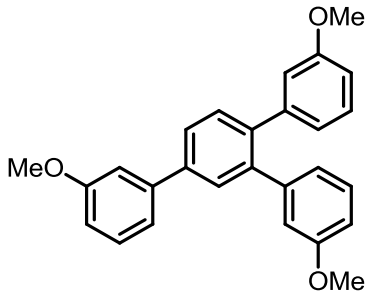

90 % yield, white solid after chromatographic purification using hexanes/ ethyl acetate (99:1).

^{1}H-NMR: (300 MHz, $CDCl_3$) δ 7.77 – 7.65 (m, 2H), 7.56 (d, J = 7.9 Hz, 1H), 7.41 (d, J = 7.9 Hz, 1H), 7.37 – 7.17 (m, 6H), 6.96 (m, 1H), 6.93 – 6.69 (m, 4H), 3.91 (s, 3H), 3.68 (s, 3H), 3.67 (s, 3H).

GC-MS: t_R = 18.775 min, (EI, 70 eV): m/z = 396

The analytical data were in agreement with literature. [247]

1,2,4-tris-(3'-benzyloxyphenyl)benzene **(3-22)**

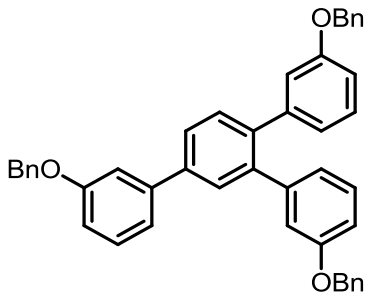

98 % yield, yellowish wax after chromatographic purification using pentane/ diethyl ether (95:5).

^{1}H-NMR: (300 MHz, $CDCl_3$) δ 7.76 – 7.12 (m, 28H), 6.88 (d, J = 8.9 Hz, 2H), 5.17 (s, 2H), 4.91 (s, 2H), 4.90(s, 2H).

^{13}C-NMR: (75 MHz, $CDCl_3$) δ 159.29, 158.50 (2C), 142.89, 142.53(2C) , 142.07 , 140.81(2C), 140.26, 139.54, 137.05 , 137.00, 130.95(2C), 129.94(2C), 129.29 (2C), 129.08(2C), 128.69(2C),

128.61(2C), 128.08(2C), 127.96(2C), 127.63(2C), 127.49, 126.26, 122.70(2C), 122.64, 119.94, 116.28(2C), 116.22, 113.89(2C), 113.78, 70.17, 70.03 (2C).

HRMS:(EI, m/z): found 624.266189 [M^+] (calculated 624.26590).

IR(neat): υ= 556 (med), 683(str), 733(str), 777(med), 1015(med), 1202(med), 1471(med), 1577(med), 2853 (wk), 2926(wk) cm^{-1}.

1,2,4-tris-(3‘,4‘-dimethoxyphenyl)benzene **(3-23)**

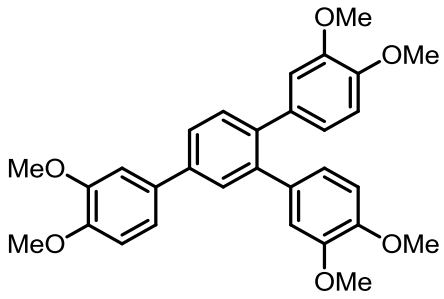

98 % yield, white solid after chromatographic purification using hexanes/ ethyl acetate (99:1).

^{1}H-NMR: (300 MHz, $CDCl_3$) δ 7.68 – 7.48 (m, 3H), 7.17 (m, 2H), 6.98 (d, J = 8.3 Hz, 1H), 6.88 – 6.78 (m, 4H), 6.66 (m, 2H), 3.96 (s, 3H), 3.94 (s, 3H), 3.88 (s, 6H), 3.63 (s, 3H), 3.62 (s, 3H).

^{13}C-NMR: (75 MHz, $CDCl_3$) 149.22, 148.76, 148.32, 148.25, 147.86, 147.77, 140.60, 140.11, 138.83, 134.37, 133.95, 133.65, 130.82, 128.83, 125.75, 121.86 (2C), 119.43, 113.46, 113.40, 111.51, 110.80 (2C), 110.36, 56.02 (2C), 55.90, 55.88, 55.73, 55.68.

The analytical data were in agreement with literature. [248]

1,2,4-tris-(2’-methyl-4’-methoxyphenyl)benzene **(3-24)**

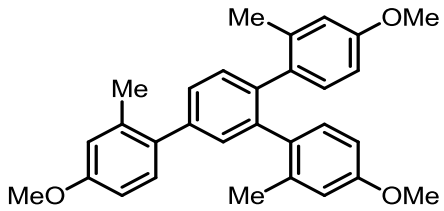

95 % yield, white solid after chromatographic purification using pentane/ dietethyl ether a (98:2).

^{1}H-NMR: (300 MHz, $CDCl_3$) δ 7.68 – 7.48 (m, 3H), 7.17 (m, 2H), 6.98 (d, J = 8.3 Hz, 1H), 6.88 – 6.78 (m, 4H), 6.66 (m, 2H), 3.96 (s, 3H), 3.94 (s, 3H), 3.88 (s, 6H), 3.63 (s, 3H), 3.62 (s, 3H).

^{13}C-NMR: (75 MHz, $CDCl_3$) δ 158.72, 158.15, 139.80, 137.09, 136.97, 136.82, 134.25, 131.99, 131.00, 130.74, 129.08, 128.27, 127.60, 115.79(2C), 115.02, 111.17, 110.50, 55.28, 55.06 (2C), 21.03 (3C).

HRMS:(EI, m/z): found 438.2187 [M^+] (calculated 438.22895).

Melting point: 176-178 °C

IR(neat): υ = 556 (med), 591(wk), 806(str), 843(med), 1038(med), 1059(med), 1232(str), 1291(str), 1476 (str), 1606(str), 2853(med), 2923(med), 2954(med) cm^{-1}.

1,2,4-tris-(6-methoxynaphthyl)benzene **(3-25)**

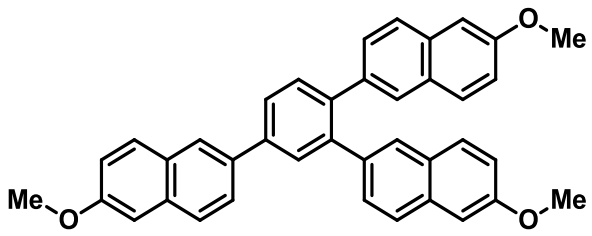

93 % yield, white solid after chromatographic purification using hexanes/ ethyl acetate (98:2).

^{1}H-NMR: (300 MHz, $CDCl_3$) 8.12 (s, 1H), 7.92 (d, J = 1.7 Hz, 1H), 7.86 (s, 1H), 7.81 (d, J = 1.3 Hz, 3H), 7.74 – 7.62 (m, 3H), 7.47 (dd, J = 8.5, 4.4 Hz, 2H), 7.20 (d, J = 7.5 Hz, 4H), 7.14 (ddd, J = 8.9, 4.2, 1.8 Hz, 3H), 7.06 (s, 2H), 3.96 (s, 3H), 3.90 (s, 6H).

^{13}C-NMR: (75 MHz, $CDCl_3$) δ 157.85, 157.69, 141.03, 140.35, 139.33, 137.16, 136.72, 135.78, 133.92, 133.29, 133.23, 131.64, 129.89, 129.80, 129.59, 129.25, 128.96, 128.25, 128.24, 128.20, 127.40, 126.23, 126.17, 126.16, 126.10, 125.99, 125.66, 119.27, 118.81, 118.78, 105.61, 105.56, 55.38, 55.32 (2C).

HRMS:(EI, m/z): found 546.21818 [M^+] (calculated 546.21895).

Melting point: 188-190 °C.

IR(neat): υ = 480 (str), 678(med), 806(str), 848(str), 1029(str), 1203(str), 1496(med), 1631(med), 1684 (str), 2898(wk), 3058(wk) cm^{-1}.

1,2,4-tris-(4‘-*N*,*N*-dimethylamino)benzene **(3-26)**

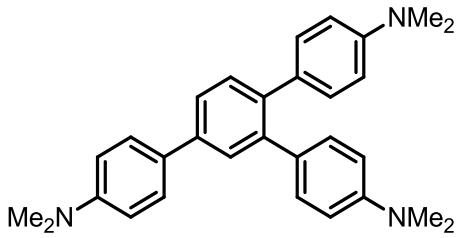

95 % yield, yellow solid after chromatographic purification using hexanes/ ethyl acetate (99:1).

^{1}H-NMR: (300 MHz, $CDCl_3$) δ 7.64 – 7.49 (m, 4H), 7.42 (d, J = 7.9 Hz, 1H), 7.12 (m, 4H), 6.82 (d, J = 8.7 Hz, 2H), 6.65 (m, 4H), 3.00 (s, 6H), 2.94 (s, 6H), 2.94 (s, 6H).

^{13}C NMR (75 MHz, $CDCl_3$) δ 148.55, 148.31 (2C), 142.98, 141.55, 139.49, 130.28, 129.20 (2C), 128.61, 128.46 (2C), 128.46, 128.39 (2C), 128.39, 128.31 (2C), 127.96, 126.33, 125.91, 114.40, 114.01 (2C), 113.50, 113.14, 42.01,41.70 (2C).

The analytical data were in agreement with literature.[249]

1,2,4-tris-(4‘-trifluoromethylphenyl)benzene **(3-27)**

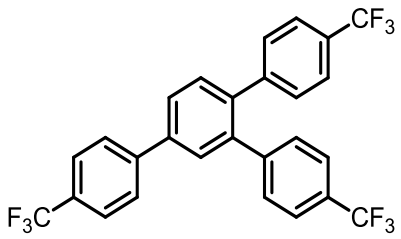

98 % yield, white solid after chromatographic purification using hexanes/ ethyl acetate (99:1).

^{1}H-NMR: (300 MHz, $CDCl_3$) δ 7.83–7.70 (m, 5H), 7.67 (d, J = 1.7 Hz, 1H), 7.60–7.48 (m, 5H), 7.29 (m 4H).

^{19}F NMR (282 MHz, $CDCl_3$) δ -62.94 (s).

^{13}C-NMR: (75 MHz, $CDCl_3$) δ 144.14, 143.25, 143.53, 139.92, 138.99(2C), 131.48, 130.11(2C), 130.07, 129.62(2C), 129.03(2C), 129.05, 127.46, 127.17(2C), 125.98, 125.93(2C),125.24,125.25, 125.26.

The analytical data were in agreement with literature. [247]

1,2,4-tris-(4‘-fluorophenyl)benzene **(3-28)**

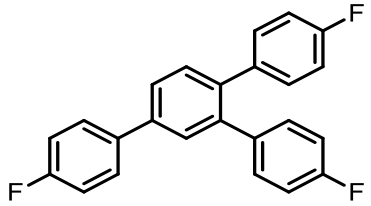

94 % yield, brown solid after chromatographic purification using hexanes/ ethyl acetate (99:1).

^{1}H-NMR: (300 MHz, $CDCl_3$) δ 7.73–7.55 (m, 4H), 7.48 (m, 1H), 7.27 (m, 1H), 7.15 (m, 7H), 6.96 (m, 1H).

^{19}F NMR (282 MHz, $CDCl_3$) δ -115.59 (m), -116.07 (m), -116.19 (m).

The analytical data were in agreement with literature.[246]

1,2,4-tris-(4'-chlorophenyl)benzene **(3-29)**

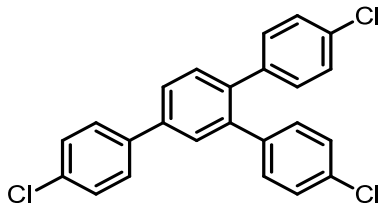

55 % yield, white solid after chromatographic purification using hexanes/ ethyl acetate (98:2).

^{1}H-NMR: (300 MHz, $CDCl_3$) δ 7.65–7.54 (m, 3H), 7.51–7.41 (m, 4H), 7.26–7.19 (m, 4H), 7.15–7.04 (m, 4H).

GC-MS: t_R = 16.778 min, (EI, 70 eV): m/z = 408 [M^+], 338, 302, 226.

The analytical data were in agreement with literature. [246]

1,2,4-tri-*tert*-butylbenzene **(3-30)**

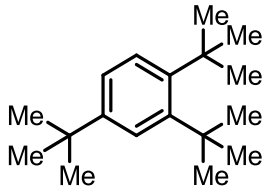

80 % yield, transparent liquid after filtration over silica gel with ethyl acetate as eluent and evaporation of the starting material under vacuum.

^{1}H-NMR: (300 MHz, $CDCl_3$) δ 7.62 (d, J = 2.3 Hz, 1H), 7.51 (d, J = 8.5 Hz,1H), 7.19 (s, 1H), 1.56 (s, 9H), 1.54 (s, 9H), 1.31 (s, 9H).

GC-MS: t_R = 7.32 min(1,3,5), 8.39 min (1,2,4) (EI, 70 eV): m/z = 246 [M^+], 231.

The analytical data were in agreement with literature. [225k]

1,2,4-tris(prop-1-en-2-yl)benzene **(3-31)**

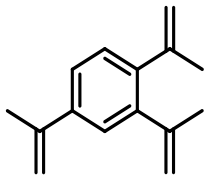

70 % yield, yellowish liquid after filtration of the crude reaction through a plug of silica gel (ethyl acetate).

^{1}H-NMR: (300 MHz, $CDCl_3$) δ 7.37 – 7.25 (m, 2H), 7.16 (d, J = 7.9 Hz, 1H), 5.38 (d, J = 0.6 Hz, 1H), 5.13 – 5.09 (m, 1H), 5.09 – 5.06 (m, 2H), 5.02 (m, 2H), 2.16 (s, 3H), 2.06 (s, 6H).

GC-MS: t_R = 7.529 min (1,2,4) (EI, 70 eV): m/z = 198 [M+], 183,168,155,141, 128, 115.

The analytical data were in agreement with literature. [250]

Trimethyl 1,2,4-benzenetricarboxylate **(3-32)**

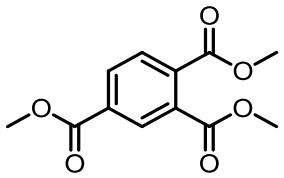

70 % yield, liquid after filtration through a plug of silica gel (ethyl acetate) and evaporation of the starting material in vacuum.

^{1}H-NMR: (300 MHz, $CDCl_3$)) δ 8.43 (d, J = 1.6 Hz, 1H), 8.20 (dd, J = 8.0, 1.7 Hz, 1H), 7.75 (d, J = 8.0 Hz, 1H), 3.96 (s, 3H), 3.94 (s, 6H).

^{13}C-NMR (75 MHz, CDCl3, δ) 168, 167, 165.5, 136.4, 132.8, 132.56, 132, 130.43, 129, 53.07, 53.00(2C)

The analytical data were in agreement with literature. [251]

1,2,4-tri-*n*-hexyl benzene **(3-33)**

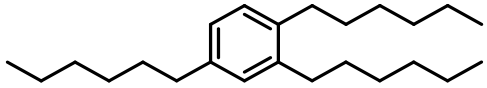

90% yield, yellowish liquid after filtration through a plug of silica gel (ethyl acetate) and evaporation of starting material in vacuum.

^{1}H-NMR: (300 MHz, $CDCl_3$) δ 7.06 (d, J = 7.5 Hz, 1H), 6.95 (m 1H), 6.83 (s, 1H), 2.66 – 2.49 (m, 6H), 1.60 (m, 4H), 1.33 (m, 20H), 0.91 (m, 9H).

^{13}C-NMR (75 MHz, $CDCl_3$): δ 140(2C), , 137.6, 129.(2C), 126, 35.3, 34(2C), 33.60(2C), 32.5, 32.0, 22.89, 23, 22.6, 22.5, 14.0.

The analytical data were in agreement with literature. [252]

1,2,4 tricyclopropyl benzene **(3-34)**

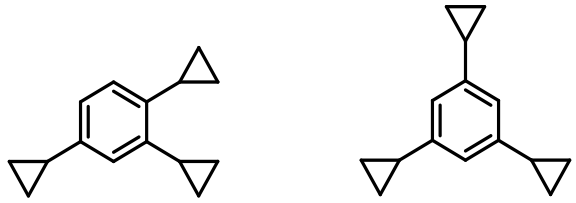

A B

An inseparable mixture of A and B was obtained in 60 % yield as white solids after filtration through a plug of silica gel (ethyl acetate) and evaporation of the starting material in vacuum.

A: ^{1}H-NMR: (300 MHz, $CDCl_3$) δ 6.80 (d, J = 1.8 Hz, 1H), 6.78 (d, J = 1.8 Hz, 1H), 6.71 (d, J = 1.6 Hz, 1H), 1.95 – 1.72 (m, 3H), 0.77 – 0.57 (m, 12H).

B: ^{1}H-NMR: (300 MHz, $CDCl_3$) δ 6.86 (s, 1H), 6.57 (s, 2H), 2.25 – 2.08 (m, 3H), 1.02 – 0.83 (m, 12H).

GC-MS: t_R = 8.845 min (A), 8.903 min (B) (EI, 70 eV): m/z = 198 [M^+], 183, 169, 155, 141, 129, 115.

The analytical data were in agreement with literature. [253]

1,2,4-Triphenyl(deuterated)benzene

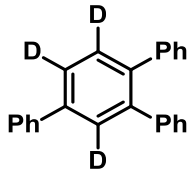

^{1}H-NMR: (300 MHz, CDCl3) δ 7.77–7.66 (m, 4H), 7.56 (d, J = 7.7 Hz, 1H), 7.50 (t, J = 7.4 Hz, 2H), 7.45–7.36 (m, 1H), 7.34–7.17 (m, 10H).

GC-MS: t_R = 12.66 min (EI, 70 eV): m/z = 309 [M^+], 292, 230, 217.

The analytical data were in agreement with literature. [254]

1,2,4-trimethyl-3,5,6-triphenylbenzene **(3-35)**

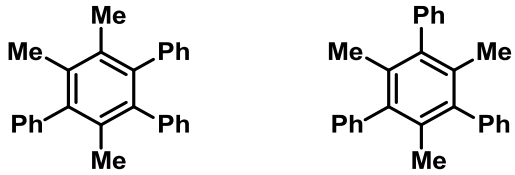

85% yield after removal of the unreacted starting material in vacuum.

^{1}H-NMR: (300 MHz, $CDCl_3$) δ 7.55 – 6.92 (m, 15H), 2.05 (s, 6H), 1.72 (s, 3H).

GC-MS(1,2,4) isomer: t_R = 12.465 min(1,2,4), 120.46 min (1,3,5) (EI, 70 eV): m/z = 348[M^+], 333, 318, 303, 289, 271, 255.

GC-MS(1,3,5) isomer: t_R = 12.645 min (1,2,4-isomer), 120.46 min (1,3,5-isomer) (EI, 70 eV): m/z = 348[M^+], 333, 318, 303, 289, 271, 255.

The analytical data were in agreement with literature.[255]

1,3,6,8-tetrahydro-2,7-dioxa-as-indacene **(3-36)**

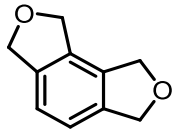

85% yield, yellowish liquid after filtration through silica gel (ethyl acetate) of the crude reaction.

^{1}H-NMR: (300 MHz, $CDCl_3$) δ 7.15 (s, 2H), 5.18–5.08 (m, 4H), 5.08–4.99 (m, 4H).

^{13}C-NMR: (75 MHz, CDCl3) δ 138.69, 132.34, 119.91, 73.45, 72.23.

GC-MS: 7.93 min, (EI, 70 eV): *m/z* = 162 [M^+], 133, 104, 77, 63, 51.

The analytical data were in agreement with literature. [245]

Diethyl 5-methyl-6-phenyl-1H-indene-2,2(3H)-dicarboxylate **(3-37)**

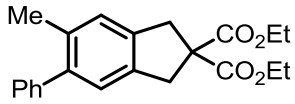

65 % yield, white solid after chromatographic SiO_2 column purification using hexanes/ethyl acetate (98:2) as eluent.

^{1}H-NMR: (300 MHz, $CDCl_3$) δ 7.48 – 7.16 (m, 5H), 7.06(s, 1H), 7.01(s, 1H), 4.17 (d, J = 7.1 Hz, 4H), 3.56 (m 4H), 2.16 (s, 3H), 1.22 (t, J = 7.1 Hz, 6H).

^{13}C-NMR: (75 MHz, CDCl3) δ 171.78(2C) , 142.13 , 140.81, 139.15, 137.53, 134.10, 129.25(2C), 128.03(2C) , 126.65, 125.92, 125.49, 61.73(2C), 60.53(2C), 40.29, 40.19, 20.47, 14.07(2).

GC-MS: 7.93 min, (EI, 70 eV): *m/z* = 162 [M^+], 133, 104, 77, 63, 51.

HRMS:(EI, m/z): found 352.16754 [M^+] (calculated 352.16944).

The analytical data were in agreement with literature. [256]

2,4,5-triphenyl toluene **(3-38)**

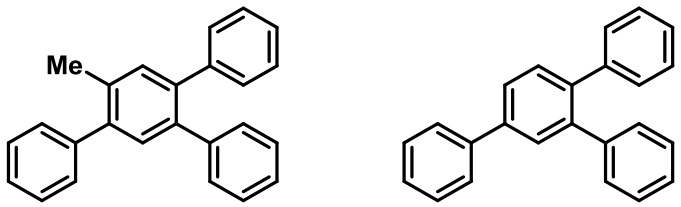

An inseparable mixture of these two compounds was obtained in 60 % yield as white solid after filtration through a plug of silica gel (ethyl acetate) and evaporation of the starting material in vacuum.

^{1}H-NMR: (300 MHz, $CDCl_3$) 7.80–7.64 (m, 4H), 7.54 (d, J = 7.7 Hz, 1H), 7.39–7.27 (m, 1H), 7.25–7.14 (m, 11H)., 1.95 (s, 3H).

GC-MS: t_R = 12.34 min (1,2,4), 12.40 min (1,3,5) (EI, 70 eV): m/z = 320 [M]

The analytical data were in agreement with literature. [257]

Conclusions and outline for the future

During this three years of PhD, we explored and tacked different problems, all of them somehow related to the concept of sustainable chemistry.

We successfully demonstrated the possibility of using $HSiCl_3$ as metal-free, reducing agent under continuous flow conditions for the preparation of selected molecules, direct precursor of APIs (Scheme 4-1), as reported in Chapter 1. We used a cheap and achiral Lewis Base for the activation of the trichlorosilane, in combination with different chiral auxiliaries(CA), in particular phenyl ethyl amine and its derivatives. When a chiral sulfoxide was employed as CA we were also able to obtain the primary amine in a complete metal free process.

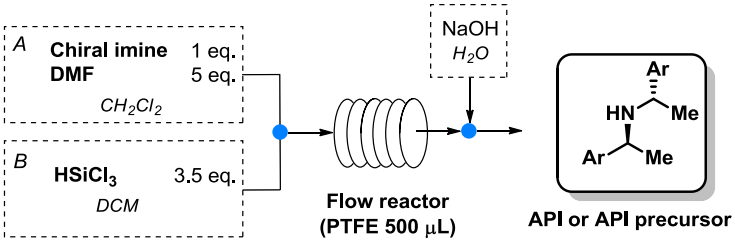

Scheme 4-1

Instead of using DMF it is also possible to use a catalytic amount of an a chiral LB for the activation of $HSiCl_3$; in this field we effectively developed a new and very efficient chiral catalyst, based on a chiral scaffold easily synthesized from readily available aminoacids. This picolinamide-based catalyst was used to perform enantioselective imine reduction, in high yields and selectivities (Scheme 4-2). We also demonstrated the possibility of using an organocatalyst at very low loading in a gram scale reaction. (Chapter 1)

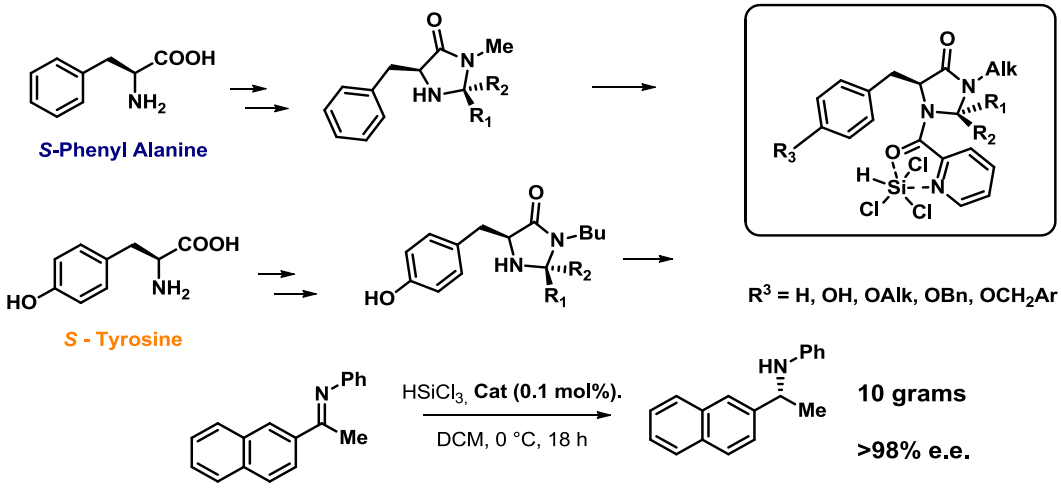

Scheme 4-2

We also explored, for the first time the use of 3D printing as technology for the preparation of meso and macro reactors for stereoselective chemical transformations. In particular we focused our attention on a stereoselective Henry reaction between different benzaldehydes and nitroethane, to obtain chiral nitro alcohols. These compounds were subsequently hydrogenated, in flow with an H-

Cube mini apparatus equipped with a Pd/C cartridge, for the synthesis of chiral amino alcohols (scheme 4-3). The *ad hoc* design of a new type of reactor allowed us to perform an all-in flow process for the precursor of norephedrine.

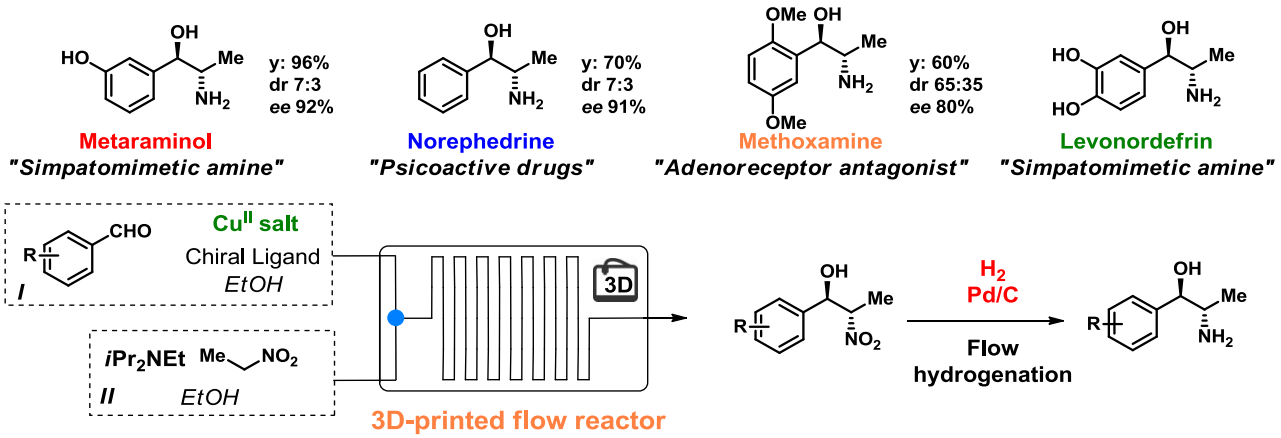

Scheme 4-3

Regarding the use of iron catalysis, we explored two different areas. First, we used a well known, and easy to handle iron cyclopentadienone-based catalyst for the stereoselective hydrogenation of chiral imines. In this case the yield that we were able to achieve were quite low and in addition only aromatic imines were successfully reduced, however we demonstrated the possibility to use this family of catalysts in this type of transformation (scheme 4-4). In our opinion, in this field the development of new chiral ligands will be crucial, to open the possibility of performing enantioselective catalytic reductions using stable iron catlaysts instead of precious metals.

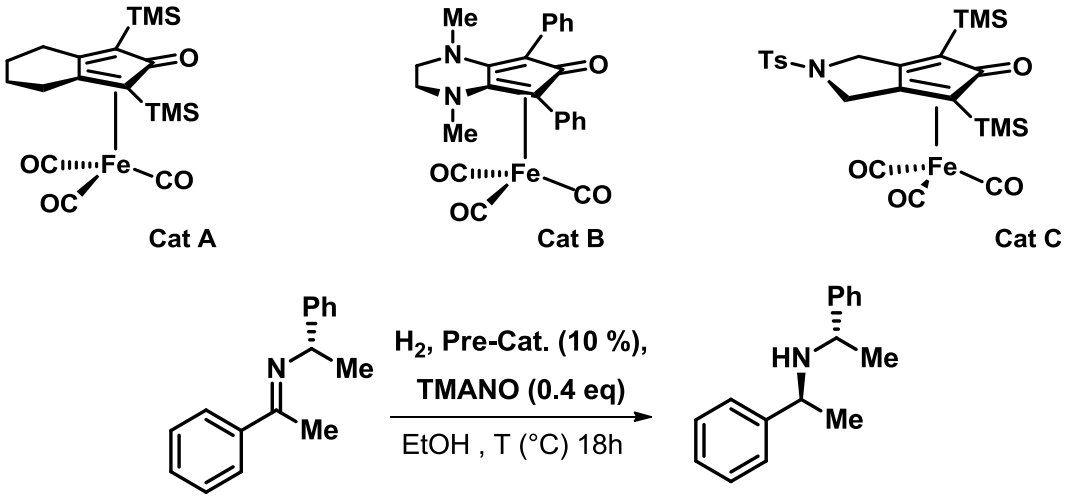

Scheme 4-4

During my stay in Regensburg university in the group of professor Axel Jacobi we also explored the use of an easy source of iron, $Fe(hmds)_2$ for alkyne trimerization reactions; in particular we demonstrated the possibility of running the reaction in the absence of any external reducing agent (scheme 4-5). However, it should be noted that the catalyst is really sensitive to air and moisture. Different alkynes were successfully trimerized with excellent yields and selectivities towards the

1,2,4 isomer; different functional groups were tolerated such as esters, cyclopropyl ring, halogens and ether.

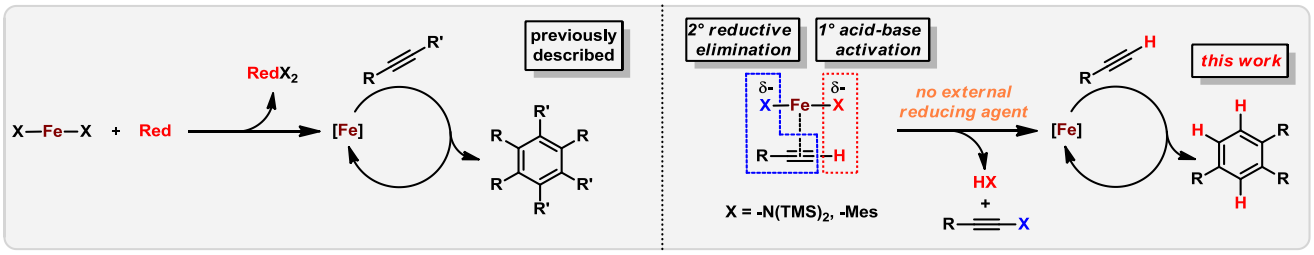

Scheme 4-5

In this field, very often the high activity of an iron catalyst is compromised by issues of low stability and necessity of a careful handling. The present study could open the wat towards new systems, in which a high reactivity meets an easy handling and storage of the catalyst.

[1]https://www.acs.org/content/acs/en/greenchemistry/what-is-green-chemistry/principles/12-principles-of-green-chemistry.html

[2]For extensive reviews on the activation of $HSiCl_3$ see: a) S. Rendler, M. Oestreich, *Synthesis* **2005**, *11*, 1727; (b)Y. Orito, M. Nakajima, *Synthesis* **2006**, *9*, 1391. For a review on hypervalent silicates-mediated reactions see: M. Benaglia, S. Guizzetti, L. Pignataro, *Coord. Chem. Rev.* **2008**, 252, 492.

[3] F. Iwasaki, O. Onomura, K. Mishima, T. Kanematsu, T. Maki, Y. Matsumura *Tetrahedron Lett.* **2001**, *42*, 2525-2527.

[4] a) S. Guizzetti, M. Benaglia, R. Annunziata, F. Cozzi, *Tetrahedron* **2009**, *65*, 6354-6363; b) S. Guizzetti,M. Benaglia, M. Bonsignore, L. Raimondi, *Org. Biomol. Chem.* **2011**, *9*, 739-743; c) A. Genoni, M. Benaglia, E. Massolo, S. Rossi, *Chem. Commun.*, **2013**, *49*, 8365-8367; d) S. Guizzetti, M. Benaglia, F. Cozzi, S. Rossi, G. Celentano, *Chirality* **2009**, *21*, 233-238; e) C. P. Barrulas, A. Genoni, M. Benaglia, A. J. Burke, *Eur. J. Org. Chem*, **2014**, 7339-7342; f) P. Barrulas, M. Benaglia, A. Burke *Tetrahedron, Asymm.*, 2014, 25, 923-935; g) A. Genoni, M. Benaglia, E. Mattiolo, Sergio Rossi, L. Raimondi, P. C. Barrulas, A. J. Burke *Tetrahedron. Lett.*, **2015**, *56*, 5752-5756, h) S. D. Fernandes, R. Porta, P. C. Barrulas, A. Puglisi, A. J. Burke, M. Benaglia *Molecules*, **2016**, *21*, 1182.

[5] S. Guizzetti, M. Benaglia, C. Biaggi, G. Celentano, *Synlett* **2010**, 134-136.

[6] D. Brenna, M. Benaglia, R. Porta, S. Fernandes, A. Burke *Eur. J. Org. Chem*, **2017**, 39.

[7] D. Brenna, M. Pirola, L. Raimondi, M. Benaglia *Bioorg. Med. Chem.*· **2017** DOI: 10.1016/j.bmc.2017.01.023.

[8] Astellas Pharma Inc., Patent: US2014/88080 A1, 2014. J.T. Colyer, N.G. Andersen, J.S. Tedrow, T.S. Soukup, M.M. Faul, *J. Org. Chem.*, **2006**, *18*, 6859.

[9] S. Rossi, R. Porta, D. Brenna, A. Puglisi, M. Benaglia, *Angew. Chem. Int. Ed.*, **2017**, *56*, 4290.

[10] D. Brenna, S. Rossi, F. Cozzi, M. Benaglia *Org. Biomol. Chem*, **2017**, *15*, 5685.

[11] For the prices of noble metals, in particular Pd see: http://www.monex.com/prods/palladium_chart.html.

[12] , D. Brenna, M. Villa, T. N. Gieshoff, F. Fischer, M. Hapke, A. Jacobi von Wangelin, *Angew. Chem. Int. Ed.* **2017**, *56*, 8451 (hot paper).

[13] a) G. Domìnguez, J. Pérez-Castells, *Chem. Soc. Rev.*, **2011**, 40, 3430; b) B. R. Galan, T. Rovis, *Angew. Chem. Int. Ed.* , **2009**, 48, 2830; c) P. R. Chopade, J. Louie, *Adv. Synth. Catal*. , **2006**, 348, 2307.

[14] Selected examples of Ru catalysed [2+2+2]: a) Y. Yamamoto, K. Hata, T. Arakawa, K. Itoh, *Chem. Commun*. **2003**, 1290. b) Y. Yamamoto, T. Arakawa, R. Ogawa, K. Itoh, *J. Am. Chem.*

Soc. **2003**, *125*, 12143; c) Y. Yamamoto, J. Ishii, H. Nishiyama, K. Itoh, *J. Am. Chem. Soc.* **2004**, *126*, 3712; d) Y. Yamamoto, J. Ishii, H. Nishiyama, K. Itoh, *J. Am. Chem. Soc*. **2005**, *127*, 9625; e) F. Xu, C. Wang, X. Li, B. Wan, *ChemSusChem* **2012**, *5*, 854.

[15] Selected examples of Rh catalysed [2+2+2]: a) R. Grigg, R. Scott, P. Stevenson, *Tetrahedron Lett.* **1982**, *23*, 2691; b) H. Kinoshita, H. Shinokubo, K. Oshima, *J. Am. Chem. Soc.* **2003**, *125*, 7784; c) K. Tanaka, G. Nishida, A. Wada, K. Noguchi, *Angew. Chem. Int. Ed.* **2004**, *43*, 6510; d) H. Hara, M. Hirano, K. Tanaka, *Org. Lett.*, **2008**, *10*, 2537.

[16] Selected examples of Co catalysed [2+2+2]: a) K. P. C. Vollhardt, *Acc. Chem. Res.* **1977**, *10*, 1 – 8; b) R. L. Funk, K. P. C. Vollhardt, *J. Chem. Soc. Chem. Commun.* **1976**, 833; c) R. L. Funk, K. P. C. Vollhardt, *J. Am. Chem. Soc.* **1977**, *99*, 5483; d) R. L. Hillard, III, K. P. C. Vollhardt, *J. Am. Chem. Soc.* **1977**, *99*, 4058; e) Hilt, T. Volger,W. Hess, F. Galbiati, *Chem. Commun.* **2005**,1474 – 1475; f) I. Thiel, H. Jiao, A. Spannaenberg, M. Hampke *Chem. Eur. J.* **2013**, *45*, 2003.

[17] Selected examples of Ir catalysed [2+2+2]: a) R. Takeuchi, M. Kashio, *Angew. Chem. Int. Ed. Engl.***1997**, *36*, 263 – 266; b) R. Takeuchi, *Synlett* **2002**, 1954 – 1965; c) R. Takeuchi, Y. Akiyama, *J. Organomet. Chem.* **2002**, *651*, 137 – 145.

[18] Selected examples of Ni catalysed [2+2+2]: a) W. Reepe, J. Liebigs, *Ann. Chem.* **1948**, 560, 1. b) F. Teplý, I. G. Stará, I. Starý, A. Kollárovič, D. Šaman, L. Rulíšek, P. Fiedler, *J. Am. Chem. Soc.* **2002**, *124*, 9175; c) K. R. Deaton, M. S. Gin, *Org. Lett.* **2003**, *5*, 2477; d) Y. Zhong, N. A. Spahn R. M. Stolley, H. M. Minh, J. Louise, *Synlett* **2015**, *26*, 307.

[19] Selected examples of Pd catalysed [2+2+2]: V. Gevorgyan, U. Radhakrishnan, A. Takeda, M.Rubina, M. Rubin, Y. Yamamoto, *J. Org. Chem.* **2001**, *66*, 2835 – 2841; b) D. Pena, D. Perez, E. Guitian, L. Castedo, *Eur. J. Org.Chem.* **2003**, 1238.

[20] Selected examples of Ti catalysed [2+2+2]: a) O.V. Ozerov, F. T. Ladipo, B. O. Patrick, *J. Am. Chem. Soc.* **1999**, *121*, 7941; b) M. J. Sung, J. Pang, S. Park, J. K. Cha, *Org. Lett.* **2003**, *5*, 2137.

[21] N. Yoshikai, S.-L. Zhang, K.-I. Yamagata, H. Tsuji, E. Nakamura, *J. Am. Chem. Soc.* **2009**, *131*, 4099.

[22] I. Bauer, H.-J. Knölker, *Chem. Rev.* **2015**, *115*, 3170.

[23] W. Hüberl, C. Hoogzand C. *Chem. Ber.* **1960**, *93*, 103.

[24] a) N. Saino, D. Kogure, S. Okamoto, *Org. Lett.* **2005**, 7, 3065; b) N. Saino, D. Kogure, K. Kase, S. Okamoto, J. *Organomet. Chem.* **2006**, 691, 3129.

[25] A. Fürstner, K. Majima, R. Martín, H. Krause, E. Kattnig, R. Goddard, C. W. Lehmann *J. Am. Chem. Soc.* **2008**, *130*, 1992.

[26] Y. Liu, X. Yan, N. Yang, C. Xi *Catal. Commun.* **2011**, *12*, 489.

[27] H. Chowdhury, N. Chatterjee, A. Goswami *Eur. J. Org. Chem.* **2015**, 7735.

[28] M. I. Lipschutz, T. Chantarojsiri, Y. Dong, T. D. Tilley *J. Am. Chem. Soc.* **2015**, *137*, 6366.

[29] Examples of other iron catalysed 2+2+2 reaction for heterocycles and benzene rings formations: a) C. Wang, X. Li, F. Wu, B. Wan, *Angew. Chem. Int. Ed.* **2011**, *50*, 7162; b) K. Nakajima, W. Liang, Y. Nishibayashi, *Org. Lett.* **2016**, *18*, 5006; c) N. A. Spahn, M. H. Nguyen, J. Renner, T. K. Lane, and J. Louie, *J. Org. Chem.* **2017**, *82*, 234; d) V. Richard, M. Ipouck, D. S. Mérel, S. Gaillard, R. J. Whitby, B. Witulski and J. Renaud, *Chem. Commun.*, **2014**, *50*, 593; e) L. Ilies, A Matsumoto, M. Kobayashi, N. Yoshikai, E. Nakamura, *Synlett.* **2012**, *23*, 2381; e) M. Minakawa, T. Ishikawa, J. Namioka, S. Hirooka, B. Zhou, M. Kawatsura, *RSC Adv.*, **2014**, *4*, 41353; f) B. R. D'Souza, T. K. Lane, J. Louie, *Org. Lett.* **2011**, *13*, 2936; g) S. Karpiniec, D. S. McGuinness, G. J. P. Britovsek, J. Pate, *Organometallics* **2012**, *31*, 3439; h) K. Nakajima, S. Takata, K. Sakata, Y. Nishibayashi *Angew. Chem. Int. Ed.* **2015**, *54*, 7597; i) C. Wang, D. Wang, F. Xu, B. Pan, B. Wan, *J. Org. Chem.* **2013**, *78*, 3065; j) B. A. Frazier, V. A. Williams, P. T. Wolczanski, S. C. Bart, K. Meyer, T. R. Cundari, E. B. Lobkovsky, *Inorg. Chem.* **2013**, *52*, 3295; k) C. Breschi, L. Piparo, P. Pertici, A. M. Caporusso, G. Vitulli, *J. Organomet. Chem.* **2000**, *607*, 57.

[30] R. A. Andersen, K. Faegri, J. C. Green, A. Haaland, M. F. Lappert, W.-P. Leung, *Inorg. Chem.* **1988**, *27*, 1782.

[31] T. N. Gieshoff, U. Chakraborty, **M. Villa**, and A. J. Wangelin *Angew. Chem. Int. Ed.* **2017**, *56*,3585 –3589

[32] Selected recent examples: a) M. I. Lipschutz, T. Chantarojsiri, Y. Dong, T. D. Tilley, *J. Am. Chem. Soc.* **2015**, *137*, 6366; b) L. C. H. Maddock, T. Cadenbach, A. R. Kennedy, I. Borilovic, G. Aromí, E. Hevia, *Inorg. Chem.* **2015**, *54*, 9201; c) T. Hatakeyama, R. Imayoshi, Y. Yoshimoto, S. K. Ghorai, M. Jin, H. Takaya, K. Norisuye, Y. Sohrin, M. Nakamura, *J. Am. Chem. Soc.* **2012**, *134*, 20262; d) J. Yang, T. D. Tilley, *Angew. Chem. Int. Ed.* **2010**, *49*, 10186; e) J. Yang, M. Fasulo, T. D. Tilley, *New J. Chem.* **2010**, *34*, 2528.

[33] Reported by Dr. Vittorio Farina in ISPROCHEM **2017**, file:///C:/Users/Davide/Desktop/ISPROCHEM/open_me.html

[34] The Top Pharmaceuticals That Changed The World Vol. 83, Issue 25 (6/20/05), Chemical and eng. news

[35] M. Reist, P. A. Carrupt, E. Francotte, B. Testa *Chem. Res. Toxicol.* **1998**, *11*, 1521 - 1528

[36] Book of Jonahm, Chapther 4 verse 11.

[37] M. Echelbaum, A. Gross *Adv. Drug. Res.* **1996**, *28*, 1 -64.

[38] J. A. Bristol, A. M. Doherty "To Market, to market in annual reports in medicinal chemistry, 25-36, academic press. San Diego, California, 1990 – 2001.

[39] J. Caldwell *Modern Drug. Discov.* **1999**, *2*, 51-60.

[40] http://www.mcc-sci.com/pharma_profiling.htm

[41] I. Agranat, H. Caner, J. Caldwell *Nature Rev. drug discovery*, **2002**, *1*, 753- 768.

[42] http://www.ich.org/products/guidelines.html

[43] S. L. Lee, T. F. O'Connor, X. Yiang, C. N. Cruz, S. Chatterjee, R. D. Madurawe, C. M. V. Moore, L. X. Yu, J. Woodcock J. Pharm. Innov. **2015**,*10*, 191.

[44]

[45] C. J. Mallia, I. R. Baxendale, *Org. process. Res. Dev.* **2016**, *20*, 327.

[46] B. J. Reizman, K. F. Jensen, *Acc. Chem. Res.* **2016**, *49*, 1786.

[47]For two recent review see: a) R. Porta, M. Benaglia, A. Puglisi *Org. Process Res. Dev.*, **2016**, *20*, 2–25; b)B. Guntmann, D. Cantillo, O. C. Kappe, Angew. Chem. Int. Ed. 2015, 54, 6688-6728.

[48] a) B. L. Trout *et al. Angew. Chem. Int. Ed.***2013**, *52*, 12359; b) K. F. Jensen *et al., Org. Process Res. Dev.* **2014**, *18*, 402.

[49] A. Adamo, T. F. Jamison, F. F. Jensen *et al. Science* **2016**, 352, 61.

[50] a) V. Hessel *et al. ChemSusChem***2013**, *6*, 746; b) J. Wegner, S. Ceylan, A. Kirschning, *Adv. Synth. Catal.* **2012**, *354*, 17.

[51] Chiral Amine Synthesis: Methods, Developments and Applications (Ed.: T. C. Nugent), Wiley-VCH, Weinheim, **2010**.

[52] Recent general reviews on asymmetric hydrogenation: a) A. M. Palmer, A. Zanotti-Gerosa, Current Opinion *in Drug Discovery and Development*, **2010**, *13*, 698; b) G. Shang, W. Li, X. Zhang. Transition Metal-Catalyzed Homogeneous Asymmetric Hydrogenation, in: Catalytic Asymmetric Synthesis, 3rd ed., I. Ojima Ed., Wiley, Hoboken, **2010**; c) for a special issue on hydrogenation and transfer hydrogenation see: M. J. Krische, Y. Sun, Eds. *Acc. Chem. Res.* **2007**, *40*, *1237*-1419.

[53] For reviews on organocatalyzed enantioselective reductions see: a) M. Benaglia, A. Genoni, M. Bonsignore, Enantioselective organocatalytic reductions in Stereoselective Organocatalysis: From C-C to C-heteroatom bond formation, **(**Ed. R. Rios Torres) Wiley, **2012**; b) S. Rossi, M. Benaglia, E. Massolo, L. Raimondi, Catal. Science Technol. **2014**, 9, 2708-2723.

[54] X. Lianhong, K. Ravi "Trichlorosilane" Encyclopedia of Reagents for Organic Synthesis, **2006**. doi:10.1002/047084289X.rt213.pub2

[55] For a review on HSiCl3 mechanism and reactivity see: S. Denmark, E. Wynn *J. Am. Chem. Soc.* **2001**, *123*, 6199.

[56] S. Guizzetti, M. Benaglia, S. Rossi, *Org. Lett.* **2009**, *11*, 2928-2932.

[57] a)S. Kobayashi, K. Nishio, *Tetrahedron Lett.* **1993**, *34*, 3453-3456; b) S. Kobayashi, K. J. Nishio, *Org. Chem.* **1994**, *59*, 6620-6628.

[58] S. Guizzetti, M. Benaglia, C. Biaggi, G. Celentano, *Synlett* **2010**, 134-136.

[59] S. Guizzetti, M. Benaglia, *Eur. J. Org. Chem.* **2010**, 5529-5541; S. Jones C.J. A. Warner, *Org. Biomol. Chem.* **2012**, *10*, 2189-2200.

[60] S. Kobayashi, M. Yasuda and I. Hachiya, *Chem. Lett.* **1996**, 407-408.

[61] F. Iwasaki, O. Onomura, K. Mishima, T. Kanematsu, T. Maki, Y. Matsumura, *Tetrahedron Lett.* **2001**, *42*, 2525-2527.

[62] A. V. Malkov, A. Mariani, K. N. MacDougal, P. Kočovský, *Org. Lett.* **2004**, 6, 2253-2256.

[63] Selected picolinamides catalysts: a) O. Onomura, Y. Kouchi, F. Iwasaki, Y. Matsumura, *Tetrahedron Lett.* **2006**, *47*, 3751-3754; b) H. Zheng, J. Deng, W. Li, X. Zhang, *Tetrahedron Lett.* **2007**, *48*, 7934-7937; c) S. Guizzetti, M. Benaglia, R. Annunziata, F. Cozzi, *Tetrahedron* **2009**, *65*, 6354-6363; d) S. Guizzetti, M. Benaglia, S. Rossi, *Org. Lett.* **2009**, *11*, 2928-2931; e) Y. Jiang, X. Chen, Y. Zheng, Z. Xue, C. Shu, W. Yuan, X. Zhang, *Angew. Chem. Int. Ed.* **2011**, 50, 7304-7307; f) Y. Jiang, X. Chen, X. Hu, C. Shu, Y. Zhang, Y. Zheng, C. Lian, W. Yuan, X. Zhang, *Adv. Synth. Catal.* **2013**, *355*, 1931-1936; g) A. Genoni, M. Benaglia, E. Massolo, S. Rossi, *Chem. Commun.* **2013**, *49*, 8365-8367.

[64] O. Onomura, Y. Kouchi, F. Iwasaki, Y. Matsumura, Tetrahedron Lett. **2006**, *47*, 3751.

[65] S. Guizzetti, M. Benaglia, European Patent Application **November 30 2007**; PCT/EP/2008/010079, nov. 27, **2008**. WO2009068284-A2, 2009-06-04.

[66] H. Zheng, J. Deng, W. Lin, X. Zhang, *Tetrahedron Lett.* **2007**, *48*, 7934.

[67] Guizzetti, S.; Benaglia, M.; Bonsignore, M.; Raimondi, L., *Org. Biomol. Chem.* **2011**, *9*, 739-743.

[68] A. Genoni, M. Benaglia, E. Massolo, S. Rossi, *Chem. Commun.*, **2013**, *49*, 8365-8367.

[69] S. Guizzetti, M. Benaglia, F. Cozzi, S. Rossi, G. Celentano, Chirality **2009**, 21, 233-238.

[70] a) C. P. Barrulas, A. Genoni, M. Benaglia, A. J. Burke *Eur Joc*, **2014**, 7339-7342; b) P. Barrulas, M. Benaglia, A. Burke *Tetrahedron, Asymmetry*, **2014**, *25*, 923-935; c) A. Genoni, M. Benaglia, E. Mattiolo, S. Rossi, L. Raimondi, P. C. Barrulas, A. J. Burke *Tetrahedron. Lett.*, **2015**, *56*, 5752-5756.

[71] S. D. Fernandes, R. Porta, P. C. Barrulas, A. Puglisi, A. J. Burke, M. Benaglia *Molecules*, **2016**, *21*, 1182-1190.

[72] a) D. Brenna, M. Benaglia, R. Porta, S. D. Fernandes, A. J. Burke *Eur. J. Org. Chem*, **2017**, 1, 39-44.; b) D. Brenna, M. Pirola, L. Raimondi, A. J. Burke, M. Benaglia *Bioorg. Med. Chem.*, **2017**, DOI: 10.1016/j.bmc.2017.01.023; c) D. Brenna, R. Porta, E. Massolo, L. Raimondi, M. Benaglia *ChemCatChem*, **2017**, *9*, 941-945.

[73] For recent reviews on chiral amine synthesis: a) T. C. Nugent, M. El-Shazly, *Adv. Synth. Catal.* **2010**, *352*, 753–819; b) N. Fleury-Br¦geot, V. de La Fuente, S. Castillýn, C. Claver, *ChemCatChem* **2010**, *2*, 1346–1371; c) for a review on fluorinated chiral compounds, including amines: J. Nie, H.-C. Guo, D. Cahard, J.-A. Ma, *Chem. Rev.* **2011**, *111*, 455-529.

[74] For a pioneer work on the use of a-phenyl-ethylamine as auxiliary in imine reduction see: a) C. G. Overbergenr, N. P. Marullo, R. G. Hiskey *J. Am. Chem. Soc.* **1961**, *83*, 1374-1378; for other, representative metal-catalyzed reductions of N-1-phenylethyl imines see: b) M. B. Eleveld, H. Hogeveen, E. P. Schudde , *J. Org. Chem.* **1986**, *51*, 3635-3638; c) B. C. Ranu, A.

Sarkar, A. Majee, *J. Org. Chem.* **1997**, *62*, 1841-1842; d) for a recent contribution on a sequential reductive amination-hydrogenolysis see T. C. Nugent, D. E. Negru, M. El-Shazly, D. Hu, A. Sadiq, A. Bibi, *Adv. Synth. Catal.* **2011**, *353*, 2085–2092 and references cited; for organocatalytic reductions of chiral imines, see: e) M. Fujii, T. Aida, M. Yoshihara, A. Ohno *Bull Chem. Soc. Jpn.* **1989**, *62*, 3845-3847; f) J. M. Farrell, Z. M. Heiden, D. W. Stephan, *Organometallics* **2011**, *30*, 4497-4500; g) S. Guizzetti, M. Benaglia, S. Rossi, *Org. Lett.* **2009**, *11*, 2928-2932;

[75] Reviews: a) J.-H. Xie, S.-F. Zhu, Q.-L. Zhou, *Chem. Rev.* **2011**, *111*, 1713–1760; b) D.-S. Wang, Q.-A. Chen, S.-M. Lu, Y.-G. Zhou, *Chem. Rev.* **2012**, *112*, 2557–2590; for a recent contribution on the catalytic synthesis of N-alkyl chiral amines, see: V. N. Wakchaure, P. S. J. Kaib, M. Leutzsch, B. List, *Angew. Chem. Int. Ed.* **2015**, *54*, 11852–11856.

[76] Recent reviews: a) I. Atodiresei, C. Vila, M. Rueping, *ACS Catal.* **2015**, *5*, 1972-1985; b) A. Puglisi, M. Benaglia, R. Porta, F. Coccia, *Current Organocatalysis* **2015**, *2*, 79-101; c) R. Munirathinam, J. Huskens, W. Verboom, *Adv. Synth. Catal.* **2015**, *357*, 1093-1123; d) C. Rodríguez-Escrich, M. A. Pericàs, *Eur. J. Org. Chem.* **2015**, 1173-1188; some very recent examples of continuous flow synthetic methods: e) J-S. Poh, D. N. Tran, C. Battilocchio, J. M. Hawkins, S. V. Ley, *Angew. Chem. Int. Ed.* **2015**, *54*, 7920-7923; f) D. C. Fabry, M. A. Ronge, M. Rueping, *Chem. Eur. J.* **2015**, *21*, 5350-5354; g) D. N. Tran, C. Battilocchio, S-B. Lou, J. M. Hawkins, S. V. Ley, *Chem. Sci.* **2015**, *6*, 1120-1125.

[77] For examples of diastereoselective reductions aimed to the synthesis of Rivastigmine, see: a) ref. 6b; b) M. Hu, F.-L. Zhang, M. H. Xie, *Synth. Commun.* **2009**, *39*, 1527-1533; c) V. R. Arava, L. Gorentla, P. K. Dubey, *Der Pharma Chemica* **2011**, *3*, 426-433.

[78] http://thalesnano.com/products/h-cube-series/H-Cube_Mini

[79] H., Meng, Z. Fu-Li, X. Mei-Hua *Synthetic Communications*, **2009**, *39*, 1527-1533

[80] R. K. Henderson, C. Jemenez-Gonzalez, D. C. Constable, S. R. Alston, G. G. A. Inglis, G. Fisher, J. Sherwood, S. P. Binks, A. D. Curzons, *Green Chem.* **2011**, *13*, 854-862.

[81] For the application of flow chemistry for multistep organic synthesis see: a) S. Newton, C. F. Carter, C. M. Pearson, L. C. Alves, H. Lange, P. Thansandote, S. V. Ley, *Angew. Chem. Int. Ed.* **2014**, *53*, 4915-4919; b) J. Wegner, S. Ceylan, A. Kirschning, *Adv. Synth. Catal.* **2012**, *354*, 17-57; c) M. Baumann, I. R. Baxendale, S. V. Ley, *Mol. Divers.* **2011**, *3*, 613-630. For some other recent, representative contributions see also: d) M. Chen, S. Buchwald, *Angew. Chem. Int. Ed.* **2013**, *52*, 4247-4250 and e) I. R. Baxendale, S. V. Ley, A. C. Mansfield, C. D. Smith, *Angew. Chem. Int. Ed.* **2009**, *48*, 4017-4021.

[82] Reviews on the synthesis of APIs under continuous flow conditions: a) B. Gutmann, D. Cantillo, C. O. Kappe, *Angew. Chem. Int. Ed.* **2015**, *54*, 6688-6728; b) R. Porta, M. Benaglia, A. Puglisi, *Org. Process Res. Dev.* **2016**, *20*, 2-25.

[83] Review on continuous flow hydrogenation: P. J. Cossar, L. Hizartzidis, M. I. Simone, A. McCluskey, C. P. Gordon, *Org. Biomol. Chem.* **2015**, *13*, 7119-7130.

[84] a) M. S. Sudhir, R.V. Nadh, *Drug Invent. Today*, **2013**, *5*, 133–138. b) M. Fernández, S. Negro, K. Slowing, A. Fernández-Carballido, E. Barcia, *Int. J.Pharm.*, **2011**, 271–280. c) O. Weinreb, T. Amit, P. Riederer, M.B.H. Youdim, *S.A. in: International Review of Neurobiology*, Academic Press: NewYork, **2011**. pp. 281.

[85] M. Fernández, E. Barcia, A. Fernández-Carballido, L. Garcia, K. Slowing, S. Negro, *Int. J. Pharm.*, **2012**, 266–278.

[86] D.R.P. Guay,; *Am. J. Geriatr. Pharmacother.* **2006**, 330–346.

[87]For selected examples of kinetic resolution see: a)L. Selic, WO Patent 064 216 ,2011, to LEK Pharmaceuticals b) M.B.H. Youdim, J.P.M. Finberg, R. Levy, J. Sterling, D. Lerner, T. Berger-Paskin, H. Yellin, A. Veinberg, US Patent 5 532 415 , **1996**, to Teva PharmaceuticalIndustries, Ltd. and Technion Research and Development Foundation Ltd.; c)R. Lidor, E. Bahar, WO Patent 21 640 , 1996, to Teva Pharmaceutical Industries,Ltd. and Lemmon Company; Patent 068 376 ,2002, to ISP Finetech Ltd. d) C.-H. Yao, T.-T. Chen, US Patent 0 218 361 , 2011, to Everlight USA, Inc.; e) A.A. Thanedar, S.A. Deshmukh, S.S. Zope, L.M. Kelkar, J.P. Koilpillai,; J.M. Gajera, WO Patent 048 612 ,2011, to Glenmark Generics Limited. For selected examples of enzymatic preparation see: f) H. Leisch, S. Grosse, H. Iwaki, Y. Hasegawa, P.C.K. Lau, *Can. J. Chem.*, **2012**, 39–45. g) M.S. Malik, E-S. Park; J-S Shin, *Green Chem.*, **2012**, *14*, 2137–2140. c) M. Päiviö, P. Perkiö, L.T. Kanerva, *Tetrahedron Asymm.*, **2012**, *191*, 230–236. h) G. Ma, Z. Xu, P. Zhang, J. Liu, X. Hao, J. Ouyang, P. Liang, S. You, X. Jia, *Org. ProcessRes. Dev.*, **2014**, *5*, 1169–1174. For selected examples of stereoselective reduction of ketones see: i) B. Clapham, C.-W. Cho, K.D. Janda, *J. Org. Chem.*, **2001**, *66*, 868–873. j) A.C. Spivey, D.P.Leese, F. Zhu, S.G. Davey, R.L. Jarvest, *Tetrahedron* , **2004**, *60*, 513–4525. k) H. Shiigi; H. Mori; T. Tanaka, Y. Demizu, O. Onomura, *Tetrahedron Lett.* **2008**, *49*, 5247–5251. l) C.I. Sheppard, J.L. Taylor, S.L. Wiskur, *Org. Lett.*, **2011**, *13*, 3794–3797. For catalytic and stereoselective metal based methodologies see: m) H. Brunner, R. Becker, S. Gauder, *Organometallics*, **1986**, *5*, 739–746. n) I. Takei, Y. Nishibayashi, Y. Ishii, Y. Mizobe, S.Uemura, M. Hidai, *Chem. Commun.*, **2001**, *44*, 2360–2361.

[88] sdafdsad

[89] C. Lu, Q. Zhou, J. Yan, Z. Du, L. Huang, X. Li, *Eur. J. of Med. Chem.* ,**2013** , *62*, 745-753

[90] R. Glennon, A. Ismaiel, M. Smith, J., D. Yousif, M. El-Ashmawy, M. Herndon, J. L. Fischer, J. B. Howie, K. J. B. Served, *A. C. J. Med. Chem.*, **1991**, *34*, 1855-1859.

[91] A. Gutman, M. Etinger, G. Nisnevich, F. Polyak, *Tetrahedron: Asymmetry*, **1998**, *9*, 4369–4379

[92] Astellas Pharma Inc., Patent: US2014/88080 A1, 2014. J.T. Colyer, N.G. Andersen, J.S. Tedrow, T.S. Soukup, M.M. Faul, *J. Org. Chem.*, **2006**, 6859–6862.

[93] D. Brenna, S. Rossi, F. Cozzi and M. Benaglia, OBCDOI: 10.1039/c7ob01123g

[94] Porta, R.; Benaglia, M.; Puglisi, A. *Org. Process Res. Dev.* **2016**, *20*, 2-25.

[95] For a review on low-loading chiral organocatalysts see: F. Giacalone, M. Gruttadauria, P. Agrigento, R. Noto, *Chem. Soc. Rev.*, **2012**, *41*, 2406-2447.

[96] See S. G. Ouellet, J. B. Tuttle, D.W. C. Mac-Millan, *J. Am. Chem. Soc*, **2005**, *127*, 32 and references cited.

[97] R.Porta, M. Benaglia, R. Annunziata, A. Puglisi, G. Celentano *Adv. Synth. Cat* DOI: 10.1002/adsc.201700376

[98] As reported in Scheme 1-15, also chiral picolinamides 3a and 3b promoted the reduction with excellent results, but they proofed to be catalysts of less general applicability, compared to 3c, that was selected as catalyst of choice.

[99] The definition of ACE was recently proposed in the attempt to compare and evaluate the efficiency of different catalysts, considering the level of enantioselectivity and the yield guaranteed by the catalyst, the molecular weight of the product and of the catalysts itself. See: S. El-Fayyoumy, M. H. Todd, C. J. Richards, Beilstein *J. Org. Chem.* **2009**, *5*, 67.

[100] S. Jones, C. J. A. Warner, *Org Biomol. Chem.*, **2012**, *10*, 2189-2200.

[101] W. Yuan, Z. Shang, X. Qiang, Z. Tan, Y. Deng, *Res Chem Intermed* ,**2014**, *40*, 787.

[102] M. K. Sethi, S. R. Bhandya, A. Kumar, N. Maddur, R. Shukla, V.S.N. J. Mittapalli *Journal of Molecular Catalysis B: Enzymatic*, **2013**, *91*, 87.

[103] M. B. Eleveld, H. Hogeveen, E. P. Schudde *J. Org. Chem.*, **1986**, *51* 3635.

[104] BASF AKTIENGESELLSCHAFT Patent: WO2006/136538 A1, 2006 ;

[105]W. Ou,; S. Espinosa; H. J. Melendez; S. M. Farre; J. L. Alvarez; V. Torres; I. Martinez; K. Santiago, M.; M. O.-Marciales, *J. Org. Chem*, **2013** , 78, p. 5314.

[106] M. Atobe, N. Yamazaki, C. Kibayashi J. Org. Chem., **2004**, 69, 17.

[107] D. R. J. Hose, M. F. Mahon, K. C. Molloy, T. Raynham, M. Wills, *J. Chem. Soc., Perkin Trans. 1* **1996**, 691–703.

[108] H. C. Hansen, S. L. Buchwald, *Org.Lett.* **2000**, 2, 713-715.

[109] X. Verdaguer, U. E. W. Lange, S. L. Buchwald, *Angew. Chem. Int. Ed.*, **1998**, *37*, 1103-1107.

[110] A. L. Gutman, M. Etinger, G. Nisnevich, F. Polyak, *Tetrahedron Asymm.*, **1998**,4369–4379.

[111] P. Martins, K. Mihail, K. Toms, S. Krill, S**.** J. Edgars, *Org. Chem.* , **2014** , *79*, 3715-3724.

[112] A. V. Malkov, V. Kvetoslava, S. Sigitas, P. Kocovsky, *J. Org. Chem.*, **2009** , *74*, 5839–5849.

[113] J. Ramon, C. J. Luis, *Chem. Comm.*, **2013** , *49*, 9194 - 9196

[114] O. Pablo, D. Guijarro, G. Kovacs, A. Lled, G. Ujaque, M. Yus, *Chem. Eur. J.*, **2012**, *18*, 1969– 1983.

[115] L. Chuanjun, Z. Qi, Y. Jun, D. Zhiyun, H. Ling, L. Xingshu, *Eur. J. Med. Chem.*, **2013**, *62*, 745–753.

[116] M. Lourdes, A. M. Rodriguez, G. Rosell, B. Pilar, M. G. Angel, *Org. Bio. Chem.*, **2011** , *9*, 8171- 8177

[117]C. Francisco, B. Pilar, M. G. Angel, *Tetrahedron Asymmetry*, **2000** , *11*, 2705 – 2717.

[118] K. A. Ahrendt, C. J. Borths, D. W. C. MacMillan, *J. Am. Chem. Soc.*, **2000**, *122*, 4243.

[119] N. Vale, F. Nogueira, V. E. Rosario, P. Gomes, R. Moreira, Eur. *J. Med. Chem.* **2009**, *44*, 2506.

[120] C. M. Holland, J. B. Metternich, C. Daniliuc, W. B. Schweizer, R. Gilmour, *Chem Eur. J.* **2015**, *21*, 10031.

[121] A. P. P. Chevrier, F. Cantagrel, K. Le Jeune, C. Philouze, P. Y. Chavant *Tetrahedron: Asymmetry* **2006**, *17*, 1969.

[122] ICIPatent: DE2007751 , 1970 ;Chem.Abstr., 1970 , vol. 73, # 120318

[123] R. Porta, M. Benaglia, V. Chiroli, F. Coccia, A. Puglisi, *Israel Journal of Chemistry*, **2014** , *54*, 381.

[124] X.W. Liu, Y. Yan, Y. Q. Wang, C. Wang, J. Sun, Chem. Eur. J. **2012**, 18, 9204.

[125] A. V. Malkov, M. Figlus, S. Stoncius, P. Kocovsky, *J. Org. Chem.* **2006**, *72*, 1315.

[126] S. Hoffmann, A. M. Seajad, B. List, *Angew. Chem. Int. Ed.* **2005**, *44*, 7424.

[127] R. I. Storer, D. E. Carrera, Y. Ni, D. W. C. MacMillan, *J. Am. Chem. Soc.* **2005**, *128*, 84.

[128] A. Chelouan, R. Recio, L. G., Borrego, E. Alvarez, N. Khiar, I. Fernandez *Org. Lett.* **2016**, *18*, 3258-3261.

[129] Franc¸ois-Moana Gautier, S. Jones, X. Lia, S. J. Martin *Org. Biomol. Chem.*, **2011**, *9*, 7860.

[130] Patent US5121329 A.

[131] https://www.mediaworld.it/mw/stampanti-3d

[132] Jones D, (writing as Daedalus) Ariadne column. *New Sci* **1974.**

[133] US Patent 4041476.

[134] U.S. Patent 4,575,330.

[135] https://www.nasa.gov/topics/technology/3-D-printing/archive.html

[136] https://www.fieldready.org/

[137] J. M. Pearce, *Science* **2012**, *337*, 1303-1304.

[138] C. Zhang, N. C. Anzalone, R. P. Faria, J. M. Pearce, *Plos One* **2013**, *8*, 59840.

[139] Halford, B., Chem. Eng. News **2004,** *92*, 32–33.

[140] B. Wijnen, E. J. Hunt, G. C. Anzalone, J. M. Pearce, Plos One **2014**, *9*, 107216.

[141] a) P. J. Kitson, M. D. Symes, V. Dragone, L. Cronin, *Chem Sci* **2013**, *4*, 3099; b) M. D. Symes, P. J. Kitson, J. Yan, C. J. Richmond, G. J. Cooper, R. W. Bowman, T. Vilbrandt, L. Cronin, *Nat Chem* **2012**, *4*, 349-354.

[142] G. Chisholm, P. J. Kitson, N. D. Kirkaldy, L. G. Bloor, L. Cronin, *Energ Environ Sci* **2014**, *7*, 3026-3032.

[143] J. S. Mathieson, M. H. Rosnes, V. Sans, P. J. Kitson, L. Cronin, *B. J. Nanotech.* **2013**, *4*, 285-291.

[144] a) J. L. Erkal, A. Selimovic, B. C. Gross, S. Y. Lockwood, E. L. Walton, S. McNamara, R. S. Martin, D. M. Spence, Lab on a chip **2014**, 14, 2023-2032; b) B. Y. Ahn, E. B. Duoss, M. J. Motala, X. Guo, S. I. Park, Y. Xiong, J. Yoon, R. G. Nuzzo, J. A. Rogers, J. A. Lewis, Science **2009**, 323, 1590-1593.

[145] M. Lee, B. Wu, in Computer-Aided Tissue Engineering, Vol. 868 (Ed.: M. A. K. Liebschner), Humana Press, **2012**, pp. 257-267.

[146] E. N. Antonov, V. N. Bagratashvili, M. J. Whitaker, J. J. A. Barry, K. M. Shakesheff, A. N. Konovalov, V. K. Popov, S. M. Howdle, *Advanced Materials* **2005**, *17*, 327-330.

[147] a) S. Bose, S. Vahabzadeh, A. Bandyopadhyay, *Materials Today* **2013**, *16*, 496-504; b) A. Butscher, M. Bohner, S. Hofmann, L. Gauckler, R. Müller, *Acta Biomaterialia* **2011**, *7*, 907-920.

[148] a) J. N. Hanson Shepherd, S. T. Parker, R. F. Shepherd, M. U. Gillette, J. A. Lewis, R. G. Nuzzo, Advanced Functional Materials **2011**, *21*, 47-54; b) Y. B. Lee, S. Polio, W. Lee, G. Dai, L. Menon, R. S. Carroll, S. S. Yoo, Experimental Neurology **2010**, *223*, 645-652.

[149] a) B. C. Gross, J. L. Erkal, S. Y. Lockwood, C. Chen, D. M. Spence, *Analytical chemistry* **2014**, *86*, 3240-3253; b) A. Waldbaur, H. Rapp, K. Lange, B. E. Rapp, *Analytical Methods* **2011**, *3*, 2681-2716; c) D. Therriault, S. R. White, J. A. Lewis, *Nat Mater* **2003**, *2*, 265-271.

[150] K. B. Anderson, S. Y. Lockwood, R. S. Martin, D. M. Spence, *Analytical chemistry* **2013**, *85*, 5622-5626.

[151] C. Chen, Y. Wang, S. Y. Lockwood, D. M. Spence, *Analyst* **2014**, *139*, 3219-3226.

[152] G. Comina, A. Suska, D. Filippini, *Lab on a chip* **2014**, *14*, 424-430.

[153] V. Dragone, V. Sans, M. H. Rosnes, P. J. Kitson, L. Cronin, B. J. Org. Chem. **2013**, *9*, 951-959.

[154] L. Henry, C. R. *Acad. Sci. Paris* **1895**, *120*, 1265; b) L. Henry, *Bull. Soc. Chim. Fr.* **1895**, *13*, 999.

[155] H. Sasai, T. Suzuki, S. Arai, T. Arai, M. Shibasaki, *J. Am. Chem. Soc.* **1992**, *114*, 4418.

[156] a) J. Boruwa, N. Gogoi, P. P. Saikia, N. C. Barua, *Tetrahedron Asymmetry* **2006**, *17*, 3315; b)C. Palomo, M. Oiarbide, A. Laso, *Eur. J. Org. Chem.* **2007**, 2561.

[157] Y. Alvarez-Casao, E. Marquez-Lopez, R. P. Herrera, *Symmetry* **2011**, *3*, 220.

[158] G. Blay, V. Hernandez-Olmos, J. R. Pedro *Synlett* **2011,** *9*, 1195.

[159] C. Christensen, K. Juhl, K. A. Jørgensen, *Chem. Commun.* **2001**, 2222.

[160] D. A. Evans, D. Seidel, M. Rueping, H. Lam, J. Shaw, C. Downey, *J. Am. Chem. Soc.* **2003**, *125*, 12692.

[161] G. Blay, L. R. Domingo, V. Hernández-Olmos, J. R. Pedro, J. R. *Chem. Eur. J.* **2008**, *14*, 4725.

[162] Kee VR. Hemodynamic pharmacology of intravenous vasopressors. Crit Care Nurse. **2003** *4* 79-82.

[163] S. Enthaler, K. Junge, M. Beller, *Angew. Chem. Int. Ed.* **2008**, *47*, 3317-3321.

[164] http://www.monex.com/prods/palladium_chart.html.

[165] Padron, J. I.; Martín, V. S. Top. *Organomet. Chem.* **2011**, *33*, 1.

[166] D. Astruc, *Nanoparticles & Catalysis*, Wiley-VCH, Weinheim, **2008**.

[167] C. Vollmer, C. Janiak, Coord. *Chem. Rev.* **2011**, *255*, 2039-2057, and references cited nerby.

[168] Y. C. Han, H. G. Cha, C. W. Kim, Y. H. Kim, Y. S. Kamg, *J. Phys. Chem. C* **2007**, *111*, 6275-6280.

[169] P.-H Phua, L. Lefort, J. A. F. Boogers, M. Tristany, J. G. de Vries, *Chemm. Commun.* **2009**, 3747-3749; C. Rangheard, C. de Juliàn Fernandàndez, P-H Phua, J. Hoorn, L. Lefort, J. G. de Vries, *Dalton Trans.* **2010**, *39*, 84694-8471.

[170]a) A. Welther, M. Bauer, M.Mayer, A. Jacobi von Wangelin, *ChemCatChem* **2012**, *4* 1088-1093; b) for similar catalysts used in isomerization see: M. Mayer, A. Welther, A. Jacobi von Wangelin *ChemCatChem* **2011**, *3*, 1567-1571.

[171] M. Stein, J. Wieland, P. Steurer, F. Tölle, R. Mühaupt, B. Breit, *Adv. Synth. Catal.* **2011**, *353*, 523- 527.

[172] J. F. Sonnerberg, N. Coombs, P. A. Dube, R. H. Morris, *J. Am. Chem. Soc.* **2012**, *134*, 5893-5899.

[173] R. Dey, N. Mukherjee, S. Ahammed, B. Ranu, Chem. Comm. **2012**, *48*, 7982-7984.

[174] R. Bedford, M. Betham, D. W. Bruce, S. A. Davis, R. M. Frost, M. Hird, *Chem. Commun.* **2006**, 1398 -1400.

[175] L.-M Lacroix, S. Lachaize, A. Falqui, T. Blon, J. Carrey, M. Respaud, F. Dumestre, C. Amiens, O. Margeat, B. Chaudret, P. Lecante, E. Snoeck, *J. Appl. Phys.* **2008**, *103*, article 07D521.

[176] A. Meffre, S. Lachaize, C. Gatel, M. Respaud, B. Chaudret, *J. Mater. Chem.* **2011**, *21*, 13464-13469.

[177] S. Oropeza, M. Corea, C. Gòmez-Yànez, J. J. Cruz-Rivera, M. E. Navarro-Clemente *Mater. Res. Bull* **2012**, *47*,1478-1485.

[178] a) L. A. Berben, B. de Bruin, A. F. Heyduk, *Chem. Commun.* **2015**, *51*, 1553-1554; b) S. Blanchard, E. Derat, M. Desage-El Murr, L. Fensterbank, M. Malacria, V. Mouries-Mansuy, *Eur. J. Inorg. Chem.* **2012**, *2012*, 376-389; c) A. Fuerstner, *ACS Cent. Sci.* **2016**, *2*, 778-789; d) W. Kaim, *Eur. J. Inorg. Chem.* **2012**, 343-348; e) V. Lyaskovskyy, B. De Bruin, *ACS Catal.* **2012**, *2*, 270-279; f) P. J. Chirik, K. Wieghardt, *Science* **2010**, *327*, 794.

[179] E. C. Alyea, P. H. Merrell, *Synth. React. Inorg. Met.-Org. Chem.* **1974**, *4*, 535-544.

[180]) S. K. Russell, E. Lobkovsky, P. J. Chirik, *J. Am. Chem. Soc.* **2011**, *133*, 8858-8861; b) A. M. Tondreau, C. C. H. Atienza, J. M. Darmon, C. Milsmann, H. M. Hoyt, K. J. Weller, S. A. Nye, K. M. Lewis, J. Boyer, J. G. P. Delis, E. Lobkovsky, P. J. Chirik, *Organometallics* **2012**, *31*, 4886-4893; c) J. H. Docherty, J. Peng, A. P. Dominey, S. P. Thomas, Nat Chem 2017, advance online publication; d) A. M. Tondreau, E. Lobkovsky, P. J. Chirik, *Org. Lett.* **2008**, *10*, 2789-2792; e) K. T. Sylvester, P. J. Chirik, *J. Am. Chem. Soc.* **2009**, *131*, 8772-8774; f) B. L. Small, M. Brookhart, *J. Am. Chem. Soc.* **1998**, *120*, 7143-7144; g) B. L. Small, M. Brookhart, A. M. A. Bennett, *J. Am. Chem. Soc.* **1998**, *120*, 4049-4050; h) G. J. P. Britovsek, M. Bruce, V. C. Gibson, B. S. Kimberley, P. J. Maddox, S. Mastroianni, S. J. McTavish, C. Redshaw, G. A. Solan, S. Stroemberg, A. J. P. White, D. J. Williams, *J. Am. Chem. Soc.* **1999**, *121*, 8728-8740; i) G. J. P. Britovsek, V. C. Gibson, B. S. Kimberley, P. J. Maddox, S. J. McTavish, G. A. Solan, A. J. P. White, D. J. Williams, *Chem. Commun.* **1998**, 849-850; j) M. W. Bouwkamp, E. Lobkovsky, P. J. Chirik, *J. Am. Chem. Soc.* **2005**, *127*, 9660-9661.

[181] S. C. Bart, E. Lobkovsky, P. J. Chirik, *J. Am. Chem. Soc.* **2004**, *126*, 13794-13807.

[182] a) A. A. Danopoulos, J. A. Wright, W. B. Motherwell, *Chem. Commun.* **2005**, 784-786; b) J. M. Darmon, Z. R. Turner, E. Lobkovsky, P. J. Chirik, *Organometallics* **2012**, *31*, 2275-2285; c) R. P. Yu, J. M. Darmon, J. M. Hoyt, G. W. Margulieux, Z. R. Turner, P. J. Chirik, *ACS Catal.* **2012**, *2*, 1760-1764.

[183] a) R. Langer, Y. Diskin-Posner, G. Leitus, L. J. Shimon, Y. Ben-David, D. Milstein, *Angew. Chem. Int. Ed.* **2011**, *50*, 9948-9952; b) R. Langer, G. Leitus, Y. Ben-David, D. Milstein, *Angew. Chem. Int. Ed.* **2011**, *50*, 2120-2124.

[184] E. Alberico, P. Sponholz, C. Cordes, M. Nielsen, H. J. Drexler, W. Baumann, H. Junge, M. Beller, *Angew. Chem. Int. Ed.* **2013**, *52*, 14162-14166.

[185] S. Chakraborty, H. Dai, P. Bhattacharya, N. T. Fairweather, M. S. Gibson, J. A. Krause, H. Guan, *J. Am. Chem. Soc.* **2014**, *136*, 7869-7872.

[186] S. Chakraborty, W. W. Brennessel, W. D. Jones, *J. Am. Chem. Soc.* **2014**, *136*, 8564-8567.

[187] S. Lange, S. Elangovan, C. Cordes, A. Spannenberg, H. Jiao, H. Junge, S. Bachmann, M. Scalone, C. Topf, K. Junge, M. Beller, *Catal. Sci. Technol.* **2016**, *6*, 4768-4772.

[188] a) P. O. Lagaditis, A. J. Lough, R. H. Morris, *Inorg. Chem.* **2010**, *49*, 10057-10066; b) N. Meyer, A. J. Lough, R. H. Morris, *Chem. Eur. J.* **2009**, *15*, 5605-5610; c) A. Mikhailine, A. J. Lough, R. H. Morris, *J. Am Chem. Soc.* **2009**, *131*, 1394-1395; d) A. A. Mikhailine, R. H. Morris, *Inorg. Chem.* **2010**, *49*, 11039-11044; e) R. H. Morris, *Chem. Soc. Rev.* **2009**, *38*, 2282-2291; f) P. E. Sues, A. J. Lough, R. H. Morris, *Organometallics* **2011**, *30*, 4418-4431; g) C. Sui-Seng, F. Freutel, A. J. Lough, R. H. Morris, *Angew. Chem. Int. Ed.* **2008**, *47*, 940-943; h) C. Sui-Seng, F. N. Haque, A. Hadzovic, A.-M. Pütz, V. Reuss, N. Meyer, A. J. Lough, M.

Zimmer-De Iuliis, R. H. Morris, *Inorg. Chem.* **2009**, *48*, 735-743; i) W. Zuo, A. J. Lough, Y. F. Li, R. H. Morris, *Science* **2013**, *342*, 1080.

[189] D. E. Prokopchuk, R. H. Morris, *Organometallics* **2012**, *31*, 7375-7385.

[190] A. A. Mikhailine, M. I. Maishan, A. J. Lough, R. H. Morris, *J. Am. Chem. Soc.* **2012**, *134*, 12266-12280.

[191] A. Quintard, J. Rodriguez, *Angew. Chem. Int.* **2014**, *53*, 4044-4055

[192] W. Reppe, H. Vetter Liebigs *Ann. Chem.* **1953**, *582*, 133.

[193] G. N. Schrauzer, *J. Am. Chem. Soc.***1959**, *81*, 5307.

[194] a) I. Wender, R. A. Friedel, R. Markby, H.W. Sternberg, *J. Am.Chem. Soc.***1955**, *77*, 4946; b)I. Wender, R. A. Friedel, R. Markby, H.W. Sternberg, *J. Am. Chem. Soc.***1956**, *78*, 3621; G. N. Schrauzer, *Chem. Ind.***1958**, 1403; c) E. Weiss, R. Merenyi, W. Hubel, *Chem. Ind.***1960**, 407.

[195] Y. Blum, D. Czarkie, Y. Rahamim, Y. Shvo, *Organometallics* **1985**, *4*, 1459; Y. Shvo, D. Czierkie, Y. Rahamin, D. F. Ghodosh, *J. Am.Chem. Soc.***1986**, *108*, 7400.

[196] H.-J. Knölker, E. Baum, H. Goesmann, R. Klauss, *Angew. Chem.***1999**, *111*, 2196; *Angew. Chem. Int. Ed.***1999**, *38*, 2064

[197] D. Chen, H. Zhang, Y. Zhang, G. Zhang, J. Liu, *Dalton Trans.*, **2010**, *39*, 1972.

[198] A. Quintard, J. Rodriguez, Op. Cit., p. 53

[199] C. P. Casey, H. Guan, *J. Am. Chem. Soc.***2007**, *129*, 5816

[200] A. Pagnoux-Ozherelyeva, N. Pannetier, M. D. Mbaye, S. Gaillard, J.-L. Renaud, *Angew. Chem.* **2012**, *124*, 5060; *Angew. Chem. Int. Ed.* **2012**, *51*, 4976.

[201]S. Moulin, H. Dentel, A. Pagnoux-Ozherelyeva, S. Gaillard, A. Poater, L. Cavallo, J.-F. Lohier, J.-L. Renaud, *Chem. Eur. J.* **2013**, *19*, 17881.

[202] D. S. M_rel, M. Elie, J.-F. Lohier, S. Gaillard, J.-L. Renaud, *ChemCatChem*, **2013**, *5*, 2939.

[203] T. T. Thai, D. S. Mérel, A. Poater, S. Gaillard, J.-L. Renaud, *Chem. Eur. J.* **2015**, *21*, 7066-7070.

[204] For and extensive review on iron catalyzed reaction see: Bauer, I. and Knölker, H., J. *Chem. Rev.* **2015**, *115*, 3170–3387.

[205] For a recent review on metal toxicity see: Egorova K., S.; Ananikov, V., P *Angew. Chem. Int. Ed.* **2016**, *55*, 12150 – 12162.

[206] For selected examples of Stereoselective ketones reductions see: a) Berkessel, A.; Reichau, S. ; Von der Höh, A.; Leconte, N.; Neudörfl, J., M.; *Organometallics*, **2011**, *30*, 3880–3887, b) Gajewski, P.; Renom-Carrasco, M.; Vailati Facchini, S. ; Pignataro, L.; Lefort, L.; de Vries, J. G.; Ferraccioli, R.; Forni, A.; Piarulli, U.; Gennari, C. *Eur. J. Org. Chem.* , **2015**, 1887–1893.

[207] Zhou, S.; Fleischer, S.; Junge, K.; Das, S.; Addis, D. Beller, M. *Angew. Chem. Int. Ed.* **2010** , *49*, 8121 –8125

[208] Prokopchuk, D. E. ; Lough, A. J. ; Rodriguez-Lugo, R. E.; *Morris* R. H.; Grützmacher, *H*. *Science* ***2013***, *342*, *1080-1083.*

[209] Yan, T.; Feringa, B., L.; and Barta, K. ACS Catal. **2016**, 6, 381-388

[210] a) G. Domìnguez, J. Pérez-Castells, *Chem. Soc. Rev.*, **2011**, *40*, 3430–3444. b) B. R. Galan, T. Rovis, *Angew. Chem. Int. Ed.* , **2009**, *48*, 2830-2834. c) P. R. Chopade, J. Louie, *Adv. Synth. Catal.* , **2006**, *348*, 2307 – 2327.

[211] Selected examples of Ru catalysed [2+2+2]: a) Y. Yamamoto, K. Hata, T. Arakawa, K. Itoh, *Chem. Commun.* **2003**, 1290 – 1291; b) Y. Yamamoto, T. Arakawa, R. Ogawa, K. Itoh, *J. Am. Chem. Soc.* **2003**, *125*, 12143 – 12160; c) Y. Yamamoto, J. Ishii, H. Nishiyama, K. Itoh, *J. Am. Chem. Soc.* **2004**, *126*, 3712 – 3713; d) Y. Yamamoto, J. Ishii, H. Nishiyama, K. Itoh, *J. Am. Chem. Soc.* **2005**, *127*, 9625 – 9631; e) F. Xu, C. Wang, X. Li, B. Wan, *ChemSusChem* **2012**, *5*, 854-857.

[212] Selected examples of Rh catalysed [2+2+2]: a) R. Grigg, R. Scott, P. Stevenson, *Tetrahedron Lett.* **1982**, *23*, 2691 – 2692; b) H. Kinoshita, H. Shinokubo, K. Oshima, *J. Am. Chem. Soc.* **2003**, 125, 7784 – 7785; c) K. Tanaka, G. Nishida, A. Wada, K. Noguchi, *Angew. Chem. Int. Ed.* **2004**, *43*, 6510– 6512; d) H. Hara, M. Hirano, K. Tanaka, *Org. Lett.*, **2008**, *10*, 2537 – 2540.

[213] Selected examples of Co catalysed [2+2+2]: a) K. P. C. Vollhardt, *Acc. Chem. Res.* **1977**, *10*, 1 – 8; b) R. L. Funk, K. P. C. Vollhardt, *J. Chem. Soc. Chem. Commun.* **1976**, 833 – 835; c) R. L. Funk, K. P. C. Vollhardt, *J. Am. Chem. Soc.* **1977**, *99*, 5483 – 5484; d) R. L. Hillard, III, K. P. C. Vollhardt, *J. Am. Chem. Soc.* **1977**, *99*, 4058 – 4069; e) Hilt, T. Volger,W. Hess, F. Galbiati, *Chem. Commun.* **2005**,1474 – 1475; f) I. Thiel, H. Jiao, A. Spannaenberg, M. Hampke *Chem. Eur. J.* **2013**, *45*, 2003-2008.

[214] Selected examples of Ir catalysed [2+2+2]: a) R. Takeuchi, M. Kashio, *Angew. Chem. Int. Ed. Engl.***1997**, *36*, 263 – 266; b) R. Takeuchi, *Synlett* **2002**, 1954 – 1965; c) R. Takeuchi, Y. Akiyama, *J. Organomet. Chem.* **2002**, *651*, 137 – 145.

[215] Selected examples of Ni catalysed [2+2+2]: a) W. Reepe, J. Liebigs, *Ann. Chem.* **1948**, *560*, 1. b) F. Teplý, I. G. Stará, I. Starý, A. Kollárovič, D. Šaman, L. Rulíšek, P. Fiedler, *J. Am. Chem. Soc.* **2002**, *124*, 9175 –9180; c) K. R. Deaton, M. S. Gin, *Org. Lett.* **2003**, *5*, 2477 – 2480; d) Y. Zhong, N. A. Spahn R. M. Stolley, H. M. Minh, J. Louise, *Synlett* **2015**, *26*, 307-312.

[216] Selected examples of Pd catalysed [2+2+2]: V. Gevorgyan, U. Radhakrishnan, A. Takeda, M.Rubina, M. Rubin, Y. Yamamoto, *J. Org. Chem.* **2001**, *66*, 2835 – 2841; b) D. Pena, D. Perez, E. Guitian, L. Castedo, *Eur. J. Org.Chem.* **2003**, 1238 – 1243.

[217] Selected examples of Ti catalysed [2+2+2]: a) O.V. Ozerov, F. T. Ladipo, B. O. Patrick, *J. Am. Chem. Soc.* **1999**, *121*, 7941-7942; b) M. J. Sung, J. Pang, S. Park, J. K. Cha, *Org. Lett.* **2003**, *5*, 2137 – 2140.

[218] N. Yoshikai, S.-L. Zhang, K.-I. Yamagata, H. Tsuji, E. Nakamura, *J. Am. Chem. Soc.* **2009**,*131*, 4099–4109.

[219] W. Hüberl, C. Hoogzand *C. Chem. Ber.* **1960**, *93*, 103.

[220] a) N. Saino, D. Kogure, S. Okamoto, *Org. Lett.* **2005**, *7*, 3065-3067; b) N. Saino, D. Kogure, K. Kase, S. Okamoto, *J. Organomet. Chem.* **2006**, *691*, 3129-3136.

[221] A. Fürstner, K. Majima, R. Martín, H. Krause, E. Kattnig, R. Goddard, C. W. Lehmann *J. Am. Chem. Soc.* **2008**, *130*, 1992-2004.

[222] Y. Liu, X. Yan, N. Yang, C. Xi *Catal. Commun.* **2011**, *12*, 489-492.

[223] H. Chowdhury, N. Chatterjee, A. Goswami *Eur. J. Org. Chem.* **2015**, 7735–7742.

[224] M. I. Lipschutz, T. Chantarojsiri, Y. Dong, T. D. Tilley *J. Am. Chem. Soc.* **2015**, *137*, 6366−6372.

[225] Examples of other iron catalysed 2+2+2 reaction for heterocycles and benzene rings formations: a) C. Wang, X. Li, F. Wu, B. Wan, *Angew. Chem. Int. Ed.* **2011**, *50*, 7162-7166; b) K. Nakajima, W. Liang, Y. Nishibayashi, *Org. Lett.* **2016**, *18*, 5006−5009; c) N. A. Spahn, M. H. Nguyen, J. Renner, T. K. Lane, and J. Louie, *J. Org. Chem.* **2017**, *82*, 234−242; d) V. Richard, M. Ipouck, D. S. Mérel, S. Gaillard, R. J. Whitby, B. Witulski and J. Renaud, *Chem. Commun.*, **2014**, *50*, 593 - 595; e) L. Ilies, A Matsumoto, M. Kobayashi, N. Yoshikai, E. Nakamura, *Synlett.* **2012**, *23*, 2381 – 2384; e) M. Minakawa, T. Ishikawa, J. Namioka, S. Hirooka, B. Zhou, M. Kawatsura, *RSC Adv.*, **2014**, *4*, 41353–41356; f) B. R. D'Souza, T. K. Lane, J. Louie, *Org. Lett.* **2011**, *13*, 2936-2939; g) S. Karpiniec, D. S. McGuinness, G. J. P. Britovsek, J. Pate, *Organometallics* **2012**, *31*, 3439−3442; h) K. Nakajima, S. Takata, K. Sakata, Y. Nishibayashi *Angew. Chem. Int. Ed.* **2015**, *54*, 7597 – 7601; i) C. Wang, D. Wang, F. Xu, B. Pan, B. Wan, *J. Org. Chem.* **2013**, *78*, 3065 – 3072; j) B. A. Frazier, V. A. Williams, P. T. Wolczanski, S. C. Bart, K. Meyer, T. R. Cundari, E. B. Lobkovsky, *Inorg. Chem.* **2013**, *52*, 3295 – 3312; k) C. Breschi, L. Piparo, P. Pertici, A. M. Caporusso, G. Vitulli, *J. Organomet. Chem.* **2000**, *607*, 57 – 63.

[226] R. A. Andersen, K. Faegri, J. C. Green, A. Haaland, M. F. Lappert, W.-P. Leung, *Inorg. Chem.* **1988**, *27*, 1782.

[227] T. N. Gieshoff, U. Chakraborty, M. Villa, and A. J. Wangelin *Angew. Chem. Int. Ed.* **2017**, *56*,3585 –3589

[228] Selected recent examples: a) M. I. Lipschutz, T. Chantarojsiri, Y. Dong, T. D. Tilley, *J. Am. Chem. Soc.* **2015**, *137*, 6366-6372; b) L. C. H. Maddock, T. Cadenbach, A. R. Kennedy, I. Borilovic, G. Aromí, E. Hevia, *Inorg. Chem.* **2015**, *54*, 9201-9210; c) T. Hatakeyama, R. Imayoshi, Y. Yoshimoto, S. K. Ghorai, M. Jin, H. Takaya, K. Norisuye, Y. Sohrin, M. Nakamura, *J. Am. Chem. Soc.* **2012**, *134*, 20262 - 20265; d) J. Yang, T. D. Tilley, *Angew. Chem. Int. Ed.* **2010**, *49*, 10186- 10188; e) J. Yang, M. Fasulo, T. D. Tilley, *New J. Chem.* **2010**, *34*, 2528- 2354.

[229] D. R. Anton, R. H. Crabtree, Organometallics 1983, 2, 855; b) G. Franck, M. Brill, G. Helmchen, *J. Org. Chem.* **2012**, *89*, 55; c) D. Gärtner, A. L. Stein, S. Grupe, J. Arp, A. Jacobi von Wangelin, *Angew. Chem. Int. Ed.* **2015**, *54*, 10545.

[230] H.-J. Knölker, E. Baum, H. Goesmann, R. Klauss, *Angew. Chem. Int. Ed.* **1999**, *38*, 2064 – 2068.

[231] S. Moulin, H. Dentel, A. Pagnoux-Ozherelyeva, S. Gaillard, P. Sylvain; A. Poater, L. Cavallo, J. F. Lohier, J. L. Renaud, *Chem. Eur. J*, **2013**, *19*, 17881 – 17890.

[232] M. Heiden, D. W. Stephan *Chem. Commun.,* **2011**, *47*, 5729 – 5731.

[233] R. D. Guthrie, J. L. Hedrick *J. Am. Chem. Soc.*, **1973**, *95*, 2971 – 2977.

[234] M. B. Eleveld, H. Hogeveen, E. P. Schudde *J. Org. Chem.,* **1986***, 51* 3635*.*

[235] R. Gracheva, *Zhurnal Organicheskoi Khimii*, **1973**, *9*, 1265-1267.

[236] V. N. Johannes, C.G. Pandit, K. Upendra *Tetrahedron*, **1985**, *41*, 6005 – 6012.

[237] S. Guizzetti, M. Benaglia, S. Rossi *Organic Letters*, **2009**, *11*, 2928 – 2931.

[238] Chuanjun, L.; Qi, Z.; Jun, Y.; D. Zhiyun; Ling, H.; Xingshu, L. *Eur. J. Med. Chem.*, **2013**, *62*, 745–753.

[239] BASF AKTIENGESELLSCHAFT Patent: WO2006/87321 A1, **2006**.

[240] a) R. Slavko, S. Michel, M. Barbara *Eur. J. Org. Chem.*, **2015**, 2214 – 2225; b) H. Fernández-Pérez, J. Benet-Buchholz, A. Vidal-Ferran, *Chem. Eur. J*, **2014**, *20*, 15375 – 15384.

[241] A. Andersen, K. Faegri, J. C. Green, A. Haaland, M. F. Lappert, W. P. Leung, K. Rypdal, *Inorg. Chem.* **1988**, *27*, 1782.

[242] B. Kaiser, D. Hoppe *Angew. Chem. Int. Ed. Engl.* **1995**, *34*, 323

[243] a) N. Weding, R. Jackstell, H. J. Jiao, A. Spannenberg, M. Hapke, *Adv. Synth. Catal.* **2011**, *353*, 3423; b) R. G. Iafe, J. L. Kuo, D. G. Hochstatter, T. Saga, J. W. Turner, C. A. Merlic, *Org. Lett*. **2013**, *15*, 582.

[244] J. Aleman, V. del Solar, C. Navarro-Ranninger, *Chem. Commun.* **2010**, *46*, 454.

[245] M. Fernández, M. Ferré, A. Pla-Quintana, T. Parella, R. Pleixats, A. Roglans, *Eur. J. Org. Chem.* **2014**, 6242.

[246] M. Rehan, S. Maity, L. K. Morya, K. Pal, P. Ghorai, *Angew. Chem. Int. Ed.* **2016**, *55*, 7728.

[247] S. Reimann, P. Ehlers, M. Sharif, A. Spannenberg, P. Langer, *Tetrahedron* **2016**, *72*, 1083.

[248] L. Xu, R. Yu, Y. Wang, J. Chen, Z. Yang, *J. Org. Chem.* **2013**, *78*, 5744.

[249] G. J. Rodriguez, R. Martin-Villamil, I. Fonseca, *J. Chem. Soc. Perkin Trans.* **1997**, *1*, 945.

[250] G. Hilt, T. Vogler, W. Hessa, F. Galbiatia, *Chem. Commun.* **2005**, 1474.

[251]K. R. Sanjeewa, I. V. Powell, M. G. Coleman, J. A. Krause, H. Guan, *Org. Biomol. Chem.* **2013**, *44*, 7653.

[252] K. Tanaka, K. Toyoda, A. Wada, K. Shirasaka, M. Hirano, *Chem. Eur. J.* **2005**, *11*, 1145.

[253] S. Pal, C. Uyeda, *J. Am. Chem. Soc.* **2015**, *137*, 8042.

[254] G. Kalikhman *Bul. Acad. Sciences of the USSR, Div. Chem. Sci. (Engl. Transl.)*, **1969**, 1714.

[255] J.-S. Yang, H.-H. Huang, S.-H. Lin, *J. Org. Chem.* **2009**, *74*, 3974.

[256]Y. Kenta, I. Morimoto, K. Mitsudo, H. Tanaka, *Tetrahedron* **2008**, *64*, 5800.

[257]*P. García-García, A. Martínez, A. M. Sanjuán, M. A. Fernández-Rodríguez, R. Sanz, Org. Lett.*, **2011**, *13*, 4970.